uOttawa

L'Université canadienne
Canada's university

FACULTÉ DES ÉTUDES SUPÉRIEURES ET POSTOCTORALES

uOttawa

L'Université canadienne
Canada's university

FACULTY OF GRADUATE AND POSDOCTORAL STUDIES

Michel G. Houlé
AUTEUR DE LA THÈSE / AUTHOR OF THESIS

Ph.D. (Earth Sciences)
GRADE / DEGREE

Department of Earth Sciences
FACULTÉ, ÉCOLE, DÉPARTEMENT / FACULTY, SCHOOL, DEPARTMENT

Physical Volcanology and Metallogenesis of Komatiitic Rocks in the Abitibi Greenstone Belt, Superior Province, Ontario, Canada

TITRE DE LA THÈSE / TITLE OF THESIS

Tony Fowler
DIRECTEUR (DIRECTRICE) DE LA THÈSE / THESIS SUPERVISOR

Mike Lesher
CO-DIRECTEUR (CO-DIRECTRICE) DE LA THÈSE / THESIS CO-SUPERVISOR

EXAMINATEURS (EXAMINATRICES) DE LA THÈSE / THESIS EXAMINERS

Stephen J. Barnes

Keiko Hattori

Mark Hannington

Harold Gibson

Gary W. Slater
Le Doyen de la Faculté des études supérieures et postdoctorales / Dean of the Faculty of Graduate and Postdoctoral Studies

Physical Volcanology and Metallogenesis of Komatiitic Rocks in the Abitibi Greenstone Belt, Superior Province, Ontario, Canada

Michel G. Houlé

Thesis submitted to the
Faculty of Graduate & Postdoctoral Studies
University of Ottawa
in partial fulfillment of requirements for the
Ph.D. degree in Earth Sciences

Ottawa-Carleton Geoscience Centre
and
University of Ottawa
Ottawa, Canada

Your file Votre référence
ISBN: 978-0-494-48655-9
Our file Notre référence
ISBN: 978-0-494-48655-9

ABSTRACT

Komatiites occur in many Archean and Proterozoic greenstone belts worldwide, provide critical information about the nature of early Earth volcanism and the stratigraphy, structure, and crustal evolution of greenstone belts, and locally host Ni-Cu-(PGE) sulfide deposits. Despite their importance, many aspects of the physical volcanology of komatiites are not well understood. The Western Abitibi Greenstone Belt (WAGB) contains some of the best exposed and well-preserved komatiites on Earth, including several areas with spectacular glacially-polished and well-preserved outcrops, and is one of the best places to address some of the fundamental questions regarding the physical volcanology of komatiites.

Komatiites form a wide range of volcanic facies (e.g., textural, morphological, lithological, and volcanological facies) and geochemical types (e.g., ADK: Al-depleted, TEK: Ti-enriched, AUK: Al-undepleted, TDK: Ti-depleted) that occur sporadically throughout the Superior Province. The western Abitibi greenstone belt is one of the youngest volcano-plutonic greenstone belts in the Superior Province and is characterized by approximately equal proportions of supracrustal (53%) and intrusive rocks (47%). Komatiitic volcanism spaned over 40 Ma and occurs as minor component in 4 volcano-sedimentary assemblages: the Pacaud assemblage (2750-2735 Ma) contains ~4% komatiites with abundant differentiated flows (ortho- to mesocumulate lower zones and poorly developed spinifex-textured upper zones) and less abundant undifferentiated flows (olivine-phyric or ortho- to mesocumulate) characterized by TDK geochemical type, the Stoughton-Roquemaure assemblage (2723-2720 Ma) contains ~3% komatiites with undifferentiated flows, pillowed flows with lesser differentiated flows characterized by ADK-TEK≈AUK geochemical types, and the Kidd-Munro assemblage (2719-2711 Ma) with ~11% komatiites and the Tisdale assemblage (2710-2704 Ma) with ~7% komatiites both contain undifferentiated flows with abundant ortho- to adcumulate rocks with fewer olivine-phyric rocks, and differentiated flows with thick orthocumulate lower zones and thin spinifex-textured upper zones characterized by AUK > ADK-TEK. Thus, the younger assemblages (Kidd-Munro and Tisdale) contain larger volumes of komatiitic rocks, in particular larger volumes of thick, highly magnesian cumulate lava channels and channelized sheet flows than the older assemblages (Pacaud and Stoughton-Roquemaure). This might

reflect higher magma discharge rates, emplacement closer to the eruptive site, and/or selective preservation.

Substrate erosion by modern lava flows and Archean komatiite lava flows has been debated for many years, but is now recognized by most workers to be one of the most dominant mechanisms in the genesis of komatiite-associated Ni-Cu-(PGE) deposits worldwide. Field relationships at the Alexo Mine in Dundonald Township provide unequivocal evidence for thermomechanical erosion of andesite by komatiite. The evidence includes: 1) nested footwall embayments occur on scales from 100s of meters to a few centimetres; 2) the morphologies of the embayments vary from concave to re-entrant; 3) the basal contact is very sharp but scalloped and clearly transgresses the footwall rocks without any evidence of a regolith, shearing, or folding; 4) there is evidence for contact metamorphism along the entire length of the contact, but it appears to be thicker and more intense around embayments; 6) xenoliths are more common within embayments; and 7) komatiitic dikes penetrate downward into the host andesites primarily along the lateral margins of embayments. The spatial association between thermomechanical erosion and Fe-Ni-Cu sulfide mineralization indicates a clear relationship between those two critical mechanisms in the genesis of komatiite-associated Ni-Cu-(PGE) deposits.

Inflation processes have been recognized as an important mechanism in the emplacement of basaltic flow fields in Hawaii and in continental flood basalts, and have been inferred to have been important in the emplacement of komatiite flows in Western Australia and South Africa. Detailed mapping at Pyke Hill in Munro Township and Serpentine Mountain in McArthur Township indicates that thin komatiite sills/dikes present within those komatiite sequences, which have been previously interpreted as segregation veins, represent new pulses of hotter magma into cooler, semi-consolidated but permeable cumulate materials during endogenous growth of lava conduits (i.e., lava tube to lava channel). This interpretation is supported by a more complex organization of the spinifex-textured zone than is normally observed in lava flows, coarsening of olivine crystals at the margins of the sills, and concentric overgrowth shells or dendritic olivine overgrowths that grew from the cumulate-sill contact toward the sill interior. These intrusions suggest that these systems were more dynamic and may indicate preferred lava pathways or tubes that served to focus lava flow. Despite the fact that thin spinifex-textured sills appear to have been observed only within unmineralized komatiitic lava flows, this volcanic environment is permissive for thermomechanical erosion. Furthermore, spinifex-textured sills might also be used to aid in the identification and delineation of nearby larger lava pathways that could be more prospective and potentially host Ni-Cu-(PGE) mineralization within subvolcanic-volcanic komatiite lava flow fields.

Komatiitic rocks are well known to occur as lava flows but also occurs as hypabyssal and abyssal intrusions providing important constraints on the architecture of the komatiite volcanic-subvolcanic sequences in the Abitibi greenstone belt. An intrusive origin for some komatiites previously interpreted as extrusive is supported by transgressive relationships with overlying rocks, symmetric differentiation (upper and lower chilled margins characterized by fine-grained spinifex-textured rocks) in comparison to asymmetric differentiation within komatiite flows (A and B zones), and/or peperites along the upper contacts. Recognition of direct linkages between intrusive and extrusive komatiitic rocks in Dundonald Township suggest that density and rheology of the near-surface rocks governs whether they will be emplaced as lava flows, invasive flows, or sills and also influences the localization of Ni-Cu-(PGE) sulfide deposits. The initial eruptions in lava-dominated environments are typically most voluminous and, if erupted at sufficient flow rates, form channelized flows conducive to thermomechanical erosion of sulfur-rich footwall rocks. In subvolcanic-volcanic environments, however, channelized units may also occur within the subvolcanic plumbing system. Where only the sills are channelized (e.g., Thompson belt), mineralization will occur only within the subvolcanic environment, where only the flows are channelized (e.g., Damba-Silwane), mineralization will occur only within the volcanic environment, but where both sills and lava flows are channelized (e.g., Dundonald, Shaw Dome, possibly Raglan), the distribution of the mineralization is more diverse and may occur within both environments as sub-seafloor and seafloor Ni-Cu-(PGE) sulfide deposits.

ACKNOWLEDGEMENTS

This research project would not have been possible without the financial support of several organizations, including research grants from the Ontario Geological Survey and from the Natural Sciences and Engineering Research Council of Canada (NSERC) to Dr. C.M. Lesher, student fellowships from "Le Fonds québécois de la recherche sur la nature et les technologies" (formely "Fonds pour la Formation de Chercheurs et l'Aide à la Recherche"), from the University of Ottawa, and from the Society of Economic Geologists *(Hugh E. McKinstry Grant)* to M.G. Houlé.

I also want to acknowledge the support of many individuals and companies who provided access to field exposures, drill cores, geological data, and thoughtful discussions on the geology of these areas over the years, including P. Davis (Hucamp Mines Ltd., Larchex Inc., Canadian Arrow Mines Ltd., First Nickel Inc.); K. Montgomery (Hucamp Mines Ltd., First Nickel Inc.); D. Gamble (Dave Gamble Geoservices Inc.); E. Bettiol and E.W. Harrison (Millstream Mines Ltd.); D. Rogers, F. Santaguida, and N. Dupras (Falconbridge Ltd.).

My sincere thanks go to my thesis supervisor Dr. C.M. Lesher at Laurentian University for his friendship, guidance, advice, and great generosity since the beginning of my doctorate. It has been an extremely enriching experience to work with one of the top researchers in komatiites. His tremendous knowledge on every aspect of komatiites and his professionalism allowed me to grow as a researcher and to reach a higher standard. I am also grateful to him for introducing me to high-level research and for the opportunity to meet so many well-established researchers from around the world. I also thank my co-supervisor Dr. A.D. Fowler at University of Ottawa, who provided guidance and encouragement during the course of this thesis. This project has greatly benefited from his knowledge of textures and structures of volcanic rocks, including spinifex textures. I am also grateful to him for introducing me to student's supervision and giving me the opportunity to co-organize an international field trip in the Abitibi greenstone belt (Lenny G. Berry Summer School, GAC MAC Field Trip). I am grateful to both for sharing their knowledge on komatiites and giving me the free reign to explore many aspects of the komatiite physical volcanology in a variety of directions.

I also want to acknowledge the continuous scientific and moral support of my entire advisory committee. I am particularly grateful to Dr. Gibson for sharing his knowledge and passion about physical volcanology. It is always an incredible experience to do field work with him and his enthusiasm for looking at rocks as a first and primordial key observation before complementing by other investigation is highly contagious and refreshing. Dr. Thurston introduced me to Sudbury and to Laurentian University in late 90s, when I first met him in LG-3 in the James Bay in northern Québec. He suggested that I contact Dr. Lesher about an interesting physical volcanology project on komatiites conducted in collaboration with the Ontario Geological Survey and Laurentian University. As Abitibi Group leader for the Ontario Geological Survey, Dr. Ayer, give me the opportunity to get involved in special themes within the Discover Abitibi and Targeted Geoscience Initiatitive III programs. Those commitments provided me an opportunity to complement, at different scales, my learning on komatiites. Dr. Sproule has greatly facilitated my integration into the Mineral Exploration Research Centre at Laurentian University. She rapidly became more than a co-worker, a good friend in this new environment for me and my family. Sharing an office with her was always entertaining and allowed me to benefit from her knowledge of geochemistry and komatiites.

I want also to thank my current employer, the Ontario Geological Survey, for the support and resources they provided toward the accomplishment of my PhD and to give me the opportunity to learn more on komatiites in the Abitibi greenstone belt and elsewhere in Ontario. The support of the Mineral Exploration Research Centre of Laurentian University and the Department of Earth Sciences of University of Ottawa was greatly appreciated. I also want to thank Natalie Lafleur-Roy for her friendship and all the technical support that she provided me. She facilitated all logistic and administrative tasks during the entire study.

Thank you to my family who never failed to be there for me and support me in every way they could during all those years. They always encouraged me to pursue my way through university. I would like to thank my mother for her entire support behind the scene all those years. She did not completely understand the science behind my work, but she was always interested in what I was doing. I know she loved me very much and that she would be extremely proud of her son for the completion of this study.

Finally, I thank Isabelle, my wife, who agreed many years ago to start a new chapter of our life far away from home, in Sudbury. I am grateful for her constant and inestimable support, understanding, encouragement, and patience over the years and also for the time she spent without the attention of her husband over the past seven years. I am also thankful of my little daughter, Catherine, who gives me the ultimate reason to finally finish it.

TABLE OF CONTENTS

LIST OF TABLES

List of Figures

CHAPTER 1 - INTRODUCTION

The spectacular textures and structures of komatiites have captured the imagination and attention of geologists since their interpretation as extrusive rocks by Viljoen and Viljoen (1969) in the Barberton Mountain Land in South Africa. Several attempts have been made to classify komatiites and other high-magnesium volcanic rocks, and distinguishing between komatiites, komatiitic basalts, and picrites is still a matter of debate (see Le Bas, 2000; Kerr and Arndt, 2001; Le Bas, 2001; Arndt, 2008). However, it is generally accepted by most workers that komatiites are ultramafic volcanic rocks or intrusive equivalents that are characterized by very high MgO (>18%), moderately low SiO_2 and Al_2O_3, and very low K_2O and TiO_2 contents.

Spinifex textures were once considered diagnostic of an extrusive origin, but have since been shown to occur in both flows and high-level intrusions (e.g., Donaldson, 1974; Arndt et al., 2004; Houlé et al., 2004). Spinifex texture was first defined by Nesbitt (1971) because of the resemblance with spinifex grass in Western Australia (Fig. 1.1), but the same texture had been previously recognized and referred to "chicken-track" texture by Naldrett and Mason (1968) in their study of ultramafic rocks in Dundonald Township in the Abitibi greenstone belt.

Komatiites and komatiitic basalts are almost entirely restricted to Archean cratons and Proterozoic mobile belts (see review by Arndt, 2008), but rarely occur in younger environments (e.g., Gorgona Island: Columbia) (Fig. 1.2). Komatiites form a wide range of volcanic facies (e.g., Arndt et al., 1979; Lesher et al., 1984; Hill et al., 1995), some of which locally host magmatic Ni-Cu-(PGE) deposits (e.g., Lesher, 1989; Lesher and Keays, 2002; Naldrett, 2004). Komatiites have been interpreted by most workers to have formed by a high degree of partial melting (e.g., Nesbitt and Sun, 1976; Arndt, 1977) in mantle plumes (e.g., Fyfe, 1978; Campbell et al., 1989; Herzberg et al., 2000; Arndt, 2008) or in subduction-like environments (e.g., Allègre, 1982; Parman et al., 2004). Regardless, they appear to have erupted as voluminous, highly mobile flows capable of travelling long distances (~10s to 100s km long) once channelized (e.g., Lesher et al., 1984; Huppert and Sparks, 1985; Williams et al., 1998). A significant amount of research has been directed toward understanding the metallogenesis of komatiites, as komatiite-hosted magmatic Fe-

Ni-Cu sulfide deposits represent approximately 20% of the global nickel resources in the world (Hoaston et al., 2006).

Figure 1.1 Spinifex grass in Western Australia (courtesy of Rebecca Sproule).

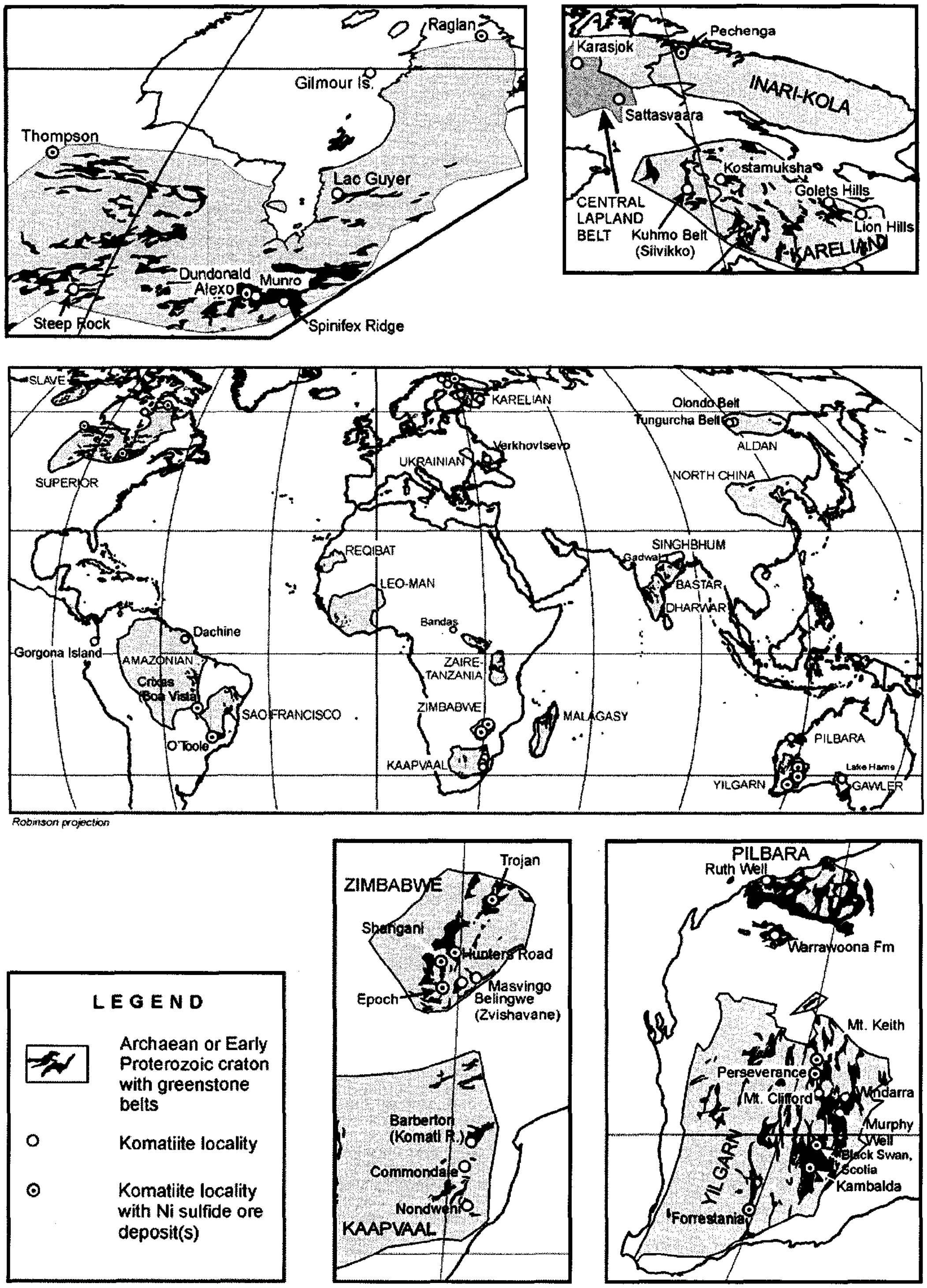

Figure 1.2 Komatiites and komatiitic basalts distribution around the world, with major nickel districts associated with komatiitic rocks (from Arndt et al., 2008).

1.1 Statement of problem

Komatiites and komatiitic basalts represent only a small proportion of supracrustal sequences within Archean or Proterozoic greenstone belts around the world. However, understanding komatiite physical volcanology provides critical information about the nature of early Earth volcanism, the stratigraphy, structure and crustal evolution of Archean and Proterozoic greenstone belts, and the genesis of komatiite-associated Ni-Cu-(PGE) deposits.

A large amount of research over the past 40 years has been focused on the petrologic and geochemical characteristics of komatiites and their source regions compared to the amount of research conducted on the physical volcanology of komatiites. This discrepancy is in part a reflection the fact that no historic komatiite eruptions are known and most komatiites are only preserved within deformed and metamorphosed Archean and Proterozoic volcanic belts in which mapping komatiites physical characteristics and modelling their physical volcanology are extremely challenging.

Komatiite lava field models (Hill et al., 1990; 1995), inspired from previous subaqueous mafic flow models in Archean greenstone belts (e.g., Abitibi: Dimroth et al., 1978), depict them as an anastomosing network of lava rivers and levee facies. Recent advances in understanding physical volcanology of Hawaiian basalts (Hon et al., 1994) and flood basalts (Self et al., 1996; 1997), led Hill (2001) to further interpret komatiite lava flow fields as a direct analogues of modern inflationary basaltic lava flow fields. However, basalts have much lower eruption temperatures, significantly higher viscosities, appreciably smaller intervals between the liquidus and solidus temperatures, and significantly higher specific heat contents (see Chapter 2). Moreover, those in Hawaii erupted subaerially onto low-relief, near-horizontal surface, so they are probably not good analogs for komatiites (Barnes and Lesher, 2008). Subaqueous flood basalts would be better analogues, at least for thicker komatiite flows, but their volcanology is even less well constrained.

Several aspects of komatiite physical volcanology are still hotly debated, and require further study. These can be grouped into three broad topics: physical behaviour of komatiite lava flows and sills, volcanic-subvolcanic architecture, and geodynamic setting. These points include:

Geodynamic setting

- What is the geodynamic setting of komatiites? Were they plume-related, subduction-related, or did they result from plume-arc interaction, or some other process?
- What is the significance of komatiite (e.g., proportion and distribution) within a greenstone belt?

Volcanic (-subvolcanic) architecture

- What are the relationships between intrusive and extrusive komatiites?
- If spinifex texture is not diagnostic of an extrusive environment, is there a difference between spinifex texture in intrusive versus extrusive komatiites?
- How the flows are organized in terms of their internal zonation and how does this change in or across a flow field differ from the internal zonation of intrusive komatiites?
- What is the architecture of komatiite lava flow fields at the greenstone belt-scale?
- What is the role of the physical volcanology (i.e., volcanic-subvolcanic architecture) on metallogenetic models for komatiite-associated deposits?

Physical behaviour of komatiite lava flows/sills

- Were komatiites dry or wet?
- Were they capable of thermomechanical erosion?
- Were they capable of vesiculation and explositivity?
- Were they inflationary?

This is a broad range of critical questions that must be asked regarding the physical volcanology and the nature of komatiites in general. This thesis does not attempt to answer all of then. However, several chapters bring new insights to several questions within those three broad areas.

1.2 Aim and Objectives

The principal aim of this thesis is to better understand, using a volcanological facies analysis approach, the physical volcanology and the metallogenesis of komatiites in the western part of the Abitibi greenstone belt (WAGB). A better understanding of the volcanic architecture of komatiites will help constrain stratigraphic, tectonic, and metallogenic models throughout the WAGB that may aid in the development of similar models in other greenstone belts.

In order to accomplish those goals, the following specific objectives were defined: 1) establishment of a komatiite facies classification scheme for the WAGB; 2) determination of regional (i.e., belt-scale) facies variations for komatiites in the WAGB; 3) determination of local (i.e., Township-scale, outcrop-scale) facies variations for komatiites in the WAGB; 4) evaluation of the role of komatiite sills and dikes within the WAGB; and 4) determination of the prevalent processes responsible for the formation of nickel sulfide deposits associated with komatiites in the WAGB.

The WAGB, which includes the Kidd-Munro and Tisdale assemblages (Ayer et al., 2002), is an ideal area for the study because it is easily accessible and contains well-exposed glacially-polished outcrops that preserved the primary volcanic structures and textures of the rocks. The belt has also been the focus of a recent comprehensive geoscience program undertaken by the Ontario Geological Survey, which included extensive geochronological analysis (e.g., Ayer et al., 1997; 1999a; 1999b; 2002; 2005), and a regional geochemical study on komatiite geochemistry and petrogenesis undertaken collaboratively by Mineral Exploration Research Centre of Laurentian University (Sudbury) and the Ontario Geological Survey (Sproule et al., 2002; 2003; 2005). These studies provide excellent stratigraphic and geochemical controls on the komatiites in the WAGB, allowing more detailed examination of the spatial and temporal variations in their physical volcanology at various scales throughout the WAGB.

1.3 Organization and Co-Authorship

This dissertation is presented in 7 chapters. Chapters 2 and 3 have been written as manuscripts for publication in a refereed government publication and chapters 4, 5, and 6 have been written as manuscripts for publication in refereed scientific journals. To a certain degree these chapters overlap and the nomenclature used within each chapters varies slightly (reflecting variations in the time of publication), but considerable effort has been made to minimize these issues within this dissertation.

A number of collaborators provided supervision and scientific guidance at different stages of the manuscript preparation. They encouraged scientific exchanges that stimulated my thinking on different aspects of komatiite physical volcanology and komatiite genesis. However, as senior author, I acquired most or all of the field and laboratory data, made the primary interpretations of the data, drafted all the diagrams, wrote the first drafts of all the manuscripts, made all of the revisions, submitted all of the manuscripts, and communicated with the journal editors.

Chapter 1 introduces the reader to the problems, the aims and objectives, the methodology used to achieve those objectives, the organization of this study, and information about co-authorships on multi-authored papers.

Chapter 2 is written as a manuscript entitled "***Physical Volcanology of Komatiites in the Abitibi Greenstone Belt***" (published in *Summary of Field Work and Other Activities 2001*: OFR 6070). It summarizes the nomenclature and the volcanic terminology used for komatiites, proposes revised komatiite classification scheme, presents an overview of the komatiite physical volcanology, and summarizes the geochronological and stratigraphic framework of komatiites in the WAGB. Minor modifications were made from the published version.

The co-authors that have collaborated to this publication are: *Lesher, C.M.*, *Gibson, H.L.*, and *Sproule, R.A.*, Mineral Exploration Research Centre, Department of Earth Sciences, Laurentian University, 933 Ramsey Lake Road, Sudbury, Ontario P3E 6B5 Canada; *Fowler, A.D.*, Ottawa-Carleton Geoscience Centre, Department of Earth Sciences, University of Ottawa, 140 Louis Pasteur, Ottawa, Ontario K1N 6N5 Canada.

Chapter 3 is written as a manuscript entitled "***Physical Volcanology and Economic Potential of Komatiite-Associated Ni-Cu-(PGE) Deposits, Bannockburn Township Area***" (published in *Summary of Field Work and Other Activities 2005*: OFR 6172). It summarizes the physical volcanology and the potential for komatiite-associated Ni-Cu-(PGE) mineralization in the Bannockburn area within the southern part of the western Abitibi greenstone belt, and provides a brief description of an unusual occurrence where the Fe-Ni-Cu sulfide ore is a major component of the host unit. Minor modifications were made from the published version.

The co-authors that have collaborated to this publication are: *Préfontaine, S.* and *Berger, B.R*, Precambrian Geosciences Section, Ontario Geological Survey, 933 Ramsey Lake Road, Sudbury, Ontario P3E 6B5 Canada.

Chapter 4 is written as a manuscript entitled "***Komatiitic Sills and Multi-Generational Peperite at Dundonald Beach, Abitibi Greenstone Belt, Ontario: Volcanic Architecture and Nickel Sulfide Distribution***" (published in Economic Geology, volume 103, 2008). It summarizes the subvolcanic and volcanic architecture of a komatiite-dominated volcano-sedimentary sequence in Dundonald Township, and provides new insights on the influence of the near-surface rocks in the construction of the volcanic edifice and where the nickel sulfide mineralization occurred within this edifice.

The co-authors that have collaborated to this publication are: *Lesher, C.M.* and *Gibson, H.L.*, Mineral Exploration Research Centre, Department of Earth Sciences, Laurentian University, 933 Ramsey Lake Road, Sudbury, Ontario P3E 6B5 Canada; *Davis, P.C.*, First Nickel Inc., Suite 206, 120 Front Street East, Toronto, Ontario M5A 4L9 Canada.; *Cas, R.A.F.*, and *Beresford, S.W.*, School of Geosciences, Monash University, Victoria 3800 Australia ; *Arndt, N.T.*, LGCA, Université Joseph-Fournier à Grenoble, 1381 Rue de la Piscine, 38401 St Martin d'Hères, France.

Chapter 5 is written as a manuscript entitled "***Endogenous Growth in Komatiite Lava Flows: Evidence from Spinifex-Textured Sills at Pyke Hill and Serpentine Mountain, Western Abitibi Greenstone Belt, Northeastern Ontario, Canada***" (accepted, pending revisions for publication in *Bulletin of Volcanology*). It summarizes new results acquired from detailed mapping and petrographic work done at two very well-preserved komatiite flows within the western Abtibi greenstone belt: Serpentine Mountain (McArthur Township) and Pyke Hill (Munro Township), and provides new insights on the significance of inter-formational spinifex-textured sills within the komatiite lava flow field. This work includes research done as part of a B.Sc thesis written by Préfontaine at University of Ottawa and supervised by Fowler and Houlé

The co-authors that have collaborated to this publication are: *Préfontaine, S.* and *Fowler, A.D.*, Ottawa-Carleton Geoscience Centre, Department of Earth Sciences, University of Ottawa, 140 Louis Pasteur, Ottawa, Ontario K1N 6N5 Canada; *Gibson, H.L.*, Mineral Exploration Research Centre, Department of Earth Sciences, Laurentian University, 933 Ramsey Lake Road, Sudbury, Ontario P3E 6B5 Canada.

Chapter 6 is written as a manuscript entitled "***Thermomechanical Erosion and Genesis of Komatiite-Associated Ni-Cu-(PGE) Mineralization at the Alexo Mine, Abitibi Greenstone Belt***" (to be submitted in spring 2008 for publication in *Economic Geology or Mineralium Deposita*). It summarizes new results acquired from detailed mapping, petrographic work, and geochemical analysis on hydraulically-cleaned glacially-polished exposures at the Alexo mine in Dundonald Township, provides unequivocal evidence for thermomechanical erosion of andesite by komatiite, and proposes that this mechanism was a key process in the genesis of the komatiite-associated Ni-Cu-(PGE) deposits in the area.

The co-authors that have collaborated to this publication are: *Lesher, C.M.*, Mineral Exploration Research Centre, Department of Earth Sciences, Laurentian University, 933 Ramsey Lake Road, Sudbury, Ontario P3E 6B5 Canada; *Davis, P.C.*, First Nickel Inc., Suite 206, 120 Front Street East, Toronto, Ontario M5A 4L9 Canada.

Chapter 7 summarizes the new insights on the physical volcanology and metallogenesis of komatiite from this study.

1.4 Statement of Original Contributions

The following points focus on the main original contributions presented in this study to our knowledge on the physical volcanology of komatiites in the western Abitibi greenstone belt.

1) This study demonstrates that there is a close association between intrusive and extrusive komatiites in the WAGB, identifies the critical role of the near-surface rocks in controlling extrusive and intrusive emplacement, and defines the potential influence of the volcanic-subvolcanic architecture on the localization of the komatiite-associated Ni-Cu-(PGE) mineralization;

2) This study identifies thin spinifex-textured sills that have intruded their own volcanic piles as evidence of endogenous growth (i.e., inflation) in a komatiite lava flow field;

3) This study presents one of the best examples of the interaction between a mineralized komatiite and its footwall rocks, providing unequivocal evidence for thermomechanical erosion of andesite by komatiite.

CHAPTER 2 - PHYSICAL VOLCANOLOGY OF KOMATIITES IN THE ABITIBI GREENSTONE BELT

2.1 Introduction

Komatiites are ultramafic volcanic rocks with greater than 18% MgO (Arndt and Nisbet, 1982). Since the recognition of komatiites as lavas by Viljoen and Viljoen (1969), it has been appreciated that komatiites must have had unusual physical properties, including very high liquidus temperatures (up to 1640°C), very low dynamic viscosities (down to 0.1 $Pa \cdot s^{-1}$), very high specific heats (up to 1760 $J \cdot kg^{-1} \cdot °C^{-1}$), and a very large range between the liquidus and solidus (up to 400°C), which permitted them to form very mobile flows with the potential to flow long distances and to crystallize large amounts of olivine before solidifying (see reviews by Nisbet, 1982; Huppert and Sparks, 1985; Lesher, 1989; Williams et al., 1998). Much work has subsequently been done on their physical properties, phase equilibria and crystallization, geochemistry, and textural variability. However, because there have been no historic komatiite eruptions and because the Archean and Proterozoic volcanic belts in which most komatiites are preserved are folded and faulted, interpretations of their volcanology have been limited to relatively small scales (e.g., Pyke et al., 1973; Arndt et al., 1979; Lesher et al., 1984; Hill et al., 1990; Cas et al., 1999). Because of variations in discharge rate, topography, temperature, composition, volatile content, and viscosity, not all facies will be present in the same area, which further hampers correlations between different areas within the same komatiite flow field. Models have been developed on the scale of entire volcanic successions based on observed stratigraphic relationships (Lesher, 1989) or on the scale of entire flow fields based on models developed for Hawaiian basalts (e.g., Hill et al., 1990; 1995). However, basalts had much lower eruption temperatures, much higher viscosities, much narrower crystallization intervals, and much lower heat contents, and those in Hawaii erupted subaerially onto greater slopes, so they are not good analogues for komatiites. Subaqueous flood basalts would be better analogues, at least for thicker, more channellized komatiite flows, but their volcanology is even less well constrained. Nevertheless, the determination of volcanic facies is particularly important as it will be shown that such information facilitates recognition of favourable volcanic sequences that may host magmatic nickel-copper-platinum group elements (PGE) sulphide mineralization (Lesher, 1989; Barnes et al., 1999).

This project is part of a PhD study based at Laurentian University and the University of Ottawa, under the supervision of Drs. C.M. Lesher and A.D. Fowler. The principal aims of the project are to establish variations in the volcanic facies of komatiites within the Abitibi greenstone belt (AGB), to test and refine current stratigraphic, tectonic, and metallogenic models for the AGB (Jackson and Fyon, 1991; Jackson et al., 1994; Heather, 1998; Ayer et al., 1997; 1999a; 1999b), and to help constrain the volcanic architecture of komatiite flow fields. The AGB was selected for study because of the excellent mineralogical and textural preservation of the rocks, the abundance of glacially polished outcrops, and the excellent geological, geochemical, and geochronological database. A better understanding of the volcanic architecture of komatiites will help constrain stratigraphic, tectonic, and metallogenic models throughout the AGB and may aid in the development of similar models in other greenstone belts. Three broad topics have been addressed thus far: 1) classification of komatiite lava flow facies; 2) determination of regional facies variations of komatiites in the AGB; and 3) determination of local facies variations of komatiites in the AGB. A komatiite lava flow classification has been developed to provide an internally consistent framework for the classification of komatiites in the AGB. Regional facies variations of komatiites in the AGB have been studied by compiling data from both the literature and from previous projects by Drs. Lesher and Fowler, supplemented by field work in critical areas. Local facies variations of komatiites have been studied by detailed mapping of key areas with unparalleled exposure. This multi-scale, integrated approach has been critical in constraining interpretations regarding komatiite facies, and aid ultimately interpretations of the volcanic architecture of komatiite flow fields.

2.2 Physical Volcanology

2.2.1. Komatiite Lava Flow Classification

Previous volcanological classifications of komatiites have included *textural facies* (e.g., Pyke et al., 1973; Donaldson, 1982), *morphological facies* (e.g., Arndt et al., 1979; Imreh, 1980), *flow facies*, and *volcanic facies* (e.g., Lesher et al., 1984; Lesher, 1989; Hill et al., 1995; Barnes et al., 1999). Because komatiites exhibit such a wide range of textural, morphological, flow, and volcanic facies, we have utilized a 3D matrix method to classify komatiite facies in which the order of classification is from small- to large-scale observations.

Komatiite *textural facies* occur on the scale of individual flow profiles and vary with lava composition, temperature, viscosity, flow rate, cooling, nucleation, and crystallization rates (e.g., Donaldson, 1982), forming an extremely wide range of textures including adcumulate, mesocumulate, orthocumulate, porphyritic, platy spinifex, acicular spinifex, aphyric, flow-aligned and autoclastic textures. Textural facies of komatiites are controlled primarily by the eruption rate, cooling rate, degree of olivine accumulation, degree of differentiation, degree of inflation, and timing of ponding.

Komatiite *morphological facies* occur on the scale of individual flow units and vary within and between flow fields depending on eruption rate and style, mode and environment of emplacement, lava viscosity, flow rate, and flow regime, resulting in channels, sheets, lobate sheets, flattened pillows, spherical pillows, autoclastic lavas, and pyroclastic units. Each morphological facies is distinguished by a width:height aspect ratio (Fig. 2.1). Sheet flows (high aspect ratio) are a common morphological facies in Archean komatiites. Pillowed flows (spherical or flattened with low aspect ratio) are less common in komatiites than in basalts, although lobate flows (intermediate aspect ratio) are common and perhaps broadly equivalent, reflecting the higher flow rates and lower viscosities of komatiites. Autoclastic rocks, formed by quench fragmentation at the contact of hot lava and cold water, occur along the upper margins of some subaqueous komatiite flows, but thick autoclastic flows are much rarer in komatiites than in basalts, also reflecting the higher flow rates and lower viscosity of komatiites. Pyroclastic komatiites are relatively rare in most areas, probably reflecting their low volatile contents (a consequence of high degrees of partial melting of depleted mantle with no evidence of any metasomatic component in most cases), and deeper water emplacement for most komatiites.

Komatiite *flow facies* include simple and compound flows and volcaniclastic deposits. Simple flows comprise single cooling units, defined by chilled margins in contact with substrate or aqueous environment, whereas compound flows comprise multiple cooling units, commonly resulting from "piling up" of individual flow units (e.g., Walker, 1972). An outstanding problem is whether the thin differentiated (spinifex- and cumulate-textured) lobate sheets that are common in many komatiite

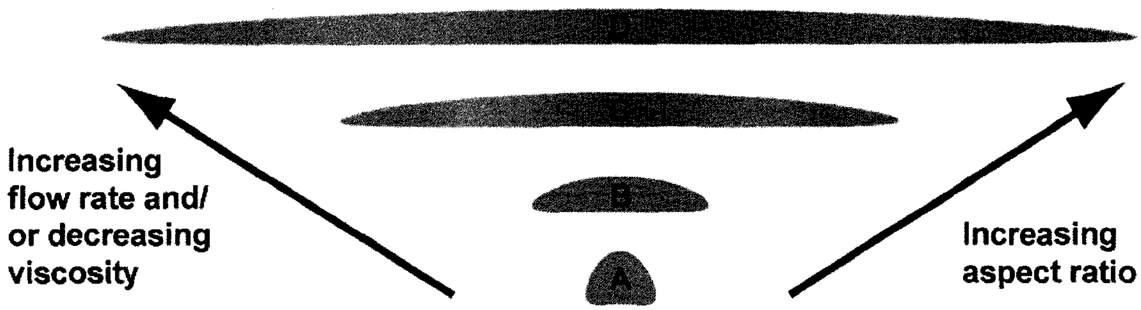

Figure 2.1 Classification scheme for morphological facies based on width:height (W:H) aspect ratio: A, spherical pillow (<2:1); B, flattened pillow (2:1–5:1); C, lobate sheet (5:1–20:1); and D, sheet (>20:1).

sequences are simple or compound flows. Volcaniclastic deposits may produced by quench fragmentation (autoclastic), explosive eruption (pyroclastic), or redeposition (epiclastic).

Komatiite *volcanic facies*, established by stratigraphic mapping in smaller scale areas (e.g., Lesher et al., 1984) and by inference on a larger scale (e.g., Lesher, 1989; Hill et al., 1990; 1995; Barnes et al., 1999), include vent pyroclastic facies, sheet flow facies, lava channel facies with or without overbank facies, lava pond facies, lobate sheet facies, and distal pyroclastic and/or epiclastic facies. The basal flows in many komatiite sequences are commonly thicker and are often separated by interflow sediments, whereas the flows in the upper parts are commonly thinner and devoid of sediments (Lesher et al., 1984) indicating that the initial eruptions were more voluminous and more episodic, that later eruptions were less voluminous and more continuous, and that the lava facies regressed over time (Lesher, 1989).

A classification scheme has been developed that focusses on the relationship between three major processes to generate a wide range of facies as function of olivine accumulation, differentiation, and aspect ratio provide the most systematic and useful basis for mapping and classifying komatiites (Fig. 2.2).

However, it is important to appreciate that the axes in this classification scheme indirectly include many other factors that are important to the physical volcanology of komatiitic rocks. For example, the olivine accumulation axis reflects the amount of magma that can be moved in the pathway (i.e., level of replenishment). The differentiation axis reflects the crystallization rate and timing of lava ponding during emplacement. The aspect ratio axis varies within and between flow fields depending on eruption rate and style, mode (laminar versus turbulent) and environment of emplacement, lava viscosity, and flow regime.

This 3D matrix komatiite lava flow classification scheme allows us to establish the relationship between textural and morphological facies that define flow facies and volcanic facies. Komatiite volcanic facies are assumed to vary on the scale of an entire flow field and on the scale of individual flow units, and to have included vent pyroclastic facies, sheet flow facies, lava channel facies with or without overbank facies, lava pond facies, lobate sheet facies, and distal pyroclastic and/or epiclastic facies. However, because no komatiite flow fields have been mapped and because the individual volcanic facies in the parts of flow fields that have been mapped may extend for distances of up to 100 km or more (Lesher et al., 1984; Hill et al., 1995), the proportions of these facies and their spatial configurations are unknown.

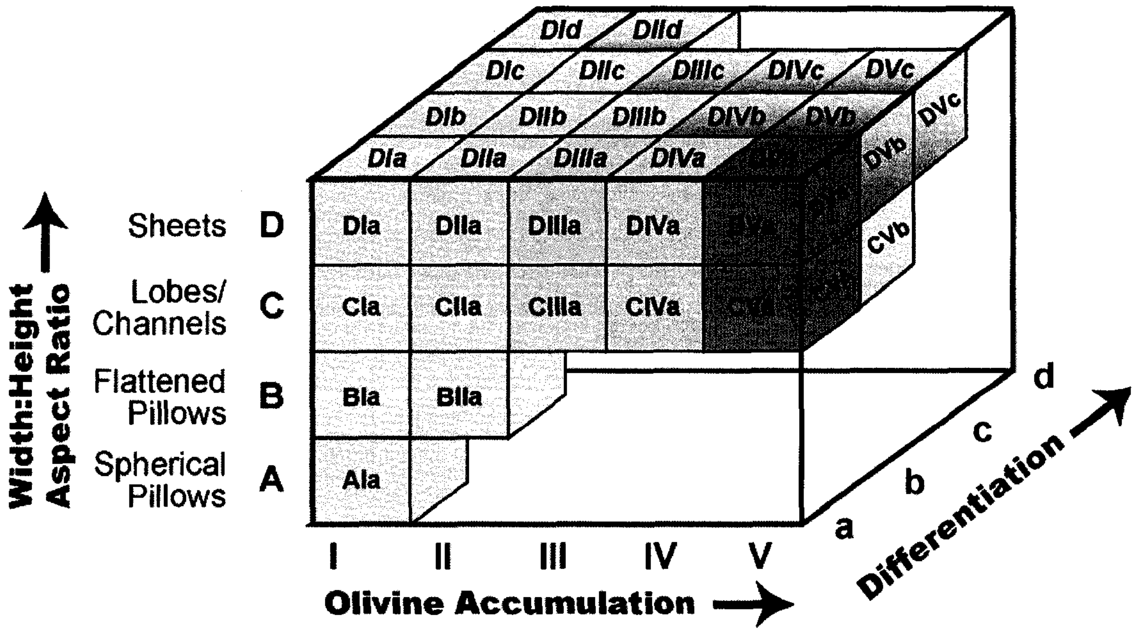

Figure 2.2 3D matrix facies classification scheme based on degree of olivine accumulation (horizontal axis), morphology (vertical axis), and degree of differentiation (depth axis). Examples of facies types in komatiites and komatiitic basalts include: undifferentiated, aphyric pillowed flows (**AIa**); undifferentiated, aphyric lobate flows (**CIa**); weakly differentiated, non-cumulate lobate flows (**CIb**); moderately differentiated, non-cumulate lobate flows (**CIc**); strongly differentiated, non-cumulate lobate flows (**CId**); moderately differentiated olivine-phyric lobate flows (**CIIc**); moderately differentiated olivine orthocumulate lava channels (**CIIIc**); moderately differentiated olivine mesocumulate lava channels (**CIVc**); moderately differentiated, olivine mesocumulate sheet flows (**DIVc**); and weakly differentiated, olivine adcumulate sheet flows (**DVb**).

2.3 Regional Facies Variations of Komatiites in the Abitibi Greenstone Belt

The Abitibi greenstone belt (AGB) is located in the Superior Province, the largest Archean craton in the world. It is characterized by a high ratio of supracrustal to intrusive rocks (Fig. 7.3) and generally low metamorphic grades: predominantly lower greenschist and local prehnite-pumpellyite facies with amphibolite facies occurring adjacent to large granitic plutons (Jolly, 1982). It also contains world-class orogenic lode gold deposits, world-class volcanic-associated copper-zinc (-lead) massive sulphide deposits, and minor magmatic nickel-copper (-PGE) and PGE (-copper) deposits (Jackson and Fyon, 1991). The AGB has been divided in 2 volcanic zones: the "Northern Volcanic Zone" (NVZ) and the "Southern Volcanic Zone" (SVZ) (Dimroth et al., 1982; Ludden et al., 1986; Chown et al., 1992). Felsic, intermediate, and mafic volcanic rocks occur in both zones, but picrites, komatiitic basalts, and komatiites occur predominantly in the SVZ.

Previous work demonstrated that the AGB is composed of a large number of lithologically and tectonically different assemblages (Jackson and Fyon, 1991). However, Ayer et al. (1997; 1999a; 1999b; 2002) have subdivided the AGB in Ontario into 9 stratigraphically distinct assemblages, 7 of which are dominantly volcanic and 2 of which are dominantly sedimentary. This subdivision has been modified recently by Thurston et al. (2008) where some volcanic assemblages were combined to redefine only 6 volcanic assemblages instead than 7 as previously defined by Ayer and co-workers (Fig. 2.3; Fig. 7.2). Only 4 of the assemblages contain ultramafic rocks: the Pacaud assemblage (PCA), the Stoughton–Roquemaure assemblage (SRA), the Kidd–Munro assemblage (KMA), and the Tisdale assemblage (TSA). The komatiitic rocks represent only a minor proportion of each assemblage (Sproule et al., 2002; see also Fig. 7.4): the PCA contains less than 1% (by volume) komatiitic rocks, which occur primarily in the upper part of the volcanic sequence associated with more abundant massive to pillowed tholeiitic basalts; the SRA assemblage contains approximately 2% komatiitic rocks, which generally occur near the base of the assemblage associated with more abundant mafic volcanic rocks; and the KMA and TSA contain approximately 5% komatiitic rocks, which occur near the base of volcanic sequences overlying intermediate to felsic volcanic rocks and underlying mafic volcanic rocks. A second sequence of komatiitic

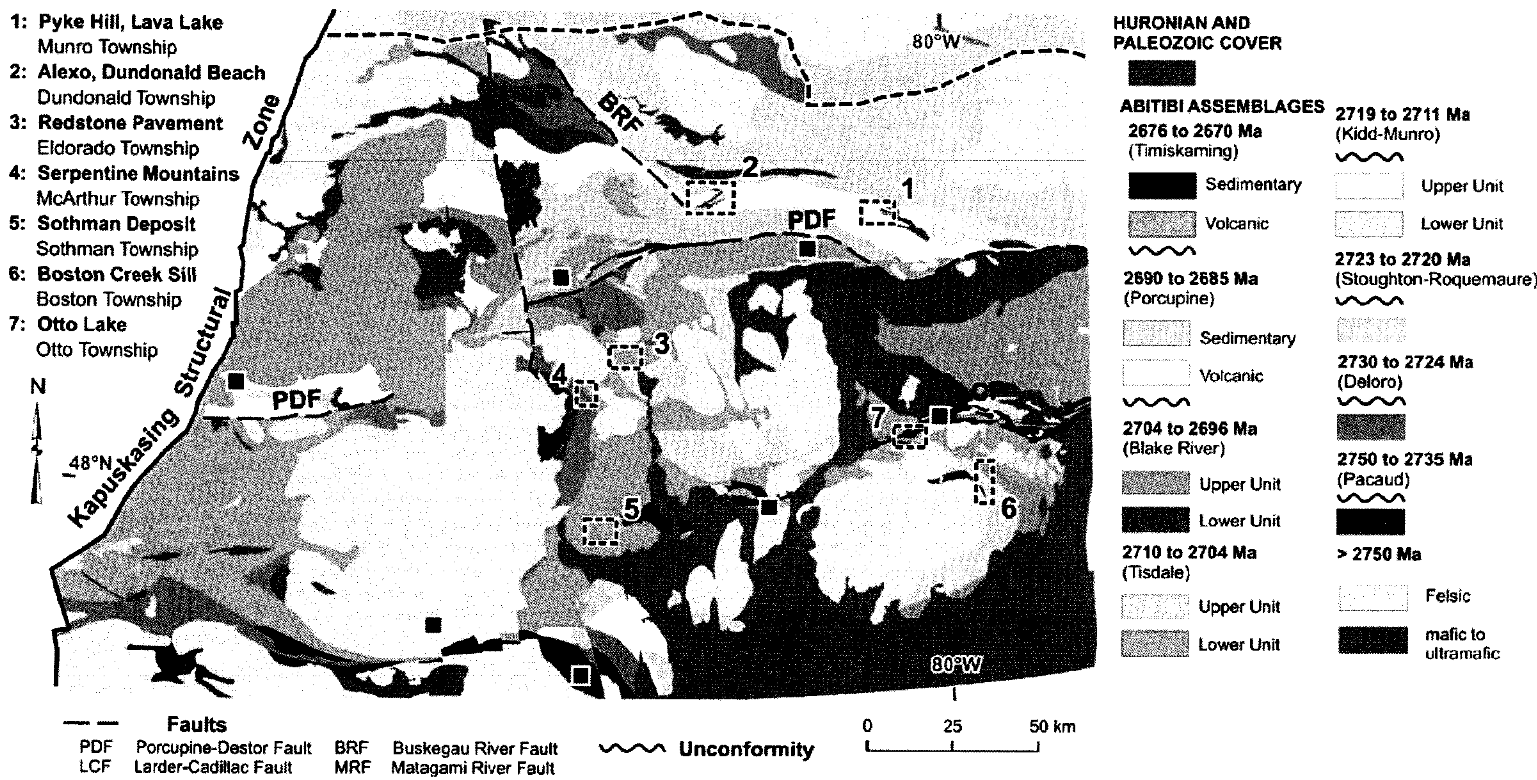

Figure 2.3 Simplified lithotectonic assemblages map showing the different location sites for this study in the Western Abitibi greenstone belt (adapted from Thurston et al., 2008).

rocks may be present near the top of the Tisdale assemblage, however, they could be a structural repetition of a lower sequence (J.A. Ayer, OGS, personal communication, 2001).

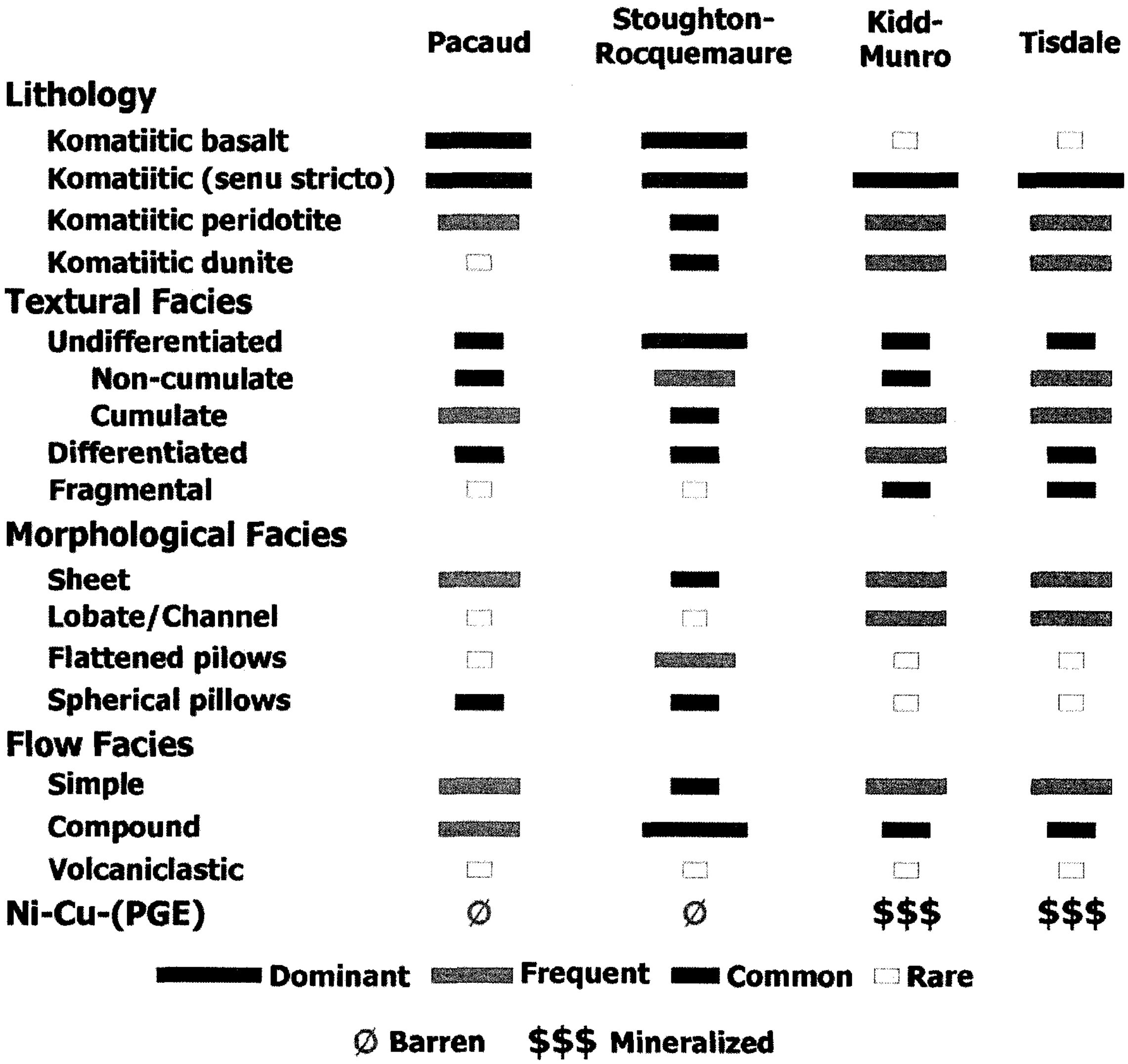

Figure 2.4 Summary of geochemical (or lithological) and textural facies for the komatiitic rocks in different assemblages of the Abitibi greenstone belt.

Interpreting volcanic environments is difficult as the environments may be complicated by primary factors (e.g., more than one eruptive centre in each assemblage, differences in eruption rate and style, mode and environment of emplacement) and secondary factors (e.g., metamorphism, alteration, structural complexity). However, there are clear lithological, geochemical, textural, and volcanological differences between the komatiitic rocks in the different assemblages of the AGB. Lithological, textural, and volcanological differences are summarized in Figure

2.4 (see also Table 7.2); geochemical differences are summarized in Sproule et al. (2002) (see also Table 7.1).

The PCA is dominated by simple flows with lesser compound flows. The simple flows include abundant differentiated flows (ortho- to mesocumulate lower zones and poorly developed spinifex-textured upper zones) and less abundant massive flows (olivine-phyric or ortho- to mesocumulate). The SRA is dominated by compound flows with lesser simple flows. Massive flows are frequently associated with compound flows, whereas differentiated flows only occur in specific parts of the SRA. The TSA and KMA contain more simple flows than compound flows. Both massive and differentiated flows are commonly present in these assemblages, however, the massive flows are characterized by abundant ortho- to adcumulate lithologies with fewer olivine-phyric lithologies and differentiated flows are characterized by thick orthocumulate lower zones with thin spinifex-textured upper zones.

Volcaniclastic komatiitic rocks occur in the KMA and TSA, and are typically autoclastic (i.e., flow top breccia hyaloclastite or reworked hyaloclastite rather than pyroclastic rock). Only the KMA and TSA contain a large proportion of komatiitic peridotite and komatiitic dunite in massive cumulate lithologies, which are interpreted to represent lava channels or the channel-flow facies of channellized sheet flows and high-level sills. These environments are important, as they are the favoured facies to host nickel-copper (-PGE) mineralization (Lesher, 1989). This is consistent with the presence of komatiite-hosted nickel-copper (-PGE) deposits only within the KMA (e.g., Marbridge, Alexo, and Dundonald) and TSA (e.g., Texmont, Redstone, Hart, and Langmuir deposits).

2.4 Local Facies Variations of Komatiites in the Abitibi Greenstone Belt

2.4.1. Kidd-Munro Trend

The Kidd-Munro trend is a belt of tholeiitic and komatiitic, felsic to ultramafic volcanic and associated intrusive rocks (representing the majority of the KMA) that trends east-northeast over a distance of 80 km on the north side of the Destor-Porcupine fault. The komatiites in the belt have been subdivided into three areas: 1) eastern Kidd-Munro area (Munro, McCool and Warden townships); 2) central Kidd-Munro area (Clergue, Dundonald and Stock townships), and 3) western Kidd-Munro area (southwestern Little, southwestern Tully, Prosser, Wark, Carnegie and Kidd townships). This is the same subdivision used in our complementary study on the geochemistry of komatiites in the AGB (Sproule et al., 2002). The remainder of this chapter describes the various facies observed in komatiites across the Western Abitibi greenstone belt. Further details are given on particular areas in subsequent chapters or references as noted at the start of most of the following sections.

2.4.1.1. Eastern Kidd-Munro Area

The eastern Kidd-Munro area includes Munro, McCool and Warden townships, but our field work thus far has focussed on the area of the Potter Mine in Munro Township, which contains abundant komatiitic, lesser mafic, and rare felsic volcanic rocks. Minor nickel-copper (-PGE) mineralization occurs at the Mickel showing in Dee's Flow in the southern part of Munro Township (Davis, 1997; Davis and Shore, 1999; Péloquin et al., 2005) and significant volcanic-associated massive copper-zinc(-lead) mineralization occurs at the Potter and Potter–Doal mines in the north-central part of Munro Township. The Potter Mine area is bordered by the McCool Hill syncline to the north, the Centre Hill fault to the south, and the mafic-ultramafic Centre Hill complex to the east. The Potter Mine volcanic succession may be subdivided into 3 lithostratigraphic sequences including 1) a lower komatiitic sequence; 2) a middle tholeiitic basalt hyaloclastite sequence with co-magmatic peperitic basalt sills, argillaceous sediments, and komatiites; and 3) an upper komatiitic sequence (Gamble and Gibson, 2000). "Lava lake" (Arndt, 1986) and Pyke Hill (Pyke et al., 1973) occur in the upper komatiitic sequence. The metamorphic grade in Munro Township is very low (prehnite-pumpellyite to lower greenschist facies) with excellent preservation of original igneous textures and geological relationships.

Pyke Hill (Munro Township)

Pyke Hill (e.g., Pyke et al., 1973; Péloquin et al., 2005; Houlé et al., 2006a) is located in the northeastern part of Munro Township, approximately 1 km ESE of the Potter Mine, and represents one of the best preserved and best exposed sequences of thin differentiated (spinifex-textured) and massive komatiite flows in the world. It is being studied to determine whether it represents a series of simple flows or a number of compound flows. At least 60 flows have been identified over an exposure width of approximately 125 m (Pyke et al., 1973). Individual flows range in thickness from 0.5 to 15 m, averaging approximately 3 m (Pyke et al., 1973). The relative proportions of spinifex-textured "A" zones and cumulate-textured "B" zones vary within individual flows, owing to irregularities along the contact between the zones in response to different rates of cooling. The ratio averages approximately 2:1 at both Pyke Hill (Pyke et al., 1973) and Spinifex Ridge in Quebec (Mueller et al., 1999), confirming that these areas contain primarily non-cumulate rather than cumulate flows. However, preliminary data indicate that the proportion of A:B zones decreases with increasing thickness, consistent with increases in flow thickness increasing with the amount of olivine accumulation, a trend also observed in Western Australia (Lesher et al., 1984; Lesher, 1989). The southern (stratigraphically lower) part of Pyke Hill is dominated by thin and thick differentiated non-cumulate flows, the central part by thin undifferentiated non-cumulate flows, and the northern (stratigraphically upper) part by thin differentiated non-cumulate flows, indicating that the eruption rates waned and waxed through the sequence. However, well-differentiated flows are interlayered within sequences dominated by poorly differentiated flows, indicating that the timing of ponding varied on a flow-by-flow basis. Poorly differentiated, non-cumulate flows, especially those with lobate sheet and flattened-pillow forms (rather than sheet flows) are spinifex textured along their margins and along fractures, indicating rapid crystallization due to extensive hydrothermal cooling and thermally constrained crystallization (Shore and Fowler, 1999). Flattened pillows contain shelves that were interpreted by Shore (1996) as molten lava breakouts. However, the thicker parts of some lobate flows exhibit incomplete secondary selvages inside the major external selvages, possibly indicating growth occurred by progressive inflation.

Lava Lake (Munro Township)

"Lava lake" (Arndt, 1986; Péloquin et al., 2005; Houlé et al., 2006a) is located in the north-central part of Munro Township, immediately west of the Centre Hill complex and approximately 1 km west of Pyke Hill. It is also very well exposed and is being studied as an example of a possible komatiite lava lake. The area is dominated by massive to weakly layered, medium-grained olivine adcumulate and was interpreted by Arndt (1986) to be an approximately 120 m thick lava lake that youngs toward the north. However, recent work by the Hunter Dickenson Group, based on logging and interpretation of new diamond drill cores, suggests that the Centre Hill complex and the komatiitic horizon have both been folded by regional deformation into a west-closing anticline. Our geological mapping and drill core logging, using chilled margin polarities, asymmetric differentiation within flow units, and vesicle orientations, suggest that the "Lava lake" is stratigraphically equivalent to the rocks exposed at

Pyke Hill, but that it lies on the southern limb of the anticline and therefore faces south rather than north, and that it may represent a thick series of thick sheet flows or a thin series of thick sheet flows overlain by a thin lava lake additional. Field work is in progress to further test these interpretations.

2.4.1.2. Central Kidd-Munro Area

The central Kidd–Munro area includes Clergue, Dundonald and Stock townships, but our work has been focussed on newly stripped exposures around the Alexo Mine (along the boundary of Dundonald and Clergue townships) and Dundonald Beach (southeastern corner of Dundonald Township). The geology of Dundonald Township has been summarized by Davis (1997, and references therein) and is characterized by a major westward-plunging "Z" fold. The rocks in the sequence include abundant intermediate to mafic volcanic rocks, lesser felsic volcanic rocks, a mafic-ultramafic sill (Dundonald Sill), and a regionally extensive komatiitic unit. The komatiitic horizon hosts several nickel-copper (-PGE) deposits, including the Alexo Mine and Kelex zone, Dundeal zone, Dundonald Beach, and Dundonald South.

Alexo Mine (Dundonald Township)

The Alexo Mine (Houlé et al., 2008b; see also Chapter 6) area is located on the northeast-dipping central limb of the Dundonald fold structure and is being studied because it could represent one of the best preserved and best exposed mineralized cumulate komatiite lava channels in the world. The stratigraphic succession in this area comprises four sequences of komatiitic rocks intercalated with intermediate volcanic rocks (Davis, 1999). The younging indicators in the komatiitic units (e.g., flow-top breccias, asymmetrically zoned spinifex textures, transgressive lower margins of lava channels, disseminated and/or net-textured and/or massive ore segregation profiles) and the andesites (e.g., flow-top breccias, pillows) consistently face northward to eastward, and, because the compositions of the andesites change systematically from more tholeiitic in the south to more calc-alkaline in the north, the sequence is interpreted to represent an intact sequence of intercalated komatiites and andesites (P.C. Davis, MPH Consulting Ltd., personal communication, 2001). This means that the Alexo Mine, the Alexo "small pit", and the Kelex zone all occur within distinct komatiite units (Davis, 1999).

The komatiite–andesite contact east and west of the Alexo Mine horizon was stripped by Hucamp Mines Ltd. in 2001, exposing the basal contact of the mineralized lava channel. Because the metamorphic grade in the Alexo area is only lower greenschist facies, these areas provide almost complete exposure of glacially polished outcrops of the well-preserved contact between footwall pillowed, massive, and hyaloclastic andesite and the overlying cumulate komatiite unit. The contact is generally very sharp between the two lithologies and outlines a pronounced topographic depression that clearly transgresses massive andesite and associated hyaloclastite without any evidence for a regolith. The presence of andesitic fragments in the lower part of the komatiite, komatiitic dikes projecting downwards into pillowed andesite, and pervasive contact metamorphic alteration adjacent to the contact indicate that, similar to many other areas where nickel-copper (-PGE) sulphides have formed, lava emplacement was channellized and most likely turbulent (Huppert and Sparks, 1985; Williams et al., 1998), not passive and laminar (cf. Beresford and Cas, 2001), and most likely involved thermomechanical erosion (see Lesher et al., 1984; Lesher, 1989). Further field work is in progress to completely characterize this exceptionally well-preserved and well-exposed channellized komatiite flow.

Dundonald Beach (Dundonald Township)

The Dundonald Beach (Houlé et al., 2008b; see also Chapter 4) is an area of stripped outcrop on the southeast-dipping, southern limb of the Dundonald fold structure. It is being studied because it contains excellent exposures of thin komatiitic basalt flows intruded into graphitic sediments (Davis, 1997; 1999) and provides unique insights into the behaviour of invasive komatiite flows that have thus far only been inferred from drill core observations (Gillies, 1993; Beresford and Cas, 2001). The area exposes a sequence of thin komatiitic basalt flows, intercalated graphitic argillaceous metasedimentary rocks and associated peperites, thick olivine meso- to adcumulate komatiite flows, and thick differentiated olivine cumulate/pyroxene spinifex flows overlying a felsic heterolithic breccia (Davis, 1997; 1999). The footwall felsic volcanic rocks contain thin (~10 cm) dikes of spinifex-textured komatiite (Davis, 1997). The main exposure was cleared by Falconbridge Ltd. in 1989 and adjacent exposures to the east and south were cleared by Hucamp Mines Ltd. in 2000.

The lower part of the komatiitic sequence is composed of pyroxene spinifex-textured komatiitic basalt flows and very fine-grained, massive komatiitic basalt flows and sills. There are 2 types of intrusive units: 1) relatively thick (~4 m), fine- to medium-grained massive intrusions with thin (~2 to 3 cm), very fine-grained chilled margins; and 2) relatively thin (<50 cm), fine-grained intrusions with very thin (<1 cm), very fine-grained chill margins possessing both globular and irregular textures suggesting contamination by the country rocks. The second type has been injected into previous komatiitic basalt flows, producing thin *en échelon* sills, or into unconsolidated graphitic argillitic sediments, producing both *blocky and fluidal peperites* containing both clasts of sediment within komatiite and clasts of komatiite within sediment. Peperites with the clasts of komatiite surrounded by sediment occur on larger scales (metres) than the peperites with the clasts of sediments surrounded by komatiites (centimetres). Both textures generally occur close to each other: along the margins of the intrusions; or they form distinctive globular textures within the intrusions, where they form distinctive "egg-shell breccia" textures (Davis, 1997, 1999). Thus, this area provides considerable insights into the mechanisms of komatiite intrusion into unconsolidated sediments. Additional field work is currently underway in this area to characterize the nature of lava emplacement.

2.4.2. Shaw Dome

The Shaw Dome (Atkinson et al., 2005; Houlé et al., 2008a) area is located approximately 20 km southeast of Timmins and is composed primarily of volcanic rocks with minor felsic intrusive rocks (Pyke, 1978; 1982). Although the komatiites in this area are more deformed, more altered (local talc-carbonate alteration), and metamorphosed to lower greenschist facies (Larson, 1996), geological relationships and relict igneous textures are locally well preserved in stripped outcrops that expose transgressive contacts between thick, weakly differentiated cumulate flows.

The Shaw Dome is cored by calc-alkaline mafic and felsic volcanic rocks, intruded in the upper parts by differentiated mafic to ultramafic sills, and is overlain by tholeiitic basalts intercalated with komatiites, komatiitic basalts, and minor sulphide-facies iron formation. These komatiites are correlated with the Tisdale assemblage (Ayer et al. 1999b). They have been described by Larson (1996) and Baird (1999) and are the main hosts to the nickel-copper (-PGE) deposits in the area (e.g., Langmuir 1 and 2, McWatters, Hart, Redstone and Galata) (Coad, 1979; Green and Naldrett, 1981).

2.4.2.1. Redstone Pavement

One of the best exposures of the komatiites occurs in a stripped outcrop approximately 1 km south of the Redstone Mine site in the western part of Eldorado Township. Three flows are exposed in the outcrop, but only the middle flow has its lower and upper contacts exposed. All three flows have relatively thick (~20 m) lower cumulate "B" zones, which are locally intensely polysutured, but are composed mainly of texturally well-preserved meso- to orthocumulate komatiite containing serpentine pseudomorphs after medium-grained (1 to 2 mm) euhedral olivine. The two flows with exposed upper contacts have relatively thin (~4 m) upper "A" zones composed of very coarse-grained olivine crescumulate komatiite and coarse- to medium-grained random olivine spinifex-textured komatiite, but no fine-grained random spinifex-textured komatiite or flow-top breccia. Thus, these are cumulate flows, intermediate in terms of degree of olivine accumulation between thin non-cumulate Pyke Hill-type flows and the thick cumulate flows that host the majority of the nickel-copper (-PGE) mineralization in the Shaw Dome (e.g., Green and Naldrett, 1981) and elsewhere (Lesher, 1989). The contacts with overlying flows are very sharp and wavy (contact between Flow 1 and Flow 2) or very sharp and jigsaw-textured with small dikes of fine-grained komatiite injected into the overlying cumulate rock (contact between Flow 2 and Flow 3). The cumulate zones of the lower two flows contain small (average size 5 cm) subrounded pods of fine- to medium-grained olivine spinifex-textured rock with very sharp margins that may represent pockets of trapped liquid or xenoliths. They are common in the lower parts of the cumulate zones and are absent in the upper parts of the cumulate zones, supporting the latter interpretation and suggesting that they have been derived by mechanical erosion of the upper spinifex-textured parts of the underlying flows. The jigsaw-shaped, locally intrusive contact between flows 2 and 3 is interpreted to represent compaction of the underlying partially molten spinifex-textured zone by the overlying cumulate zone after mechanical erosion of the upper spinifex-textured parts of the underlying flows. This explains the presence of spinifex xenoliths. Thus, this outcrop provides considerable insights into the processes of thermomechanical erosion in komatiites, especially in flows that are intermediate in terms of thickness and degree of olivine accumulation between classic Pyke Hill-type (thin, non-cumulate) flows and Kambalda-type (thick, cumulate) flows. Petrographic work is being be done to further clarify the nature of the contacts in this area.

2.4.3. Bartlett Dome

The Bartlett Dome is located approximately 40 km south of Timmins and is interpreted to be stratigraphically equivalent to and contiguous with the Shaw Dome to the north (Jensen, 1985). It is composed of supracrustal metavolcanic and metasedimentary rocks intruded by very large batholiths of felsic intrusive rocks (e.g., Adams Pluton, Geikie Pluton, and the Peterlong Lake Complex). The volcanic sequence is composed of a lower sequence of intermediate to mafic volcanic rocks, a central sequence of komatiitic rocks that is laterally most extensive and best exposed in McArthur and Geikie townships, and an upper sequence of mafic volcanic rocks (Houlé et al., 2008a). Some of the best exposures occur in the Serpentine Mountain area, which is probably the stratigraphic equivalent of the komatiites at the Texmont Mine, which was exploited in the 1970s (e.g., Atkinson, 1999). The metamorphic grade in the Bartlett Dome is relatively low (mainly greenschist facies) with locally good preservation of original igneous textures and geological relationships, but the rocks are locally sheared and altered to talc-carbonate assemblages.

2.4.3.1. Serpentine Mountain

The komatiitic rocks at Serpentine Mountain (Houlé et al., 2008a; in press; see also Chapter 5) are located between the gravel road and the power line near the Mountjoy River in central McArthur Township. An outcrop close to the road has been described by Atkinson (1999) and is characterized by abundant spinifex-textured komatiite dikes within a sequence composed primarily of massive komatiites and one well-differentiated flow (including a well-defined B1 horizon). An outcrop under the power line is composed of fine-grained random olivine spinifex-textured komatiite containing small (20 to 30 cm) spherical to ellipsoidal fragments of medium-grained olivine cumulate rock with polysutured joints. There are 2 possible interpretations of this outcrop: 1) it may represent a spinifex-textured dike, similar to that exposed near the road, that has ripped up and partially assimilated cumulate komatiite wall rocks, or 2) it may represent a spinifex-textured flow exhibiting a relationship the reverse of that observed at the Redstone pavement (*see* "Shaw Dome"). However, the latter interpretation would require erosion of the entire spinifex-textured upper zone and part or the entire underlying cumulate zone of an unexposed underlying flow, entrainment of the cumulate rock fragments, and preservation in the upper spinifex-textured zone, which seems unlikely. More work is being done to aid in the interpretation of these exposures.

2.4.4. Halliday Dome

The Halliday Dome area is located approximately 80 km south of Timmins. It represents a major antiformal structure that trends eastward from Sothman Township across Halliday Township into Midlothian Township before disappearing beneath

Proterozoic sediments. The dome is cored by massive or pillowed intermediate volcanic and fragmental felsic volcanic rocks overlain by an extensive komatiitic horizon that can be traced over 40 km (Mullen, 1983). A few pods of ultramafic rock have been found in the core of the Halliday Dome, which may represent sills analogous to those in the Shaw Dome (*see* "Shaw Dome"). The metamorphic grade in the Halliday Dome is relatively low (mainly lower greenschist facies) with good preservation of original igneous textures and geological relationships.

2.4.4.1. Sothman Deposit (Sothman Township)

The Sothman nickel-copper (-PGE) deposit (Houlé et al., 2003; Atkinson et al., 2005) occurs along the south-southwestern-dipping, southwestern limb of the Halliday Dome, along the southern border Sothman Township, approximately 30 km east of Highway 144. It is hosted by a thick ultramafic body with a dunite core and peridotite margins that has been previously interpreted to be a sill intruded into intermediate volcanic rocks (e.g., Watkins, 1972), but is most likely a lava channel. An area along the basal contact of the body was stripped in 2000 by Hucamp Mines Ltd., providing near complete exposure of glacially polished outcrops of the embayed contact between footwall massive andesite and the overlying cumulate komatiite unit.

Field work done in this area during Summer 2001 did not reveal any evidence for an extrusive or intrusive origin for this ultramafic body, as the stripped area exposes only the basal part and not the upper part which might exhibit extrusive (e.g., flow-top breccia and upper spinifex-textured zone, conformable unmetamorphosed hanging-wall rocks) or intrusive (e.g., contact metamorphosed hanging-wall rocks, discordant contacts) features. Nevertheless, this environment clearly represents a channellized flow or channellized sill where magma flow was focussed within a topographic and/or thermomechanically produced embayment similar to those observed at Alexo. The underlying andesites exhibit patchy alteration and silica veining within 30 cm of the contact with overlying olivine pyroxenite, which are most pervasive at the base of the channel, suggesting that they represent a contact metamorphic feature. Thin (~10 to 50 cm) felsic dikes, which crosscut the komatiitic unit at a high angle and terminate at the basal contact, may represent partial melts of the andesite produced during thermal erosion of the environment (P.C. Davis, MPH Consulting Ltd., personal communication, 2001).

The mineralization occurs approximately 0.8 m above the basal contact within olivine pyroxenite and is composed of interlayered net-textured sulphides, disseminated sulphides, and barren olivine pyroxenite. However, disseminated mineralization always overlies net-textured mineralization, suggesting that the sequence youngs toward the south, consistent with the regional geology. The presence of barren komatiitic cumulate rocks within the main mineralized horizon and the apparent disruption of mineralized zones by olivine pyroxenites suggest that the environment was quite dynamic and was characterized by successive replenishment of magma and sulphides into the channel. Additional mapping is planned to constrain the origin and dynamics of this channellized environment.

2.4.5. Round Lake Dome

The Round Lake Dome area occurs approximately 15 km south of Kirkland Lake. It is defined by a large felsic intrusive body, the Round Lake batholith, which is bordered on the north, east, and south by mafic and ultramafic metavolcanic rocks of the Stoughton–Rocquemaure and Tisdale assemblages. The komatiitic rocks in the Stoughton–Rocquemaure assemblage are underlain and overlain by mafic and lesser intermediate volcanic rocks (Ayer and Trowell, 2000). The metavolcanic rocks are penetratively deformed along the margins of the batholith and within faults and shear zones, but are much less deformed away from the batholith (Jackson, 1994). The metamorphic grade in the komatiitic rocks around the Round Lake Dome is higher than in many other areas of the Abitibi greenstone belt (lower greenschist to locally lower amphibolite facies), but there is good preservation of original igneous textures and geological relationships in many areas.

2.4.5.1. Boston Creek Unit (Boston Township)

The Boston Creek unit (Houlé et al., 2004) and Misema komatiite occur on the eastern side of the Round Lake Dome and are the most extensive ultramafic units in the Abitibi Greenstone Belt. They define an arc-shaped pattern around the eastern margin of the Round Lake Dome, trending broadly north for more than 30 km. Thus far, only the Boston Creek unit has been studied as part of this project.

The Boston Creek unit is best known because it appears to be derived from a ferropicritic magma (Stone et al., 1987). It is approximately 100 m thick and exhibits the following internal differentiation, from base to top (Stone et al., 1987): a thin basal pyroxenite (~3.5 m), olivine cumulate (~30 m), pyroxene cumulate (~9 m), gabbro (~15 m), parallel-oriented acicular pyroxene spinifex (~30 m), randomly oriented pyroxene spinifex (~0.30 m), and a very thin fine-grained upper chill margin (~1 to 2 cm). The peridotite zone appears to be laterally restricted and is interpreted as channellized environment (Stone et al., 1996). Although no flow-top breccia has been identified, the Boston Creek unit has been interpreted to be extrusive on the basis of the presence of spinifex textures and the presence of vesicles in the upper chilled margin (Stone et al., 1995). However, spinifex textures only indicate rapid crystallization of an ultramafic liquid and also form in veins (see below) and vesicles only indicate exsolution of volatiles and also form in shallow intrusions (i.e. miarolitic cavities) . In order to further investigate the environment of emplacement of the Boston Creek unit, it has been studied in 2 sections near O'Donald Lake in the southeastern part of Boston Township, approximately 2 km from the old shaft of the mine. Particular attention was focussed on the upper contacts between the Boston Creek unit and overlying volcanic rocks.

Section A

The upper contact of the Boston Creek unit along section 2 of Stone et al. (1996) is sheared, but well exposed. The upper random pyroxene spinifex-textured zone grades very rapidly over a distance of 20 to 30 cm into a very thin fine-grained, locally vesicular random spinifex-textured upper margin. No aphanitic rocks or autoclastic breccias similar to those preserved at the tops of most komatiite flows are present. The rocks above the contact are sheared "intermediate" volcanic rocks containing discontinuous bands of quartz. The overlying "intermediate" volcanic rocks do not show any mesoscopic evidence of contact metamorphism, but they may represent contact metamorphosed mafic volcanic rocks, so work is in progress to constrain the nature of the rocks more distant from to the contact.

Section B

The upper contact of the Boston Creek unit along section 1 of Stone et al. (1996) is very similar to the that described above, except that the contact is not sheared and it shows evidence suggestive of an intrusive origin for the Boston Creek unit. The upper part of the Boston Creek unit in this area contains clasts of the overlying "intermediate" volcanic rocks and the overlying "intermediate" volcanic rocks contain several thin veins of more mafic material, similar in composition to the Boston Creek unit. The fragments are very fine grained and have altered rims. Petrographic and geochemical work is presently in progress to determine the composition of the fragments and the overlying rocks to help constrain the environment of emplacement of the Boston Creek unit, but, at this stage of interpretation, it seems possible that it is a sill, not a flow.

2.4.5.2. Otto Lake (Otto Township)

Several excellent outcrops of Tisdale Assemblage komatiites occur on the southwestern shore of Otto Lake, approximately 5 km southeast of Swastika. The outcrops studied expose 3 individual flows, which, from base to top, are a partially exposed differentiated flow (Unit 1), a completely exposed differentiated flow (Unit 2), and a partially exposed pillowed flow (Unit 3). They dip steeply southwest, consistent with the regional geology.

Unit 1

Only the upper, random pyroxene spinifex-textured zone of this flow is exposed in the northeastern part of the main outcrop, but there are smaller peridotite outcrops to the northeast, which are probably part of the same flow. The grain size of the pyroxene spinifex decreases to the northwest, suggesting that the flow youngs in that direction.

Unit 2

This flow is completely exposed in the northeastern part of the outcrop and the upper part is exposed in the southwestern part of the outcrop. It is approximately 12 m thick and is underlain by pyroxene spinifex-textured rocks of Unit 1 and overlain by pillowed komatiitic basalt of Unit 3. It is strongly differentiated, comprising, from base to top, thin lower chilled margin (<5 cm), pyroxene cumulate (~6 m), B1 zone (~15 to 20 cm), parallel pyroxene spinifex, random pyroxene spinifex, random olivine spinifex (total ~5 m), and flow-top breccia (~30 cm). The ratio of A:B zones is approximately 1:1, suggesting that this is a non-cumulate flow. The B zone is polysutured and the A zone contains multiple layers of parallel pyroxene spinifex and random pyroxene spinifex indicating that the cooling and/or nucleation and/or crystallization process in the flow was more complicated than in simple Pyke Hill-type flows.

Unit 3

This flow is composed of pillowed komatiitic basalt. The pillows are slightly elongate in a northeast to southwest orientation and appear to young toward the northwest. The pillows selvages are thin, and discontinuous, but are well defined in the upper part of the flow, but the rocks grade downwards into random olivine spinifex of Unit 2. This suggests that Units 2 and 3 possibly represent a transition between a simple to compound unit, reflecting a change in eruption rate, magma supply, etc. during emplacement. Petrographic and geochemical analysis work is in progress to test this hypothesis.

2.5 Future Work

Additional work is in progress in all of these areas. Some areas, including Redstone, Serpentine Mountain and Otto Lake, require follow-up petrographic and geochemical work. Other areas, including Pyke Hill, Lava lake, Alexo, Dundonald Beach and Boston Creek, require additional field work with follow-up petrographic and appropriate geochemical study. Additional areas will also be studied, including fragmental ultramafic deposits in Halliday Township. Sequence-scale stratigraphic studies are planned at Alexo Mine and in the Potter Mine area. These data will be used to provide constraints on the regional volcanological facies interpretation.

2.6 Acknowledgements

This project has been supported under an Ontario Geological Survey (OGS)–Mineral Exploration Research Centre (MERC) Collaborative Project Agreement, and funded under a Natural Sciences and Engineering Research Council of Canada (NSERC) operating grant to CML, and a "Fonds pour la Formation de Chercheurs et l'Aide à la Recherche" (FCAR, Quebec) fellowship to MH. We would like to thank Nick Arndt, John Ayer, and Phil Thurston for stimulating discussions on komatiite volcanology. We are very grateful to P.C. Davis and K. Montgomery from MPH Consulting Ltd. (Hucamp Mines Ltd.) for their advice and assistance with the field work and core examination at Alexo and Dundonald; E. Bettiol, E.W. Harrison, and D. Gamble for their advice and assistance with the field work and core examination in the Potter Mine area; D. Rogers and N. Dupras (Falconbridge Ltd., Timmins) for their assistance and permission to access internal company reports; B. Atkinson (OGS Resident Geologist Program, Timmins) for advice and assistance with field work in the Timmins area; and G. Grabowski (OGS Resident Geologist Program, Kirkland Lake) for advice and assistance with field work in the Kirkland Lake area.

CHAPTER 3 - PHYSICAL VOLCANOLOGY AND ECONOMIC POTENTIAL OF KOMATIITE-ASSOCIATED DEPOSITS, BANNOCKBURN TOWNSHIP AREA

3.1 Introduction

The Precambrian Geoscience Section of the Ontario Geological Survey (OGS) conducted bedrock mapping, at a scale of 1:20 000, in Cairo Township in 2002 (Berger and Leblanc, 2002) and in Montrose, Bannockburn and Powell townships in 2005 (Berger and Préfontaine, 2005; Préfontaine and Berger, 2005) as part of an ongoing project to update geological mapping in the Matachewan area. The goal of this contribution is to complement the Ontario Geological Survey bedrock mapping project in assessing the distribution, the physical volcanology and the economic potential of the komatiitic rocks in this area.

3.2 General Geology

The Bannockburn Township area is located west of theTown of Matachewan in the southern part of the western Abitibi greenstone belt. The map area is underlain by Neoarchean ultramafic, mafic, intermediate and felsic metavolcanic rocks and clastic metasedimentary rocks. Several intrusions cut through the supracrustal rocks. These are dominated by ultramafic to mafic rocks and alkalic rocks (syenite, feldspar porphyry) and mafic to intermediate rocks (gabbro, quartz diorite) (Figs. 3.1 and 3.2).

Clastic sedimentary rocks cover a large part of the map area and are correlated with the Proterozoic Gowganda Formation of the Cobalt Group of the Huronian Supergroup that unconformably overlies the Archean rocks. Diabase dikes observed in the mapped area are attributed to the Sudbury and Matachewan swarms.

Four major faults crosscut the Bannockburn area at high to moderate angles with the stratigraphy: the east-west trending Cadillac–Larder Lake deformation zone, the Galer Lake fault trending southwest to northeast, the Mistinikon Lake fault and the Montreal River faults that trend north - south. The reader is referred to Berger and

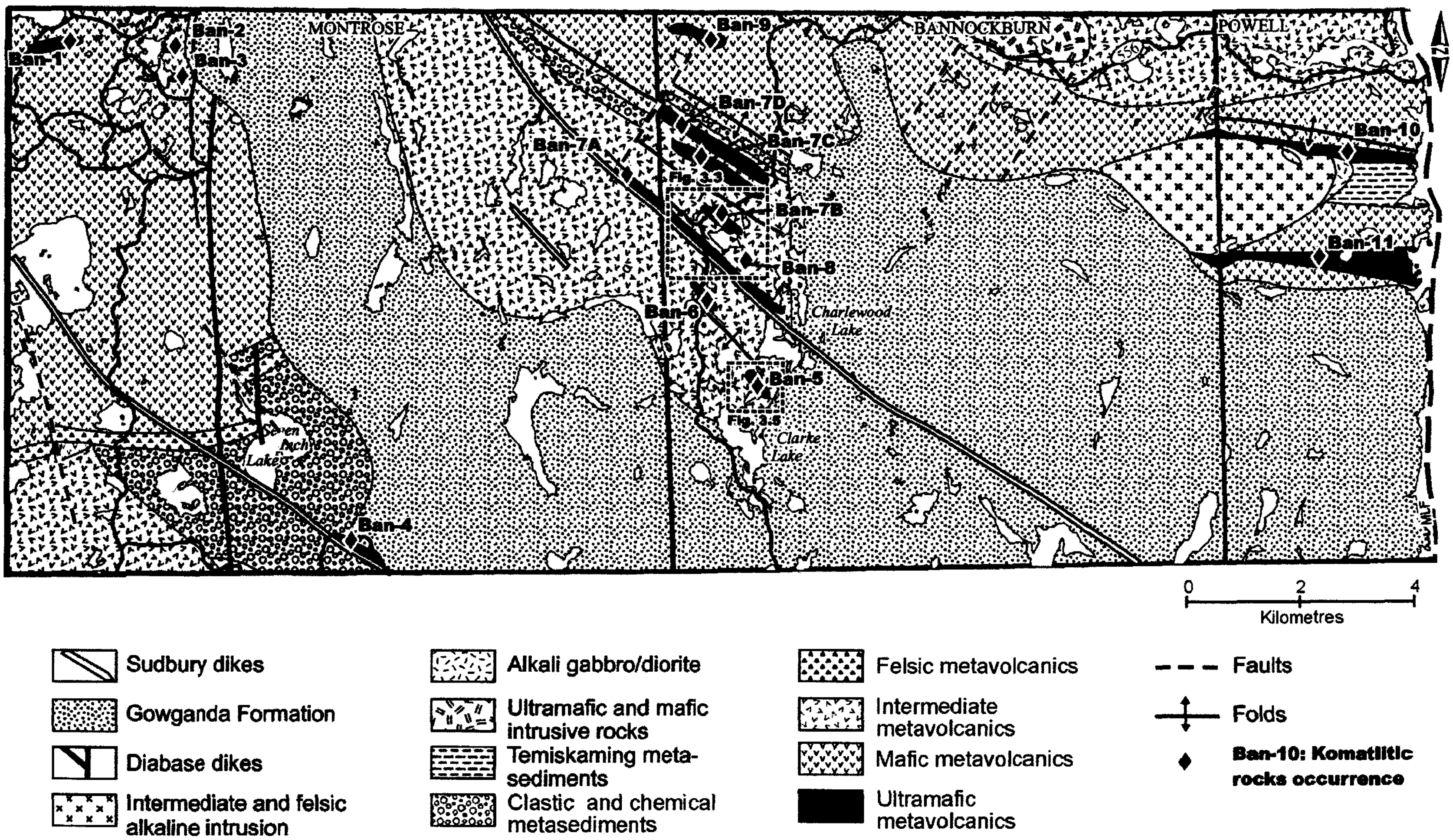

Figure. 3.1. General geology of Montrose, Bannockburn, and part of Powell townships (adapted from Berger and Préfontaine, 2005; and Préfontaine and Berger, 2005). The location of Fig. 3.3 and Fig. 3.5 are shown on the map.

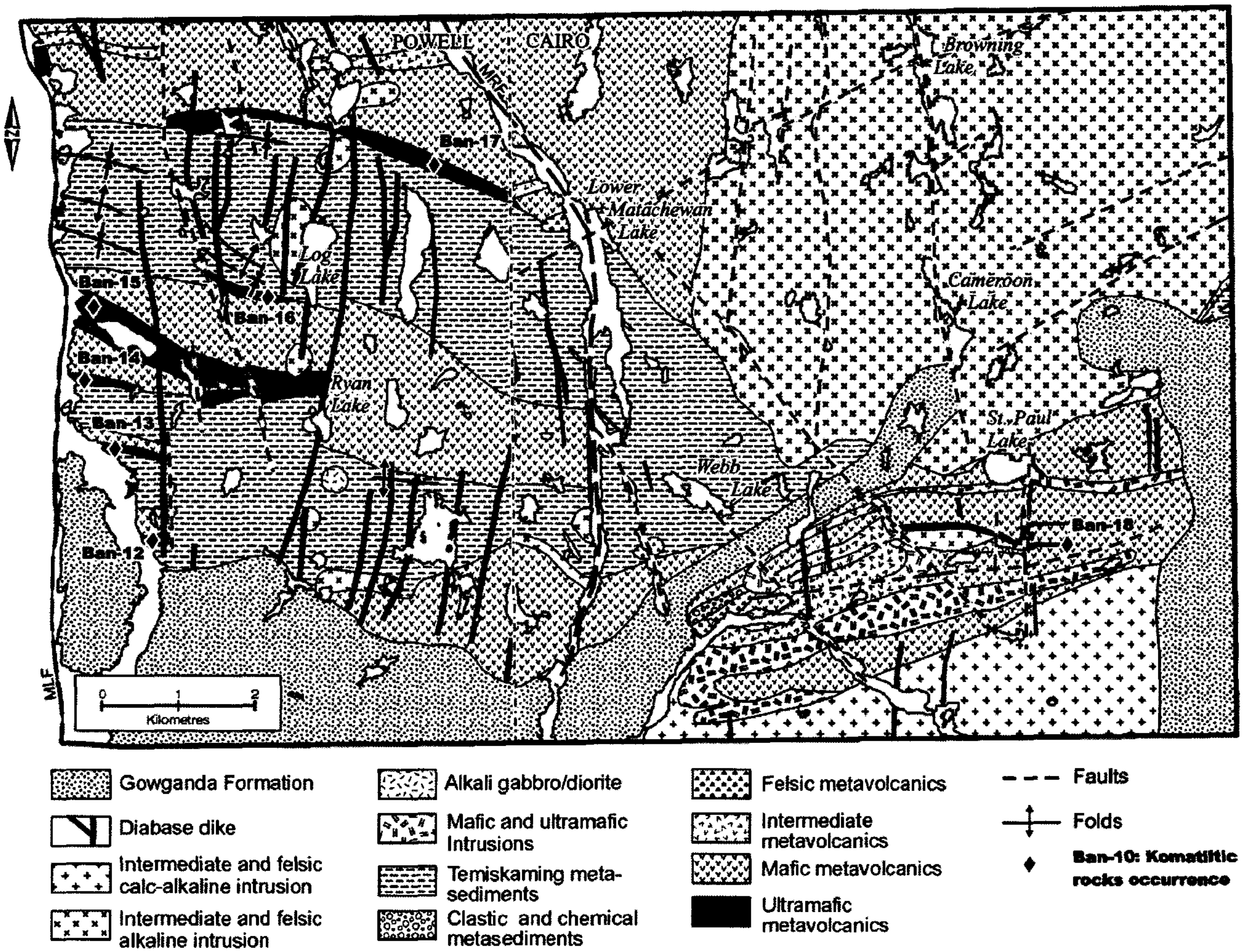

Figure 3.2. General geology of Cairo and part of Powell townships (adapted from Berger and Préfontaine, 2005; and Berger and Leblanc 2002).

Préfontaine (2005), Préfontaine and Berger (2005); and Berger and Leblanc (2002) and Leblanc and Berger (2003: Cairo Township) for a more detailed geological context.

3.3 Exploration History

Nickel-copper-(platinum group element) (PGE) discoveries in the Abitibi greenstone belt (AGB) were discovered sporadically over the years since the 20th century, as exploration waxed and waned (Ayer et al., 2005) and Ni-Cu-(PGE) mineralization continues to be discovered whenever there is sufficient exploration activity.

The Bannockburn area is not an exception; before 1995, minimal nickel exploration was conducted as the area was essentially recognized for its gold potential (e.g., Ashley gold mine: ~50 000 ounces Au). Although prior to 1995, ultramafic rocks in this area were targeted for their asbestos potential, for example, in the late 1930's by the Asbestos Company Limited, and during the late 1960's and early 1970's, by Canex Aerial Exploration Limited. Outokumpu Mines Ltd. undertook an intense exploration program (e.g., geophysical surveys, surface geological mapping, various geochemical surveys, and diamond drilling) between 1995 and 1999 of the area to assess the potential for komatiite-associated Ni-Cu-(PGE) deposits (*see* Harron, 2005 for more detailed descriptions). Much of the significant, known komatiite-associated Ni-Cu-(PGE) mineralization in this area was discovered by Outokumpu Mines Ltd. during this intense exploration (Thalweg: 1996; Bannockburn: 1998; Rahn Lake: 1998). Since acquiring the property in 2003, Mustang Minerals Corp. has completed a large exploration program (e.g., geophysical surveys, assays, and diamond drilling) that focussed on previous known occurrences and on new targets generated by geophysical surveys (Harron 2005). One of the most recent discoveries of komatiite-associated Ni-Cu-(PGE) mineralization (C-Zone/C-Offset: 2003) in the Abitibi greenstone belt was found during this exploration program.

3.4 Distribution and Volcanological Facies of Komatiitic Rocks

In the following section, the map area is divided into three blocks based on geological context (map patterns) and major breaks: the *Montrose–Bannockburn Block*, the *Powell Block*, and the *Cairo Block* (*see* Figure 3.1 and 3.2). The Montrose–Bannockburn Block corresponds to the area located west of the Mistinikon Lake fault.

The Powell Block corresponds to the area located between the Mistinikon Lake fault and the Montreal River fault. The Cairo Block corresponds to the area located east of the Montreal River fault. Komatiitic rocks occur in different proportions in each of these blocks. Table 3.1 summarizes the distribution and the komatiite volcanological facies in the map area.

3.4.1. Montrose-Bannockburn Block

Komatiitic rocks are relatively abundant in the Montrose–Bannockburn Block and compose up to 4% of the supracrustal rocks. All komatiitic rock outcrops in this block are distributed over eleven komatiite occurrences (from Ban-1 to Ban-11: *see* Figure 3.1). Only three komatiite occurrences (Ban-5, 7 and 8) possess enough exposure to evaluate their textural facies variations. These komatiite occurrences correspond, respectively, to the Thalweg Zone, the Bannockburn-Rahn Lake Zone, and the C-Zone. Overall, the komatiitic rocks in this sector exhibit several different textural facies such as massive (aphyric and cumulate), spinifex texture, flow breccia, and polysutured jointing. In the Montrose–Bannockburn Block, massive cumulate komatiite and lesser massive aphyric komatiite are the dominant textural facies that occur throughout the area.

3.4.1.1. Bannockburn-Rahn Lake-C-Zone Area

The Bannockburn–Rahn Lake–C-Zone komatiite occurrences (Ban-7 and Ban-8) represent most of the komatiite occurrences in the western half of Bannockburn Township. Figure 3.3 shows a simplified geological map of this area and represents a preliminary geological interpretation based on field data and diamond drill core data from Outokumpu Mines and Mustang Minerals. Recent work conducted by the OGS (Préfontaine and Berger, 2005; this contribution) has increased our knowledge of this area, however, our understanding is incomplete and many questions remain.

The Bannockburn Zone (Ban-7A) is composed of thick zones of komatiitic dunite and komatiitic peridotite with lesser and thinner komatiitic pyroxenite and komatiitic gabbroic zones. Minor spinifex zones also occur at the top of the unit. The Rahn Lake Zone (Ban-7B) is composed of thick intervals of komatiitic peridotite with lesser and thinner komatiitic pyroxenite and rare gabbroic zones. Common spinifex zones occur within and at the top of the units. The C-Zone (Ban-8) is composed of thin zones of

Table 3.1. Summary of the komatiitic rocks in the Bannockburn area.

ID	Area	Type	Rock Types	Width	Komatiite Facies					Sulphides	
				(m)	Textural	Lithofacies	Morphofacies	Units	Volcanic	Species	Showing
Ban-01	Mont-Ban Block	C	Kk, Kb	180	Ma[Cu], OSx, PSx	UN, DC	Shl?	M	DSF/S	N.O.	N.K.
Ban-02	Mont-Ban Block	C	Kr	130	Ma, Sx	UN, DN	Pw, Shl?	M	DSF/S	N.O.	N.K.
Ban-03	Mont-Ban Block	C	Kr	115	Ma[Cu], Sx	UC, DC	Shl?, Pw	M	DSF/S	Py	N.K.
Ban-04	Mont-Ban Block	O	Kk	200	Ma, Sx	DN	Shl	M	USF/S	N.O.	N.K
Ban-05	Mont-Ban Block	O	KPd, Kk	20-300	Ma[Cu], Sx	UC, DN	Sh	M	CSF/S	Po, Pn	Thalweg
Ban-06	Mont-Ban Block	O	KPd	80	Ma[Cu]	UC	Sh	S	USS	N.O.	N.K
Ban-07	Mont-Ban Block	O	KPd, KDn, Kk	50-250	Ma[Cu], Sx, Fbx	UC, DC, DN	Sh	M	CSF/S	Po, Pn,	Bannockburn, Rahn Lake
Ban-08	Mont-Ban Block	O	Kk, KPd	10	Ma[Cu], Fbx	UC	Sh	M	USD	Po, Pn,	C-Zone, C-Offset
Ban-09	Mont-Ban Block	O	Kk	180	Sx, Vr	DN	Shl	M	TDF	N.O.	N.K
Ban-10	Mont-Ban Block	O	Kk	50-230	Sx, Fbx, Pj, Ma	DN	Shl	M	TDF	N.O.	N.K
Ban-11	Powell Block	O	Kk	90-650	Ma,Pj, Fbx	UN	Shl	M	CSF	Py	?
Ban-12	Powell Block	G	Kr	130	-	-	-	-	-	-	N.K
Ban-13	Powell Block	O	Kk	50-90	Ma, Fbx	UN	Shl	M-S	TUF	N.O.	N.K
Ban-14	Powell Block	G	Kr	70-140	-	-	-	-	-	-	N.K
Ban-15	Powell Block	O	Kk, KPd	80-500	Ma[Cu], Ly, Fbx, Sx, Pj	UC, DN	Sh	M	CSF	N.O.	N.K
Ban-16	Powell Block	O	Kk	50-130	Fbx	UN	Shl	M-S	TUF	N.O.	N.K
Ban-17	Powell Block	O	Kk, KPd, KPx	50-200	Ma,Fbx	UN, DC	Shl	M-S	CSF	N.O.	N.K.
Ban-18	Cairo Block	O	Kb		Ma[Cu], PSx, Hy	UC, DN	Shl	M	TDF	Sulph	N.K.

ID: komatiitic occurrence; Mont-Ban Block: Montrose-Bannockburn Block; **Type:** data acquisition, O: Observed, C: Compiled, G: Geophysical; **Rock Type:** Kr: komatiitic rocks, Kb: komatiitic basalts, Kk: komatiites, KPd: komatiitic peridotites, KDn: komatiitic dunites; **Width:** Thickness of the komatiitic occurrence; **Textural -** Ma: Massive, Cu: Cumulate, Sx: Spinifex, OSx: Olivine spinifex, PSx: Pyroxene spinifex, Fbx; Flow/magmatic breccia, Vr: Variolitic, Pj: Polysutured jointing; **Lithofacies –** UN: Undifferentiated Non-cumulate, UC: : Undifferentiated Cumulate, DN: Differentiated Non-cumulate, DC: Differentiated Cumulate; **Morphofacies –** Shl: Sheet-like, Sh: Sheet, Pw: Pillowed; **Unit:** M: multiple and S: single cooling unit; **Volcanic –** DSF/S: Differentiated Sheet Flow/Sill, CSF/S: Channelized Sheet Flow/Sill, USF/S: Undifferentiated Sheet Flow/Sill, USD: Undifferentiated Sheet Dike, TDF: Thin Differentiated Flow, TUF: Thin Undifferentiated Flow; **Species -** Po: Pyrrhotite, Pn: Pentlandite, Py: Pyrite; **N.O.:** Not observed, **N.K.:** Not known.

komatiitic peridotite overlain by thin zones of komatiitic pyroxenite and komatiitic breccias. Minor pyroxene spinifex zones also occur locally towards the top of the unit.

The Rahn Lake sector is a key area to try to understand the komatiitic architecture of the map area (*see* Figure 3.3) because elsewhere the komatiite occurrences are not well exposed and/or are composed of undifferentiated homogeneous komatiitic units.

On the northwest side of Rahn Lake, the komatiitic unit dips moderately to the southwest at 65° and is overlain by dacite metavolcanic rocks. The komatiitic unit is composed of an autoclastic sorted breccia containing rounded to subangular fragments of komatiite within an altered komatiitic matrix. Further south along the shoreline of Rahn Lake, a diamond-drill hole intersected the same contact exhibiting well-developed spinifex zones overlain by dacitic metavolcanic rocks suggesting a southwest-facing direction.

On the south side of Rahn Lake, the komatiitic unit is moderately dipping to the north-northeast at 65° and is overlain by dacite metavolcanic rocks. Here, the komatiitic unit is composed of a sorted autoclastic breccia containing rounded to subangular fragments of cumulate komatiite within an altered komatiitic matrix (*see* Figure 3.3; Photo 3.4A). Some of the cumulate fragments contain disseminated sulfides. Locally below this contact zone, the komatiitic peridotite is highly serpentinized (*see* Figure 3.3; Photo 3.4B). Following the same contact further south, the upper part of the komatiite unit exhibits a spinifex breccia to coherent olivine spinifex zone that contains several rounded cumulate komatiite fragments (*see* Figure 3.3; Photo 3.4C). In this location, the komatiite unit is moderately to steeply dipping toward the northeast, overlain by the C-Zone footwall suggesting a facing direction to the northeast.

At the stripped area (C-Zone), the komatiitic unit trends 070° and dips steeply to the south-southeast. This unit appear to be discordant (*see* Figure 3.3) with the surrounding rocks (dacitic and komatiitic rocks) and is facing to the southeast based on the distribution of the mineralization and occasional spinifex-bearing rocks. Most of the upper third of the komatiitic unit is composed of poorly sorted (fragments size from 1 to 60 cm) komatiite breccia (autoclastic) containing rounded to subangular fragments of phyric to cumulate komatiite, aphyric komatiite, and spinifex-bearing komatiite within an altered komatiitic matrix (*see* Figure 3.3; Photo 3.4D). Furthermore, volcanic structures such as pillow-like structure, "volcanic" breccias along those structures, and scattered highly vesicular zones overlying the komatiite breccias in the central part of the C-Zone strongly suggest at least limited interaction with seawater on the seafloor or subseafloor. Difficulties in interpreting the geological context arise from factors such as the reversal of facing directions in the NW-Se trending unit (northwest and south side of Rahn Lake), the presence of a discordant komatiitic unit (C-Zone), and the general lack of bedding and facing directions within the surrounding dacitic volcanic rocks.

Several hypotheses may be considered to explain the actual discordant nature of the C-Zone in the geological complexity of the Rahn Lake area, including structural emplacement (i.e., fault-bounded emplacement), komatiite flow or sill lying within a southeast-closing fold hinge, or a primary emplacement that preserved or at least partially preserved angular relationships between the C-Zone and the Rahn Lake komatiite. Evidence of interaction between the komatiite and the dacitic footwall observed on the stripped area (*see* Figures 3.8A and 3.8B) combined with a northeast-facing direction for the Rahn Lake komatiite located south of the C-Zone disproves a structural emplacement hypothesis. The possibility that the C-Zone is lying within a southeast to east fold hinge is unlikely because it does not seem to fit the overall fold pattern in this area. Based mainly on its discordant nature, we suggest that the C-Zone might represent an inclined dike. However, the true nature of the C-Zone komatiitic unit may be best determined by careful examination of the diamond-drill core that intersected the footwall and hanging wall contact between the komatiitic units and the intermediate metavolcanic rocks. Alternatively, subsequent work conducted at the C-Zone by Taranovic et al. (2008) have suggested that the C-Zone Fe-Ni-Cu sulfide deposit appears to be hosted in the east by a thin lava pathway and in the west by breccias formed via multiple lateral breakouts where the sulfide ores may have been extruded laterally from the lava pathway underneath early phases of the komatiitic breccias.

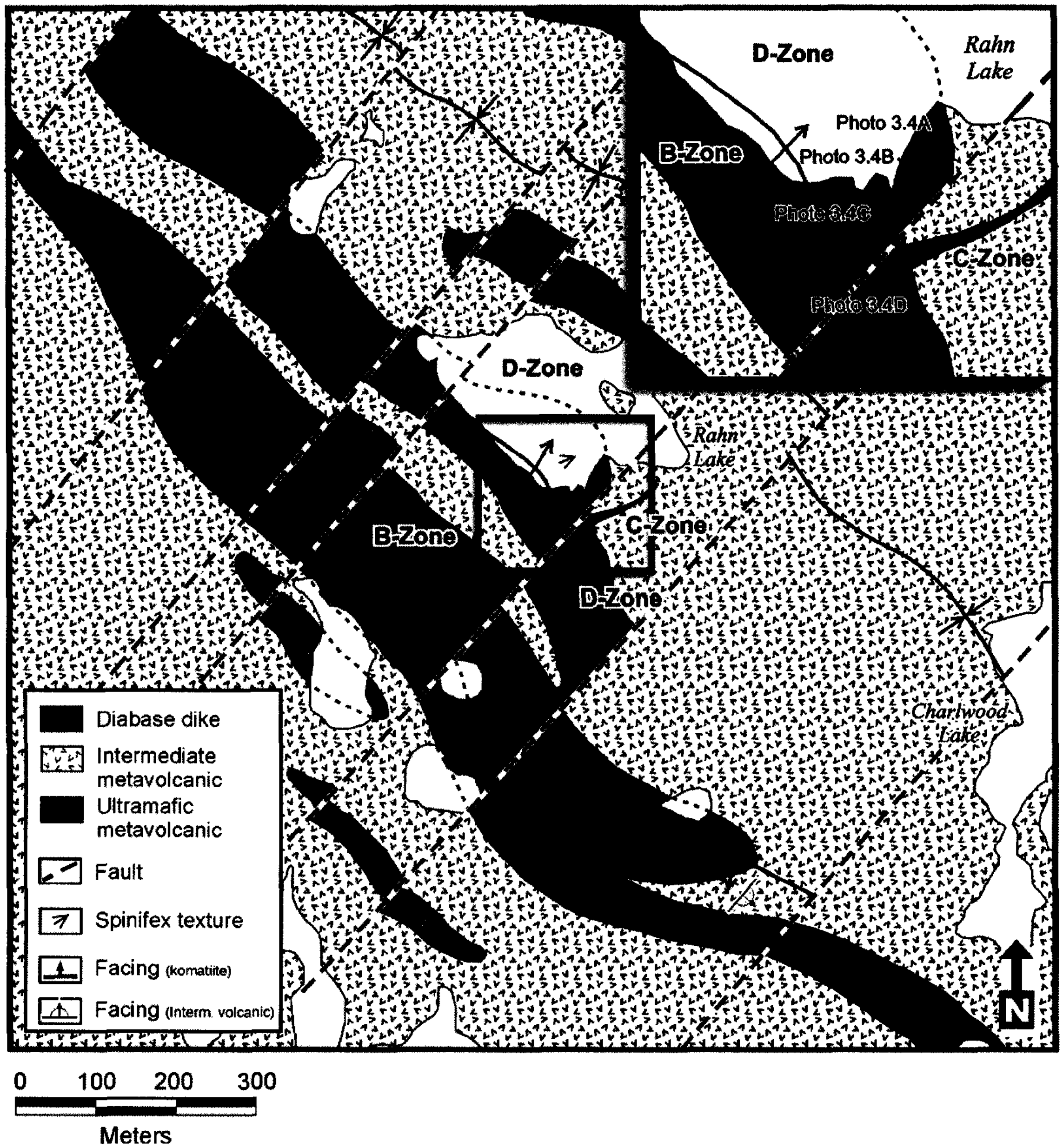

Figure 3.3. Sketch map of the surface geology in the area of the Bannockburn–Rahn Lake–C-Zone in Bannockburn Township. This preliminary interpretation of the geological context of this area is based essentially on surface geology with some insights from diamond drilling conducted by Outokumpu Mines Ltd. in the mid 1990s and, more recently, by Mustang Minerals. Location of this map is shown on Fig. 3.1.

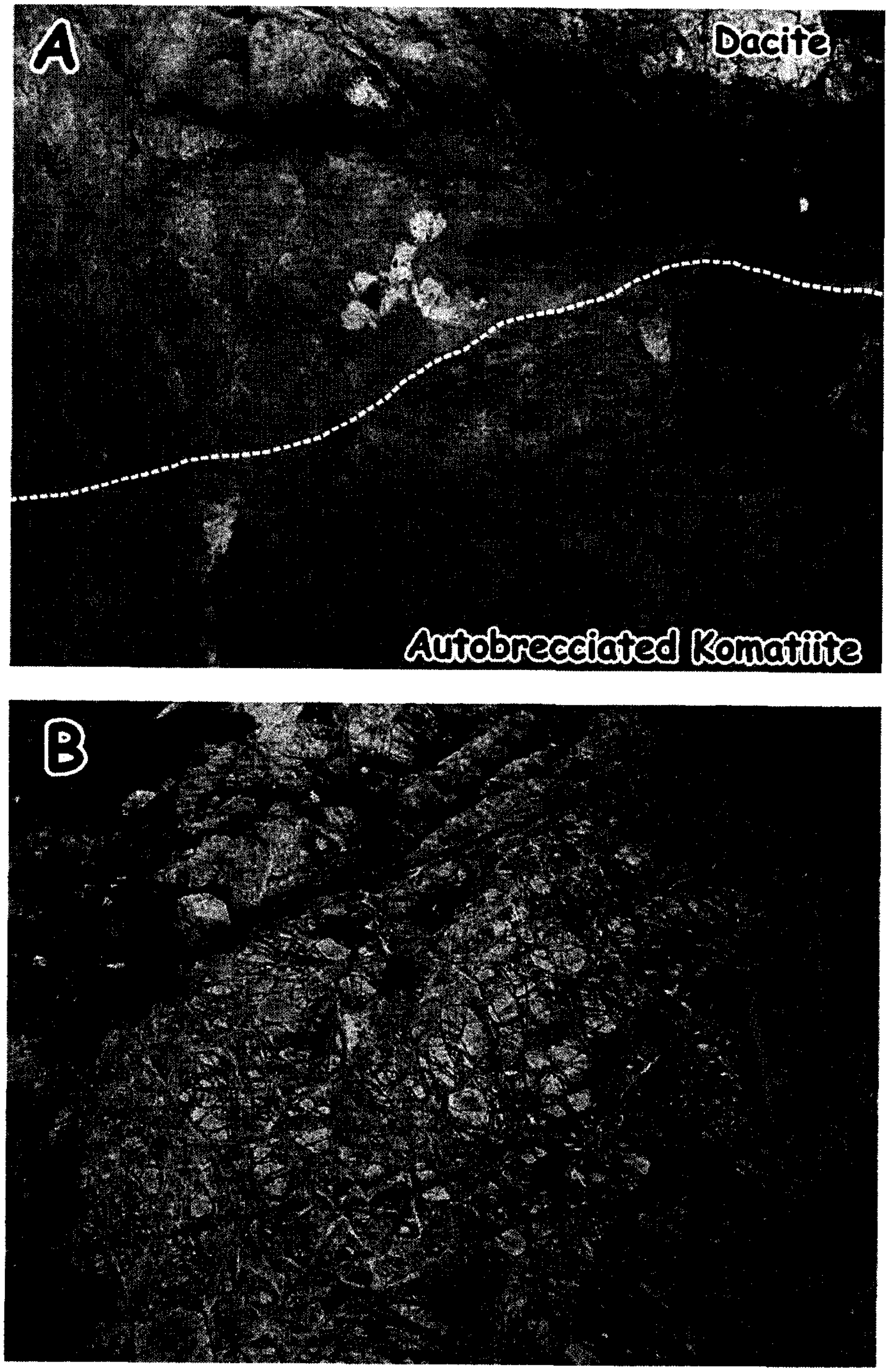

Figure 3.4. A) Contact between autobrecciated komatiitic peridotite of the Rahn Lake Zone and the dacite of the footwall of the C-Zone (UTM 507101E, 5313911N, NAD 83, Zone 17). B) Highly serpentinized komatiitic peridotite of the Rahn Lake Zone (UTM 507095E, 5313913N, NAD 83, Zone 17).

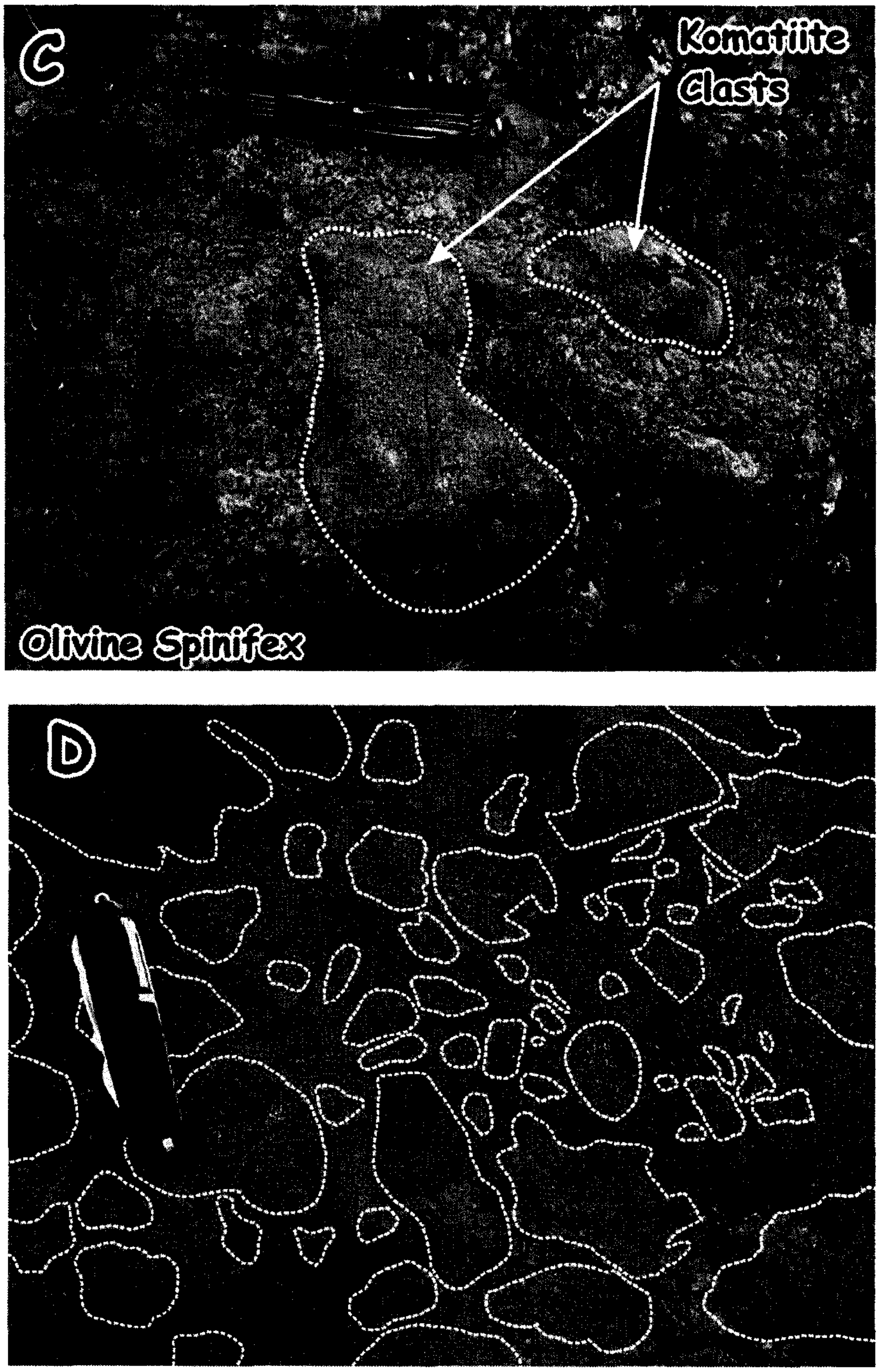

Figure 3.4. (Cont'd) C) Cumulate komatiite fragment within the spinifex-textured upper part of the Rahn Lake komatiitic peridotite. D) Autobrecciated komatiite upper zone of the C-Zone komatiitic peridotite from the western edge of the stripped area. Phyric to cumulate textures dominate within the fragments but some spinifex-bearing fragments are also present (UTM for photos C and D 507115E, 5313877N, NAD 83, Zone 17).

3.4.1.2. Thalweg Area

The Thalweg komatiite occurrence (Ban-5) is completely isolated from other komatiite occurrences in the western half of Bannockburn Township. Figure 3.5 shows a simplified geological interpretation of the Thalweg area based on field data and diamond-drill core data from Outokumpu Mines and Mustang Minerals. The Thalweg komatiite occurrence has a facing direction toward the northeast and contains at least four different komatiite units hosted in massive dacitic metavolcanic rocks. Limited iron formations are also present underlying the main komatiite unit. This sequence represents a typical channelized sheet flow or sill environment where the Thalweg sulfide mineralization occurs at the base of an embayment. The main komatiite unit is composed of thick olivine adcumulate to mesocumulate rocks, whereas the flanking facies north and south of the sulfide mineralization are thinner and more differentiated units containing spinifex-bearing komatiite. This unit has a strike length of over 1 km and varies in thickness from 100 to 150 m in the middle of the embayment to less than 30 m in the flanking area. The lateral extent of this occurrence is unknown because the southern margin is covered by the Gowganda Formation. The basal contact is characterized by an extensive and complex branching out of thin komatiitic units into the footwall. The stripped area has exposed some thin komatiitic units beneath the main komatiite unit that display complexity (Fig. 3.6). The upper part of this komatiitic sequence is characterized by numerous thin differentiated komatiitic units intercalated with dacitic flows. The geology is further complicated by a network of interpreted faults trending approximately 070° that disrupt and displace the komatiite units. The presence of some komatiitic units directly beneath some dacitic exposures, combined with contacts dipping to the northwest (*see* Figure 3.6), suggests that the komatiitic sequence is overturned and dips to the west. This speculation appears to be confirmed by the magnetic survey (P. Wood, Mustang Minerals Corp., personal communication, 2005).

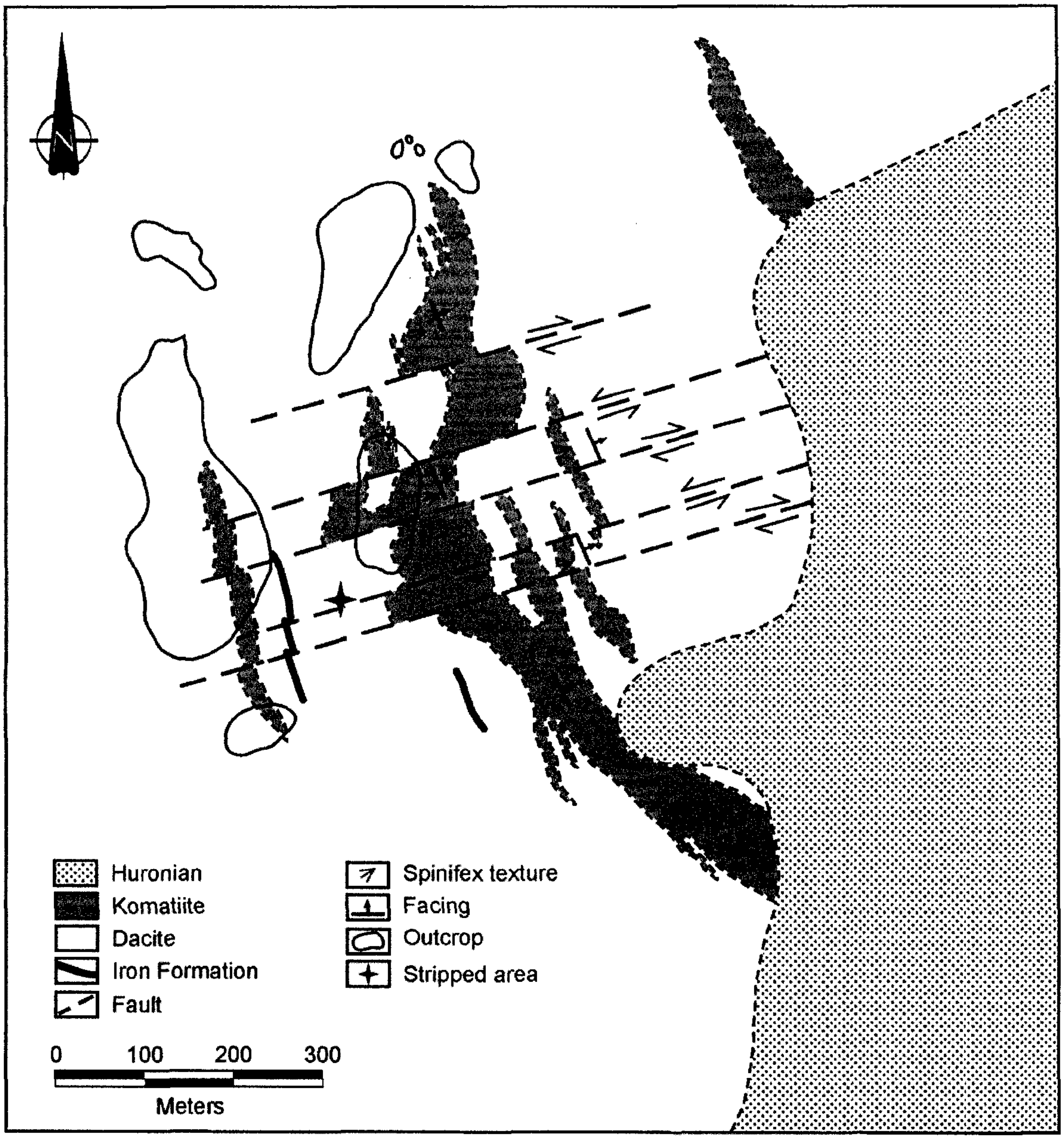

Figure 3.5. Simplified geological map of the Thalweg area based on projection to the surface of data from some of the diamond-drilling programs conducted by Outokumpu Mines and Mustang Minerals. Note that some of the komatiitic units projected to the surface are located directly underneath intermediate metavolcanic outcrops. This reconstruction is based on information extracted from the diamond-drill logs. The diamond-drill cores from Outokumpu Mines are no longer available. Location of this map is shown on Fig. 3.1.

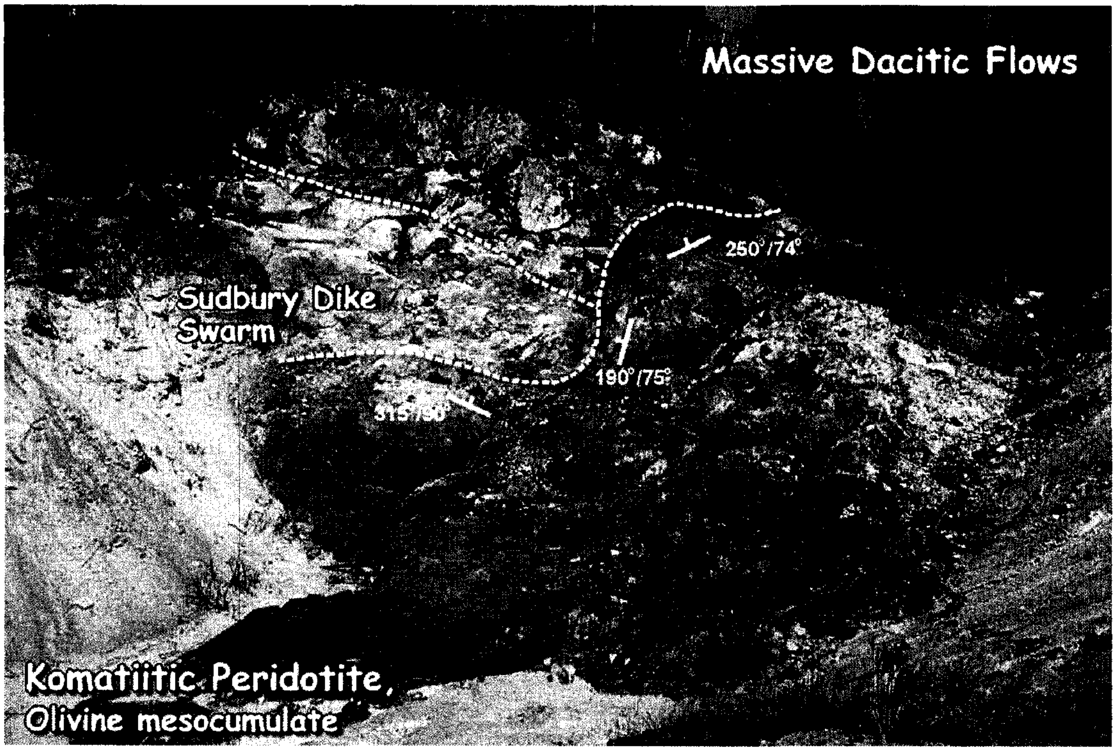

Figure 3.6. Eastern stripped area at Thalweg occurrence in Bannockburn Township showing the irregularity of the contact between the komatiitic peridotite and the massive dacitic flows. Note that the Sudbury dike terminates at the contact with the komatiitic unit (UTM 507472E, 5311752N, NAD 83, Zone 17).

3.4.2. Powell Block

Komatiitic rocks are relatively abundant in the Powell Block and comprise up to 5% of the supracrustal rocks. Most of the komatiitic rocks which outcrop in this block occur in the six labelled komatiite occurrences (from Ban-12 to Ban-17: *see* Figure 3.2). However, there are numerous other komatiitic outcrops that are not large enough to merit their own occurrence label at this scale. These units are intimately intercalated with mafic metavolcanic rocks in the central and southern parts of the Powell Block. Only two komatiite occurrences (Ban-15 and Ban-17) are sufficiently exposed to evaluate their textural facies variations. Ban-15 is located in the central part of the Powell Block and is in contact with Timiskaming metasedimentary rocks and mafic metavolcanic rocks to the south and in contact with mafic metavolcanic rocks to the north. This komatiite occurrence varies in thickness from 80 to 500 m and is composed of multiple cooling units of komatiite and cumulate komatiite trending northwest to southeast over 3.6 km. Ban-15 shows textural facies variation along strike exhibiting massive komatiitic peridotite cumulate in the eastern part to more differentiated units (i.e., massive, spinifex, flow breccia, and layered flows [massive/spinifex]) in the western part. Ban-17 is located in the northern part of the Powell Block and is in contact with Timiskaming metasedimentary rocks to the south and mafic metavolcanic rocks to the north. This komatiite occurrence varies in thickness from 50 to 200 m and is composed of multiple cooling units of komatiite and cumulate komatiite trending northwest to southeast for over 4.5 km. Ban-17 shows a textural facies variation along strike that mirrors Ban-15, with komatiitic peridotite and pyroxenite in the western part and more differentiated units (massive, flow breccia) in the eastern part.

Overall, the komatiitic rocks in this sector exhibit several different textural facies such as massive (aphyric and cumulate), spinifex texture, flow breccia, and polysutured jointing. In the Powell Block, the flow breccia textural facies (e.g., flow breccia, flow-top breccia, hyaloclastite) are well distributed throughout most of the komatiite occurrences and komatiitic outcrops.

3.4.3. *Cairo Block*

The komatiitic rocks in the Cairo Block represent only a small proportion of the rock units observed during the regional bedrock mapping in 2002 by Leblanc and Berger (2003). Only one komatiite occurrence is labelled in this area (Ban-18: *see* Figure 3.2). It crops out along the powerline south of St. Paul Lake. This komatiitic occurrence varies in thickness from 40 to 70 m and is composed dominantly of komatiitic basalt trending east to west for over 2.3 km. From west to east, this unit is in contact with alkali granite and quartz syenite, sulfide-graphite-facies iron formation, massive and autobrecciated intermediate volcanic rocks, and massive and variolitic mafic volcanic rocks along the southern contact (footwall), whereas it is in contact with massive mafic volcanic rocks along its northern contact (hanging wall).

Komatiitic basalt exhibits pale orange-brown to bone-white weathered surfaces and dark green or pale green fresh surfaces. Most exposures around the Whiskeyjack Creek fault consist of massive and sheared komatiitic basalt (western part), whereas most of the exposure in the eastern part consists of fine-grained olivine cumulate, pyroxene spinifex-bearing rocks and *in situ* komatiitic hyaloclastite. Banded iron formation is locally incorporated as xenoliths in an exposure of komatiitic basalt located under the powerline south of St. Paul Lake (Fig. 3.7A). An abundance of jigsaw-fit *in situ* hyaloclastite with an intense alteration of the clast margins (Fig. 3.7B) suggests a high water:rock interaction ratio between seawater and the komatiitic basalt flow. Furthermore, the presence of a highly vesiculated komatiitic basalt margins along the contact with the xenoliths (Fig. 3.7C) also suggests that the iron formation was not completely consolidated.

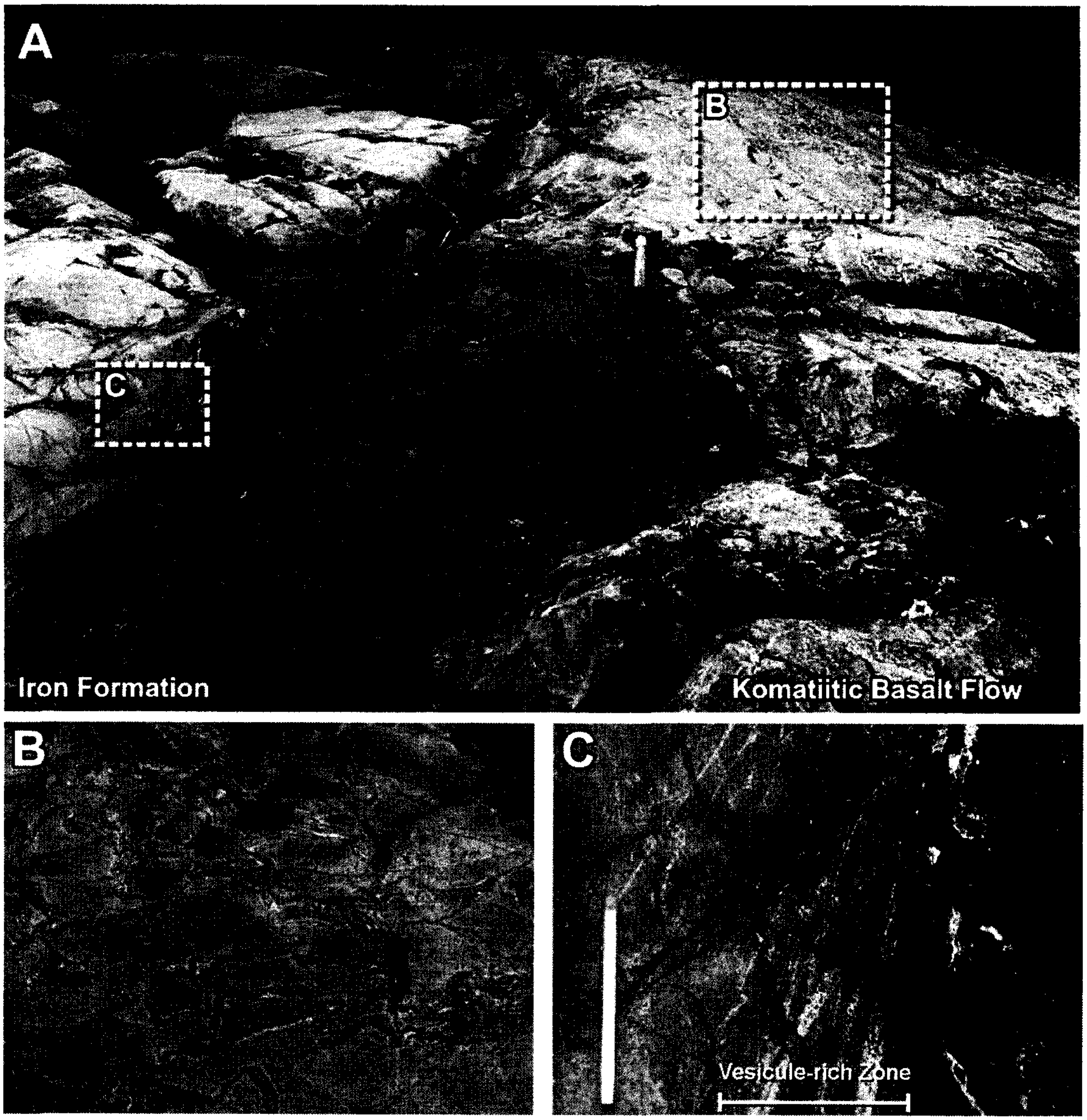

Figure 3.7. A) Iron formation xenoliths within a komatiitic basalt flow. B) Close-up from Photo 7.3A showing a jigsaw-fit *in situ* komatiitic basalt breccia. C) Close-up from Photo 7.3A showing the contact between komatiitic basalt flow and the iron formation xenolith. Note the highly vesicular zone along the contact (UTM for all photos: 531918E, 5311118N, NAD 83, Zone 17).

3.5 Volcanic and Subvolcanic Architecture

Distinguishing between extrusive and intrusive origins for komatiitic units is generally difficult because of incomplete exposure and/or deformation of contacts, and the fact that several komatiite textures (e.g., spinifex, amygdules) can occur in both extrusive and intrusive units (Arndt et al., 2004; Houlé et al., 2004). On the other hand, several komatiite textures provide unequivocal evidence for an extrusive mode of emplacement, including flow-top breccia, flow breccia, hyaloclastite, and polyhedral (polysutured) jointing (*see* Arndt et al., 2004).

In the eastern half of the map area (Powell and Cairo townships), the komatiitic units (Ban-9 to Ban-18) exhibit unequivocal evidence for extrusion such as *in situ* komatiitic hyaloclastites, flow breccias, flow-top breccias, and polysutured jointing. However, the evidence is ambiguous for the komatiitic occurrences (Ban-5 to Ban-8) in Bannockburn Township where some of the komatiitic units exhibit evidence of extrusion or intrusion. Examples include those in the northern part of the area (Ban-7D) that contain flow-top breccias or those having a high angular relationship with others units (Ban-8: C-Zone). Unequivocal evidence for an intrusive or extrusive emplacement has not been observed thus far for other occurrences in Bannockburn Township. However, several factors could suggest that these units are more likely to be intrusive rather than flows. Their include the presence of steep- and shallow-dipping units, the presence of discordant komatiitic units (C-Zone), the absence of lateral continuity (i.e., isolated blobs on the map of the magnetic survey (OGS, 1999)), large amount of sulfides within small komatiitic units (C-Zone), the absence of an obvious sulfur source in the immediate footwall and the overall complexity of the geology associated with these komatiitic units. The lack of data on the komatiitic units in the western part of Montrose Township (Ban-1 to Ban-4) precludes interpretation on their origin (i.e., flow versus intrusion).

Interpreting volcanic environments is complicated by both primary factors (e.g., more than one eruptive centre, differences in eruption rate and style, differences in mode and environment of emplacement) and secondary factors (e.g., metamorphism, alteration, structural complexity, exposure, etc.). However, there are clear volcanic facies variations in the Bannockburn Township area. The komatiites in the west-central part of Bannockburn Township contain more prospective volcanology (e.g., cumulate rocks, less differentiated, degree of channelization, underlying lithologies) than komatiites elsewhere in the area.

Based on available data, komatiitic rocks in the Bannockburn area are tentatively interpreted to be a complex sill-lava flow field, whereas, in the west-central part of Bannockburn Township, the rocks are interpreted to be high-level komatiitic subvolcanic intrusions and feeder dikes that fed channelized komatiitic sheet flows and thin differentiated flows further east in Bannockburn and Powell townships. However, further investigations are necessary to support or refute this interpretation of the volcanic architecture for this area.

3.6 Komatiite-Associated Ni-Cu-(PGE) Mineralization

Komatiite-hosted Ni-Cu-(PGE) deposits contain a variety of mineralization types (Lesher and Keays, 2002), which may be subdivided into 3 broad genetic categories: magmatic, metamorphically hydrothermally mobilized, and tectonically mobilized. Each of these categories is divisible into several types and subtypes (Lesher and Keays, 2002) (Table 3.2). The most favourable Ni-Cu-(PGE) primary mineralization types in the Bannockburn area are, in order of economic potential, stratiform basal (Type I: Kambalda-type), stratabound internal (Type II: Mt. Keith type), and stratiform internal (Type III: "reef-type").

Table 3.2. Simplified classification of primary mineralization types in komatiite-associated magmatic Ni-Cu-PGE deposits (modified from Lesher and Keays 2002) in the Abitibi greenstone belt.

Origin	**Type**		
Type	**I** **Stratiform Basal**	**II** **Stratabound Internal**	**III** **Stratiform "Reef-style"**
Sulfide distribution	At or near the bases of komatiitic peridotite or komatiitic dunite units	Within komatiitic peridotite or dunite units	At or near contact between lower ultramafic cumulate zones and upper mafic zones
Sulfide textures	Massive, net-textured, disseminated	Disseminated, interstitial	Disseminated
Timing and paragenesis	Segregated prior to or during emplacement	Segregated during crystallization of cumulate host rock	Segregated during final stages of crystallization of host rock
Examples in the Bannockburn area	- *C-Zone* - Thalweg Zone (F Zone) - *Rahn Lake Zone (D Zone)*	- *Bannockburn Zone (B Zone)*	*Unknown*

Four significant nickel sulfide mineralization zones are known in the Bannockburn area from past exploration programs. The C-Zone, the Thalweg Zone (F-Zone), and the Rahn Lake Zone (D-Zone) are related to the Kambalda-type, whereas the Bannockburn (B-Zone) is related to the Mt. Keith-type (*see* Table 3.2). Other sulfide occurrences associated with komatiitic rocks in the study area include the H-Zone

(0.4–0.7% Ni: unpublished data from Mustang Minerals) located northeast of Rahn Lake in Bannockburn Township, and trenches that contain disseminated sulfides (up to 25%: Benson, 2005) located near the boundary between Powell and Bannockburn townships. In the following section, the most significant komatiite-associated Ni-Cu-(PGE) zones are summarized from direct observations and data available from Outokumpu Mines and Mustang Minerals.

The C-Zone is the most recent discovery and is exposed over a length of 150 m (Ban-8: *see* Figure 3.1). The sulfide mineralization consists of massive and disseminated to blebby sulfides that occurs at or slightly above the contact with dacite (Fig. 3.8). Rare net-textured sulfides are also observed locally. The apparent thickness of the sulfide zone at surface ranges from 1.5 to 6 m, whereas true thickness estimated from diamond drilling ranges between 0.5 to 8 m (Harron, 2005). The ore zone is generally composed of very fine-grained and highly deformed sulfides that contain numerous talc-carbonate stringers. It is composed of pyrrhotite, pentlandite, chalcopyrite, pyrite and magnetite. In some locations, the sulfide mineralization is intensely weathered and oxidized. Table 3.3 shows the typical grade of the C-Zone mineralization over the length of the stripped area. The C Offset Zone is interpreted to be the equivalent of the C-Zone sulfide lens displaced by a north-northwest- to south-southeast-trending fault.

The Thalweg nickel sulfide mineralization is located south-southwest of Charlewood Lake in the southwest corner of Bannockburn Township (Ban-5: *see* Figure 3.1). The sulfide mineralization at Thalweg is hosted within a thick komatiitic peridotite that occurs at or near the basal contact of a footwall embayment. The sulfide mineralization is continuous over 200 m and could locally be up to 18 m wide (Bereton, 2003). This occurrence is typical of a Kambalda-type mineralization composed of massive sulfides, net-textured sulfides, and disseminated sulfides. Table 3.3 shows the typical grade of the Thalweg mineralization intersected by Outokumpu Mines and Mustang Minerals. Some mineralization is also reported within komatiite projection along the main channel (Davis, 1996).

The Bannockburn Zone (B-Zone) is located approximately 2 km north-northwest of the Thalweg Zone and approximately 200 m southwest of the C-Zone at Rahn Lake (Ban-7A: *see* Figure 3.1). The host unit of the B-Zone is an olivine adcumulate to mesocumulate trending northwest-southeast for over 3 km. The B-Zone is typical of Mt. Keith type mineralization with fine disseminated sulfides (1–3%) within a thick

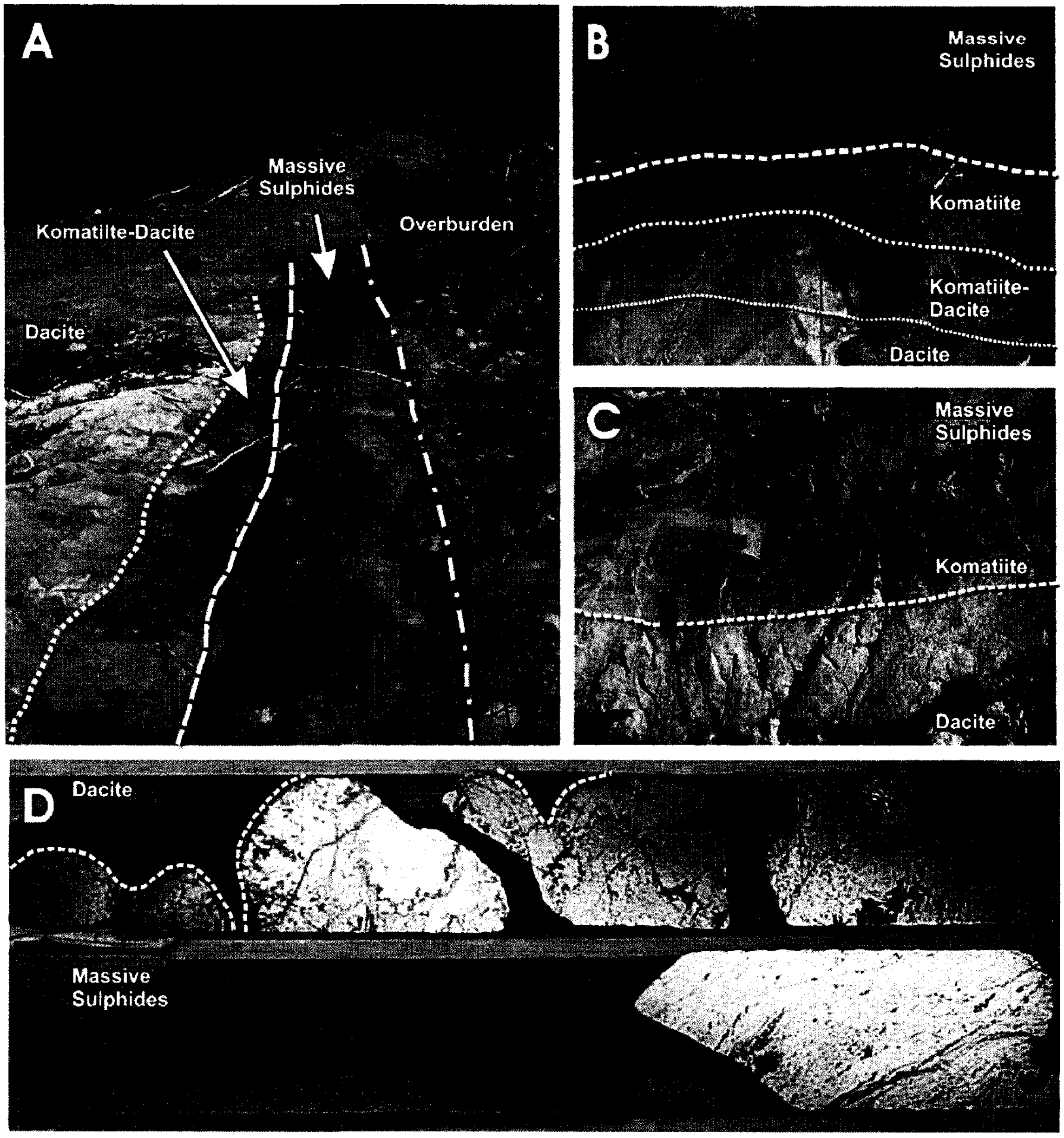

Figure 3.8. Nickel sulfide mineralization at the C-Zone in Bannockburn Township. A) The C-Zone mineralization exposed on the eastern edge of the stripped area (looking east) showing the footwall contact between massive sulfide, komatiite and dacite. B) Close-up from Photo 7.4A showing the interaction between komatiite and overlying massive sulfides and underlying plagioclase-phyric dacite. C) Footwall contact further up on the hill showing a sharp contact between komatiite and dacite underlying massive sulfides indicating little to no interaction between those units (UTM for photos A, B, and C: 507236E, 5313923N, NAD 83, Zone 17). D) Footwall contact from diamond drill core (MBC04-12) showing very irregular contact between dacite and massive sulfide.

olivine cumulate. Table 3.3 shows the typical grade of the B-Zone mineralization intersected by Outokumpu Mines and Mustang Minerals.

The Rahn Lake Zone (D-Zone) has been intersected by diamond drilling conducted by Outokumpu Mines below a swamp at the bottom of a cliff near the C-Zone and more recently by Mustang Minerals under Rahn Lake. The sulfide zone ranges in thickness from 1 to 3 m thick and is mainly composed of disseminated to net-textured sulfides that occur at or near the basal contact of a relatively thick olivine cumulate. A narrow band of massive sulfides is locally observed underlying the main ore profile.

Table 3.3 shows the typical grade of the D-Zone mineralization intersected by Outokumpu Mines and Mustang Minerals. The sulfide mineralization is composed of pyrrhotite, pentlandite and pyrite. Some disseminated sulfides (3–10% pyrite, pyrrhotite) are equally present near the upper contact with the dacite that constitutes the footwall of the C-Zone. Other fine disseminated sulfides were intersected within the D-Zone by diamond drilling under Rahn Lake. However, in accordance with the new structural interpretation, this sulfide zone may be related to the B-Zone rather than the D-Zone.

Table 3.3. Grade summary of the main nickel sulfide mineralization at the Mustang Minerals property in Bannockburn Township. Compiled *from* Bereton (2003), Harron (2005) and unpublished data from Outokumpu Mines.

Nickel Zone	Sulfide Texture	(n)	Average Ni (%)	Min Ni (%)	Max Ni (%)	Sulfides (%)
C-Zone						
Surface	D$ to B$	9	0.67	0.19	1.09	5-25
	M$	16	3.5	1.97	4.85	>90
Thalweg Zone						
	D$	21	0.39	0.14	1.06	1-10
	N$	15	1.14	0.87	2.16	15-60
	M$	3	3.42	2.5	4.54	90-97
Bannockburn Zone						
	D$	12	0.30	0.28	0.51	Tr-1%
	D$	8	0.64	0.31	0.97	2-3%
Rahn Lake						
	D$	4	0.85	0.61	1.23	5-10
	N$	2	1.19	1.16	1.21	10-40
	M$	1	3.2	–	–	90

M$: Massive sulfides, N$: Net-textured sulfides, D$: Disseminated sulfides, B$: Blebby sulfides, (n): number of analysis.

3.7 Mineral Potential Exploration

Komatiite-associated Ni-Cu-(PGE) deposits typically occur in clusters. For example, within the Abitibi greenstone belt, there are the following deposits: in the Shaw Dome, there are 5 known deposits (Langmuir #2, Redstone, Langmuir#1, McWatters, Hart); in the Dundonald area, there are 4 known deposits (Alexo, Kelex, Dundonald South, Dundeal); and in the Lamotte area in Québec, there are at least 4 deposits (Marbridge 1, 2, 3, 4: Naldrett and Gasparrini, 1971). This is also typical for komatiite-associated Ni-Cu-(PGE) deposits worldwide, as exemplified by the deposits in the Kambalda–St Ives–Tramways–Widgoemooltha–Carnilya Hill district of Western Australia (Barnes, 2004). Clearly, areas where only one or two deposits have been discovered, such as the Bannockburn area, have significant potential for discovery of additional deposits.

Several factors appear to be critical to the genesis of economically significant magmatic sulfide deposits (e.g., Lesher and Keays, 2002; Naldrett, 2004), including:

- **Source of Metal**: The magma must be initially undersaturated in sulfide so that it contains sufficient concentrations of Ni, Cu, and PGE;

- **Source of S**: The magma must have access to an external sulphur source to achieve early sulfide saturation and to segregate significant abundances of immiscible sulfides at a high (crustal) level;

- **Dynamic System**: The ores must form in a dynamic system where the magmas can interact with country rocks (to extract S) and where the sulfides can equilibrate with a sufficient amount of magma to generate high chalcophile element contents in the sulfides (i.e., high R factor);

- **Physical Trap**: The sulfides must be concentrated in some type of physical trap (embayment, inflection).

Numerous occurrences of nickel, copper and platinum group element mineralization associated with komatiitic rocks have been identified in the Bannockburn area (C-Zone/C Offset, B-Zone, F-Zone, H-Zone). Furthermore, Sproule et al. (2005) concluded that all of the host rocks were undersaturated in sulfide prior to emplacement in the Abitibi greenstone belt, including the Bannockburn area komatiites, suggesting that those rocks originally contain sufficient concentrations of metals. The presence of relatively thick olivine cumulate (within several komatiite occurrences: Ban-07, Ban-05, and Ban-06), and of numerous autobrecciated units (within the Rahn Lake and C-Zone komatiites), suggest dynamic emplacement of the komatiites. The presence of embayments and the interaction between the intermediate volcanics rocks and the komatiite units at the C-Zone and the Thalweg stripped exposures suggest contamination and localized physical traps to accumulate sulfide mineralization. As noted above, these features are all critical in the formation of magmatic Ni-Cu-(PGE) mineralization.

The recent work conducted by the Ontario Geological Survey (Préfontaine and Berger, 2005; Berger and Préfontaine, 2005) in this area increases significantly the understanding of the regional geological context. The new structural interpretation suggests that most of the komatiitic units in the Bannockburn area are part of the same komatiitic sequence. Incidentally, this highlights some important implications on the potential of this area for nickel mineralization. Firstly, the presence of northwest to southeast folding in this area is indicated by reversals in stratigraphic facing and this suggests that komatiites and associated mineralization may be repeated by folding. Furthermore, structural repetition of the komatiite stratigraphy suggests that the two komatiitic units north of the known occurrences are probably underexplored for their Ni-Cu-(PGE) potential. Secondly, without clear knowledge of the facing of a particular unit, previous diamond drill holes may have been drilled down dip and/or may not have tested the basal contacts of the komatiites for potential mineralization.

Identification of three compound sheets flows in the map (Ban-11, Ban-15 and Ban-17) that could contain lava pathways should be further investigated for nickel potential. The komatiite occurrence Ban-11 contains significant amount of sulfides within its flanking facies suggesting the presence of a sulphur source in the immediate vicinity.

Several positive gravity anomalies occur in the map area (OGS, 1999). Most of these appear to be related to high-density rocks such as komatiite and iron tholeiite basalt. One good example is the anomaly located in central Powell Township that appears to be associated with the most extensive komatiitic flows in the map area. However, contrary to the komatiite flows in central Powell Township, a positive gravity anomaly is not associated with those high-level komatiite intrusions. An unexplained positive gravity anomaly is situated east of Charlewood and Clarke Lakes beneath rocks of the Gowganda Formation. It occurs south-southeast of the komatiite occurrence Ban-07 (C-Zone, Bannockburn Zone, Rahn Lake) and north-northwest of the komatiite occurrence Ban-05 (Thalweg area). This anomaly may be related to ultramafic rocks and presents an attractive exploration target for magmatic sulfide mineralization.

Despite the lack of obvious sulphur sources in the area, the combination of a fertile komatiitic magma (metal source), abundant olivine cumulate rocks indicating high magma flux (heat source and dynamic environment), a clear interaction (contamination via thermomechanical erosion) between the komatiitic units and their footwall (dynamic environment), and embayments (localization) provides an excellent environment for forming komatiite-associated Ni-Cu-(PGE) deposits in the study area.

3.8 Acknowledgments

This contribution has been designed to complement the regional bedrock mapping, which is part of the Ontario Geological Survey core program and is part of an ongoing PhD study by M.G. Houlé based at Laurentian University (LU) and the University of Ottawa (UO) on the physical volcanology and metallogenesis of komatiites in the Abitibi greenstone belt. Peter Wood and Ken Lapierre from Mustang Minerals Corp. are thanked for their generous assistance, numerous discussions and permission to access properties and internal company data. Insightful discussions and comments from other geoscientists such as Rebecca Sproule, Mike Lesher, and Harold Gibson from Laurentian University and Paul Davis from First Nickel Inc. were greatly appreciated.

CHAPTER 4 - KOMATIITIC SILLS AND MULTI-GENERATIONAL PEPERITE AT DUNDONALD BEACH, ABITIBI GREENSTONE BELT, ONTARIO: VOLCANIC ARCHITECTURE AND NICKEL SULFIDE DISTRIBUTION

4.1 Abstract

The density and the tectonic stresses in the deep crust and the physical properties of komatiitic magmas determine the level to which they will rise, but once in the near-surface environment, the density and rheology of the near-surface rocks (consolidated and dense lava flows and sedimentary rocks versus unconsolidated sedimentary or volcaniclastic deposits) govern whether they will be emplaced as lava flows, invasive flows, or sills. Where near-surface strata are competent (i.e., flow-dominated or consolidated sedimentary/volcaniclastic successions), komatiitic magma erupts as flows and form extensive lava shields (e.g., Kambalda). However, where near-surface strata are not competent (i.e., unconsolidated volcaniclastic/sediment-dominated successions), komatiitic magmas typically are emplaced as high-level sills that increase the bulk density of the volcano-sedimentary pile and eventually allow the eruption of lava and the construction of complex subvolcanic-volcanic lava shields (e.g., Dundonald and Shaw Dome, Abitibi belt; Raglan, Cape Smith belt; Pechenga, Kola Peninsula; Thompson Ni belt, Manitoba). The latter environment is illustrated in the volcano-sedimentary succession in Dundonald Township, which is only weakly metamorphosed and deformed and superbly exposed in glacially-polished outcrops.

The volcano-sedimentary succession in this area comprises (from base to top) (1) the McIntosh formation, composed of a sequence of pillowed and massive intermediate volcanic flows, (2) the Dundonald formation, composed of a lower section of komatiite sills, argillites, and felsic volcaniclastic deposits and an upper section of komatiite flows, komatiitic sills, and pillowed intermediate volcanic flows, and (3) the Frederick House Lake formation, composed of massive and pillowed mafic flows. The distribution and thickness of argillites and felsic volcaniclastic rocks define a synvolcanic graben in which the Dundonald South and Alexo Ni-Cu-(PGE) deposits occur within the center and the margin, respectively. Sills and peperites in the lower komatiitic succession at

Dundonald Beach exhibit a multigenerational emplacement history recording progressive lithification and increases in the bulk density and rheological strength of the unconsolidated argillites, which ultimately permitted the eruption of lavas at Alexo.

Importantly, the nature of the near-surface rocks also influences the localization of Ni-Cu-(PGE) deposits. In lava shields (e.g., Kambalda), the initial eruptions are typically most voluminous and, if erupted at sufficient flow rates, form channelized flows conducive to thermomechanical erosion of sulfur-rich footwall rocks. In subvolcanic-volcanic lava shields, however, channelized units may occur within the subvolcanic plumbing system and/or within overlying lavas. Where only sills are channelized (e.g., Thompson), mineralization will occur only within the subvolcanic environment; where only the flows are channelized (e.g., Damba-Silwane, Zimbabwe), mineralization will occur only within the volcanic environment. Where both sills and lava flows are channelized (e.g., Dundonald, Shaw Dome, Raglan), the distribution of the mineralization is more diverse and may occur as subseafloor or on seafloor Ni-Cu-(PGE) deposits.

4.2 Introduction

The volcanic setting (volcanic, invasive, or intrusive) of komatiite-associated Ni-Cu-(PGE) deposits remains controversial despite intensive research over the past 30 years. After Bowen (1927) cast doubt on an extrusive mode of emplacement for ultramafic rocks, most geologists considered them to be intrusive, until Viljoen and Viljoen (1969) described ultramafic lava flows along the Komati River in the Barberton Mountain Land. This discovery led to the recognition of komatiitic lava flows in most other Archean cratons. Although some were shown to be intrusive (e.g., Muir, 1979; Williams, 1979; Duke, 1986; Stone and Stone, 2000), virtually all massive and spinifex-textured ultramafic units within Archean greenstone belts were interpreted as lava flows, including the komatiite succession associated with the Dundonald South Fe-Ni-Cu sulfide deposit in Dundonald Township (Muir and Comba, 1979).

Although many concordant ultramafic units containing spinifex textures are extrusive (e.g., Pyke et al., 1973; Nisbet et al., 1977; Thomson, 1989; Dann, 2000), field work in several areas has shown that spinifex texture is not restricted to flows but also develops in komatiitic dikes (e.g., Davis, 1997; Dann, 2000) and in high level komatiitic sills (e.g., Davis, 1999; Dann, 2000; Cas and Beresford, 2001; Houlé et al., 2002a, b, c; Arndt et al., 2004; Trofimovs et al., 2004). Spinifex is clearly not a "quench" texture, as it forms deep (dm to m) within flows. Indeed, theoretical studies (Shore and Fowler, 1999) and experimental work (Faure et al., 2006) have demonstrated that spinifex forms in a thermal gradient, as occurs in both flows and high-level intrusions. Thus, the presence of spinifex-texture cannot be used as the primary evidence for an extrusive origin for komatiitic rocks (e.g., Donaldson, 1974; Arndt et al., 2004; Houlé et al., 2004).

Komatiite-associated Ni-Cu-(PGE) deposits, which were originally thought to occur within intrusions, were subsequently reinterpreted as occurring in flows. For example, the ultramafic hosts of Type I or Kambalda-type deposits (classification scheme of Lesher and Keays, 2002) in the Kambalda District of the Norseman-Wiluna greenstone belt were initially interpreted as intrusive (Woodall and Travis, 1969) but were subsequently reinterpreted as occurring within distal lava channels (Lesher et al., 1984; Cowden and Roberts, 1990). Type II or Mt. Keith-type komatiite-associated deposits in the Perseverance-Mount Keith District of the Norseman-Wiluna greenstone belt were initially interpreted as occurring in subvolcanic intrusions (Naldrett and Turner, 1977) but were subsequently reinterpreted as occurring within proximal lava channels (e.g., Donaldson et al., 1986; Barnes et al., 1988; Hill et al., 1990) and, more recently, reinterpreted as occurring within a large sill (Trofimovs et al., 2003; Rosengren et al., 2005).

The intrusive or extrusive origin for komatiites hosting Ni-Cu-(PGE) mineralization, in part, reflects the different geodynamic environments into which komatiitic magmas have been emplaced. The purpose of this paper is to present a conceptual model of the emplacement of komatiitic magma within a volcaniclastic- and/or sediment-dominated environment and its role for the development of the komatiite volcanic architecture in Dundonald Township, Abitibi greenstone belt, Ontario.

In particular, we described a spectacular and well exposed volcanic succession at Dundonald Beach, including komatiitic sills and associated peperites, and use this description as a basis for defining on the transition from intrusive and to extrusive komatiites. We interpret the mechanisms of komatiitic sill emplacement and the development of multigenerational peperite, and explore the role of komatiitic sills in changing the density and rheological characteristics of the sedimentary rocks and how this may affect the subsurface and surface architecture of komatiitic edifices and the location of komatiite-associated Ni-Cu-(PGE) deposits. Finally, we propose a new hypothesis for the evolution and architecture of komatiitic edifices where magma is emplaced into unconsolidated sedimentary and volcaniclastic strata in the near surface environment.

4.3 Geological Setting

The Dundonald Beach area occurs within the Kidd-Munro assemblage in Dundonald Township, which is located ~45 km northeast of Timmins in Ontario (Fig. 4.1, inset). The Kidd-Munro assemblage has been subdivided in Ontario into a lower stratigraphic succession (2719-2717 Ma) and an upper stratigraphic succession (2717-2711 Ma: Ayer et al., 2005; Thurston et al., 2008). Volcanic rocks of these ages extend for more than 400 km from west of the Kidd Creek deposit in Ontario to the Grenville Front in Québec, where the Kidd-Munro assemblage is referred to the Kinojévis and Malartic Groups (Thurston et al., 2008).

In Dundonald Township, the volcanosedimentary succession consists of folded units dominated by intermediate to mafic and ultramafic metavolcanic rocks with lesser felsic metavolcanic and metasedimentary rocks approximately 3000 m in total thickness. The main structure in the area consists of a major subvertical, SW trending and -plunging fold axis offset by WNW- and NNW-trending faults (Fig. 4.1).

The Kidd-Munro assemblage in this area is tentatively subdivided into several informal mappable formations, members, submembers, and units summarized in Figure 4.2. Three informal formations are, from oldest to youngest, the McIntosh Lake, Dundonald, and Frederick House Lake formations.

The McIntosh Lake formation ranges in thickness from 50 to 400 meters and is composed of mafic to intermediate massive and pillowed flows, intermediate to mafic volcaniclastic rocks, and komatiitic volcanic rocks (Davis, 1997). The 200 to 2000 meter thick komatiitic succession occurs in the upper part of the formation (Fig. 4.2), and it is composed of individual flows that range in thickness from less than 1 m to greater than 10 m, with compositions from komatiitic basalt to komatiite and with well-developed spinifex textures (Davis, 1997). The komatiite unit is poorly exposed and the description and interpretations are based entirely on drill core data. It is not known to contain any komatiite-associated Ni-Cu-(PGE) mineralization.

The Dundonald formation consists of five informal mappable members, a lowermost felsic member and four komatiitic members (Fig. 4.2). The felsic member is

~300 m thick and consists of felsic volcanic flows, volcaniclastic units, and minor komatiitic and mafic dikes. Zircons in a sample collected from the felsic member yielded an age of 2717+/-1.2 Ma (Barrie et al., 1999). Graphitic, argillaceous metasedimentary rocks also occur within this member. The komatiitic members range in thickness from 1000 to 2000 m and are composed of komatiite and komatiitic basalt flows or sills, intercalated with lesser massive mafic flows and sparse felsic volcaniclastic rocks.

The Frederic House Lake formation is poorly constrains but is interpreted from drillcore by Davis (1997) as a ~250 m sequence of massive and pillowed mafic flows. No komatiitic rocks have been reported in this formation.

The supracrustal rocks in Dundonald Township are intruded by the ~1750 m-thick, layered, tholeiitic mafic-ultramafic, near concordant, Dundonald Sill. Zircons from a sample collected from the mafic part of the sill yielded an age of 2707.1+3/-2 Ma (Barrie et al., 1999).

The volcanic succession has been metamorphosed to lower greenschist facies and is locally faulted and/or sheared, but most of the deformation is nonpenetrative, and primary structures and textures are well preserved. We therefore describe the rocks using premetamorphic igneous and volcanic nomenclature.

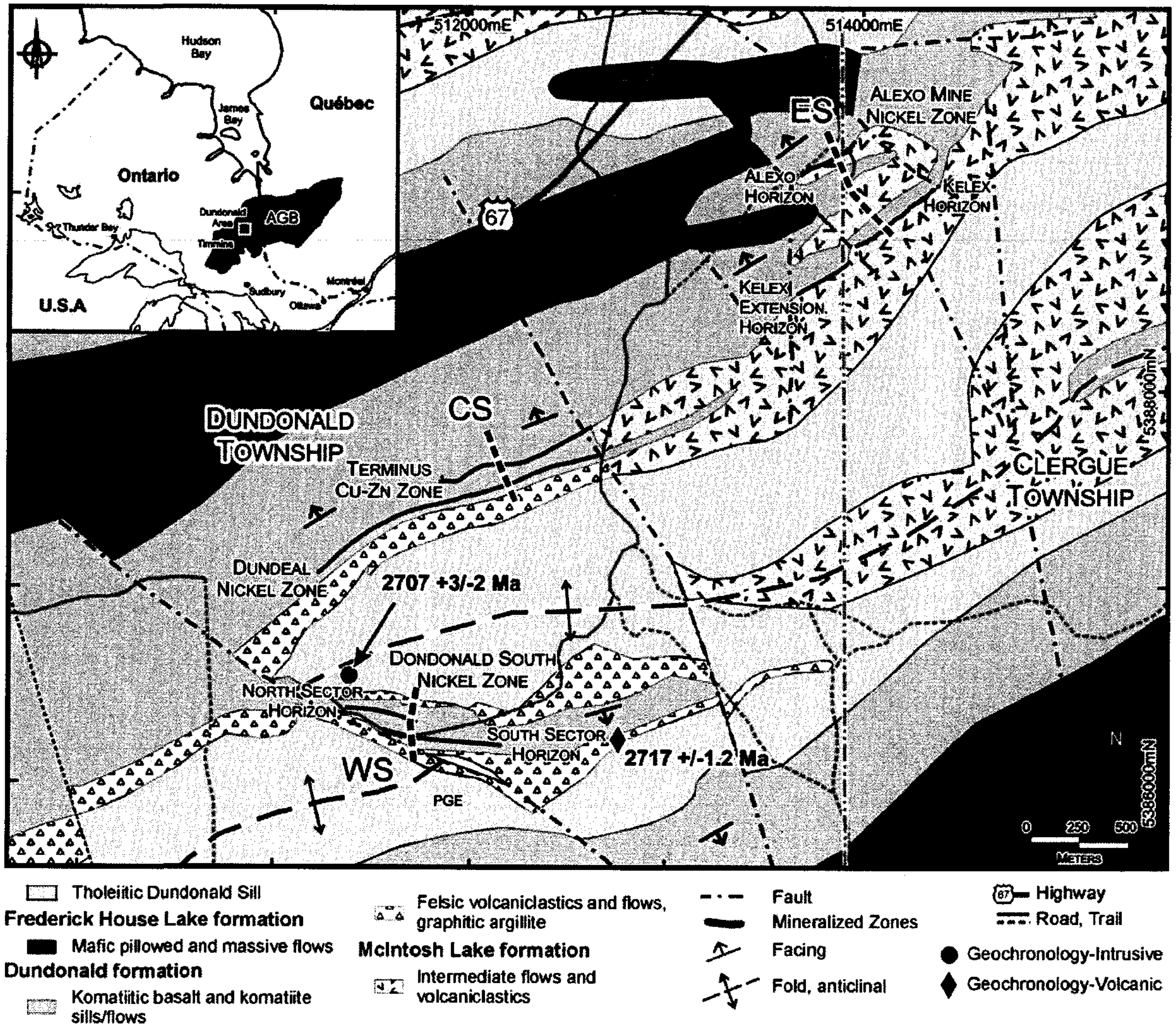

Figure 4.1 Simplified geological map of the Dundonald Township area, showing major geologic units and locations of komatiite-associated Ni-Cu-(PGE) deposits (modified from MPH Consulting Ltd., 2004). U-Pb ages are from Barrie et al. (1999). Sections WS, CS, and ES show the locations of stratigraphic columns in Figure 4.3.

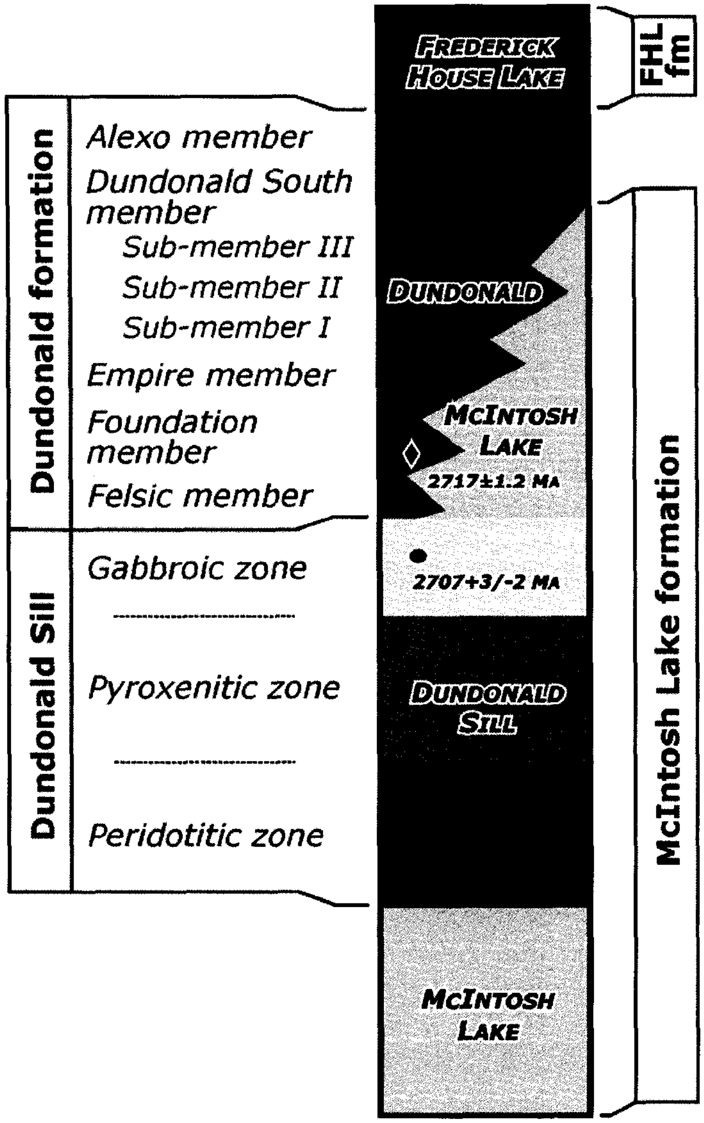

Figure 4.2 Dundonald Township tentative stratigraphic columns showing the generalized components of each informal stratigraphic unit. FHL: Frederick House Lake formation. U-Pb ages are from Barrie et al. (1999).

4.3.1. Dundonald formation

The komatiitic units in the Dundonald formation have been subdivided based on this study and previous work conducted by Falconbridge Ltd., from lowermost to uppermost, as the Foundation, Empire, Dundonald South, and Alexo members. All members contain Ni-Cu-(PGE) occurrences and deposits (e.g., Kelex: Foundation member, Dundeal: Empire member, Dundonald South: Dundonald South member, and Alexo: Alexo member; Figs. 4.1 through 4.3).

The Foundation member (Fig. 4.3) consists of a 45 m-thick, poorly-differentiated komatiitic peridotite sill or flow in the eastern section and a 100 m-thick, massive, discontinuous komatiitic peridotite sill or flow in the central section (Davis, 1997; Montgomery, 2004). It has not been identified in the western section.

The Empire member (Fig. 4.3) comprises a 100 m-thick, massive komatiitic peridotite sill or flow in the eastern section and a 180 m-thick, well-differentiated komatiitic basalt sill or flow in the central section (Vicker, 1991; Davis, 1997; Barrie et al., 1999). It has not been identified in the western section.

The Dundonald South member extends over the entire strike length of the Dundonald formation. Its thickness ranges from 100 m in the eastern section (Barnes et al., 1983; Arndt, 1986) to 80 m in the central section (Davis, 1997; Barrie et al., 1999), and 175 m in the western section (Fig. 4.3; Muir and Comba, 1979; Schofield, 1982; Davis, 1999; this study). The Dundonald South member is further subdivided into three submembers (Fig. 4.2). Submember I consists of komatiitic basalts, submember II consists of komatiitic basalts with well-developed spinifex textures, and submember III consists of komatiites with locally well-developed spinifex texture (Davis, 1999). The vertical compositional trend from komatiitic basalt upward to komatiite is the reverse of that normally found within komatiitic sequences (Fig. 4.3 and 4.4; Gresham and Loftus-Hills, 1981; Lesher et al., 1984; Lesher and Arndt, 1995; Lesher, 2007). This member is composed of complexly intercalated komatiitic basalt and komatiite sills, argillite, and peperite in the western section and thin komatiitic basalt and komatiite sills intercalated with graphitic and locally sulfidic argillite with minor peperite in the central section (Fig. 4.3). In the eastern section, it exhibits a transition between intrusive and extrusive komatiites: the lower part of the member consists of thin differentiated komatiite and komatiitic basalt sills with minor peperite, whereas the upper part of the member is composed of thin, well-differentiated komatiitic flows with hyaloclastite flow-top breccias. The extrusive nature of the komatiitic rocks in the upper part of this member is well documented from the detailed work of Barnes et al. (1983) and Arndt (1986), who focused on an excellent exposure in the upper part of the Dundonald South member underlying the Alexo deposit. In contrast, an intrusive nature of some of the komatiitic rocks in the lower part of this member is indicated by the presence of peperite at the upper margins of thin komatiitic basalts observed in drill core.

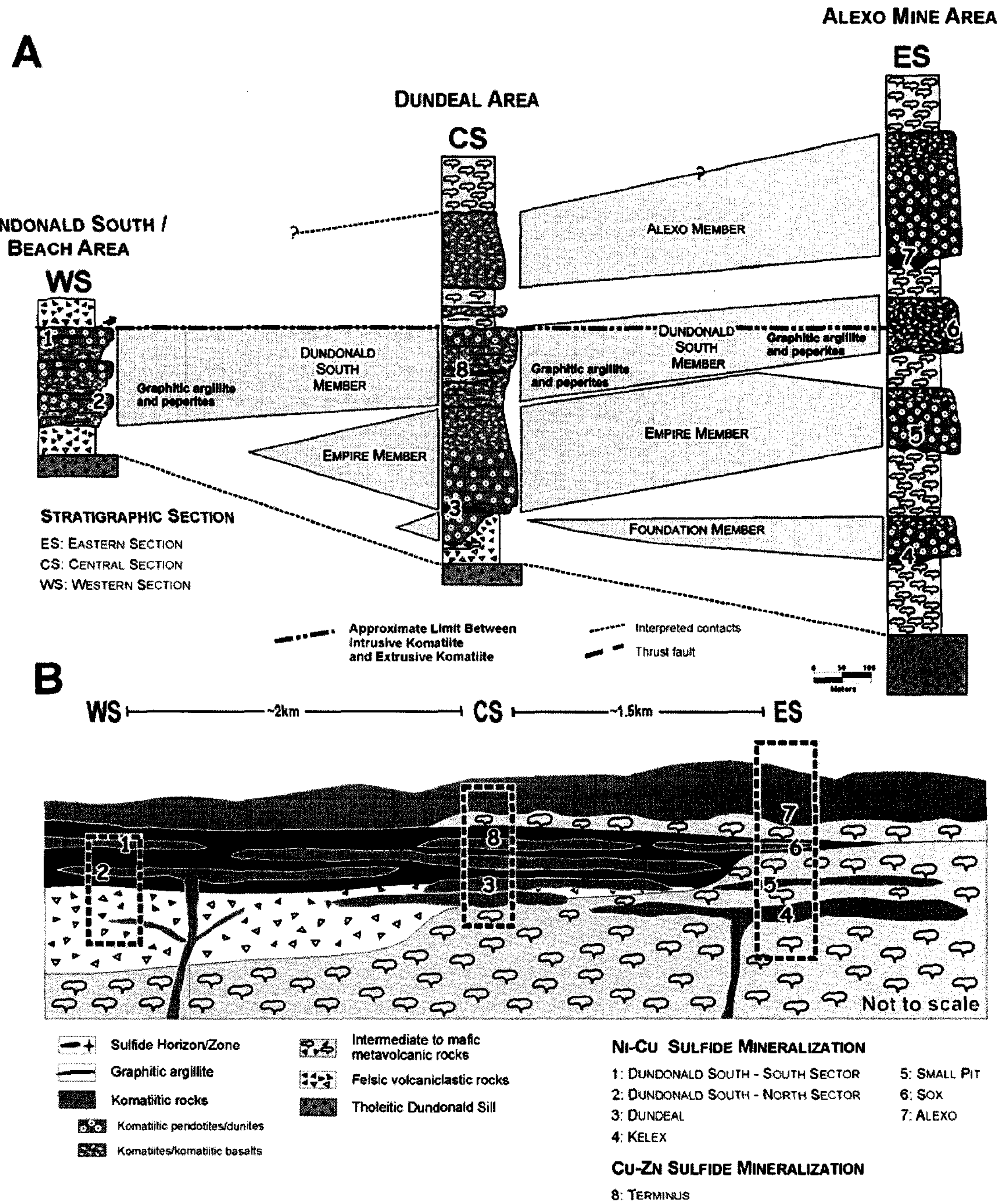

Figure 4.3 Schematic stratigraphic columns (A) and paleotopographic reconstruction (B) of the middle and upper komatiite formation showing the subvolcanic and/or volcanic architecture and locations of komatiite-associated Ni-Cu-(PGE) deposits in the *western section* (WS; this study), *central section* (CS; modified from Davis, 1997; Barrie et al., 1999), and *eastern section* (ES; P.C. Davis and Canadian Arrow Mines, unpubl. data, 1999-2005; M.G. Houlé, unpub. data). Section locations in Figure 4.1.

The Dundonald Beach outcrop provides an excellent exposure of a well-preserved section through the Dundonald South member (submember I) that was mechanically and hydraulically stripped of glacial overburden by Falconbridge Ltd. in 1989 and by Hucamp Mines in 2001, exposing ~9000 m^2 of glacially-polished outcrops. The felsic member, submember I, and the lowermost part of submember II of the Dundonald South member are exposed on this outcrop. Submember I is ~70 m-thick and is subdivided into three units (Muir and Comba, 1979; Davis, 1999; Fig. 4.4), from stratigraphic base to stratigraphic top.

Unit IA comprises multiple, thin, undifferentiated to poorly differentiated, noncumulate sills of komatiitic basalt and porphyritic komatiitic basaltic sills intercalated with graphitic argillaceous metasedimentary rocks containing fluidal and blocky peperite.

Unit IB is a differentiated, noncumulate komatiitic basaltic sill with a lower olivine-clinopyroxene cumulate zone, a thick parallel acicular ("string-beef") pyroxene spinifex-textured zone, a thin random platy olivine spinifex-textured zone, and a thin fine-grained upper chilled margin.

Unit IC consist of multiple, differentiated komatiite sills (Arndt et al., 2004) with thick, lower olivine mesocumulate zones and thin, upper olivine spinifex-textured zones. Ni-rich sulfide mineralization occurs at the bases of several of these units.

The underlying felsic member consists of poorly-bedded rhyodacitic volcaniclastic rocks (lapilli tuff to tuff breccia) and is cut by dacitic, mafic, and komatiitic dikes (Davis, 1997, 1999).

The Alexo member (Fig. 4.3) consists of a 225 m-thick sequence of massive komatiitic peridotite with local spinifex textures in the eastern section and a 100 m-thick sequence of thin differentiated komatiitic basaltic flows with well-developed parallel acicular pyroxene spinifex textures in the central section (Naldrett, 1966; Davis, 1999; M.G. Houlé, unpub. data). The Alexo member has not been identified in the western section.

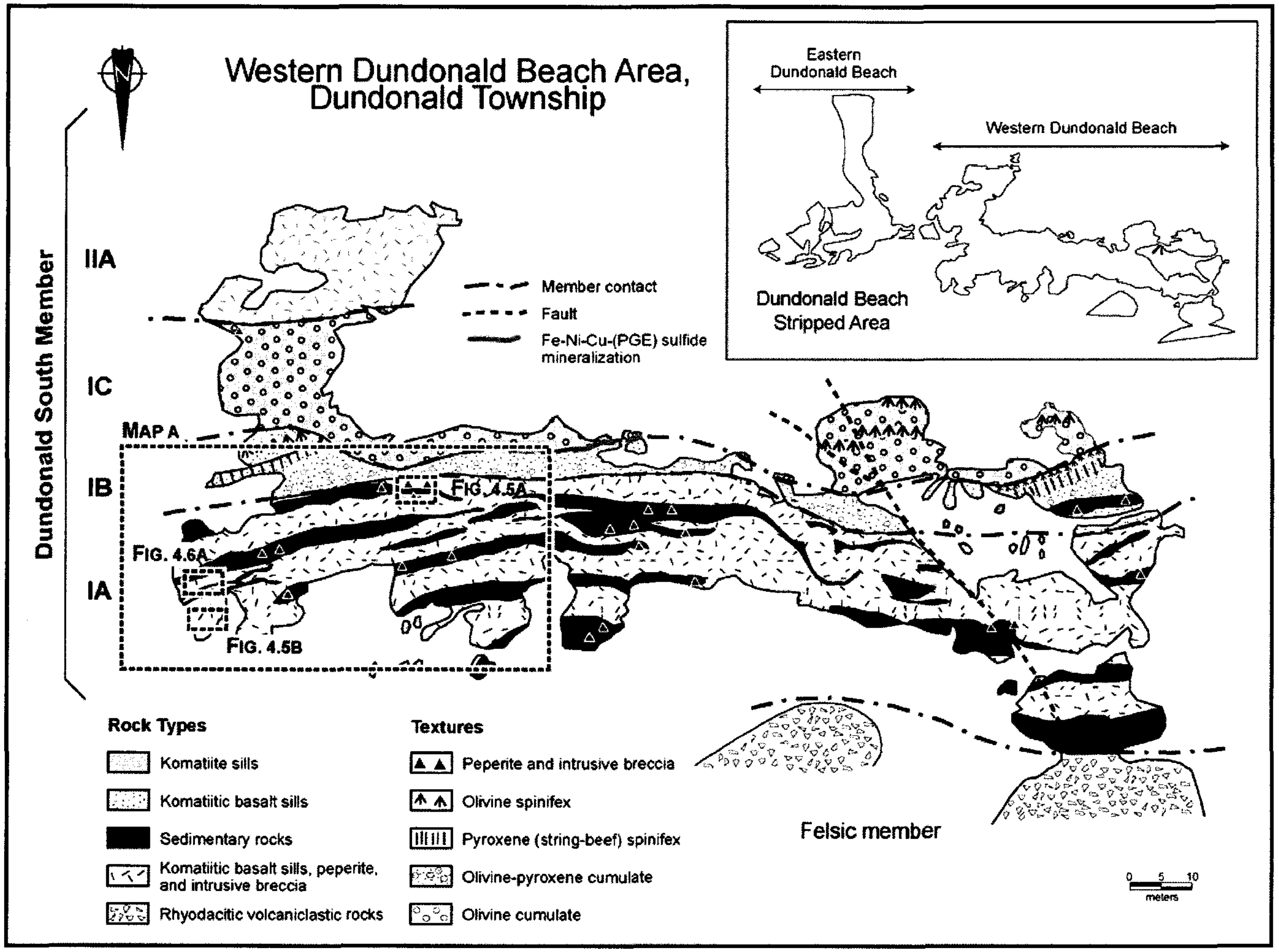

Figure 4.4 Simplified geologic map of the lower part of the Dundonald South formation at Dundonald Beach (modified from Davis, 1999 and Arndt et al., 2004). The map is drawn with north downwards so that the volcanic stratigraphy youngs upwards and corresponds to the geological sections. The outcrops in this area expose units IA, IB, and IC and unit IIA of the Dundonald South formation (UTM NAD 83, 511583E, 5386628N).

A reconstruction of the Dundonald formation, based on detailed mapping and core logging, indicates that it represents a progression from a dominantly subvolcanic intrusive lower part to a dominantly extrusive volcanic upper part (Fig. 4.3). Eruption and emplacement of komatiites was preceded by subsidence, as indicated by the accumulation of felsic volcaniclastic and argillaceous sedimentary rocks, which contain clasts of the komatiitic basalts and underlying volcaniclastic rocks, within a down-faulted basin or a topographic low (Davis, 1999: western section and central section; Fig. 4.3). The Dundonald formation displays not only a vertical lithofacies variation from sills to flows (dashed line in Fig. 4.3) but also a lateral variation, wherein portions underlain by volcaniclastic and sedimentary lithofacies are dominated by komatiitic sill lithofacies (western section and central section; Fig. 4.3) and portions underlain by coherent andesitic flow lithofacies grade from a komatiitic sill to a flow-dominated lithofacies (eastern section; Fig. 4.3). The Dundonald Beach area (western section; Fig. 4.3), which contains a thicker argillite unit, is interpreted to occur in the central part of the basin. The Dundeal area (central section; Fig. 4.3), which contains thinner argillite units, is interpreted to occur closer to the basin margin, and the Alexo area, which contains lesser, thin units of argillite and no felsic volcanic lithofacies, is interpreted to occur at the basin margin (eastern section; Fig. 4.3).

4.4 Discrimination between Komatiitic Sills and Flows

Interpretation of the emplacement of komatiitic rocks in Dundonald Township has changed over the years. They were initially interpreted by Naldrett and Mason (1968) as ultramafic intrusions, although they recognized that the skeletal "chicken track" textures that we now refer to as random olivine spinifex indicated a near-surface setting. Following the work of Viljoen and Viljoen (1969) in the Barberton Mountain Land and Pyke et al. (1973) in Munro Township, ~65 km to the east, all of the komatiitic rocks in the area were subsequently reinterpreted as flows (Muir and Comba, 1979; Schofield, 1982; Barnes, 1983). Davis (1997, 1999) identified and described mixed volcanic - graphitic sediment peperites, which were subsequently described by Cas and Beresford (2001) and Houlé et al. (2002a,b,c).

Distinguishing between an extrusive versus intrusive origin for a komatiitic unit requires detailed examination of the contact relationships of the komatiite with its enclosing rocks. Some textures and structures that are typically associated with lava flows, such as spinifex textures, amgydules, peperites along lower margins, and transgressive lower contacts, can occur in both extrusive and intrusive komatiites.

Other textures and structures such as flow-top breccias, hyaloclastites, and polyhedral jointing provide more reliable evidence for an extrusive mode of emplacement (Arndt et al., 2004). Development of peperite along upper margins and transgressive relationships with overlying units provide unequivocal evidence for an intrusive mode of emplacement (see discussions by Dann, 2000, and Arndt et al., 2004).

4.4.1. Intrusive Contacts and Transgressive Relationships

The komatiitic rocks within units IA and IC in the western part of the outcrop area at Dundonald Beach (Fig. 4.4; MAP A: BACK POCKET) have intrusive and transgressive contacts suggesting an intrusive origin. For the komatiitic units IB the situation is less clear because of poor exposure and also because its upper contact is interpreted to have been eroded by the overlying unit (IC).

The 0.2 to 4 m-thick komatiitic basaltic sills in unit IA have thin (1-2 cm) symmetric, upper and lower chilled margins that clearly cut other komatiitic basalt sills and invade the graphitic argillaceous sediments, forming fluidal and blocky peperite (Davis 1997, 1999; Cas and Beresford, 2001; Houlé et al., 2002a,b,c). However, some of the komatiitic basalt sills also transgress previous generations of peperite (Fig. 4.5A).

The komatiitic basalt sills at Dundonald Beach can be subdivided into two types. Type I sills are thin (<50 cm) and composed of fine-grained komatiitic basalt with variolitic interiors and sparsely variolitic margins. Their contacts are wavy and irregular with very thin (<1-2 cm) upper and lower chilled margins that are flow-banded parallel to contacts. Variolitic textures have been variously interpreted to reflect magma mingling, undercooling (i.e., spherulitic growths), devitrification, contamination, and alteration (see Fowler et al., 2002). The varioles in these sills appear to be related to localized alteration but may have resulted from original compositional and/or textural heterogeneities produced by contamination and/or undercooling. Type I sills appear to have interacted extensively with wall rocks and to have been injected at a stage before induration of the unconsolidated sedimentary strata (Fig. 4.5A). Type II sills are relatively thick (~4 m), composed of fine- to medium-grained komatiitic basalt, and have straight contacts with thin (~2-3 cm), fine-grained lower and upper chilled margins (Fig. 4.5B). They do not appear to have interacted extensively with their argillaceous wall rocks and are interpreted to have intruded later in the evolution of the sediment-sill succession.

Unit IC exhibits significant structural and textural variations over a strike length of ~150 m. In the southwestern part of the outcrop (Fig. 4.4), it comprises at least two cooling units. Only the lowermost is completely exposed, and it exhibits a ~1.5 m-thick upper olivine spinifex-textured zone and a ~4.5 m-thick lower olivine ortho-mesocumulate zone. To the east (Fig. 4.4), the same two sills have only very thin (0.5 m) upper olivine spinifex-textured zones. In the southeastern part (Fig. 4.4), unit 1C is a single ~20 m-thick sill composed almost entirely of olivine mesocumulate that clearly transgresses underlying komatiitic basalts (Fig. 4.4) and hosts small amounts of very high tenor Ni–Cu–PGE mineralization along its basal contact (Davis, 1999). Arndt et al. (2004) interpreted Unit 1C as a sill based on the absence of a flow-top breccia (polyhedral fracturing) along its upper contact, grain sizes at the margin that are greater than those in typical komatiite flows, and the occurrence of vesicles within 1 cm of the upper contact of the unit.

4.4.2. Peperite

Peperite is a rock formed essentially in situ by disintegration of magma intruding and mingling with unconsolidated or poorly consolidated, typically wet sediments (White et al., 2000; Skilling et al., 2002). Peperite occurs at the contacts of most komatiitic units within the lower part of the Dundonald South member but is best exposed within unit IA at Dundonald Beach where it occurs along the upper and lower contacts of komatiitic sills with graphitic sedimentary rocks (Fig. 4.4; MAP A: BACK POCKET). The formation of peperite during the emplacement of komatiitic magma into graphitic argillaceous sediments, not only along the lower but also along the upper contact, provides unequivocal evidence that the sedimentary strata were unconsolidated and wet at the time of intrusion and suggests that the intrusions are synvolcanic sills. Fluidal peperite and blocky peperite, which differ in juvenile clast morphology, and intrusive breccia have developed in decimetre- to metre-thick zones adjacent to the intrusions.

Fluidal peperite is characterized by amoeboid fragments and irregular fingerlike projections of variolitic, highly vesicular, and inclusion-rich komatiitic basalt within a matrix of desiccated graphitic argillite, and occurs as lobes within the argillite (Figs. 4.6A, 4.6C, and 4.7). Blocky peperite is characterized by blocky fragments of variolitic, highly vesicular, but inclusion-free komatiitic basalt within a matrix of desiccated graphitic argillite, and occurs as sheets within argillite.

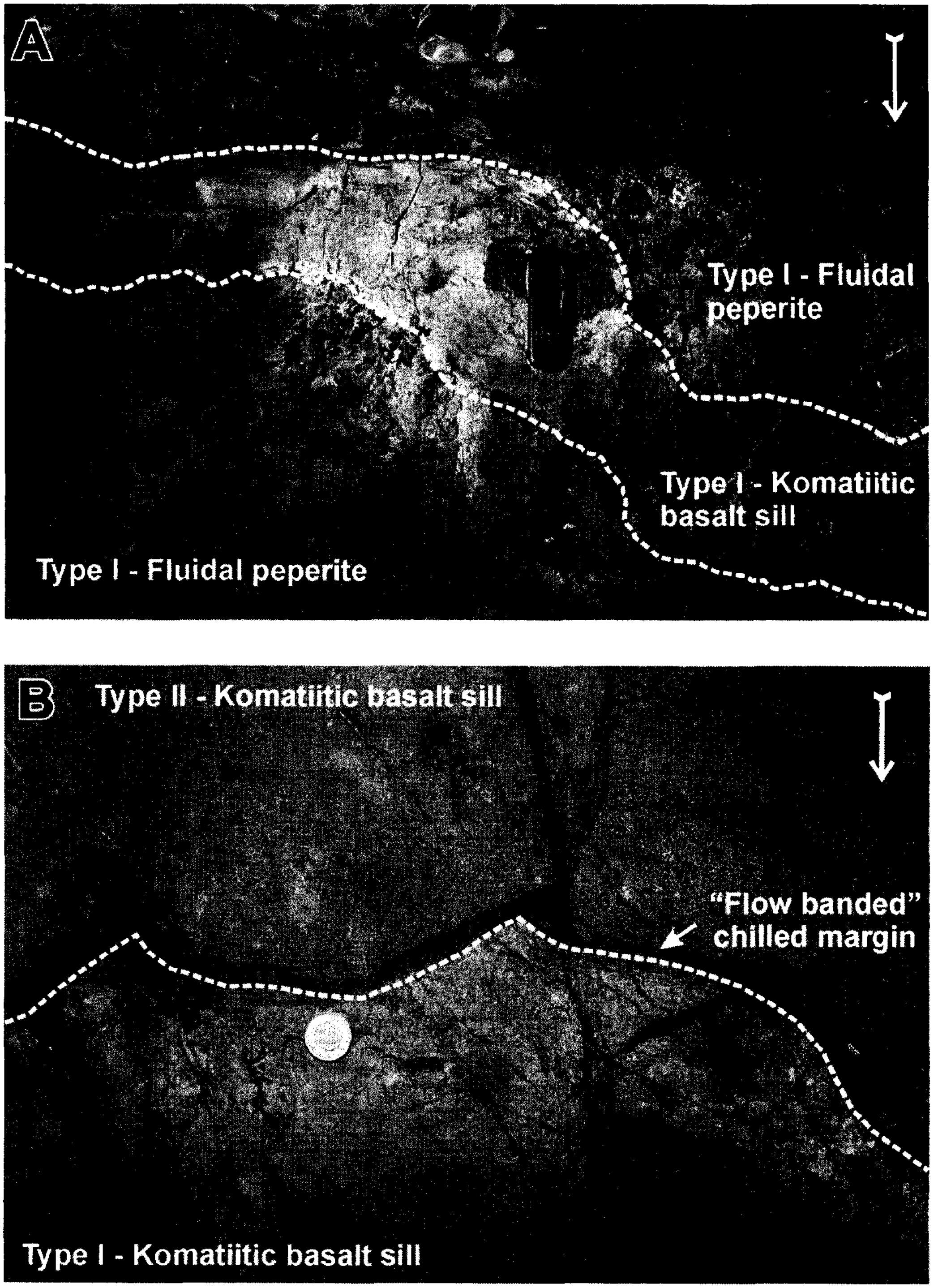

Figure 4.5 A) Type I komatiitic basalt sill transgressing komatiitic basalt - graphitic argillite peperite (UTM 511622E, 5386620N, NAD 83, Zone 17). B) Type II komatiitic basalt sill transgressing an earlier komatiitic basalt sill (UTM 511648E, 5386640N, NAD 83, Zone 17). The locations of A and B are shown in Figure 4.4. Arrows indicate the facing directions

Intrusive breccia occurs locally along the upper, and less commonly, lower contact of sills with argillites. This variety is characterized by angular, random, and jigsaw-fit clasts of desiccated graphitic argillite, in a white, silicified komatiitic basaltic matrix (Figs. 4.6A and 4.6B).

Fluidal and blocky peperite generally occur in close proximity and in many cases represent the products of two separate intrusive events. This relationship is well illustrated in Figure 4.7, which shows the distribution of blocky and fluidal peperite between two komatiite sills intersected in a drill core through unit 1C. The variolitic upper chilled margin of the lower sill is bordered by a zone of fluidal peperite containing dispersed, amoeboid fragments of komatiite with abundant fine-grained (1-3 mm) inclusions of graphitic argillite in a matrix of graphitic argillite. The chilled lower margin of the upper sill is bordered by a zone of blocky peperite containing angular jigsaw-textured fragments of inclusion-poor komatiitic basalt in a matrix of graphitic argillite (Fig. 4.7).

The development of either blocky or fluidal peperite has been interpreted by Busby-Spera and White (1987) to reflect the different rheological characteristics of the host sediment caused by differences in grain size, sorting, and water content. Both types of peperite develop in the same type of sediment at Dundonald Beach; formation of either blocky or fluidal peperite is interpreted to be strongly influenced by the degree of consolidation (rheology) of the sediment, which changed as a result of successive sill emplacement. Fluidal peperite is interpreted to have formed where sills were emplaced into wet unconsolidated sediment: this allowed the formation and maintenance of a vapor film at the magma-sediment interface, effectively insulating the ductile magma and allowing for irregular protrusion and mingling of magma and sediment to produce the irregular, amoeboid, globules typical of fluidal peperite (Squire and McPhie, 2002). Blocky peperite is interpreted to be a product of quenching and autobrecciation (mechanical fragmentation), which occurred where the komatiite intruded graphitic sediments (and peperite) that was partially dewatered and lithified by previous sill emplacement. The occurrence of peperite comprising a mixture of both blocky and fluidal clasts, which must have formed under different thermal and mechanical conditions, indicates that peperite formation at Dundonald Beach was a multistage process (see discussions by Squire and McPhie, 2002, and Skilling et al., 2002).

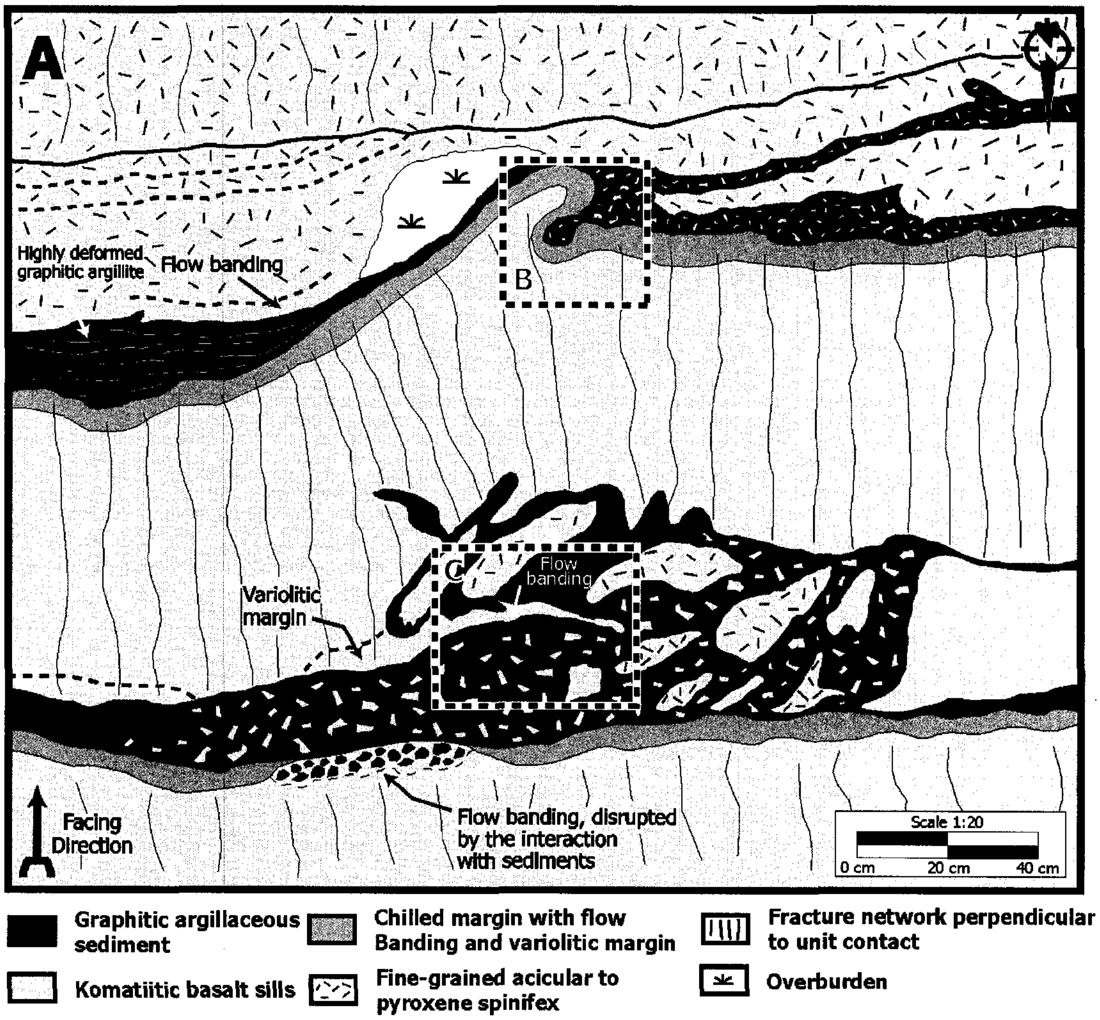

Figure 4.6 A) Detailed sketch of a komatiitic basalt sill (unit IA) bordered by fluidal peperite containing irregular apophyses of komatiitic basalt along the lower, and to a lesser extent upper, contacts of the sill (UTM 511642E, 5386631N, NAD 83, Zone 17). The irregularity of the upper and lower contacts of the sill and the presence of necked apophyses in the basal zone suggest that the peperite along both margins is the product of quench fragmentation by the intruding sill and was not produced during an earlier event.

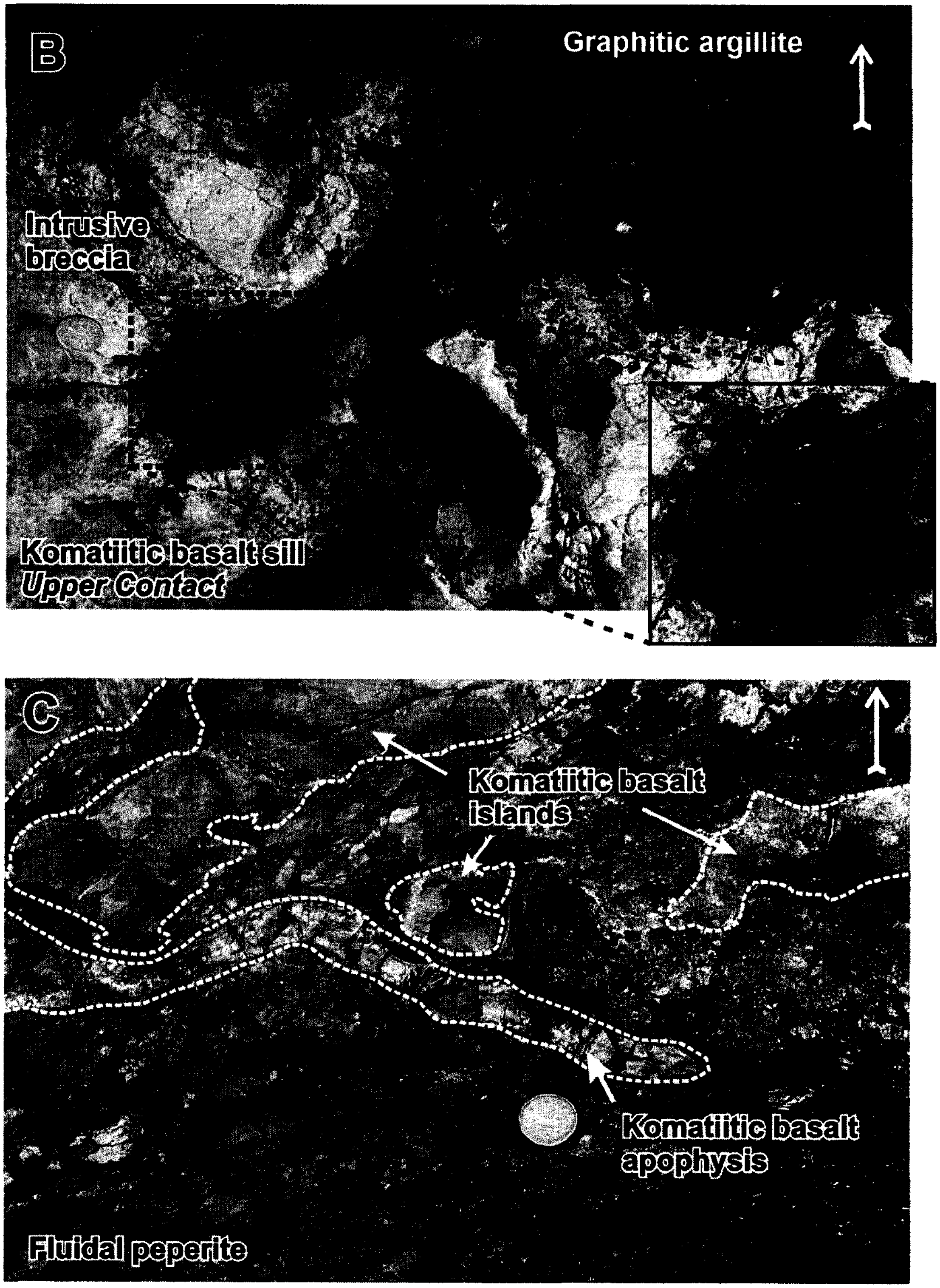

Figure 4.6 B) Intrusive breccia developed along the upper contact of a komatiitic basalt sill (UTM 511642E, 5386631N, NAD 83, Zone 17). C) Lobes and fragments of komatiitic basalt in a fluidal-blocky peperite (UTM 511642E, 5386631N, NAD 83, Zone 17). The location of Figure 4.6 is shown in Figure 4.3. Arrows indicate the younging directions.

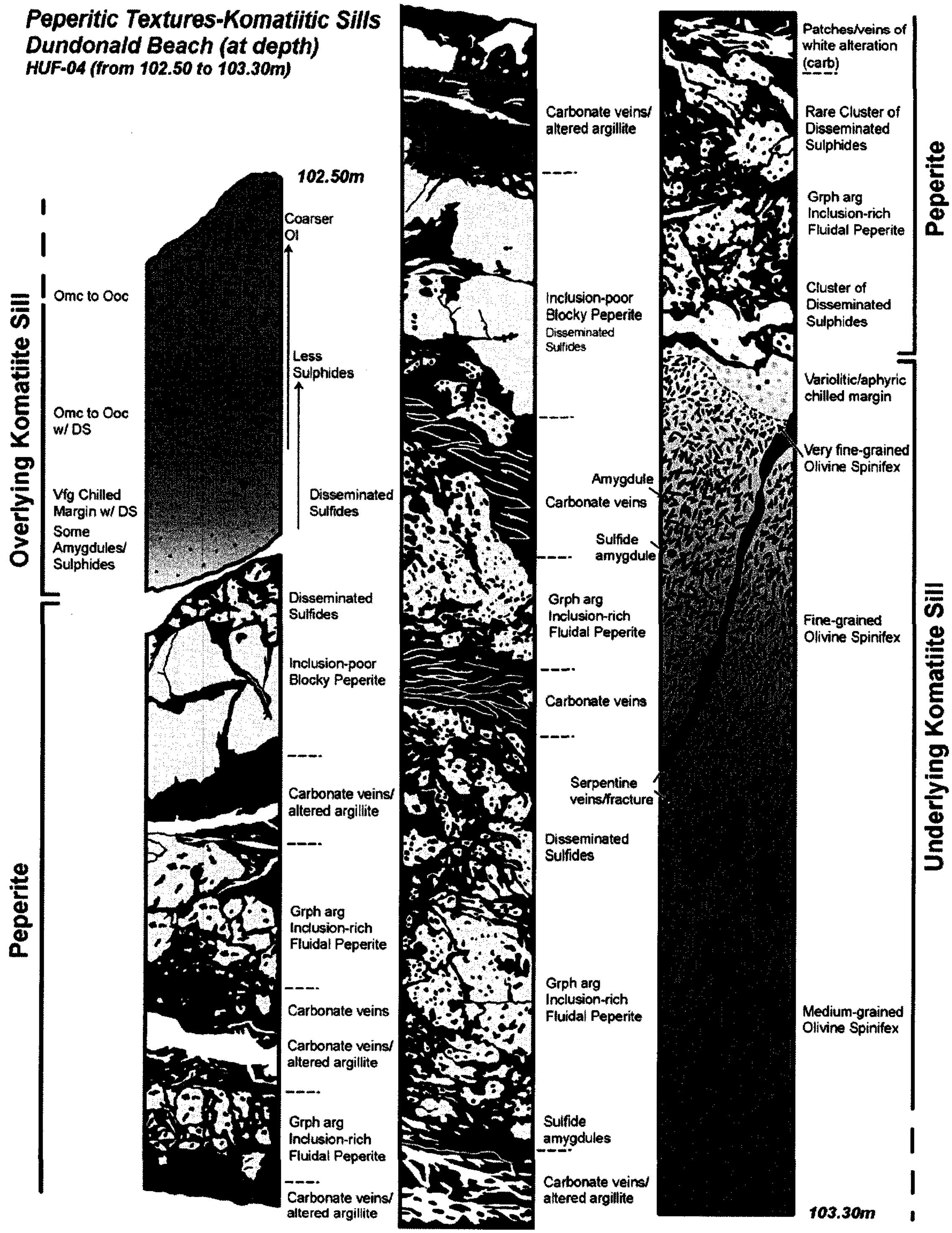

Figure 4.7 Detailed sketch of diamond drill core from drill core HUF-04 through subunit IC ~300m ESE of the Dundonald Beach outcrop, illustrating multi-genetrational peperite development adjacent to two komatiite sills. Omc: olivine mesocumulate, Ooc: Olivine orthocumulate, Vfg: very fine-grained, w/: with, carb: carbonate, D$: disseminated sulfides, Grph arg: graphitic argillite. Core width is 45 mm (NQ).

4.5 Discussion

The different geodynamic environments into which komatiitic magmas have been emplaced range from old continental crust overlain by thick sequences of basaltic strata (e.g., Kambalda), to continental margins containing a combination of basaltic and sedimentary strata (e.g., Bulawayan belt, Zimbabwe; Cape Smith Belt, Canada) to island arc/back arc settings containing a combination of felsic and mafic volcanic, volcaniclastic, and sedimentary strata (e.g., Abitibi Belt: Ayer et al., 2002). The bulk density of the crust and the density and rheology of the supracrustal rocks in these environments varies considerably, and it is the nature of the deep crustal rocks (cratonic or juvenile) and the tectonic environment (extensional versus convergent) that influences the rate of magma ascent and the location of magma emplacement (Lesher and Keays, 2002). However, in each of these environments the density and rheology of the near-surface rocks (lava flows and sedimentary rocks versus unconsolidated volcaniclastic rocks and sediments) governs the mode of emplacement (flows versus invasive flows versus sills/dikes). Thus, there is potential for a spectrum of komatiitic edifice types between those characterized by flow-dominated successions and those characterized by volcaniclastic and/or sediment-dominated successions. Recognizing that Ni-Cu-(PGE) deposits occur within the most magnesium-rich, channelized units (Lesher, 1989; Lesher and Barnes, 2008), we believe that the nature of the near-surface rocks is crucial determining the architecture of submarine komatiitic flow fields, their subvolcanic plumbing systems, and the location of Ni-Cu-(PGE) deposits.

4.5.1. Paleoenvironmental Constraints

Komatiites, tholeiitic basalts, andesites, and high-silica rhyolites of the Kidd-Munro assemblage have been interpreted as forming in a rifted arc (e.g., Jackson and Fyon, 1991; Wyman et al., 1999; Ayer et al., 2002). The presence of fine-grained, graphitic, sulfidic argillaceous sedimentary rocks and local exhalative Cu-Zn mineralization indicate a relatively deep-water environment (Davis, 1997, 1999), most likely an extensional, fault-controlled basin (Fig. 4.3). The occurrence of peperite along the margins of komatiitic sills and dikes at Dundonald Beach provides unequivocal evidence of a shallow subvolcanic environment of emplacement for at least the lower part of the Dundonald South member in that area (Fig. 4.4; MAP A: BACK POCKET).

4.5.2. Mechanisms of Emplacement

Cross-cutting relationships between sills and peperite indicate that the komatiitic basalts in unit IA were emplaced in at least 5 stages (Fig. 4.8).

Stage I: Formation of Type I peperite, consists of wispy, fluidal and blocky, highly vesicular and variolitic komatiitic basalt fragments (1-5 cm) mixed with nonlaminated graphitic argillite. Type I peperite occurs as irregular lenses several decimetres to several metres in size within otherwise argillaceous sediments. It is not associated with coherent sills and is interpreted to be a product of the total disintegration of an initial komatiitic basalt magma emplaced into unconsolidated argillite. The absence of bedding or delicate lamination within the argillite suggests that it was fluidized or partly fluidized during early sill emplacement, disintegration, and peperite formation.

Stage II: Continued emplacement of komatiitic basalt sills into unconsolidated argillite and Type I peperite produced Type II peperite. Type II peperite consists of a complex mixture of argillite and highly vesicular komatiitic basalt that cuts and engulfs Type I peperite and argillite.

Stage III: Emplacement of komatiitic magma into Type I and II peperite and associated partially-lithified sediment produced Type I sills, which are coherent and cross-cut earlier peperite. The occurrence of Type III blocky peperite along the upper and/or lower contact of these sills and angular, jigsaw-fit clasts of desiccated sediment in a silicified komatiitic basaltic matrix indicate that these sills were quenched and brecciated through interaction with the argillite.

Stage IV: Continued emplacement of komatiitic magma into earlier-formed Type I sills, Type I through III peperite, and argillite produced Type I sills that display only minimal development of peperite along their margins.

Stage V: Continued emplacement of komatiitic magma produced Type II sills with straight contacts and thin (~2-3 cm), fine-grained, lower and upper chilled margins that exhibit "flow-banding" but no trace of variolitic textures within their borders. The absence of intrusive breccias or peperite along sill margins and their straight and regular contacts indicate that Type II sills did not interact extensively with the argillaceous sediments and that the argillite was consolidated and dry. The end result of this intrusive history is the formation of a subvolcanic, sill-sediment complex characterized by multigenerational, crosscutting komatiitic basalts sills, peperite, and intercalated argillite (Fig. 4.8).

4.5.3. Volcanic and Subvolcanic Architecture

The changes in sill morphology, contact relationships, and sill-sediment interactions indicate a progressive change in the water content, density, and rheology of the host argillite in response to sill emplacement (e.g., Gibson et al., 2003). The disintegration of the initial komatiitic magma in Stage I, and the presence of abundant peperite, indicates that the argillaceous sediments were initially unconsolidated and water-saturated. The reduction in the abundance of peperite and the restriction of peperite to Type I sill margins in stages II to IV reflects progressive dewatering and consolidation of the argillaceous sediments, involving expulsion of water and cementation via growth of authigenetic minerals produced during accelerated diagenetic reactions driven by the heat of successive sill emplacement (e.g., Gibson et al., 1999, 2003). Type II sills cut across earlier sills and, less commonly, argillite and peperite, but did not generate irregular margins or peperite along their contacts. This indicates that the argillite was essentially lithified during the emplacement of Type II sills and that at this stage there were no significant rheological differences between the host argillite and previously emplaced sills. The occurrence of localized peperite along the upper and lower contacts of the thick, differentiated komatiitic basalt sill (subunit IB) (Fig. 4.4) indicates that it was emplaced into more consolidated sediments, after the emplacement of the thin undifferentiated komatiitic basalts sills in unit IA (Fig. 4.4). The thick, cumulate-textured komatiite sills of unit IC (Fig. 4.4) clearly transgress unit IB and an overlying argillite (not shown at the scale of Fig. 4.4), indicating that it postdates all of the underlying units.

The crosscutting relationships and variations in the mechanism of peperite and sill emplacement indicate that dewatering and lithification of the argillaceous sediments was progressive and resulted from the continuous emplacement of subvolcanic sills in a subseafloor environment. Sill emplacement and accompanying dewatering and lithification increased the density and modified the rheology of the sedimentary strata, resulting in substantial increases in bulk density and competency (Lesher and Keays, 1996; Burnham et al.,2003). A consequence is that successive komatiitic magmas would have reached progressively higher stratigraphic levels and eventually erupted at

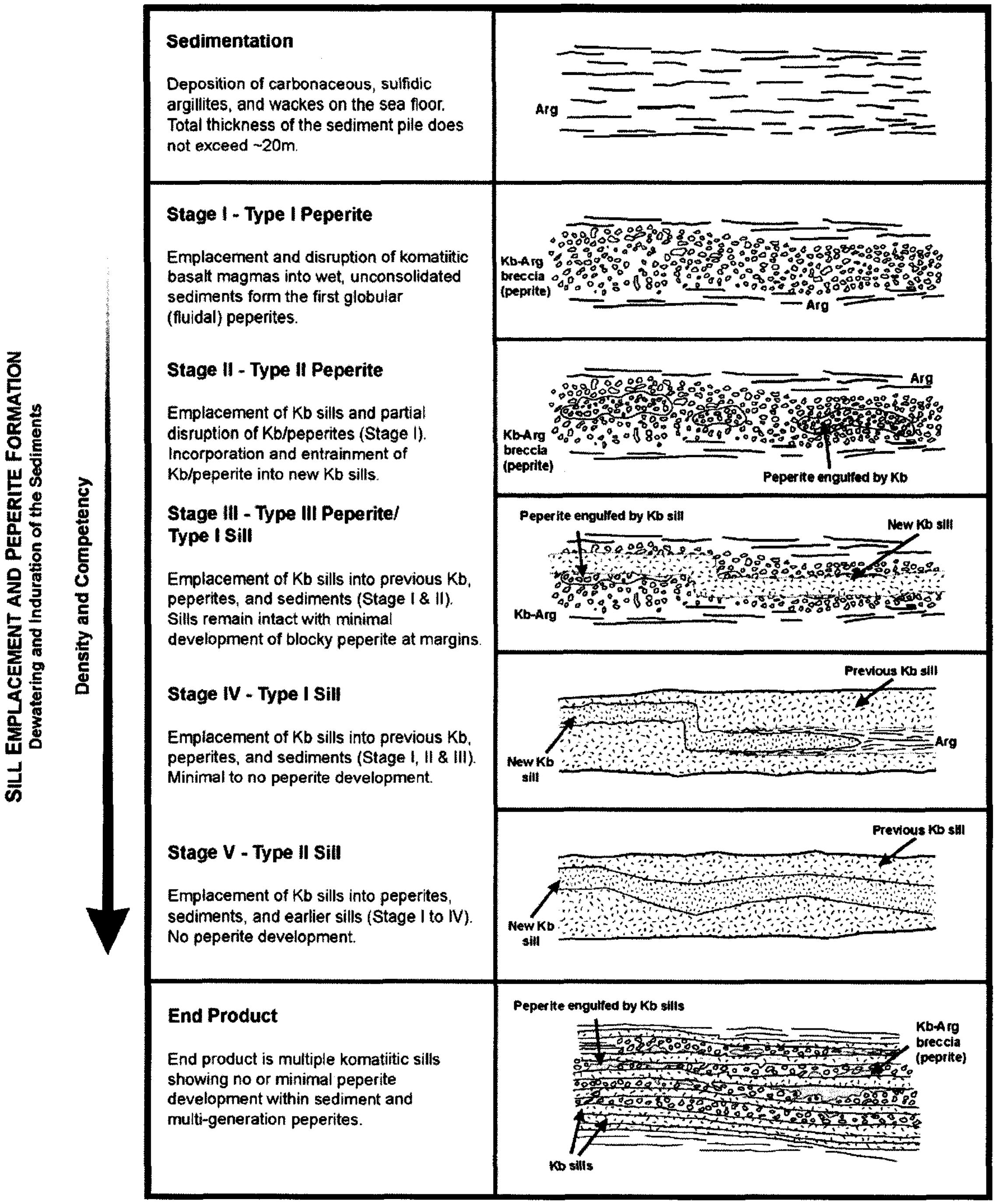

Figure 4.8 Conceptual model showing the evolution of sill architecture and concomitant peperite development at Dundonald Beach resulting from the multiple emplacements of komatiitic basalt sills within argillaceous sediments. The sequence formed in five stages (Stages I-V), produced by at least five generations of komatiitic basalt injections, three of which are manifested by sills and two, the earliest stages, are manifested by peperites. Kb: komatiitic basalt; Arg : argillite.

the surface (Fig. 4.9). The complex interactions between komatiitic sills and graphitic argillite at Dundonald Beach suggest a near-vent or proximal subvolcanic facies.

The sequence of events outline above has undoubtedly occurred in other komatiite-hosted Ni-Cu-(PGE) districts where near-surface rocks are dominated by unconsolidated sediments or volcaniclastic rocks resulting in the location of Ni-Cu-(PGE) mineralization within subseafloor sills (e.g., Mt. Keith, Western Australia: Rosengren et al., 2005; Raglan Belt, New Québec: Lévesque et al., 2003; Thompson Nickel Belt: Burnham et al., 2003; Pechenga Belt, Russia: Melezhik, 1994). This mode of komatiitic magma emplacement is significantly different from that in the Kambalda district of Western Australia, where the near-surface rocks are dominated by competent lava flows that would have produced surface eruptions rather than sill emplacement.

Because the physical characteristics of near-surface rocks play a critical role in the development of the architecture of subvolcanic/volcanic komatiite plumbing systems, the distribution of Ni-Cu-(PGE) mineralization associated with volcaniclastic/sediment-dominated successions should be different and more stratigraphically diverse than mineralization associated with flow-dominated successions where sulfur saturation is achieved through thermomechanical erosion of footwall rocks and mineralization is concentrated in lava channels, typically at or near the bases of the flow successions. The distribution of Ni-Cu (PGE) deposits and occurrences in the Dundonald area, within both flows in the upper part (Alexo) and sills above the base of the lower intrusive part (Dundonald South, Dundeal), may reflect sulfur saturation during sill emplacement that allowed Ni-Cu (PGE) mineralization to be concentrated within the subvolcanic plumbing system and within the overlying komatiitic flows. Thus, knowing the architecture of the komatiitic succession, whether intrusion-dominated or flow-dominated, allows one to predict the possible location and environments of Ni-Cu (PGE) mineralization.

Regardless of volcanic-subvolcanic architecture, Ni-Cu-(PGE) sulfide mineralization is almost always hosted within the most magnesian and channelized flows, invasive flows, or sills (Lesher and Keays, 2002). At Dundonald Beach the most magnesium-rich sills do not occur at the base of the succession but higher in stratigraphy, which may be interpreted to reflect density filtering of the more magnesian komatiite magmas prior to dewatering and lithification.

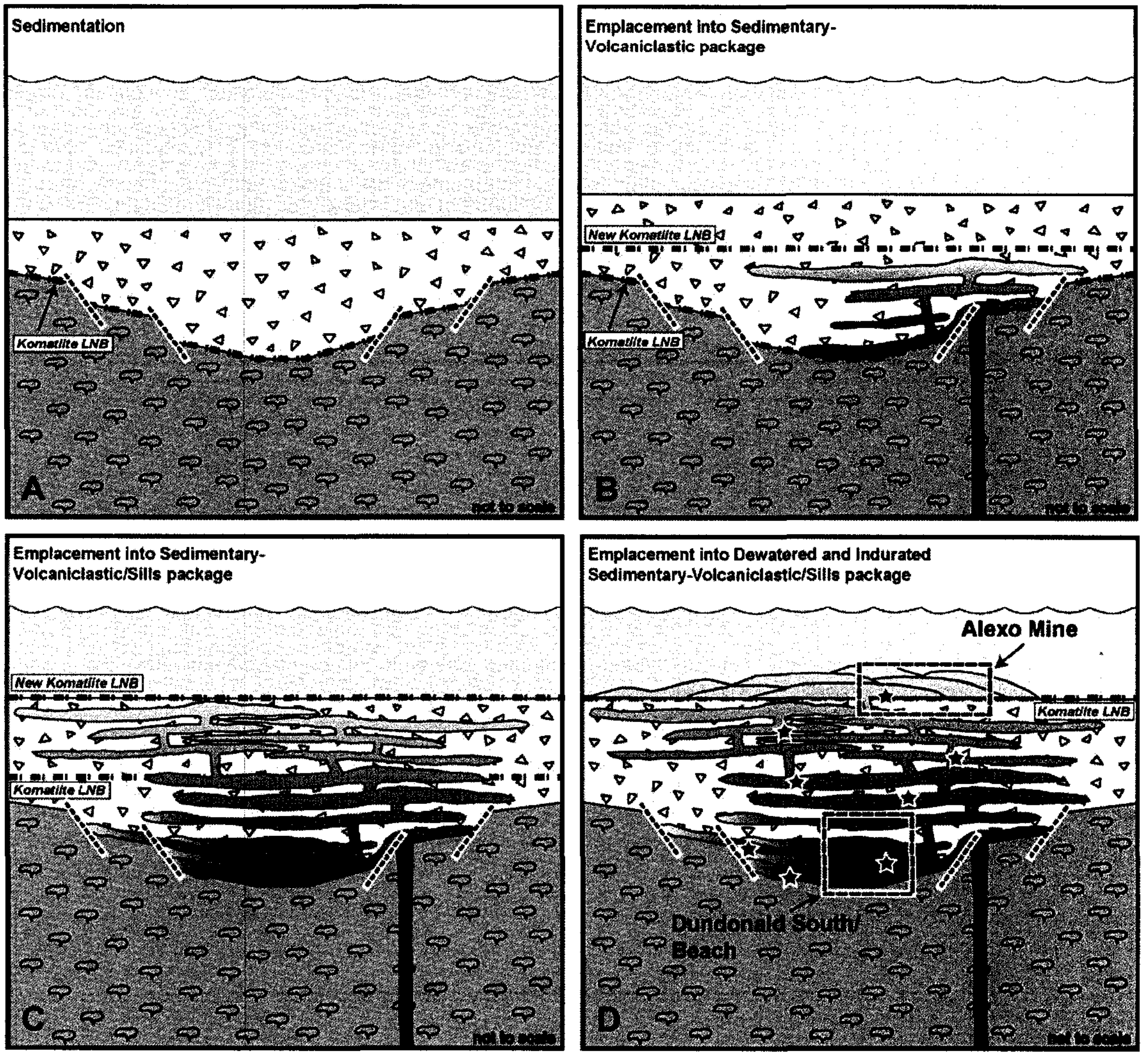

Figure 4.9 Idealized model showing the evolution of komatiitic subvolcanic/volcanic architecture (A-D) within a volcaniclastic/sediment-dominated komatiite volcanic environment (e.g., Dundonald Beach, Raglan). Dashed boxes in D represent the approximate location of Dundonald South/Beach and Alexo Mine within the komatiite volcano. Stars represent the potential location of komatiite-associated Ni-Cu-(PGE) mineralization in sediment/volcaniclastic-dominated succession. LNB: level of neutral buoyancy.

Importantly, the sequence of emplacement (and ore formation) may not necessarily be the same as the final stratigraphic sequence. Establishing the stratigraphy and understanding crosscutting relationships is crucial in terrains such as the Thompson Nickel Belt (Burnham et al., 2003), where more intense strain and higher grade metamorphism obscure the stratigraphic complexities. There is a great diversity in the architecture of komatiite volcanic-subvolcanic systems. Thus, when exploring for magmatic Ni-Cu-(PGE) deposits in volcaniclastic or sediment-dominated successions one must consider the possibility of mineralization in locations other than at the base of a komatiitic succession.

4.6 Conclusions

The temperatures, viscosities, and densities of magmas, the density of the crust, and the tectonic setting into which magmas are emplaced influence the location and morphology of volcanic systems. Close to the surface, the rheology and competency of the rocks controls the volcanic architecture of submarine lava flow fields, either komatiitic or tholeiitic. Where the near-surface strata are competent, such as environments dominated by flows, komatiitic magma erupts as flows (e.g., Kambalda). Where the near -surface strata are not competent, such as environments dominated by unconsolidated volcaniclastic rocks and sediments, komatiitic magma is initially emplaced as high level sills (e.g., Thompson, parts of Pechenga). Successive sill emplacement gradually lithifies and consolidates the volcaniclastic or sedimentary strata through the expulsion of water and cementation by secondary, diagenetic minerals. With time, the bulk density and competency of the sill-sediment/volcaniclastic package becomes sufficient to permit komatiitic magmas to reach the sea floor and erupt (e.g., Raglan, Dundonald, Shaw Dome, parts of Pechenga). With construction of a surface edifice, later komatiitic magma may eventually be emplaced as high level intrusions into a komatiitic volcanic pile (e.g., Shaw Dome, Abitibi greenstone belt: Houlé et al., 2006b).

Komatiites at Dundonald Beach erupted through juvenile crust and a thin sedimentary sequence. Low in the succession, they formed abundant thin subvolcanic sills; higher in the succession, they erupted as lava flows. The volcanic architecture and abundance of high-level subvolcanic komatiitic sills suggest a proximal to near-proximal volcanic environment.

Komatiite-associated Ni-Cu-(PGE) mineralization occurs in a wide variety of extrusive (e.g., Kambalda), invasive (e.g., Raglan), and intrusive (e.g., Thompson, Shangani, Dumont) environments (Lesher and Keays, 2002). Knowledge of the volcanic-sedimentary environment is required to predict the morphology/architecture of the komatiitic edifice and the location of Ni-Cu-(PGE) deposits in a komatiitic succession. In flow-dominated volcanic environments the highest potential for Ni-Cu-(PGE) deposits is where the komatiitic magma reached the surface and attained sulfur saturation through melting and/or assimilation of S-rich footwall rocks within large lava channels. In this environment Ni-Cu-(PGE) sulfides are more likely to form and be restricted to lava channels at the base of the komatiitic edifice. In volcaniclastic or sediment-dominated environments, the komatiitic magma may attain sulfide saturation by assimilation of sulfide-bearing sediments or volcaniclastic rocks during ascent and/or during emplacement as sills, provided that they remain channelized. In this environment Ni-Cu-(PGE) deposits are more likely to form in subsurface sills and within the overlying komatiitic flow succession.

Importantly, at Dundonald Beach, emplacement of thin basaltic komatiitic sills did not result in assimilation of sedimentary strata or achievement of sulfide saturation, probably because of an insufficient magma supply to melt and dissolve sulfur from the graphitic sediments. However, progressive lithification of the host sediments increased the bulk density and competency of the sill-sediment succession, permitting subsequently-intruded thicker channelized pyroxenitic and peridotitic komatiitic sills to thermomechanically-erode some komatiitic basalt sills and some of the graphitic, sulfidic argillaeous rocks, achieve sulfur saturation, and segregate Ni-Cu-(PGE) sulfide mineralization.

4.7 Acknowledgements

This paper is part of M. Houlé's PhD dissertation at Laurentian University and the University of Ottawa. Initial work at the Dundonald Beach stripping area was conducted by Falconbridge geologists (Nick Teasdale, PCD, Phil Vicker, and Al Coutts) following the stripping of the area in 1989, and by PCD in the 1990s as part of his M.Sc. thesis at the University of Alabama. We are grateful to our colleagues at Laurentian University (R.A. Sproule and P.C. Thurston), University of Ottawa (A.D. Fowler), Université Joseph Fournier (Y. Lacaze), Monash University (Nick Rosengren and Jesse Trofimovs), and the University of Maryland (A. Gangopadhyay) for their assistance and insights during visits to the Dundonald Beach exposure. We thank Falconbridge Ltd., Hucamp Mines Ltd., and First Nickel Inc. for providing access to field exposures, drill cores, and geological data. Kevin Montgomery is thanked for thoughtful discussions on the geology of the area. This research has been supported by a collaborative agreement between the Ontario Geological Survey and Mineral Exploration Centre (Laurentian University), Natural Sciences and Engineering Research Council of Canada operating grants to CML and HLG, "Fonds de la nature et de la technologie" fellowship, Hugh E. McKinstry Grant from the Society of Economic Geologist, and Graduate Scholarship from University of Ottawa to MGH, and a ARC operating grant to RAFC. Sergio Cattalani and Tom Hart are thanked for providing helpful comments on early draft of the paper. Steve Barnes, Wulf Mueller, John Ayer, and Mark Hannington are thanked for their reviews which helped to improve the final version of the paper.

CHAPTER 5 - ENDOGENOUS GROWTH IN KOMATIITE LAVA FLOWS: EVIDENCE FROM SPINIFEX-TEXTURED SILLS AT PYKE HILL AND SERPENTINE MOUNTAIN, WESTERN ABITIBI GREENSTONE BELT, NORTHEASTERN ONTARIO, CANADA

5.1 Abstract

Spinifex-textured sills (i.e., veins) characterized by komatiitic magmas that have intruded their own volcanic-piles have long been recognized. For instance, in the early 1970's, Pyke and coworkers, in their classic work at Pyke Hill in Munro Township, noted that not all spinifex bearing ultramafic rocks formed as lava flows, rather some were clearly emplaced as small dikes and sills. Several hypotheses have been proposed to explain spinifex-textured sills: intrusion into a cold host, filter pressing, or drainage of residual liquid. However, these do not satisfactorily explain the phenomenon. Field and petrogaphic observations at Pyke Hill and Serpentine Mountain demonstrate that the emplacement of spinifex-bearing komatiite sills and dikes are produced from inflation processes that resulted in the intrusion of new magma into cooler, semi-consolidated but permeable cumulate material. Komatiitic liquids were intruded into the olivine cumulate rocks near the boundary between the spinifex and the cumulate zones of komatiite flows. Spinifex-textured sills are generally tabular in morphology, stacked one above another, with curviplanar contacts sub-parallel to the stratigraphy. Some sills exhibit complex digitated apophyses.

Thinner sills typically have a random olivine spinifex texture similar, though generally composed of coarser crystals, to that of komatiite lava flows. Thicker sills exhibit more complex organization of their constituent crystals characterized by zones of random olivine spinifex, overlying zones of organized coarse spinifex crystals similar to that found in lava flows. They have striking coarse dendritic spinifex zones composed of very large olivine crystals, up to several centimetres long and up to 1 cm wide that are not observed in lava flows. Typically, at the sill margins, the cumulate material of the host flow is composed of euhedral to subhedral olivine crystals that are larger than those distal to the contact. Many of these margin-crystals have either concentric overgrowth shells or dendritic olivine overgrowths that grew from the cumulate-sill contact toward the sill interior. The dendrites grew on pre-existing olivine cumulate at the contact in response to a sharp temperature gradient imposed by the intrusion of hot material, whereas the concentric overgrowths formed as new melt percolated into the unconsolidated groundmass of the host-flow cumulate material. We postulate that the komatiite sills and dikes formed peripheral to lava pathways (channels/conduits) as a result of inflation that accompanied voluminous komatiitic eruptions. Thus, the occurrence of spinifex-textured sills and dikes may indicate proximity to, and aid in the identification and delineation of lava channel-ways that could potentially host Ni-Cu-PGE mineralization within subvolcanic-volcanic komatiite lava flow fields.

Keywords: Inflation, komatiite, spinifex sill, spinifex vein, Pyke Hill, Serpentine Mountain, Abitibi greenstone belt

5.2 Introduction

The ca. 2.7-Ga spinifex-textured komatiitic lava flows at Pyke Hill (Munro Township) and at Serpentine Mountain (McArthur Township) within the Abitibi greenstone belt are well known for their textural facies preservation. After Viljoen and Viljoen (1969) demonstrated the extrusive nature of ultramafic rocks within the Komati Formation of the the Barberton greenstone belt (South Africa), the classic internal subdivision (A zone: spinifex zone from A_1 to A_3 and B zone: cumulate zone from B_1 to B_4) was established (Pyke et al., 1973) for komatiite lava flows at the Pyke Hill exposure in Munro Township. Although many concordant ultramafic units containing spinifex textures are clearly extrusive, the nature (extrusive vs intrusive) of many of spinifex-bearing units is still debated. Although, initial determinations of intrusive or extrusive character were often based upon the presence of spinifex texture, Donaldson (1974) pointed out early that the texture itself was not a sufficiently strong criterion.

Spinifex texture is not a "quench" texture because it forms deep (dm-m) within komatiite flows, well below the upper chilled crust. The cooling rate below the chilled crust, within the A_3 layer (~2 m below), should be low (<1-5°C/h) whereas the spinifex crystals found within this layer reflect a much higher cooling rate (>50°C/h) based on experiments by Donaldson (1976; 1982). This discrepancy is recognized as the "spinifex paradox". Spinifex arises from crystal growth that is a result of development within a high gradient of chemical potential. In lava flows or high-level sills, it is believed that this high chemical potential gradient is provided by a thermal gradient or a gradient in chemical composition, or both.

Indeed, Shore and Fowler (1999) demonstrated that the well-organized arrays of spinifex likely result from constrained crystallization because of the efficient and anisotropic transfer of heat along forsterite's *a* crystallographic axis. Essentially favourably oriented crystals self propagate by efficiently transferring heat from, and cooling the melt in front of their tips, sustaining more growth and so on. These feedback mechanisms are the hallmark of self-organizing systems that produce patterns such as the well-organized spinifex olivine of komatiites. Faure et al. (2006) have recently reproduced olivine spinifex texture in the laboratory by growing it in a thermal gradient. In addition Grove and Parman (2006) reproduced large spinifex crystals at slow cooling rates in experiments under hydrous conditions where exsolution of volatiles (dominantly H_2O) decreased the nucleation rate and enhanced crystal growth thus creating an effective undercooling. Clearly the details of spinifex textured olivine formation remain unanswered. However, crystal growth of olivine in komatiites probably results in large part by a thermal gradient supported by the facts that the geometry of the texture is commonly related to the cooling margin and also because they are restricted to volcanic and high-level intrusive environment of emplacement.

Spinifex-textured sills, reported previously in the literature as "spinifex-textured veins" (e.g., Champagne, 2004; Scott et al., 2002; Grove et al., 1997; Pyke et al., 1973), are sub- to concordant igneous bodies that intrude earlier-formed komatiite flows and are an integral part of extrusive sequence. The term "vein" is not used in this contribution because, in our experience, it generally refers late stage secondary rather than magmatic processes. Furthermore, the term is not recommended for igneous features by the American Geological Institute. The nature of the spinifex-textured sills is not subject to debate but their mode of emplacement is poorly constrained. The exceptional exposures and degree of preservation at Pyke Hill and Serpentine Mountain, as illustrated in this paper, provide a unique opportunity to study volcanological processes at the outcrop- (macroscopic-scale) and microscopic-scales to better understand the mode of emplacement of spinifex-textured sills and komatiite flows.

Since no historic submarine komatiite (or komatiitic basalt) eruptions have been observed, our knowledge of the styles of emplacement of komatiite lava flows relies almost entirely on comparisons with modern subaerial basaltic lava flows. Inflationary processes are the dominant emplacement mechanism of modern pahoehoe basaltic lava flows on low slopes (Kauahikaua et al., 2003). Inflation is the continual growth of a lava flow by uplift of the upper crust from underneath by a molten interior that is continually replenished by fresh lava some of which is also transferred to the advancing flow front. Initially the concept of inflation was introduced by Walker (1991) and Chitwood (1994). The concept was subsequently complemented by close observations of newly emplaced pahoehoe lava flow (Mattox et al., 1993; Hon et al., 1994), by experimental study of inflating pahoehoe sheet flows (Hon et al., 1994), and by detailed geological mapping of large igneous provinces (Self et al., 1996; 1997; 1998). Pioneering research conducted by Hill and Perring (1996), Cas et al. (1999), Beresford et al. (2000a), Hill (2001), and Dann (2000; 2001) recognized "inflation features" within archean komatiite lava flows in Western Australia (Yilgarn craton) and South Africa (Barberton greenstone belt).

The purpose of this paper is to describe detailed field and petrologic relationships between komatiitic spinifex-textured sills and komatiite flows, at Pyke Hill (Munro Township) and Serpentine Mountain (McArthur Township), in order to better understand the physical volcanology of komatiite lava flows and their mode of emplacement. The morphology of the spinifex-textured sills and overgrowths (shell and dendritic) at their margins are interpreted to have formed by pulsed inflation and endogenous growth similar to modern pahoehoe lava flows (Anderson et al., 1999). It is also interpreted herein that these small pulses of komatiitic magma were injected beneath an insulated upper crust (i.e. spinifex-textured zone) into partly consolidated, hot komatiite lava flows in the vicinity of buried lava pathways/lava tubes during inflation of channelway.

5.3 Methodology

Detail geologic mapping was conducted between 2002 and 2004 and several sections of komatiitic sills and their host rocks were mapped at Pyke Hill (2 sections) and Serpentine Mountain (2 sections), at scales ranging from 1:25 to 1:50. The outcrops were first manually stripped and cleaned of overburden and lichen. In order to document all contact relationships and textures, slab samples (typically 20cm x 5cm x 5cm) were taken from komatiitic sills and the surrounding rocks using a portable diamond-blade saw. Approximately 15 such specimens were collected from different komatiitic sills for this study. A total of about 30 polished thin sections were prepared for microscopic observation, imaged and studied in detail.

5.4 Geological Setting

The Abitibi greenstone belt of the Superior Province is one of the largest and best-known Archean cratons. Its supracrustal rocks consist of well-preserved successions of Archean lavas and sedimentary rocks, which were developed in an ensimatic basin (Ayer et al., 2002). In general, the rocks are characterized by low metamorphic grades (e.g., lower greenschist facies and prehnite-pumpellyite facies: Thompson, 2005; Jolly, 1982) and are relatively unstrained except in the vicinity of deformation zones. Locally higher metamorphic grade rocks are found near large plutons. The volcano-sedimentary sequence has been divided into six volcanic-dominated and two sediment-dominated lithotectonic assemblages (Fig. 5.1). Thus far, komatiitic rocks are only recognized within four of these assemblages: the Pacaud (2750-2735 Ma), the

Stoughton-Roquemaure (2723-2720 Ma), the Kidd-Munro (2719-2711 Ma), and the Tisdale (2710-2704 Ma) assemblages.

The volcanic succession at Pyke Hill (Munro Township) is part of the eastern portion of the Kidd-Munro assemblage and is located ~90 km east of Timmins adjacent to the former Potter Mine. Here, the komatiitic-tholeiitic volcanic rocks are folded by a km-scale northwest-trending anticline (Houlé et al., 2000; Oliver et al., 1999) and are subdivided into three units - from oldest to youngest: 1) the "Lower Komatiitic Unit" (dominated by komatiite flows), 2) the "Middle Tholeiitic Unit" (dominated by basaltic volcaniclastic deposits with lesser komatiite flows/sills); and 3) the "Upper Komatiitic Unit" (dominated by komatiite flows) (Gamble, 2000).

The volcanic succession at Serpentine Mountain (McArthur Township) is part of the Tisdale assemblage located within the Bartlett Dome ~40 km south of Timmins. The volcanic-sedimentary succession is composed of a lower sequence of calc-alkalic intermediate to felsic volcanic rocks, a central sequence of komatiitic rocks, and an upper sequence of tholeiitic mafic volcanic rocks, respectively, interpreted to be a part of the Pacaud, the Deloro and the Tisdale assemblages (e.g., Houlé, 2006). The volcano-sedimentary succession in the Bartlett Dome is intruded by intrusions of a wide range of compositions (ultramafic, mafic and felsic) (e.g., Houlé, 2006; Houlé and Solgadi, 2007).

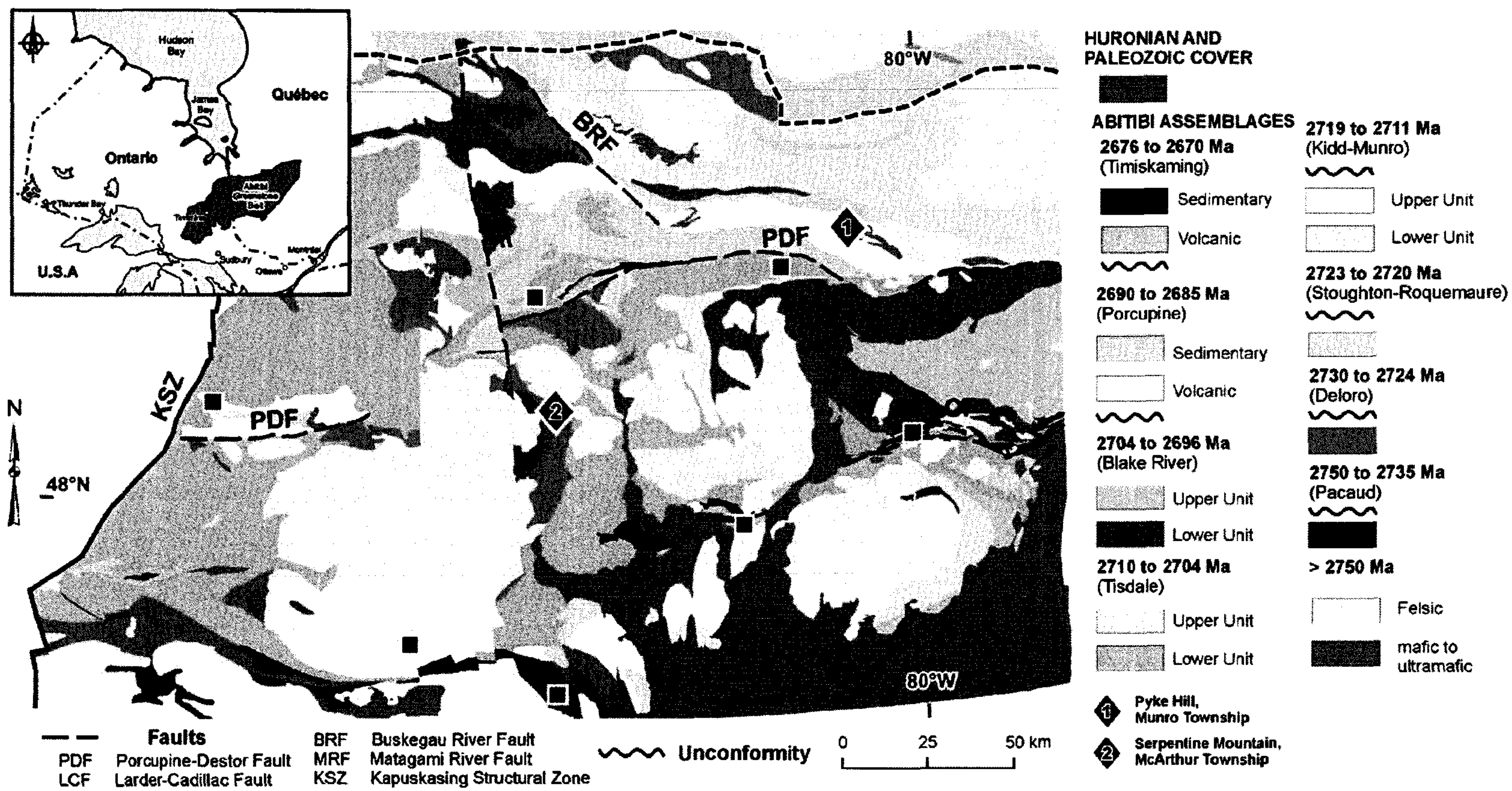

Figure 5.1 Simplified lithotectonic assemblage map of the western Abitibi greenstone belt in the Timmins and Kirkland Lake area showing the location of study areas (modified after Thurston et al., 2008).

5.5 Field Relationships

5.5.1. Pyke Hill, Munro Township

Pyke Hill, located in the northeastern part of Munro Township within the Upper Komatiitic Unit at the Potter mine, represents one of the best preserved and exposed sequences of thin spinifex-textured and massive komatiite flows known. Pyke and co-workers (1973) were first to describe the komattite flows and the spinifex bearing sills and dikes here. Sixty flows are exposed over a width of ~125 meters. They are typically about 3m thick but individual flows range from 0.5 to 15 meters in thickness. The relative proportions of spinifex-textured "A" zones and cumulate-textured "B" zones vary within and between individual flows.

Figure 5.2 is a geological map of Pyke Hill based on previous work by Pyke et al. (1973), Arndt et al. (1977) and our work. In the following discussion, the Pyke Hill outcrop is divided into a "Northern block" and a "Southern block" separated by a NW-SE trending fault (Fig. 5.2).

The nomenclature used in this paper to characterize internal textural variation within komatiitic rocks is adapted from Arndt et al. (1977). They suggest that classical komatiitic flows as described by Pyke et al. (1973) represent one end-member of a continuum from well-organized flows (exhibiting all the structural and textural subdivisions as described by Pyke and co-workers) to non-organized flows (massive flow devoid of spinifex textures). For example, a well-organized flow is internally layered with a spinifex-textured (A zone) in the upper part and a cumulus-textured (B zone) in the lower part of the flow. The A unit may be further subdivided into the A_1 (fractured upper chill zone–flow-top breccia–microspinifex), A_2 (randomly oriented spinifex), and A_3 (coarse platy spinifex) zones. The B zone may be further subdivided into the B_1 (aligned skeletal « hopper » olivine), B_2 (medium- to coarse-grained cumulate), B_3 (knobby cumulate), and B_4 (fine-grained cumulate and basal chill) zones. An organized flow is composed of A and B zones, and exhibits a thick spinifex zone, but internal subdivision such as the knobby cumulate (B_3) and skeletal olivine (B_1) zones are missing. A poorly organized flow consists of flows that developed limited spinifex textures. The flow unit can still be subdivided into an A zone and a B zone. However, the A zone is generally composed of thin A_1 and A_2 zones underlain by a thicker B zone that is generally composed of *olivine cumulate to olivine porphyritic* rich rocks. A non-organized flow is completely devoid of spinifex texture. These flows may be characterized by abundant polyhedral joints near the top (corresponding to the A zone), which become sparse and gently curved toward the centre and bottom of the flows. The B zone is generally composed of olivine porphyritic rocks, but, in general, contains less olivine than the B zone associated with more organized flows.

The western part of the Northern block at Pyke Hill comprises (from base to top): very thin (~0.75 to 2.5m) well-organized sheet flows, thick (~4 to 12m) well-organized sheet flows and thin (~3 to 4.5m) well-organized sheet flows. The uppermost section is characterized by thin sheet flows that have conspicuous textural-differentiation and represent the komatiite flow archetype described by Pyke et al. (1973) that include all the internal subdivisions (A_1 to A_3 zones and B_1 to B_4 zones) within the Area A (Fig. 5.2).

The eastern part of the Northern block at Pyke Hill comprises a series of thin (~2 to 3.5m) organized sheet flows overlain by flows having poorly defined cooling margins and little textural or structural organization. Zones of polyhedral jointing and autobreccia are prevalent. Here, the rocks are commonly intruded by spinifex-textured sills and dikes. Spinifex-textured sills (i.e. spinifex veins of Pyke et al. 1973) also occur within the western part but are uncommon (Fig. 5.2).

The Southern block consists of (from base to top): thick (~6.5 to 16m) organized sheet flows, thin (~2.5 to 4.5m) organized sheet flows, thick (~5.5 to 13.5m) organized sheet flows overlain by thin (~0.75 to 2m) organized sheet flows. Most of the komatiite flows, especially thicker ones, are not as texturally or structural organized as those of area A (Fig. 5.2). Furthermore, within the uppermost section of the Southern block (Area B, Fig. 5.2), komatiite flows also occurs as thin lobate sheets flows and flattened pillows facies that exhibit only limited spinifex textures along their cooling margins.

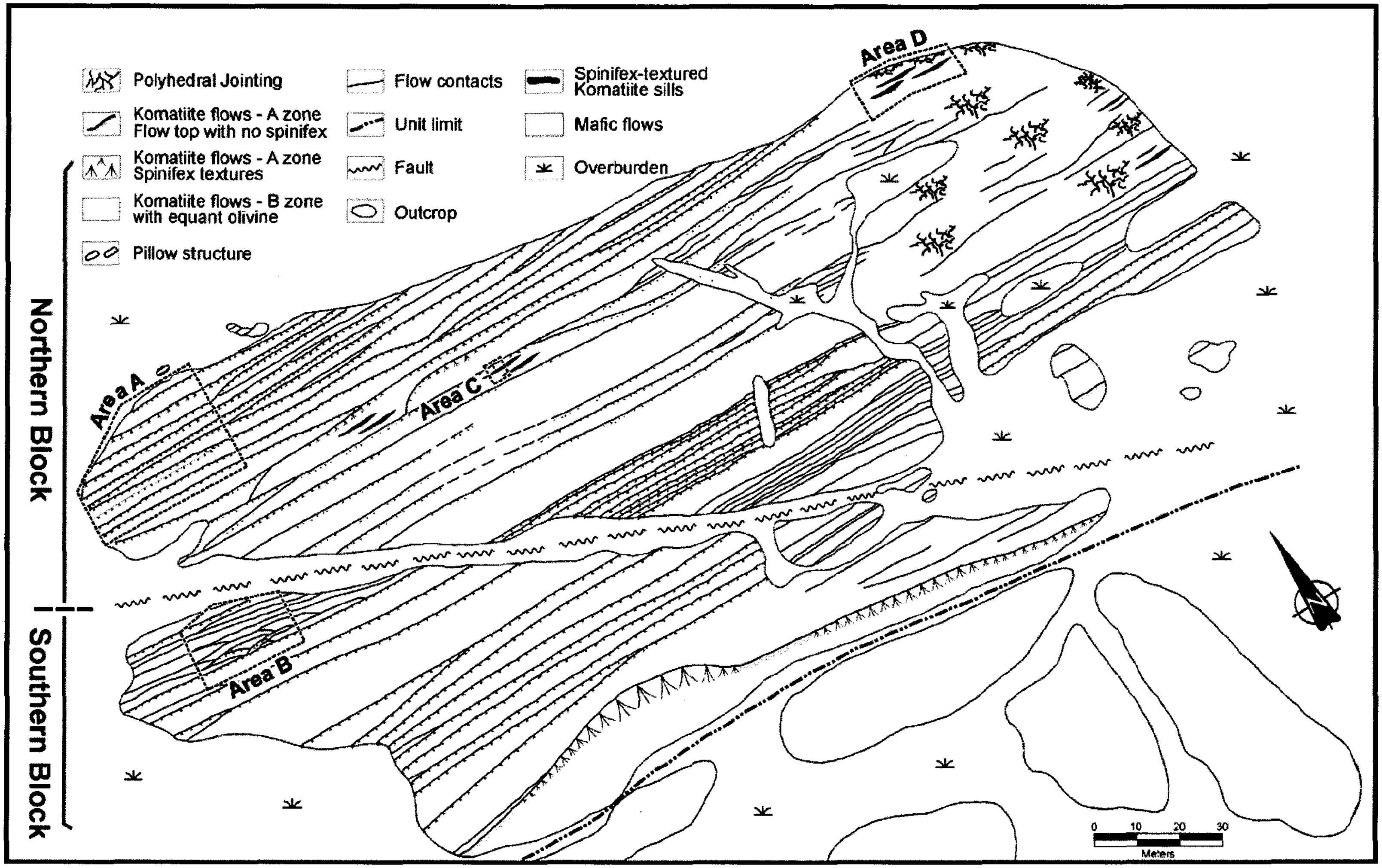

Figure 5.2 Geological map of Pyke Hill in Munro Township (modified after Pyke et al., 1973; Arndt et al., 1977).

5.5.1.1. Area C - Western Part of the Northern Block

The detailed map in Figure 5.3 provides details of a stripped and cleaned outcrop exposure containing several komatiite sills (Area C, Fig. 5.2). The host flow is a relatively thick (~13m), organized flow having a ~10 m thick olivine cumulate zone overlain by ~2.5 m thick spinifex-textured zone composed of randomly oriented, fine-grained olivine and approximately ~0.25 m of flow-top breccia. The spinifex is composed of individual blades and small "booklets" that grade from about 1-2 mm in length near the flow top, to greater than 2mm approximately one meter from the upper contact.

The sills which range from approximately 2 to 20 cm in width, stand out in positive relief, and occur in the upper part of the olivine cumulate and at its contact with the spinifex zone where they form a complex network (Fig. 5.3). Locally the cumulate crystals of the host-flow are coarser-grained immediately adjacent to the sill contacts than elsewhere within it. The spinifex crystals within the sills are homogeneously distributed and are generally oriented at high angles to the sill contacts from which they propagated (Fig. 5.4). The komatiite sills are commonly tabular shaped, stacked one above another, and have curviplanar contacts sub-parallel to the stratigraphy. The contact between sills and the host cumulate zone of the flow is always sharp and unequivocal as observed on figures 5.3 and 5.4. However, where the sills are in contact with the spinifex-textured zone of the host flow, the contact is not sharp and is difficult to trace along strike. On the figure 5.3, the contact between the sill and the spinifex-textured zone grades from sharp (a) to diffuse (b). This variation might be explained by the similarity between the two textural facies (spinifex vs. spinifex; similar grain size in b). The contact also fades out within the area c (Fig. 5.3). However, this contact does not represent the boundary between the spinifex-textured sill and the host flow but rather correspond to the contact between the spinifex and cumulate zones of the actual komatiite flow. This gradational contact rather than sharp between those two zones is not a common feature within komatiite flows at Pyke Hill. Their origins remain unclear but are not to be addressed here.

The thicker sills exhibit numerous apophyses that all terminate westward. Locally, the olivine cumulate has been completely engulfed by the sills resulting in the formation of residual patches of cumulate material. The apophyses and patches are interpreted to have resulted from a fingering process during intrusion of the komatiite sills, and the terminations of the apophyses demonstrate the sills were emplaced from east to west.

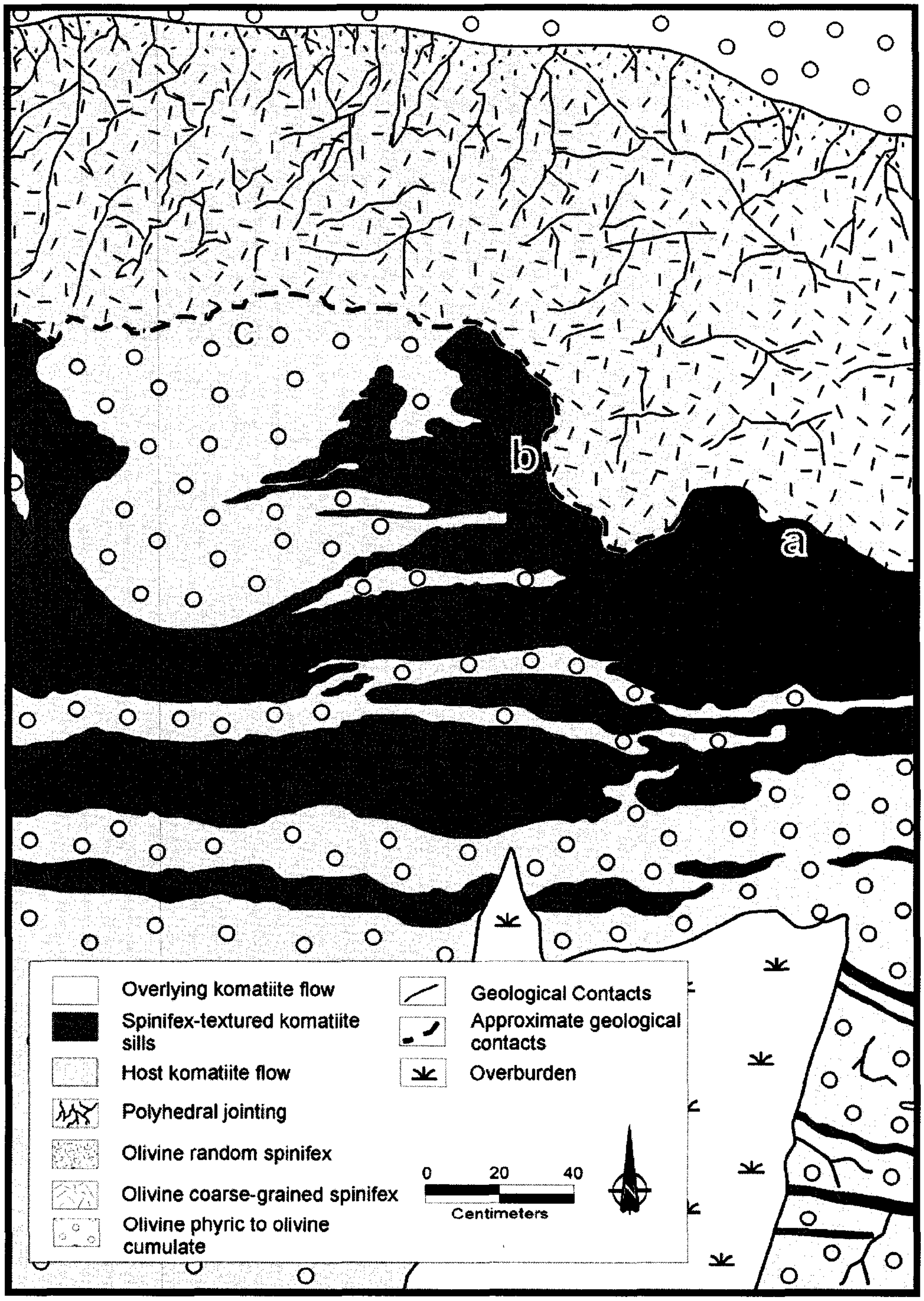

Figure 5.3 Detailed geological map of the Area C in the Northern Block at Pyke Hill, Munro Township (UTM 559130E, 5383150N, NAD 83, Zone 17). See in text for details of a, b, c. Location also on Figure 5.2.

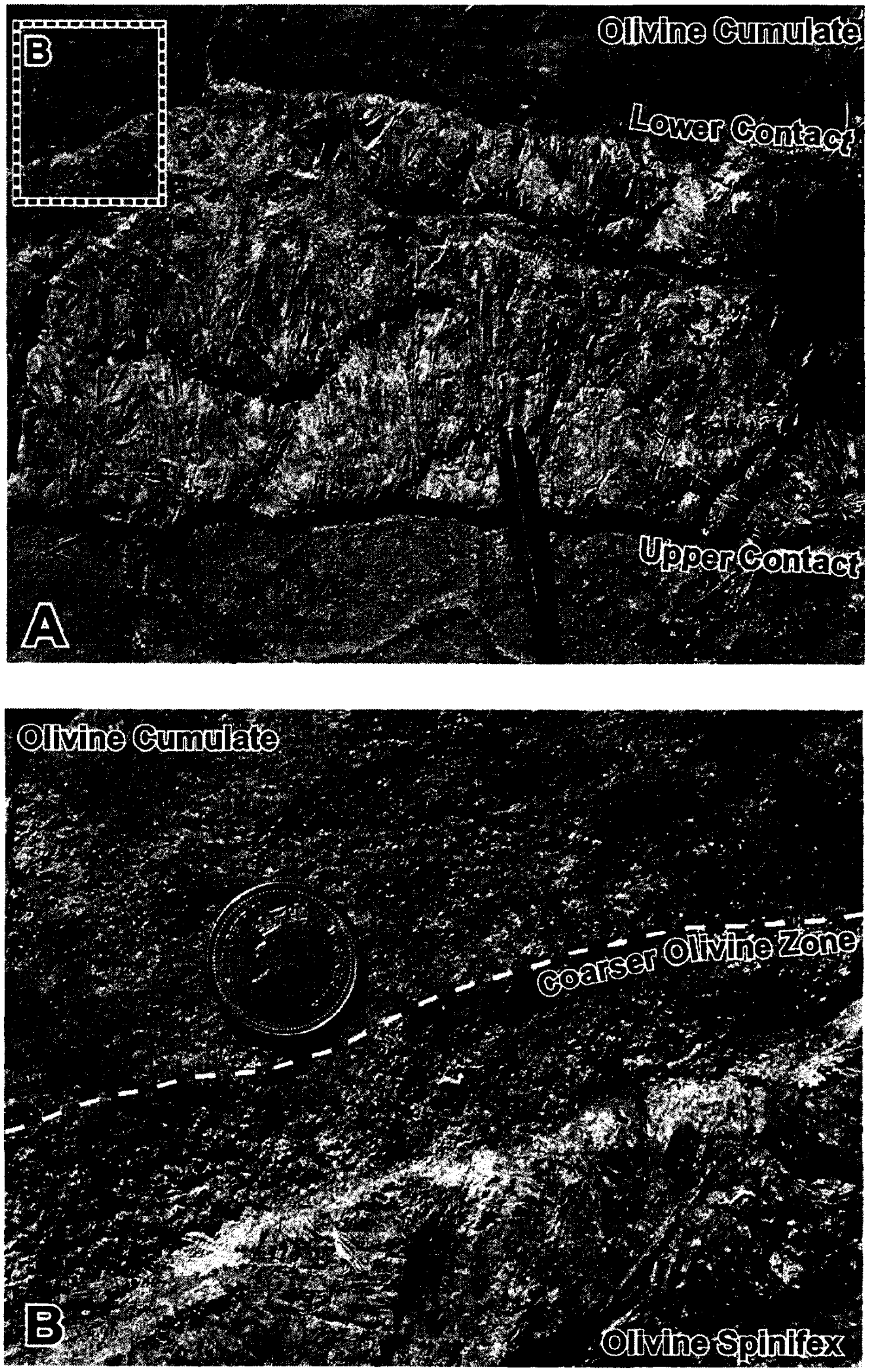

Figure 5.4 Olivine spinifex-textured sill at Pyke Hill within the Area C. A) Photograph showing spinifex crystals oriented at high angles to the sill contacts (pen for scale). B) Photograph showing the coarsening of olivine crystals within the cumulate zone of the flow near the contact with the komatiite sill. Close up of Figure 5.4A. Coin is 2.4cm in diameter.

5.5.1.2. Area D - Eastern Part of the Northern Block

The geological map in Figure 5.5 provides details of a stripped and cleaned outcrop section in the eastern part of the Northern block that exposes several komatiite dikes and sills (Area D, Fig. 5.2). Despite outcrop stripping and cleaning cooling boundaries of the host-flow were not observed. This komatiite flow, as exposed, is at least 5m thick and consists entirely of olivine cumulate. It has pronounced polyhedral jointing that occurs as meter-scale patches in the cumulate material toward the stratigraphic top (Fig. 5.6A).

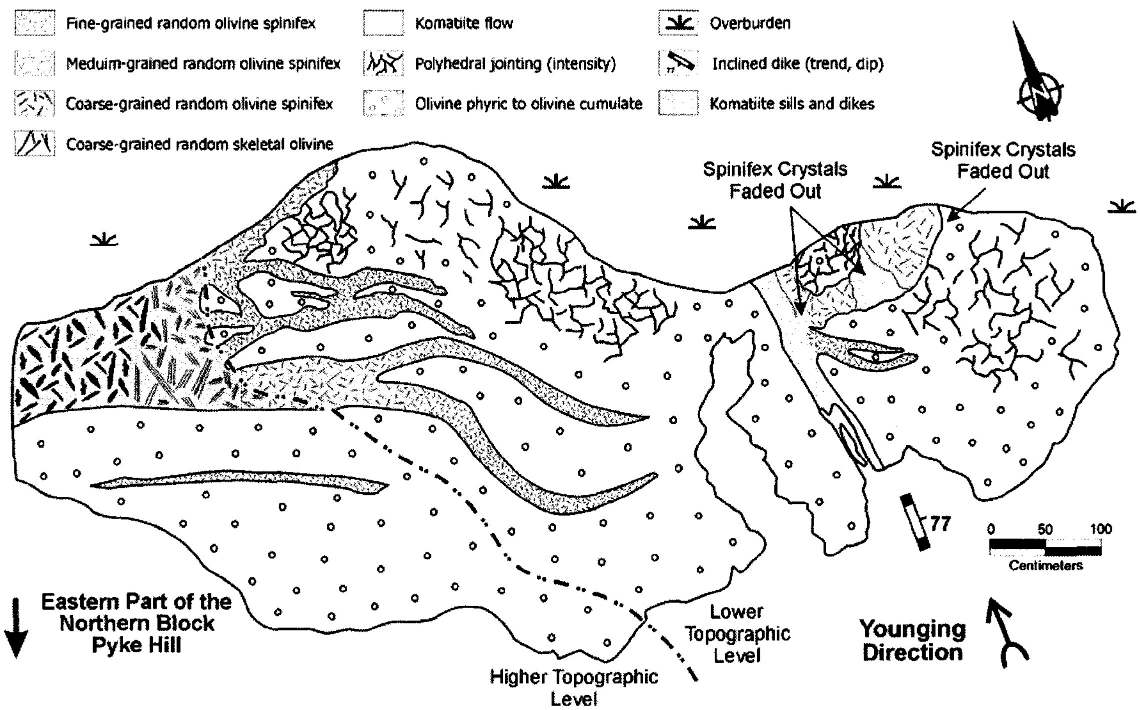

Figure 5.5 Detail geological map of the Area D in the Northern Block at Pyke Hill, Munro Township. Younging direction is inferred from differentiated komatiite flows westward (UTM 559310E, 5383135N, NAD 83, Zone 17). Location also on Figure 5.2.

In general, the komatiite sills at this location are quite similar to those previously described within Area C in the western part of the Northern block. However, some significant differences exist. Unlike the spinifex crystals within the komatiite sills of Area C (Fig. 5.2), which has homogenously distributed coarse randomly oriented olivine spinifex, komatiite sills of Area D have micro-spinifex of olivine at the margins (mm-scale) with coarse randomly oriented olivine spinifex (~3-5mm thick) interior (Figs. 5.6B and 5.6C). These sills also have a demonstrable fingering pattern. Detailed geological mapping (Fig. 5.5) shows that the apophyses are branched toward the east from a ~1.5m thick root composed of coarse randomly olivine spinifex up to 6 cm in length (Figs. 5.6D and 5.6E). In contrast to Area A (Fig. 5.2), the terminations of the apophyses demonstrate the flow direction was to the East.

A komatiite dike occurs in the eastern portion of the map area and is intruded at high angle to the flow contacts observed at Pyke Hill (Fig. 5.5). The dike is composed of fine-grained massive komatiite. Toward the stratigraphic base of the host unit, it is tabular, cross-cutting, and approximately 15 cm thick (Fig. 5.6F). Higher in the section, the komatiite dike branched to form sub-conformable apophyses having fine-grained randomly oriented spinifex textures, and a large bulbous mass of medium-grained randomly oriented spinifex textures. The spinifex textures at the edge of this komatiite mass fade (dashed line on Fig. 5.5), obscuring the contact relation with the host flow.

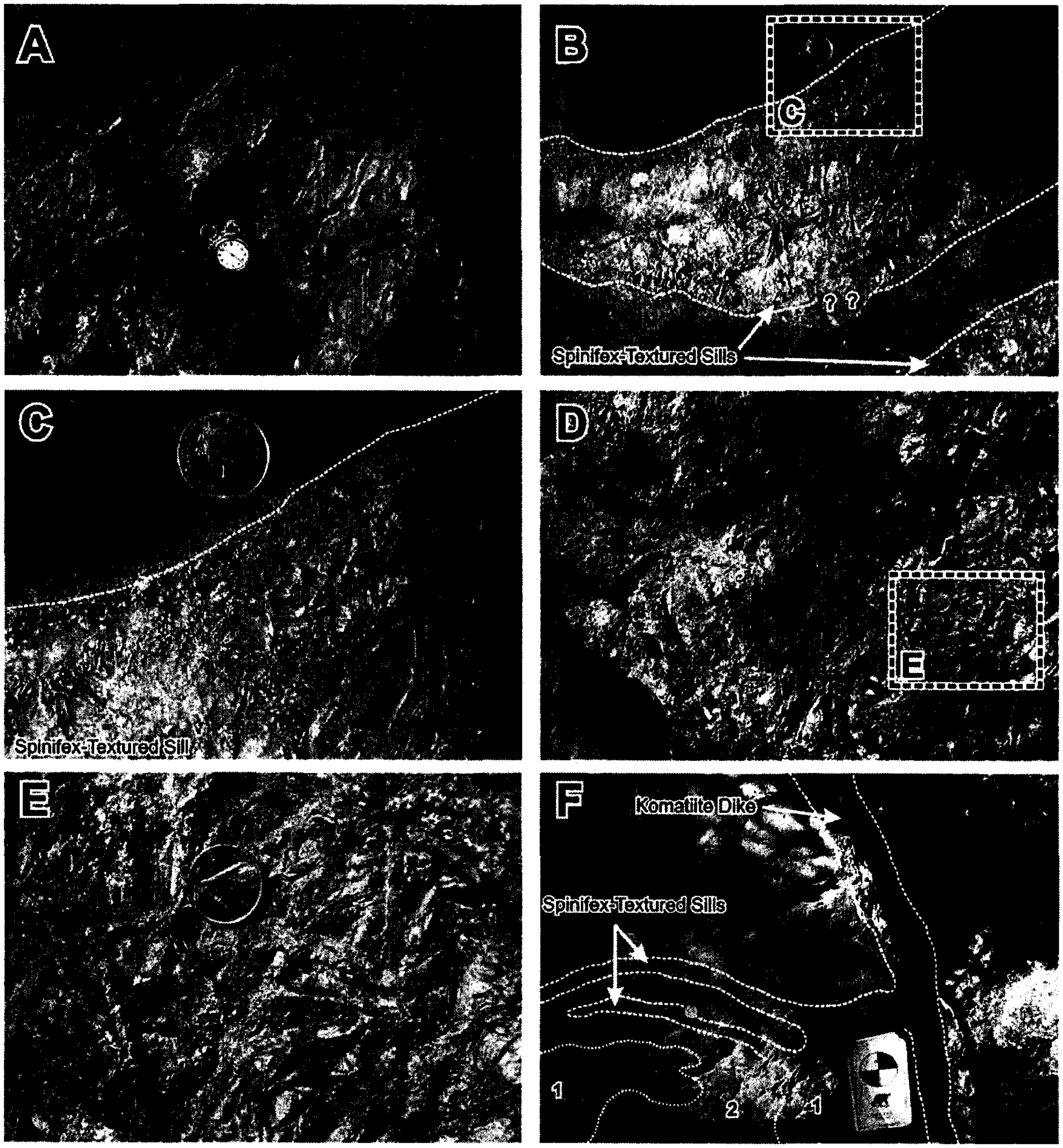

Figure 5.6 Typical textures observed within the Area D at Pyke Hill. A) Polyhedral jointing in komatiite flow. Watch is 4.8 cm in diameter. B) Spinifex-textured sills showing distribution of olivine crystals within the sill interior. Coin is 2.4cm in diameter. C) Close up of Figure 5.6B. D) Coarse-grained olivine spinifex crystals within the thickest part of the sill. Coin is 1.7cm in diameter. E) Close up of Figure 5.6D. Coin is 1.7cm in diameter. F) Komatiite flow cross-cut by a komatiite dike and by some spinifex-textured sills. 1: very fine-grained spinifex crystals that faded out laterally; 2: polyhedral jointing within komatiite flow. Note book is 18 cm long.

5.5.2. Serpentine Mountain, McArthur Township

The Serpentine Mountain area contains some of the most spectacular exposures of komatiitic rocks, in terms of the degree of preservation of their cooling and crystallization features at the macroscopic scale (Atkinson, 1999). Numerous flows have been identified over approximately 350 m on seven outcrops through a thick sequence of komatiites exposed in the area (Fig. 5.7: inset map). Individual flows range in thickness from 1 to at least 8 meters; however the exact number of flows within the sequence and the maximum thickness are uncertain because of the thick overburden that masks much of the outcrop. None of the komatiitic flows have the well-organized textural internal zonation of those documented at Pyke Hill. Generally, the flows contain only fine-grained to coarse-grained random olivine spinifex zones that overlie their olivine cumulate zones (Fig. 5.7: eastern side of the logging road). All seven outcrops contain sub-concordant spinifex-textured sills that cross-cut their host olivine cumulate. In the following, we describe two specific areas (Fig. 5.7, inset: Outcrops I and II) that have abundant and magnificent spinifex-textured sills.

5.5.2.1. Outcrop I - Area A

A detailed map was made of a manually stripped and cleaned outcrop that contains several komatiite sills (Fig. 5.8). The host organized flow is at least ~6 m thick and is composed of an olivine cumulate zone overlain by a spinifex-textured zone overlain by a flow-top breccia having characteristic polyhedral jointing.

The olivine meso to orthocumulate is composed of equant, 0.05cm to 0.1cm diameter, euhedral and subhedral crystals of altered olivine. The contact between the spinifex zone and cumulate zone of the komatiite is sharp. The ~1.5m thick olivine spinifex zone is composed of unoriented blades that tend to decrease in size toward the stratigraphic top. Within this zone, the spinifex blades are up to 21 cm in length. Some of the blades are preferentially oriented normal to the flow top. Overlying the spinifex zone, a 20cm thick breccia having a gradational contact with the spinifex zone was observed. Field observation and petrography suggest that the breccia is a flow-top breccia overprinted by a non-penetrative tectonic fabric (Fig. 5.9A). Some rounded clasts (5 to 30 cm in length) having cm-scale margins are found in the spinifex zone, and more rarely in the cumulate zones.

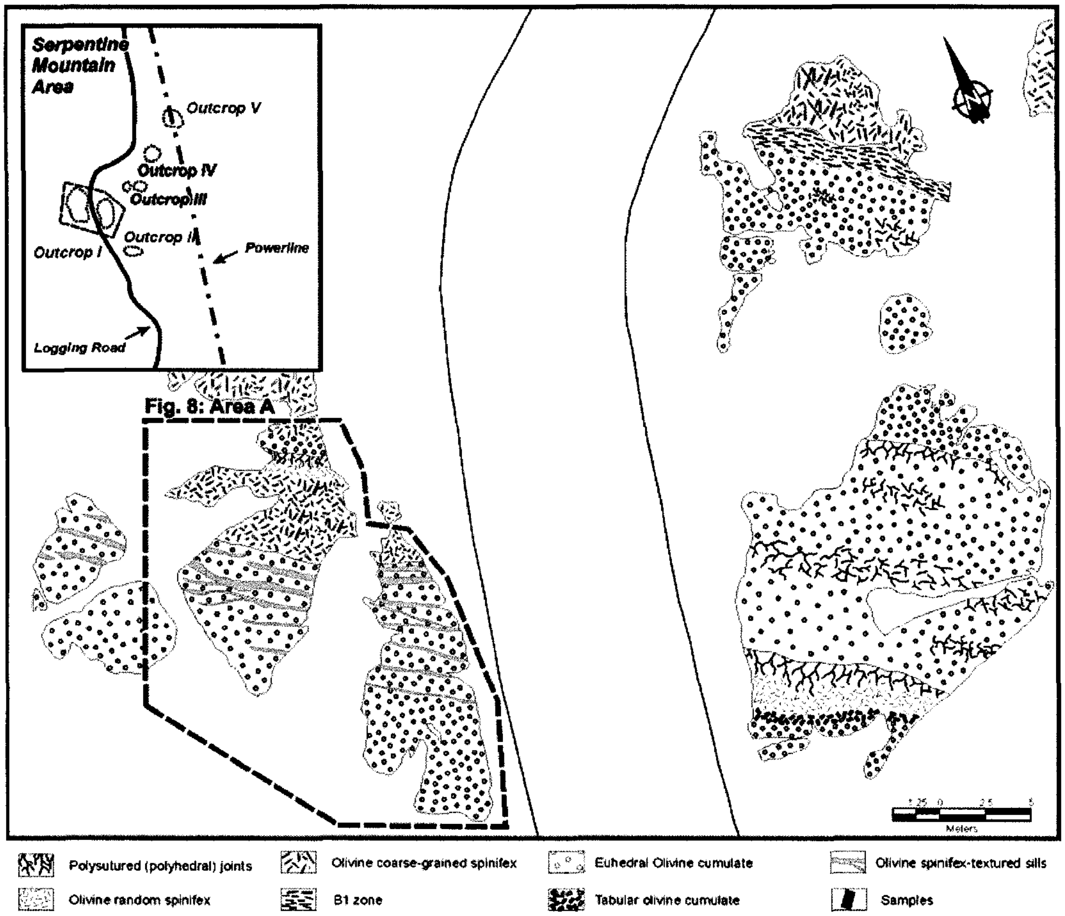

Figure 5.7 Geological map of the Outcrop I at Serpentine Mountain in McArthur Township (UTM 479708E, 5341725N, NAD 83, Zone 17: modified after Atkinson, 1999).

Conformable and semi-conformable spinifex-textured komatiite sills intrude the cumulate zone of the host flow (Figs. 5.8 and 5.9B). The sills range from 3 to 24 cm in thickness and are bordered by conspicuous cm-scale grey bands that stand out in relief against the light green colored cumulate rocks. These bands vary from 0 to 2cm in thickness and are composed of equant olivine crystals (Figs. 5.9Band 5.9C). Spinifex textures within the sills are composed of blades of altered olivine approximately 1-5 mm in thickness, ranging in length from 0.5 to 4 cm and are oriented at relatively high angles to the intrusive contacts. They occur as individual crystals or "booklets" of crystals and their distribution is non-uniform and asymmetric with respect to upper and lower sill contacts. Sills can have their larger spinifex crystals near their stratigraphic top, middle or base (Figs. 5.9 C and 5.9D).

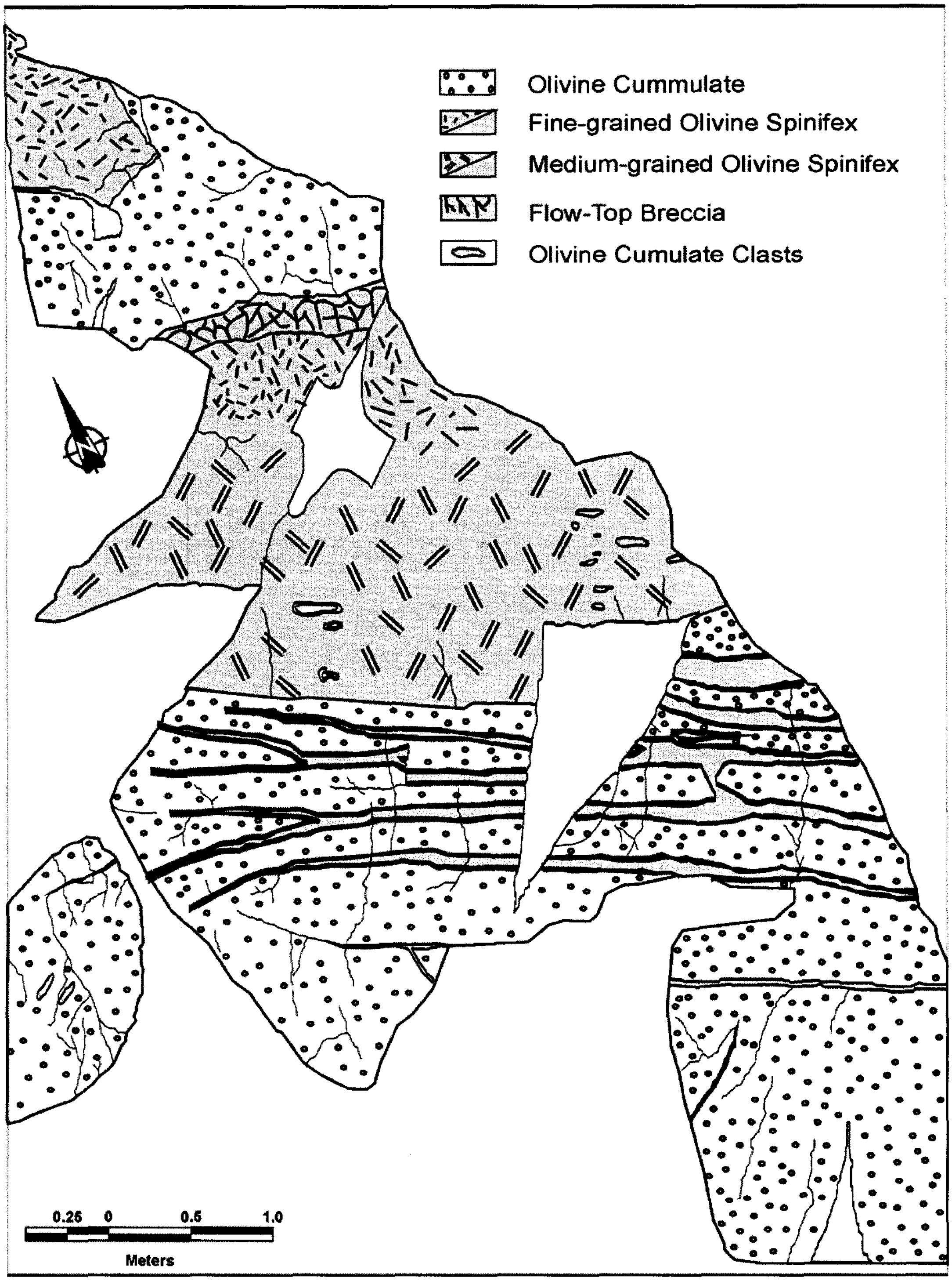

Figure 5.8 Detail geological map of the Area A within the Outcrop I at Serpentine Mountain, McArthur Township (after Préfontaine, 2003: UTM 479708E, 5341725N, NAD 83, Zone 17).

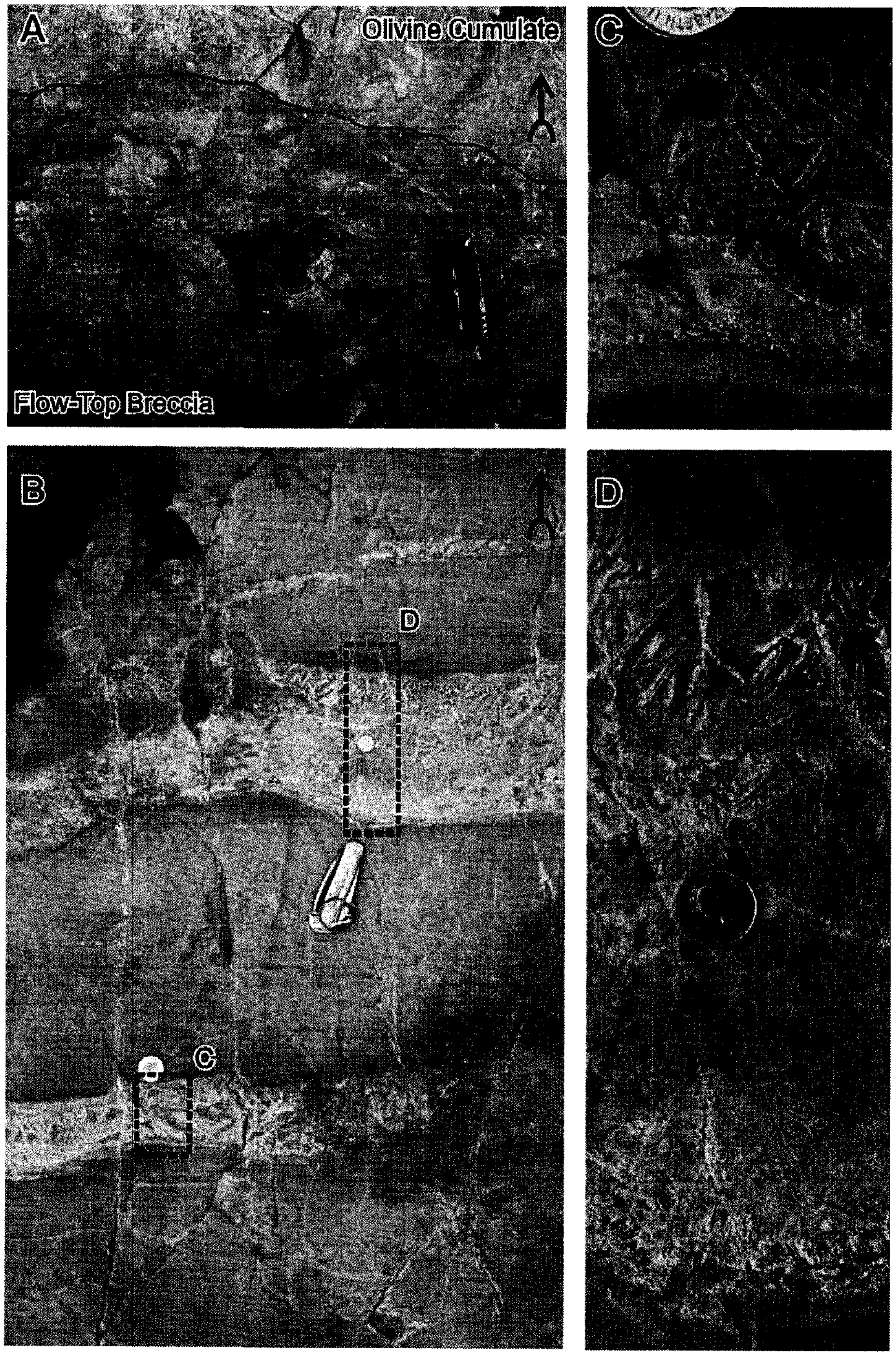

Figure 5.9 Typical structures and textures observed in the Area A within the Outcrop I at Serpentine Mountain. A) Flow-top breccia of the host komatiite flow and the overlying olivine cumulate (knife is approximarely 9 cm long). B) Typical spinifex-textured sills at Serpentine Mountain, Outcrop I (knife is approximarely 10 cm long and coin is 2.8 cm in diameter). C) Textural variation within a thin spinifex-textured sill, close-up from figure 5.9B (coin is 2.8 cm in diameter). D) Textural variation within a thicker spinifex-textured sill, close-up from figure 5.9B (coin is 2.4 cm in diameter). On all photographs, arrow indicate the younging direction.

5.5.2.2. Outcrop II - Area B

The detailed map in Figure 5.10 portrays a manually stripped and cleaned outcrop containing several komatiite sills. Although the actual cooling boundaries of the host unit were not observed, based upon the map pattern, the unit is interpreted to be a komatiite flow that is at least 4 m thick and composed entirely of olivine cumulate.

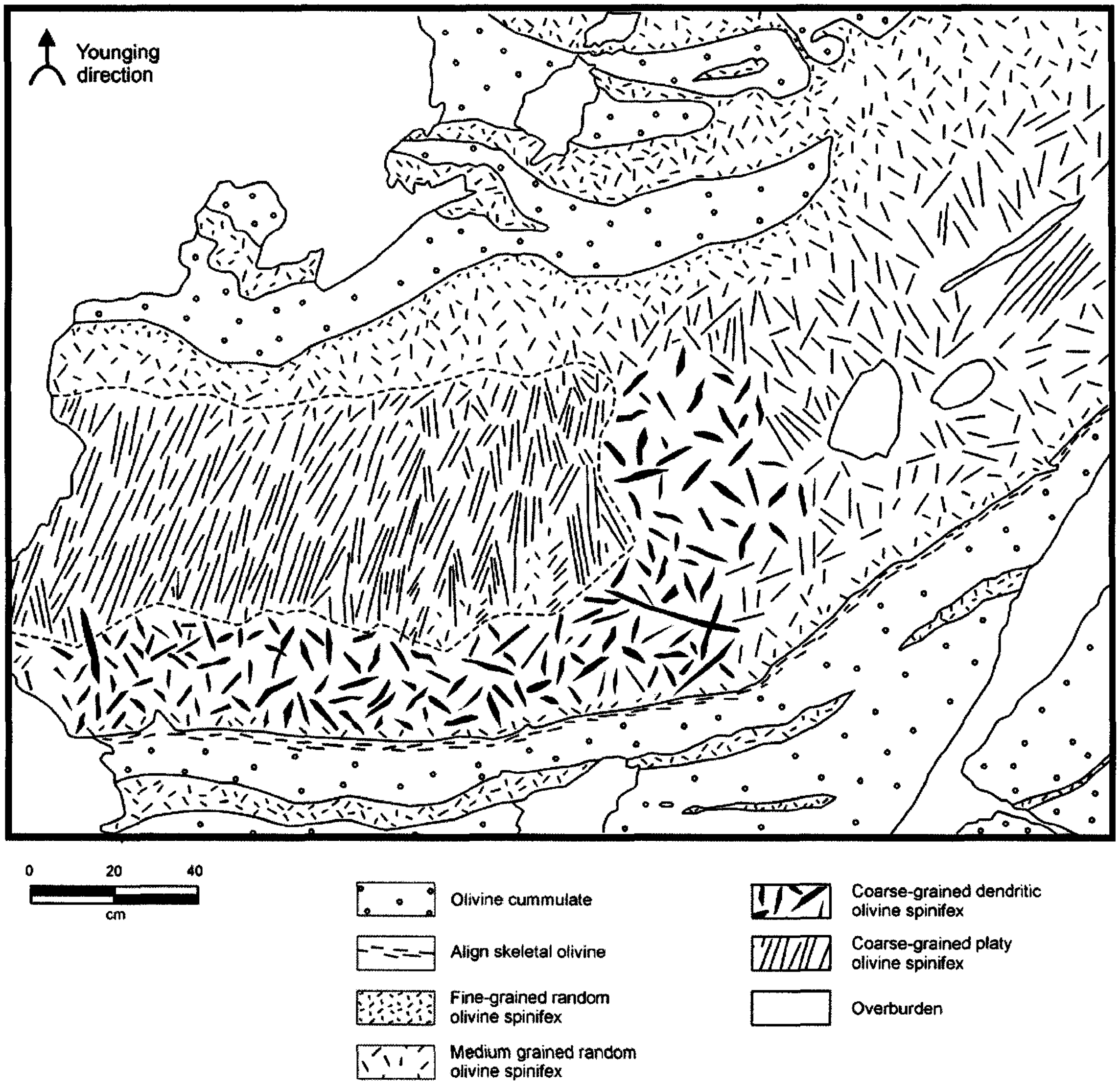

Figure 5.10 Detail geological map of the Outcrop B – Section I at Serpentine Mountain, McArthur Township (UTM 479708E, 5341685N, NAD 83, Zone 17).

The host-flow is cut by several spinifex-textured sills that range from 0.02 to 1.5 m in thickness, with the thinner ones occurring lower within the flow. In this outcrop, the thinner komatiite sills are quite similar to the sills previously described on the outcrop A. However, the thick komatiite sill here is very different and exhibits an extreme textural variation and complexity, having spinifex olivine zones organized with respect to its contacts.

This komatiite sill exhibits a more complex textural variation than a typical spinifex-textured zone of a komatiite lava flow (Fig. 5.11). The sill is composed of, from base to top, a ~45cm thick coarse random spinifex zone, a ~70cm thick very coarse aligned platy spinifex zone, and a medium-grained ~35cm thick random spinifex zone. The lower margin of the komatiite sill is largely obscured by deformation, however locally platy 0.5 cm long olivine crystals are aligned parallel the sill contact. The overlying coarse random spinifex zone consists of dendritic, platy, and fan-shaped olivine crystals that are up to 20 cm in length and ~0.5 cm wide. The aligned platy spinifex zone has crystals over 30 cm in length and ~0.01 cm wide that are organized into sheaves. Locally it contains dm-scale patches of the coarse random spinifex olivine. The lower boundary is sharp and has a wavy geometry that appears to be related to the termination of the fan-shaped sheaves of olivine crystals. The overlying random spinifex zone is composed of bladed olivine crystals that are up to 2 cm long and ~0.01 cm wide. This zone also contains dm to m-scale blocks of host rock olivine cumulate material in sharp contact with the spinifex-textured sill interior.

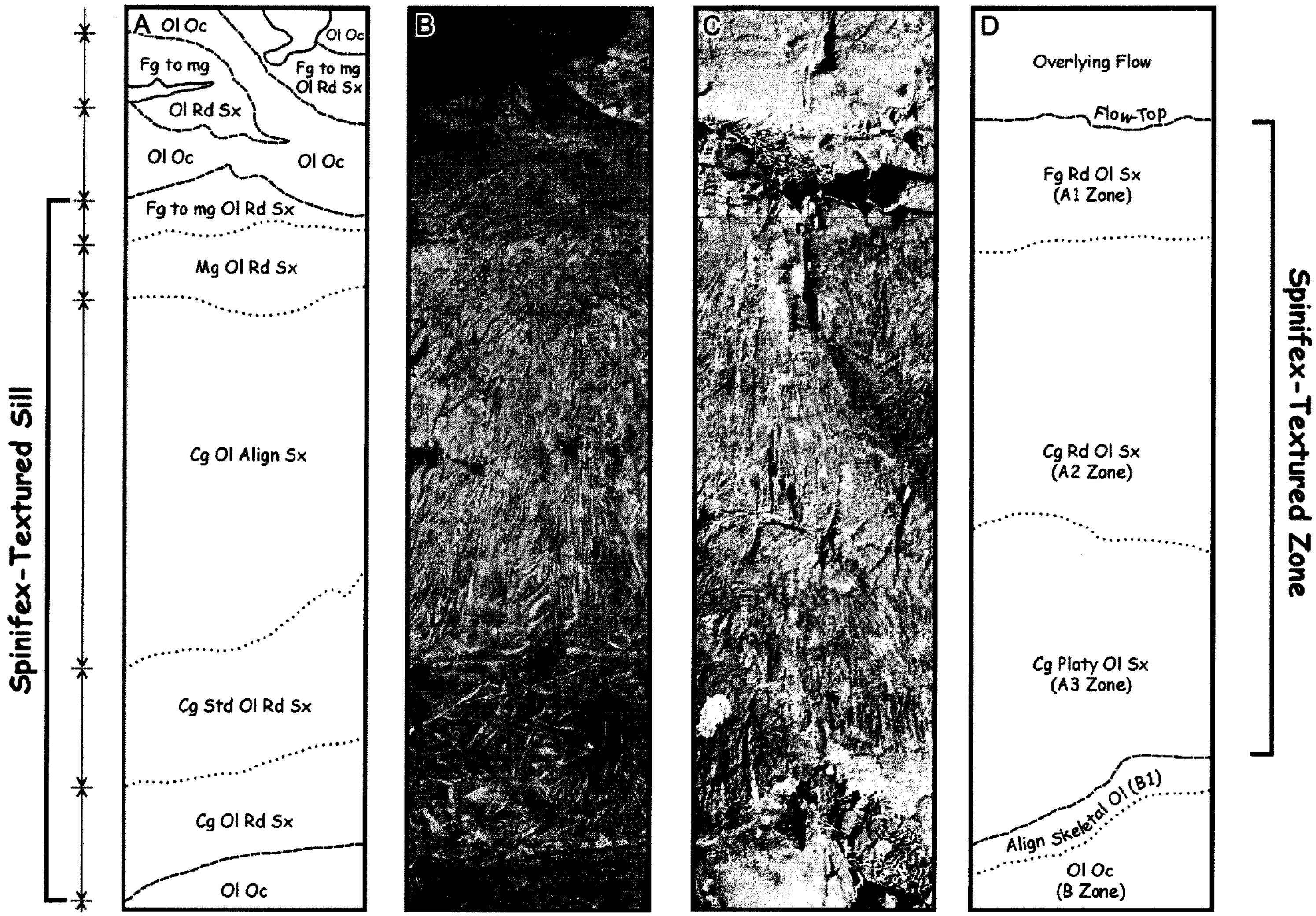

Figure 5.11 Comparison between a thick spinifex-textured sill and a typical komatiite flow. A) Scketch of a thick spinifex-textured sill, Outcrop II, Serpentine Mountain. B) Photograph of a thick spinifex-textured sill, Outcrop II, Serpentine Mountain. C) Photograph of the upper section of a komatiite flow at Pyke Hill (Area A) D) Sketch of the upper section of a komatiite flow at Pyke Hill (Area A). Cg = coarse grained, Fg = fine grained, Mg = medium grained, Oc = Olivine cumulate, Ol = olivine, Rd = random & Sx = spinifex.

5.6 Komatiite Microtexture

5.6.1. Pyke Hill, Munro Township

5.6.1.1. Host Flow

The cumulus zone of the host-flow is an olivine orthocumulate (50% to 75%) composed of subhedral, commonly rounded, equant (0.15-0.40mm) fractured and serpentinized olivine with lesser equant pyroxene crystals (Fig. 5.12A-B). Fresh olivine is present but uncommon. The groundmass is composed of skeletal and spherulitic (up to 0.5mm in length and 0.05mm in thickness) pyroxenes comprising up to 30% of the rock . The remainder of the groundmass is mostly composed of serpentine, chlorite, and ~1% of opaque minerals consisting of subhedral to euhedral Cr-spinel (from 0.05mm to 0.10mm in dimension). Magnetite is commonly found rimming chromium spinels and also as filaments surrounding olivines.

5.6.1.2. Sill Margins

Both the upper and lower contacts of the sills are commonly bordered by exterior margins ranging from 2mm to 8mm in thickness that are composed of 80% to 95% subhedral and equant olivine crystals. Two different types of overgrowths occur on olivine crystals within the sill margins: shells around equant crystals (Figs. 5.12D and 5.12E) and dendritic (Fig. 5.12F) overgrowths (Préfontaine, 2003) Equant overgrowths occur as shells around pre-existing olivine cumulate crystals typically as ~0.2mm thick shells of altered olivine. Planar faces bound the exteriors of the overgrowth whereas the interior contacts with the pre-existing cumulate crystals are generally round (Figs. 5.12B and 5.12C). The overgrown crystals at the margin are slightly larger than those found in the adjacent cumulate zone without overgrowths. A measure of 84 crystals of olivine (42 from within the cumulate zone and 42 at the sill margin) suggests that the crystals found in the margin are on average approximately 1.5 times larger than the crystals typically found in the cumulate zone (Table 1). Figures 5.12A and 5.12C demonstrates that the olivine coarsening is clearly visible at the macro and microscopic scale. The second overgrowth is defined by dendritic protrusions from individual olivine cumulate crystals. These were only observed along the contact at the margin directly adjacent the sill and the dendrite growth direction was into the sill (Fig. 5.12F).The groundmass is formed of skeletal (0.05mm and 0.50mm in length) pyroxenes that constitute up to 20% of the margin (Fig. 5.12D-E). In the sill margin, the amount of chromian spinel (< 1%) is significantly less than the amount in the cumulate zone of the host flow.

5.6.1.3. Spinifex-Textured Sills

The spinifex texture in the sills is mostly composed of olivine and pyroxene crystals. The matrix occupies approximately 20 to 30% of the sills and is made up of chlorite, serpentine, devitrified glass and amphiboles. The olivine blades are tabular or branching, form 40 to 60% of the rock, and are completely replaced by serpentine (Fig. 5.13A). Typically olivine crystals are skeletal or dendritic and commonly found as H, M or U shapes (Fig. 5.13B).They are commonly longer and wider than the pyroxene blades and crystallized first based on the observation that pyroxenes appear to have grown epitactically from the olivine crystal surfaces (e.g., Shore 1996). In addition, skeletal olivine crystals contain later-formed pyroxene blades (Fig. 5.13C). The pyroxene blades (up to 4mm) compose 10 to 20% of the spinifex within the sills and are commonly organized into ~6 by ~12mm booklets (Fig. 5.13D) or mm-scale spherulites. Chromian spinel comprises approximately 1% of the spinifex texture sills. Two different habits of chromian spinel, dendritic (~0.5 mm) and euhedral (~0.1 mm), are distributed throughout the sills. In thicker sills (> ~15 cm), the spinel dendrite morphology changes from the margin to the core. At the border, dendrites typically have a ramified habit (Fig. 5.13E) whereas in the sill interior they have a compact form (Fig. 5.13F).The second spinel habit does not change with position in the sill and consists of subhedral to euhedral crystals that form about 50% of the total chromian spinels present within the komatiite sills. Spinel crystals with either habit characteristically have thin secondary rims of magnetite formed during alteration.

5.6.1.4. Komatiite Dike

The komatiite dike is pervasively serpentinized (serpentine, chlorite and magnetite) and composed of fine-grained komatiite containing (< 0.1mm) some preserved bladed and dendritic olivine crystals. In addition it has several cm-scale clasts of olivine orthocumulate cumulate consisting of 0.2 to 0.5 mm altered olivine crystals.

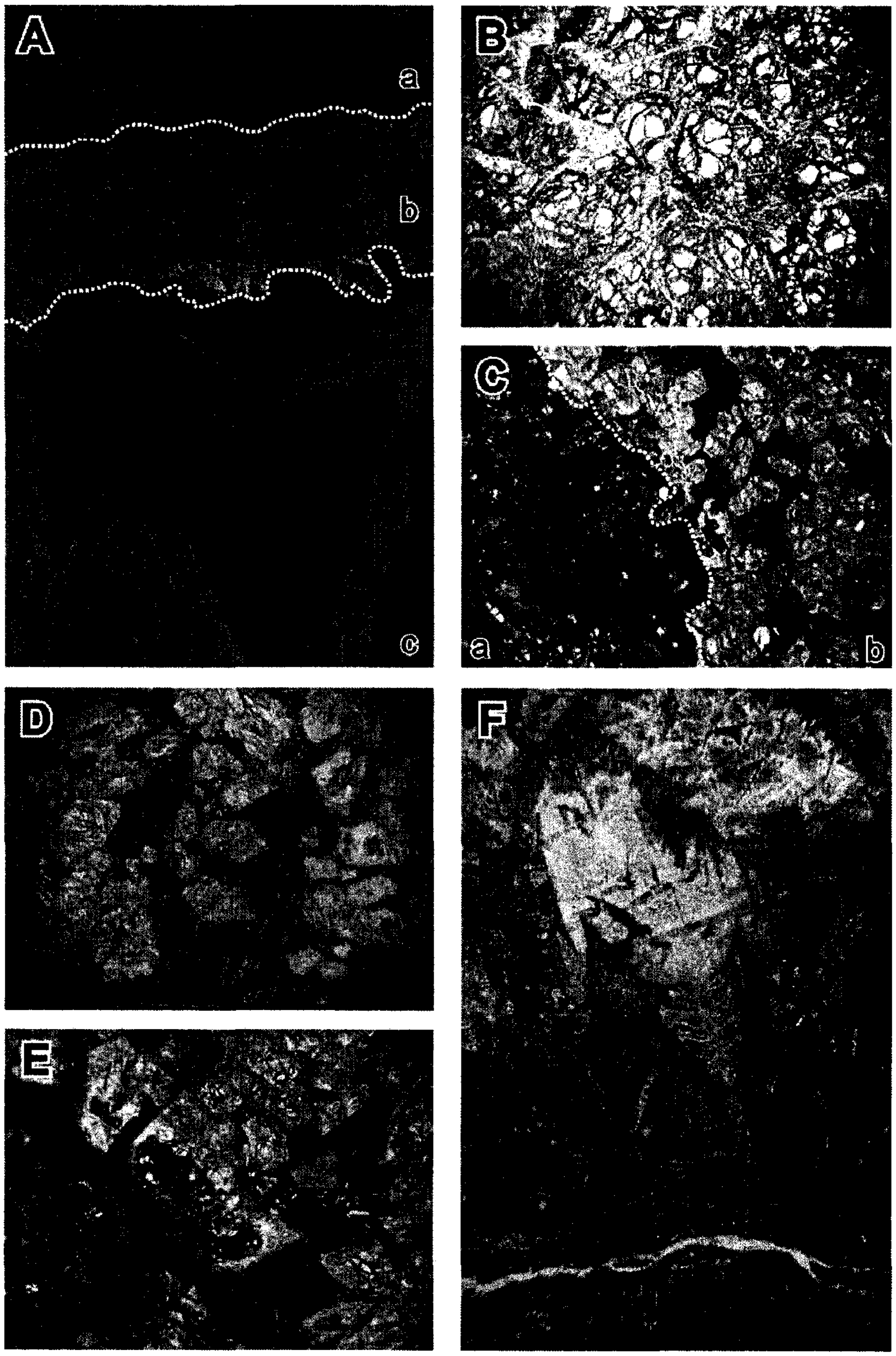

Figure 5.12 Photographs of typical textures occurring at the margins of some spinifex-textured sills and within the host komatiite flows at Pyke Hill – Area C. A) Section overview through a spinifex-textured sill and its host komatiite, (approximately 35 mm) a: olivine cumulate of a komatiite flow; b: olivine cumulate at the margin of a spinifex-textured sill; c: spinifex-textured sill (B-E photomicrographs) B) Olivine cumulate of a komatiite flow. C) Contact relationship between the olivine cumulate within the flow (a) and at the margin of the sill (b). D) Typical olivine cumulate at the margin of a spinifex-textured sill. E) Egg-shell overgrowths within the olivine cumulate at the margin of the sill. F) Dendritic overgrowth within the olivine cumulate at the margin of the sill. FOV of photomicrograps approximately 4 mm.

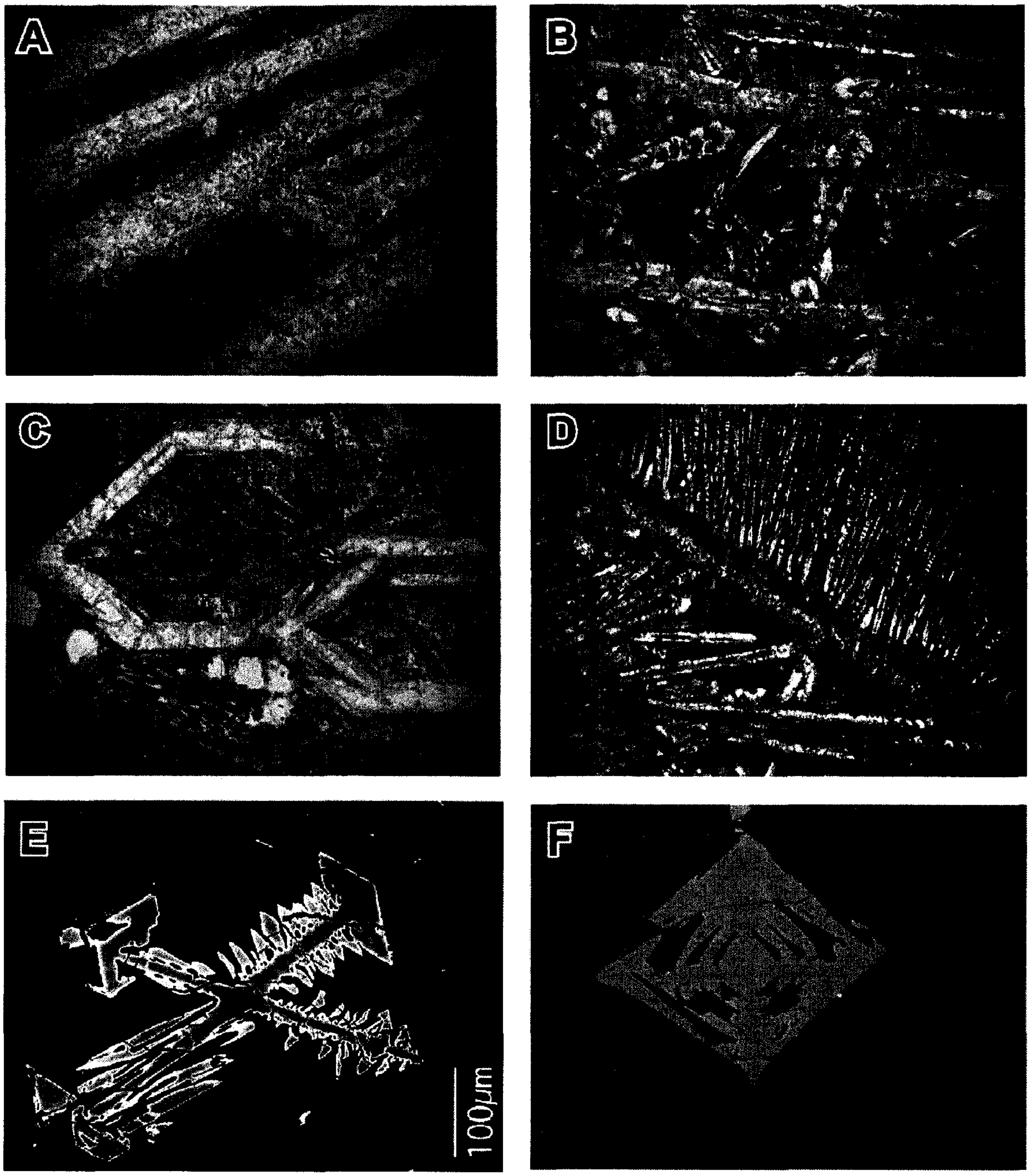

Figure 5.13 Microphotographs of typical textures occurring within spinifex-textured bearing sills at Pyke Hill – Area C. A) Entirely replaced olivine blades in the spinifex-textured sills. B) Chain-like and hopper olivine crystals in the spinifex-textured sill. C) Skeletal olivine crystals in the spinifex-textured sill. D) Subparallel pyroxene blade in the spinifex-textured sill. E) SEM backscatter microphotograph of dendritic crystal of chromite in the middle of a thin spinifex-textured sill at Serpentine Mountain (Outcrop I – Area A). F) Microphotograph of skeletal crystal of chromite in the middle of a thicker spinifex-textured sill at Serpentine Mountain (Outcrop I – Area A). FOV of a, b, c, d is approximately 4mm and 2 mm for f.

Table 5.1 Grain size distribution of olivine crystals measured within the host cumulate flow and at the margins of komatiite sills at Pyke Hill (Munro Township) and Serpentine Mountain (McArthur Township).

	Pyke Hill, Munro Township								Serpentine Mountain, McArthur Township	
Section	**Northern Block Area C**		**Northern Block Area C**		**Northern Block Area C**		**Northern Block Area C**		**Outcrop II**	
Thin Section	**S8B**		**S8O**		**S9O**		**S10B**		**186C**	
Sill Thickness	**7.5 cm**		**7.5 cm**		**17.5 cm**		**12 cm**		**150 cm**	
Contact	**Lower Contact**		**Lower Contact**		**Upper Contact**		**Upper Contact**		**Upper Contact**	
Location	**Cum**	**Margin**	**Cum**	**Margin**	**Cum**	**Margin**	**Cum**	**Margin**	**Cum**	**Margin**
	mm	**mm**	**mm**	**mm**	**mm**	**mm**	**mm**	**mm**	**mm**	**mm**
1	0.1	0.3 (2)	0.2 (3)	0.3 (3)	0.1 (3)	0.2 (4)	0.2 (8)	0.2 (1)	0.2 (3)	0.4 (4)
2	0.2 (3)	0.4	0.3 (2)	0.4 (3)	0.2 (3)	0.3 (2)	0.3 (8)	0.3 (7)	0.3 (10)	0.5 (2)
3	0.3 (4)	0.5	0.4	0.5 (2)	0.3	0.4	0.4 (4)	0.4 (12)	0.4 (6)	0.8
4		0.6 (2)	0.6					0.6	0.6 (3)	0.9 (5)
5									0.8 (3)	1.0 (3)
6									-	1.1
7									-	1.2
Average	*0.2*	*0.5*	*0.30*	*0.4*	*0.2*	*0.2*	*0.3*	*0.4*	*0.4*	*0.8*
Mrg/Cum	***2.5***		***1.3***		***1.0***		***1.3***		***2.0***	

Cum: Olivine cumulate within the flow; Margin: Olivine cumulate at the sill margin; mm: millimetre, (X) number of olivine crystals with this grain size.

5.6.2. Serpentine Mountain, McArthur Township

5.6.2.1. Host Flow

The cumulus zone of the host flow is an olivine meso to orthocumulate (~80%) composed of mostly anhedral, equant, from (0.2 to 0.5mm), subrounded, fractured, and serpentinized olivine. Olivine is uncommon and only preserved in crystal cores where it is surrounded by buff-brown coloured relict olivine. The groundmass is dominated by serpentine and chlorite with lesser opaque minerals. These comprise approximately 5 to 10% of the cumulate and occur as euhedral and equant chromian spinel (~0.1mm-0.5mm), and magnetite. Magnetite is a significant component of the oxide phase and occurs mostly as filaments surrounding olivines and also as thin rims (<10μm) around chromium spinels. Trace amounts of anhedral pyrite (< 1%) are generally associated with the spinel.

5.6.2.2. Sill Margins

The olivine cumulate crystals at the margin (~12mm in thickness) immediately exterior to the spinifex-textured sills at Serpentine Mountains are generally pervasively altered to serpentine and iron oxides. This alteration has enhanced the margin's macroscopic appearance but has destroyed most primary features. However, in one location (Outcrop II: Fig. 5.7) the degree of preservation is better, indeed unaltered olivines are apparent. Based mainly on observations from this location, the cumulate at the margin of the sill is composed of subhedral to anhedral olivine crystals ranging from 0.2 to 1.5 mm in size. A measure of 42 crystals of olivine within the cumulate zone (25 remote from the sill contact and 17 from the sill margin) suggests that the crystals found in the margin are on average approximately 1.5 times larger than the crystals typically found in the cumulate zone also suggesting an overgrowth as described at Pyke Hill (Table 5.1). Subhedral spinel (<1%) are significantly less abundant at the margin of the sill in comparison to the host cumulate.

5.6.2.3. Spinifex-Textured Sills

The spinifex texture in the sills is mostly composed of olivine and pyroxene crystals. The groundmass occupies approximately 25 to 35% of the sills and is made up of chlorite, serpentine, devitrified glass and amphiboles. The olivine blades are tabular, form 40 to 60% of the rock, and are completely replaced by serpentine. Olivine crystals are skeletal or dendritic and are commonly longer and wider than the pyroxene blades. They are aligned in crystallographic continuity thus accounting for the 0.5mm to 15mm long blades observed on outcrop. The pyroxene blades are up to 4mm in length and compose 15 to 25% of the spinifex texture within the sills. They occur as individual randomly oriented blades, mm-scale spherulites, and less commonly they are organized into booklets. Chromian spinel comprises approximately 2-3% of the spinifex textured sills. Two different habits of chromian spinel are present, dendritic (up to ~0.5 mm) and euhedral to subhedral (up to ~0.2 mm), and both are distributed throughout the sills. Dendritic and euhedral morphologies coexist within the spinifex-textured sills and their relative proportion is quite similar. Both spinel habits are surrounded by thin rims of magnetite.

5.7 Interpretations and Discussions

5.7.1. History of Spinifex-Textured Sills (i.e., Veins)

Spinifex-textured sills within komatiitic flows were described as "veins" by Pyke et al. (1973) at Pyke Hill in Munro Township. Subsequently they were also described in several other locations, for instance; the "Lava Lake" in Munro Township (Arndt, 1986), Komati Formation in Barberton Mountainland (Grove et al., 1997; Dann, 2000; 2001), Dundonald Beach in Dundonald Township (Arndt, 1994; Davis, 1999; Cas and Beresford, 2001; Houlé et al., 2002; Arndt et al., 2004; Houlé et al., 2008), and Spinifex Ridge in Lamotte Township (Champagne, 2004).

As recently pointed out (e.g., Arndt et al., 2004; Rosengren, 2005; Houlé et al., 2008), distinguishing between komatiite flows and sills is not easy. It is even more difficult distinguishing between a spinifex-textured sill and the spinifex zone of a komatiite flow although several criteria can help to discriminate between them (see also discussion in Arndt et al., 2004).

Sill contacts do not have characteristic polyhedral fractures or altered glassy zones characteristic of flow tops. In addition they are at least partially discordant and do not show a decrease in grain-size within the chilled margin. The coarsening commonly observed at the sill margins is an excellent diagnostic criteria but is not always present. Spinifex-textured sills were recognized quite early in the evolution of our understanding of komatiite volcanism; however, no satisfactorily mechanisms were invoked to explain the komatiitic injections into komatiite flows.

5.7.2. Volcanological Model

5.7.2.1. Mechanism of Emplacement

Our observations of komatiitic flows throughout the Abitibi Subprovince (Houlé, unpublished data) demonstrate that spinifex-textured sills are clustered within single flow units, are a minor component and are restricted to certain areas within many komatiite successions. Detailed mapping at Pyke Hill and at Serpentine Mountain demonstrates that the komatiitic, spinifex-textured sills were preferentially intruded into the cumulate zone of texturally-organized komatiite flows. Spinifex-textured sill emplacement may be a product of three different processes: intrusion into a cold consolidated flow (i.e. late intrusion), "auto-intrusion" as an excluded residual melt (i.e. filter pressing during flow consolidation); or intrusion of an external melt into a partially consolidated, hot flow (early intrusion coeval with flow emplacement).

Intrusion into a cold flow is consistent with spinifex textured olivine crystal growth from the host rock walls into the sills because a thermal gradient would have existed. However. it is inconsistent with the presence of overgrowths entirely surrounding cumulate olivine crystals within the pre-existing cumulate zone several mm from the flow-sill contact into the pre-existing flow. It is inconceivable that the intrusive could selectively migrate into and overgrow crystals within a solid komatiite flow; rather one would expect the sill to develop a distinct, quenched or chilled margin.

Drainage of residual liquid downward from the spinifex zone to the cumulate zone of komatiite flows, as proposed by Pyke et al. (1973) is also not likely. In this case the residual liquid would have been largely in thermal and chemical equilibrium with the crystals so spinifex or dendrites of olivine would not have formed. Close to equilibrium crystallization conditions are incompatible with the textures observed, particularly the extreme textural variation and complexity of undercooled crystals as described within some spinifex-textured sills at Serpentine Mountain (Outcrop II: Fig. 5.7).

The preferred model is the emplacement of externally derived komatiitic magma into a partially consolidated flow. The sharp contacts and their curvi-planar geometry indicate that the flow acted, at least partially, as a rigid body during sill intrusion. The overgrowth shells on the olivine crystals that resulted in cumulate crystal coarsening are interpreted to reflect permeability of the partially crystallized host flow. These textures demonstrate that magma from the sill invaded a permeable, and therefore incompletely consolidated, cumulus zone allowing the development of overgrowth shells on pre-existing olivine crystals. Neither an altered glassy margin nor a chill margin were found at the contact of the sill and the cumulate zone suggesting that a very large temperature difference did not exist between the intrusive magma and the cumulate.

However, in order to form the observed olivine dendrite overgrowths (e.g., Fig. 5.12) and the well-organized spinifex olivine texture (e.g., Fig. 5.11), a relatively high thermal gradient between the host rock and the magma that formed the spinifex-textured sills needed to exist. It has been proposed by Shore and Fowler (1999) and Faure et al. (2006) that the presence of a thermal gradient is the dominant mechanism to crystallize, under low cooling rates, the dendritic morphology of olivine similar to crystals grown at high cooling rates in laboratory experiments. Another mechanism for the development of dendritic olivine crystals, proposed by Grove et al. (1994; 1996; 2002) and Grove and Parman (2006), is crystal growth in response to exsolution of volatile phases (H_2O) that decreases the nucleation rate and enhances crystal growth producing an effective undercooling. Although the latter process may have played a role we did not observe any evidence for exsolution of volatile phases such as gas cavities within the komatiitic flows, recognizing, of course, that volatile phases could have migrated through the flows undetected. Thus, we cannot rule out the role of a volatile phases but the organization of the spinifex and dendritic olivine with respect to sill contacts argues for crystal growth driven, at least partially, by a thermal gradient.

Generally but not always thin sills (< 100cm) exhibit relatively homogeneous and symmetrical textural variation whereas thicker sills (> 100cm) exhibit more complex textural variations presumably because greater thickness implies longer cooling times and therefore more opportunity for organized crystal growth.

As a consequence of their intrusion into a rigid, semi-consolidated and permeable cumulate flow, spinifex-textured sills record the successive stages of komatiite cooling and solidification. The sill-forming process occurred after the komatiititic flow had crystallized olivine spinifex crystals from the flow crust and euhedral olivine and chromite had accumulated to form the cumulate B zone (Fig. 5.14A). We envisage that new komatiitic magma was injected into the komatiite flow that had cooled to the extent that the cumulate zone formed a rigid but not completely solidified mass resulting in sharp and curviplanar contacts with the flow (Fig. 5.14B). The increased temperature gradient at the contact caused the olivine dendrites overgrowths to form and grow from the sill contact (generally the upper one) into the sill (Fig. 5.14B). Melt then percolated into the cumulate at the sill margin forming the olivine crystal overgrowth shells (Fig. 5.14C). Nucleation and growth of olivine spinifex within the sills took place after the formation of the dendrite overgrowths and possibly coeval with the shell overgrowths (Fig. 5.14D).

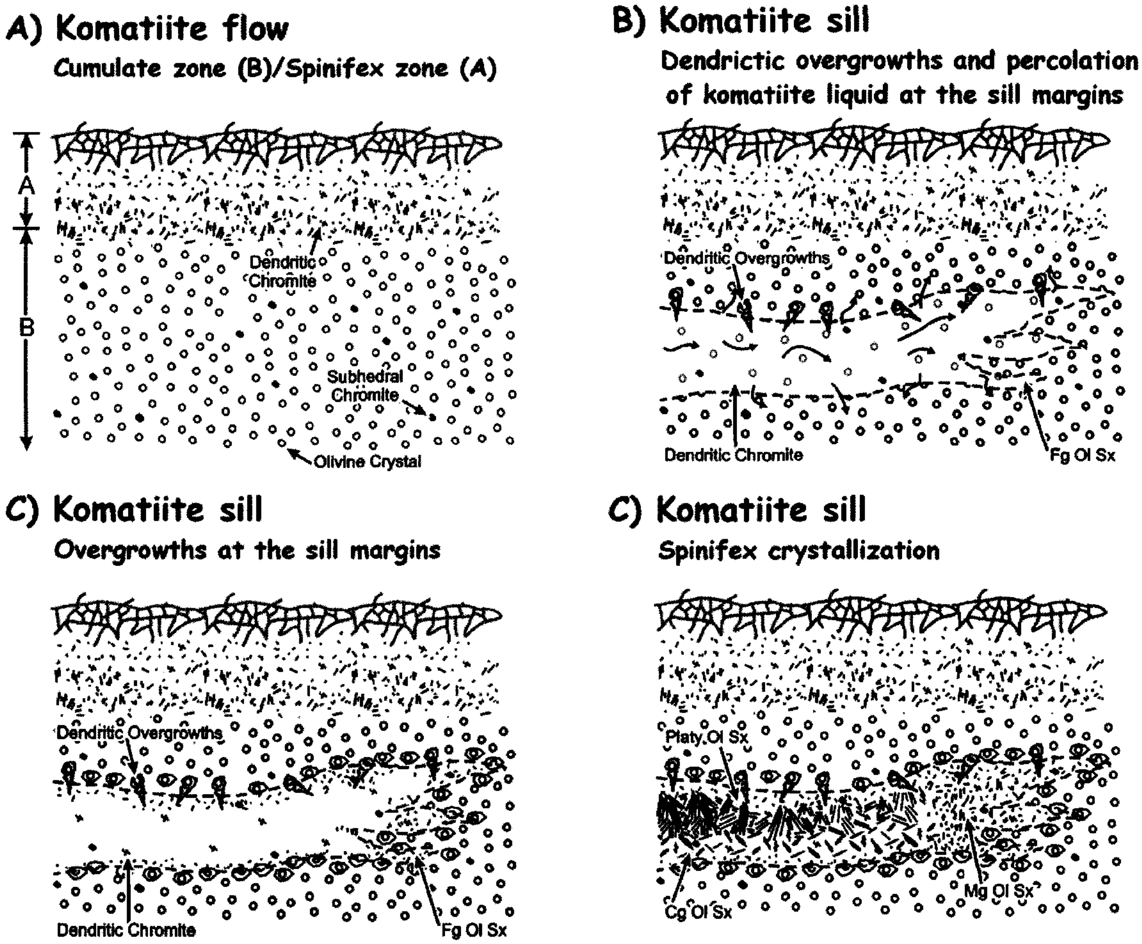

Figure 5.14 Mechanism of emplacement of spinifex-textured sills. A) Typical komatiite flow with an lower olivine cumulate zone overlain by an upper spinifex-textured zone. B) Injection of a komatiitic liquid forming the olivine crystal overgrowth dendrite in response of a thermal gradient. C) Melt percolation into the cumulate at the sill margin forming the olivine crystal overgrowth shells. D) Nucleation and growth of olivine spinifex within the sills took place after the formation of the dendrites and possibly coeval with the shells. Fg: fine-grained, Cg: coarse-grained, Mg: medium-grained, Ol: olivine, Sx: spinifex.

5.7.2.2. Model of Emplacement

Here we discuss the underlying volcanological processes involved in the emplacement of spinifex-textured komatiitic sills and their implication of on the development of komatiitic lava flow fields. Inflation, lava growth by injection under an insulated crust, is reported for many modern lava flows (e.g., Hon et al., 1994), serves as model for emplacement of large flood basalts flow fields (e.g., Self et al., 1998), and even for komatiite lava flow fields (e.g., Dann, 2001).

We postulate that inflation is also responsible for the formation and emplacement of the spinifex-textured sills described at Pyke Hill and Serpentine Mountain. Furthermore, we interpret the komatiite sills and dikes to have formed above and peripheral to buried lava pathways during periods of inflation and subsequent deflation that accompanied voluminous komatiitic eruptions as illustrated in Figure 5.15. In our model komatiitic lava moving over an irregular volcanic topography would become rapidly channelized within distributary lava rivers that, like basaltic flows, can only overrun their lava pathways when eruptions are voluminous. One such lava channel-way is illustrated in Figure 5.15A where the lava is depicted to have developed a thick crust due to ltwo main processes.

The first and initial process is the development of a continuous crust over the moving flow due to rapid cooling via conductive and convective heat loss in the subaqueous environment. The second process is the development of a thick crust via lava breakouts formed during fracturing of the channel roof during inflation of the lava channelway. Analagous to inflationary processes described in modern pahoehoe lava flows in Hawaii (e.g., Hon et al., 1994; Anderson et al., 1999). Voluminous komaiitic eruptions may have inflated the lava crust causing extension and ultimately fracturing the visco-elastic crust resulting in "breakouts" and extrusion of thin, spinifex textured lava on the crust above a moving inflated flow as illustrated in Figure 5.15. Similar inflation and breakout processes have been proposed by Dann (2001) for the lateral propogation of komatiitic lava and the development of foliated spinifex zones within komatiitic flows of the development of Komati Formation in the Barberton greenstone belt. Repeated fracture propagation of the crust during periods of flow inflation and deflation followed by extrusion during periods of inflation results in burial of the lava pathways by multiple variably organized komatiitic flows creating a thick crust produced via breakouts as depicted in Fig 5.15B.

During inflation, most fractures would tend to develop perpendicular to the crust i.e. normal to the axis of least principal stress. However, because the crust is a free surface and the breakout flows above the channel are likely only meters thick, over-pressure may locally cause dilational fractures within the crust that are horizontal rather than vertical in their orientation, as reported by Hon et al. (1994) and Anderson et al. (1999) for pahoehoe lava. In this case fractures within the relatively weak semi-consolidated cumulate zone of the flows would be parallel the flow surface and pressure relaxation after fracturing or deflation during waning eruptions would result in collapse and sealing of fractures within the channel roof essentially by trapping komatiitic magma emplaced as dikes and sills. Thus, we propose that komatiite sills and dikes described herein resulted from inflation processes during the development of buried lava channels by surface breakout flows.

Thus the occurrence of spinifex-textured sills and dikes within organized komatiitic flows (spinifex and cumulate zones) indicates proximity to buried lava pathways. This has important implications for reconstructing the architecture of komatiitic flow fields, and, by extension, for mineral exploration. Thin komatiite lava flows are generally interpreted as a product of waning eruption within a distal volcanic setting (e.g., Lesher, 1989; Hill et al., 1995). However, based on our interpretation of the emplacement mechanisms for spinifex-textured komatiitic sills, thin komatiite flows could also represent the building up of the volcanic architecture above preferred lava pathways. Given this interpretation, spinifex-textured sills may be indicators of proximity to buried or cryptic lava pathways and, therefore, providing environments permissive for the formation of nickel sulfide mineralization (e.g., Lesher et al., 1984).

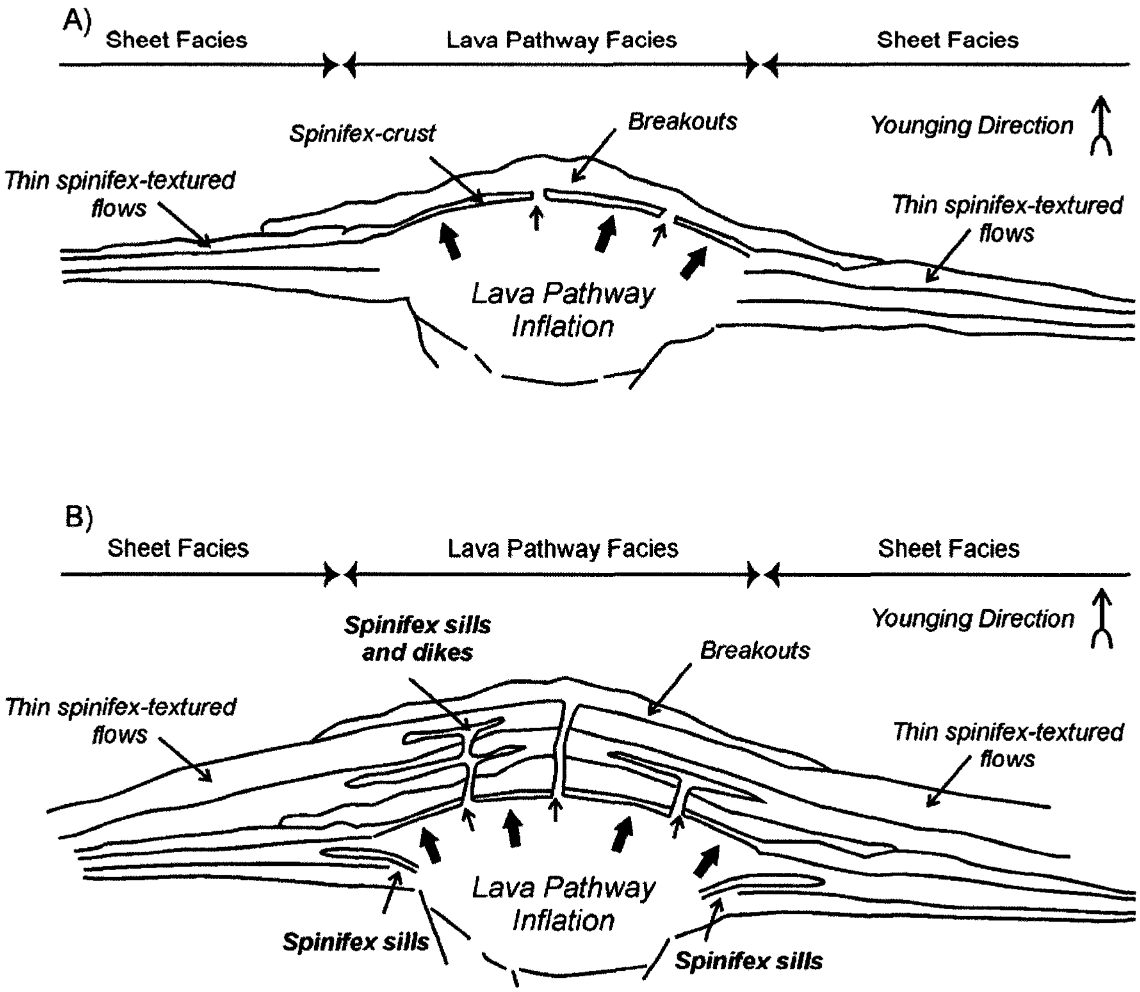

Figure 5.15 Interpretative model of emplacement for spinifex-textured sills-dikes and their distribution within a typical lava channel komatiite volcanic facies. A) Initial komatiite flows moving underneath a relatively thin crust become channelized rapidly within a pre-existent volcanic embayment that could be enhanced by thermo-mechanical erosion. An increase of the magma flux within the channel provides tension to create a break-up in the crust with new lava flows moving above it. B) Building up of the volcanic stratigraphy above the buried lava channel is produces by repeated replenishments within the lava pathway.

5.8 Conclusions

Spinifex-textured komatiitic sills, reported previously as "spinifex-textured veins", are sub- to concordant igneous bodies that intruded early komatiite flows. They are minor components, but nonetheless integral parts of many extrusive komatiitic successions in the Abitibi greenstone belt. These sills generally occur within thicker flows than the classic spinifex-textured flows. Typically they formed as multiple stacked cm-scales to meter-scale layers of spinifex-textured rocks, near the interface between the spinifex (A zone) and the cumulate (B zone) zones of a komatiite lava flows. Less commonly aphyric komatiitic dikes also occur within these host units and were intruded at high angles to the flow contacts, grading laterally to subconcordant spinifex-textured sills.

In our model of flow emplacement, the morphology of spinifex-textured sills and marginal olivine overgrowths, and crystal coarsening of the host cumulate zone adjacent to the sill margins, are interpreted to have formed by inflation and endogenous growth via multiple injections of new magma into cooler, semi-consolidated but permeable cumulate zones of thin flows that developed above and peripheral to buried lava channels. We can not rule out the role of volatile phases in the development of spinifex texture but the orientation of spinifex and dendritic olivine roughly perpendicular to sill contacts argues for growth driven by a thermal gradient. Spinifex-textured sills most likely occur within a thick crust that formed via breakouts, peripheral to or vertically above buried lava pathways that accompanied voluminous komatiitic eruptions.

5.9 Acknowledgements

This work stems from a recently completed honors project by the second author at University of Ottawa and is part of an ongoing Ph.D. by the first author under the supervision of C.M. Lesher at Laurentian University (Sudbury) and Tony Fowler at University of Ottawa (Ottawa). This research has been supported by an collaborative agreement with the Ontario Geological Survey (OGS) and the Mineral Exploration Research Centre at Laurentian University, a Natural Sciences and Engineering Research Council of Canada Discovery grant to C. Michael Lesher, a Natural Sciences and Engineering Research Council of Canada Discovery grant to ADF, a "Fonds québécois de la recherche sur la nature et les technologies"(formerly FCAR) fellowship and a Graduate Scholarship from University of Ottawa to MGH, and a Bickell Foundation fellowship to the University of Ottawa granted to SP. Brian Atkinson (Resident Geologist Office - Timmins Office) is thanked for having brought the Serpentine Mountain area to our attention and his help during some of the field work in this area. This contribution also benefit from the assistance in the field of Benoit-Michel Saumur, Justin Dignard, and Guillaume Girouard. We are very grateful to Millstreams Mines Ltd. for providing access to field exposures at Pyke Hill in the Potter mine property. The collaboration and discussions with Dave Gamble (Dave Gamble Geoservices Inc.) is gratefully acknowledged. All participants from the Len Berry Field

School (MAC-2004) and the komatiite-basalt association field trip (Field Trip A3 - GAC MAC 2006) are thanked for having stimulated discussion on the physical volcanology of komatiites on some of these specific outcrops. The present manuscript has benefited enormously from careful and thoughtful reviews by Steve Barnes, Jay Barr and Tim Grove.

CHAPTER 6 - THERMOMECHANICAL EROSION AND GENESIS OF KOMATIITE-ASSOCIATED NI-CU-PGE MINERALIZATION AT THE ALEXO MINE, ABITIBI GREENSTONE BELT, ONTARIO

6.1 Abstract

The komatiite-hosted Alexo Ni-Cu-(PGE) deposit occurs in the 2719-2711 Ma Kidd-Munro Assemblage of the Abitibi Greenstone Belt in Dundonald Township, Ontario. It was discovered in 1907 and has been mined intermittently since, most recently in 2005. The Alexo mine is the one of the localities where what is now referred to as spinifex texture was first described, where the "Billiard Ball" model for the basal segregation of massive, net-textured, and disseminated sulfides in deposits of this type was first developed, where many of the other distinctive characteristics (e.g., ore localization in footwall embayments, thick olivine cumulate host units) of deposits of this type were first identified, and where a genetic model involving incorporation of external S was first developed. Modifications of this model, involving thermomechanical erosion of footwall rocks by channelized high-temperature komatiitic magmas, have been proposed for many other deposits of this type on the basis of a wide variety of theoretical, field, stratigraphic, lithological, geochemical, and isotopic evidence, but continue to be debated. In order to further evaluate this model we have mapped a spectacular glacially-polished outcrop at the Alexo Mine that was hydraulically-cleaned of glacial overburden, providing continuous exposure of the ore zone and contact between the host komatiite and andesitic footwall rocks along a strike length of 200m. The rocks have been only locally deformed and have been metamorphosed to only prehnite-pumpellyite facies, preserving even the most subtle and delicate volcanic structures and textures. The following features provide unequivocal evidence that the host komatiite lava flow thermomechanically eroded underlying andesite flows: 1) the contact between komatiite and andesite is very sharp but delicately scalloped, marked by a thin selvedge of black devitrified glass, and clearly transgresses pillow structures and interpillow breccias in the andesite without any evidence of a regolith, shearing, or folding, producing multiple nested embayments on scales from 100s of meters to a few centimeteres; 2) the andesites have been contact metamorphosed and altered along the entire length of the outcrop and the degree of metamorphism/alteration is thicker and more intense around embayments; 3) xenoliths of andesite in komatiite are more common within embayments; 4) komatiitic dikes penetrate downward into the host andesites, primarily along the lateral margins of embayments, and 5) many of the dikes and marginal rocks exhibit geochemical evidence of contamination. This evidence for thermomechanical erosion, combined with S isotopic evidence for a major component of non-magmatic country-rock S in the ores, provides additional support for the roles of thermomechanical erosion and incorporation of country-rock S in the genesis of komatiite-associated Ni-Cu-(PGE) deposits. The detailed mapping also reveals that the stratigraphy of the ore zone is considerably more complex than previously reported, indicating that the sulfides were emplaced in several stages, confirming the dynamic nature of the ore emplacement process in komatiite-associated Ni-Cu-(PGE) deposits.

Keywords: Alexo mine, komatiite, nickel, thermomechanical erosion, embayments, Abitibi greenstone belt.

6.2 Introduction

The Alexo deposit is a small, high-grade Fe-Ni-Cu-(PGE) sulfide deposit located in Dundonald Township in northeastern Ontario (Fig. 6.1, inset). It was discovered in 1907 and appears to be the first Ni-Cu-(PGE) deposit to be discovered in what are now recognized to be komatiites. It is also one of the first localities where "chicken-track" textures (Naldrett and Mason, 1968), now referred to as spinifex textures were first decribed (Nesbitt, 1971). It was not until after the discovery of the Kambalda deposits in 1966 (Woodall and Travis, 1969; Ross and Hopkins, 1975), however, that such deposit were recognized as being an important new class of magmatic Ni-Cu-(PGE) deposits (Naldrett, 1973). The Alexo deposit is hosted by a thick olivine-rich cumulate komatiite and is localized within a pronounced embayment in the footwall rocks (Naldrett, 1966), features that are now recognized to be characteristic of Type I komatiite-associated Ni-Cu-(PGE) deposits (Lesher, 1989; Lesher and Keays, 2002; Barnes and Perring, 2006; Lesher and Barnes, 2008). The Alexo deposit is also the locality where Naldrett (1966) first proposed an external source for the S in the ores based on the similarity of the S isotopic compositions of the sulfides in the ores and andesitic country rocks and where Naldrett (1973) established his "Billiard Ball" model to explain the basal massive\net-textured\disseminated sulfide profile that characterizes many deposits of this type.

Modifications of this model, involving thermomechanical erosion of footwall rocks by channelized high-temperature komatiitic magmas, have been proposed for many other deposits of this type on the basis of an increasingly wide variety of theoretical, field, stratigraphic, lithological, geochemical, and isotopic evidence (see reviews by Lesher, 1989; Lesher and Keays, 2002; Barnes, 2006; Lesher and Barnes, 2008), but continue to be debated (e.g., Cas and Beresford, 2001; Rice and Moore, 2001; Stone and Archibald, 2002; 2004). The Alexo deposit is one of the best places to further evaluate this model, as the rocks have been only weakly metamoprphosed and are only locally penetratively deformed. Until 2001, most of the mine horizon remained covered by glacial quaternary deposits, and the only surface exposures were along the tops of a water-filled trench and mine shaft. However, between 2001 and 2003 the mine area was mechanically and hydraulically stripped, exposing spectacular glacially-polished outcrops of the lower part of the host unit, the entire width of the ore zone, and the upper part of the footwall rocks.

The purpose of this paper is to describe these outcrops and the evidence they record for thermomechanical erosion of andesite by komatiite, to discuss the physical volcanology of the mine environment, and to discuss the genesis of the Ni-Cu-(PGE) ores at the Alexo Mine.

6.3 Geological Setting

The Alexo deposit occurs within the 2719-2711 Ma Kidd-Munro assemblage of the Abitibi greenstone belt, in the northeast part of Dundonald Township approximately 45 km northeast of the city of Timmins, Ontario (Fig. 6.1). The Kidd-Munro assemblage in this area is ~3000m thick and has been subdivided into three regionally mappable formations (see Chapter 4; Houlé et al., 2008; Figs. 6.2A and 6.2B): the 50-400-m-thick *McIntosh Lake formation*, which comprises massive and pillowed intermediate to mafic flows, intermediate to mafic volcaniclastic deposits, and very minor komatiite flows; the 1000-2000m-thick *Dundonald formation*, which is composed of felsic volcanic volcaniclastic deposit, sulfidic-graphitic metasediments, and komatiite sills and flows; and the 250m-thick *Frederick House Lake formation*, which comprises primarily massive and pillowed mafic flows. The lower part of the Dundonald Formation and the upper part of the McIntosh Lake formation have been intruded by the ~1750m-thick, layered, tholeiitic mafic-ultramafic subconcordant to concordant Dundonald Sill. The rocks in the Alexo area have been metamorphosed to prehnite-pumpellyite facies (Arndt, 1986) and are locally faulted and/or sheared, but most of the deformation is non-penetrative and primary volcanic structures and textures are so well preserved that we will refer to the rocks using pre-metamorphic igneous and volcanic nomenclature.

The komatiitic rocks in the Dundonald formation in the Alexo area are intercalated with andesites of the McIntosh Lake formation; the andesites form prominent ridges, whereas the komatiites are largely covered by swamps. The komatiitic units have been subdivided into four members (see Chapter 4; Houlé et al., 2008; Fig. 6.2). The *Foundation member* is represented by a 45m-thick, poorly-differentiated komatiitic peridotite sill and the *Empire member* is represented by a 100m-thick, massive komatiitic peridotite sill. The *Dundonald South member* is ~100m thick and comprises a lower submember of thin differentiated komatiite and komatiitic basalt sills with minor peperite (Barrie et al., 1999), an an upper submember of thin, well-differentiated komatiitic flows with hyaloclastite flow-top breccias (Barnes et al., 1983;

Arndt, 1986). The *Alexo member* comprises thick, poorly-differentiated, olivine orthocumulate-mesocumulate flows, and is described in more detail below. The Alexo member is overlain by a ~250m-thick sequence of relatively thin, massive and pillowed mafic flows of the Frederick House Lake formation, which contain hydrothermally-deposited pyrite and pyrrhotite concentrated along fractures and replacing pillow selvages (Davis, 1997).

The outcrop and magnetic patterns in the Alexo area indicate that the volcanic units and the Dundonald Sill are megascopically folded and cross-cut by NW-trending faults with varying displacements (Fig. 6.1). The Dundonald formation in the vicinity of the Alexo Mine strikes ENE and dips moderately to steeply NNW with consistent NNW facing directions (indicated by brecciated and polyhedrally-jointed upper flow margins, graded spinifex-textures, and pillow polarities), and is therefore interpreted to be homoclinal (see Chapter 4; Houlé et al., 2008). We considered and cannot eliminate completely the possibility that the repetitive interlayering of komatiitic and andesitic units might be attributable to thrusting, but the exposed contacts do not appear to be faulted, there are significant differences in the volcanic-subvolcanic facies of the different members, and there is no evidence for the duplex structure required to produce structural repetition.

Fe-Ni-Cu sulfide mineralization occurs at or near the base of all four komatiite members (Fig. 6.2), but only the *Alexo Mine* (Alexo member) and the *Kelex zone* (Foundation member) have been mined thus far. The *Sox zone* (Dundonald South member) and *Small Pit zone* (Empire member) have not been mined, but are interpreted to be stratigraphically equivalent to the Dundeal and the Dundonald South deposits in the southwestern part of Dundonald Township (see Chapter 4; Houlé et al., 2008; Fig. 6.1). The Alexo Mine has been mined intermittently since its discovery, most recently in 2005, and has produced 93,000 tonnes at 3.6 percent Ni and 0.5 percent Cu (OGS, 2005; MacEachern, 2006).

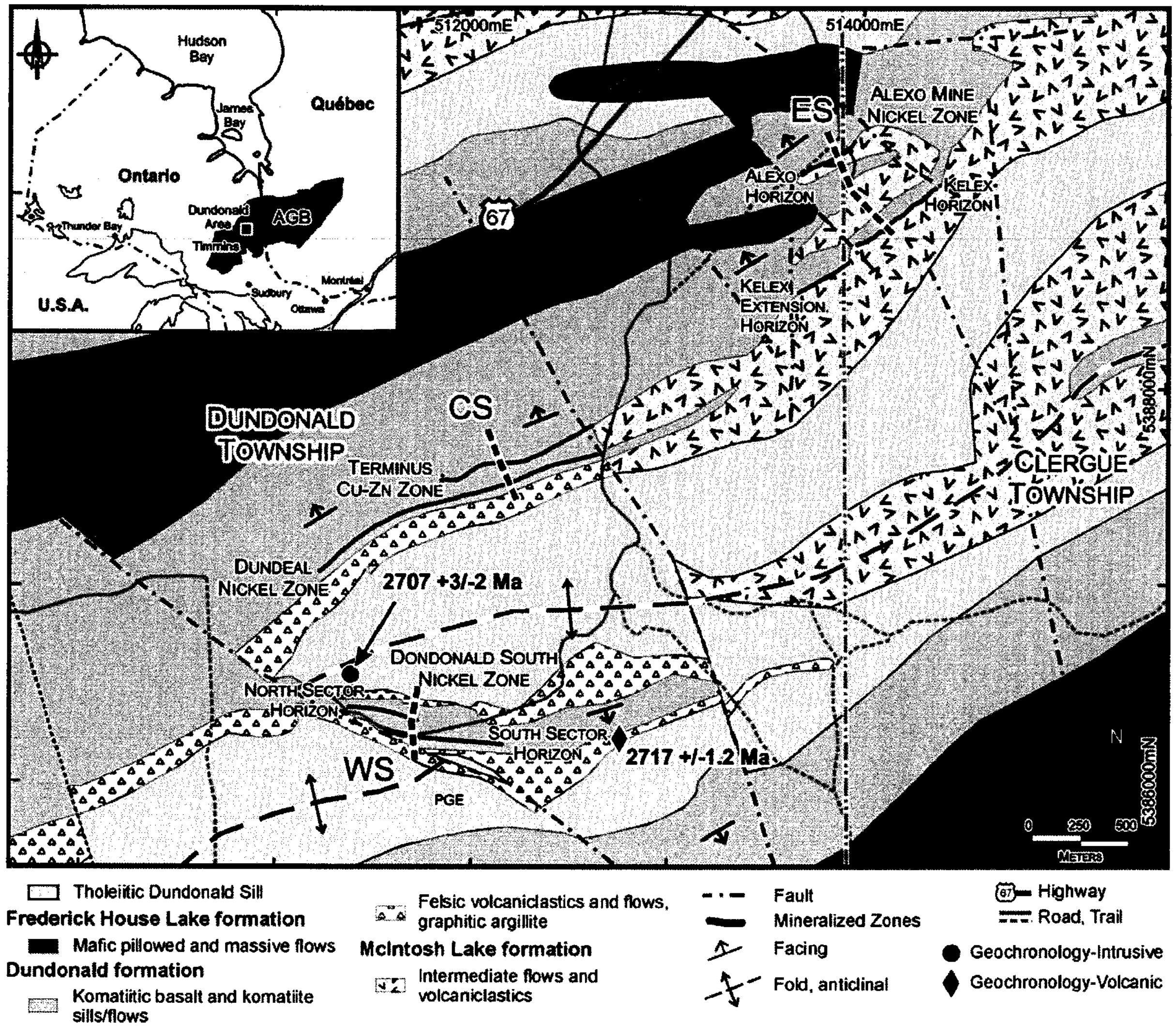

Figure 6.1 Simplified geological map of the Dundonald Township area, showing major geological units and locations of komatiite-associated Ni-Cu-(PGE) deposits (modified from MPH Consulting Ltd., 2004). U-Pb ages are from Barrie et al. (1999). Sections WS, CS, and ES are the locations of the stratigraphic columns in Figure 6.2.

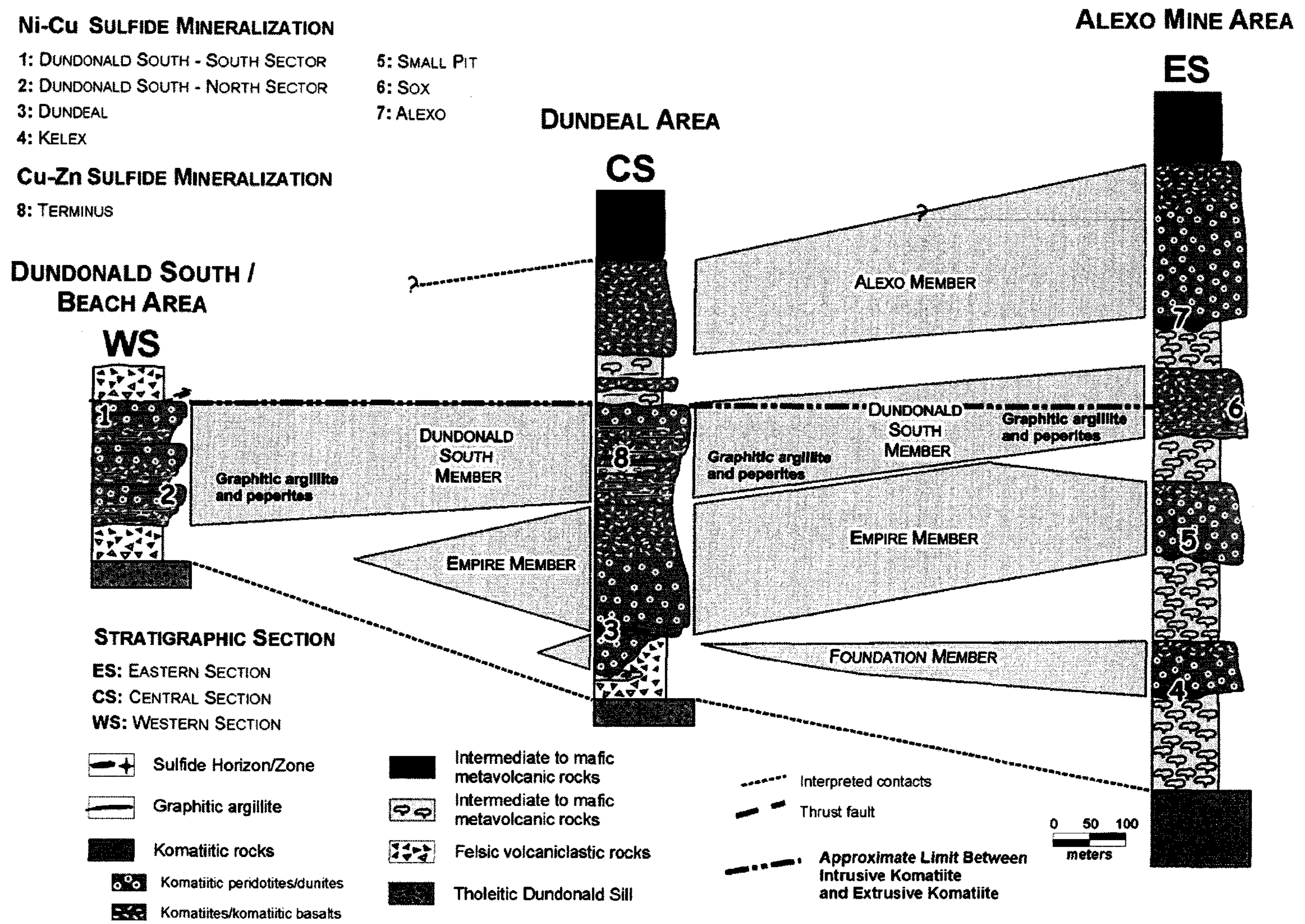

Figure 6.2 Schematic stratigraphic columns of the komatiitic succession of the Dundonald formation showing the subvolcanic/volcanic architecture and locations of komatiite-associated Ni-Cu-(PGE) deposits in the *western section* (WS: this study), *central section* (CS: modified from Davis, 1997; Barrie et al., 1999), and *eastern section* (ES: P.C. Davis and Canadian Arrow Mines, unpubl. data, 1999-2005; M.G. Houlé, this study). Section locations in Figure 6.1.

6.4 Field Relationships

Field mapping was done on glacially-polished outcrops that were mechanically-stripped and hydraulically-cleaned of glacial overburden by Hucamp Mines Ltd., Larchex Inc., and Canadian Arrow Mines Ltd. between 2001 and 2003. The stripped area exposed the lower part of the mesocumulate komatiite host unit, the entire width of the ore zone, and the upper part of the andesitic footwall rocks over a strike length of 200m and a width of 40m. The outcrops were mapped by K. Montgomery of Hucamp Mines Ltd. at 1:125 to 1:250 scales in 2001, and remapped by MGH at scales ranging from 1:10 to 1:100 between 2001 and 2002.

Regrettably, most of the exposures were lost during open-pit mining operations by Canadian Arrow Mines Ltd. between 2004 and 2005. At present, only a small section of this exceptional exposure remains at the SW end of the Alexo pit. The maps, sections, and some of the photos will be published by the Ontario Geological Survey (Houlé and Montgomery, in prep.); hard copies will be available from pubsales.ndm@ontario.ca and digital copies will be downloadable at http://www.geologyontario.mndm.gov.on.ca/.

6.4.1. Footwall Andesites

The footwall rocks to the Alexo komatiite are well-exposed along the entire length of the stripped area (Fig. 6.3) and on a prominent ridge southeast of the stripped area. They are composed of pillowed, massive, and hyaloclastitic andesitic volcanic rocks that weather a light to medium grey with a light grey-green fresh surface. The andesites form compound massive, pillowed, and fragmental flows that can be traced for 10's to 100's of metres along strike. The sequence below the ore horizon comprises, from top to bottom (Fig. 6.5A): 1) a 3-4m thick unit of closely-packed pillows with limited amounts of interpillow hyaloclastic material, 2) a 4-5m thick intermediate lapilli-tuff to tuff-breccia horizon that pinches out to west, and 3) a ~10m thick compound flow comprising a 4-6m thick upper zone of amoeboid pillows and broken-pillow breccias floating in a matrix of hyaloclastite and a 3-4m thick lower zone of pillowed andesite. Varioles, flow banding, and amygdales occur locally within pillow margins.

The andesites contain semi-massive lenses of pyrite and pyrrhotite, locally representing up to 40% of the units. Some flows are also separated by thin (<2m) discontinuous horizons of graphitic sediments containing up to 20% pyrite and pyrrhotite with trace amounts of chalcopyrite.

6.4.2. Alexo Komatiite

The Alexo komatiite is very poorly exposed and because the dips are steep and because drilling was focussed on intersecting the ore horizon, the upper contact was intersected in only one drill core ~300m WNW of the mine. This core no longer exists and only very brief descriptive logs are available. 3000m-deep diamond drill cores have been drilled through the central parts of the host unit to intersect the basal contact, but only ~300m-deep cores have been drilled through flanking parts of the unit. The serpentinized cumulate rocks of the Alexo komatiite are well defined on magnetic maps. Together, these data suggest that the Alexo member comprises one or more very thick (~250m) relatively undifferentiated olivine cumulate-rich units near the Alexo Mine, which grade laterally into multiple thick differentiated (spinifex/cumulate) units to the southwest (Fig. 6.3). The komatiites WSW of the ore zone are composed of several thin and thick (10-115m) differentiated komatiite flows with thick lower olivine cumulate zones and thin upper olivine or pyroxene spinifex zones (Fig. 6.3); some units with "flow-top breccias" and some separated by interflow graphitic sulfidic sediments were reported in cores further to the west. The komatiites ENE of the ore zone are separated from the remainder of the succession by a NW-trending fault, complicating a determination of the relationship with the ENE flank, but it appears to dominated by olivine cumulate komatiites

The komatiites above the ore zone are composed almost entirely of massive, fine- to medium-grained olivine orthocumulate and mesocumulate komatiite (Fig. 6.4A), but some parts of the olivine orthocumulate exhibit randomly oriented tabular olivine (Fig. 6.4B) or hopper olivine textures (Fig. 6.4C). These rocks have also been reported by Barnes (1985) to contain branching olivine crescumulate komatiite. The proportions of olivine and interstitial liquid vary gradually and repetitively over the thickness of the unit, and the abundance of olivine decreases near the basal contact (Naldrett, 1966). The lowermost part of the unit is marked by a 2-3m thick zone of fine-grained pyroxene peridotite to olivine pyroxenite (wehrlite) that is in sharp contact with the footwall andesites.

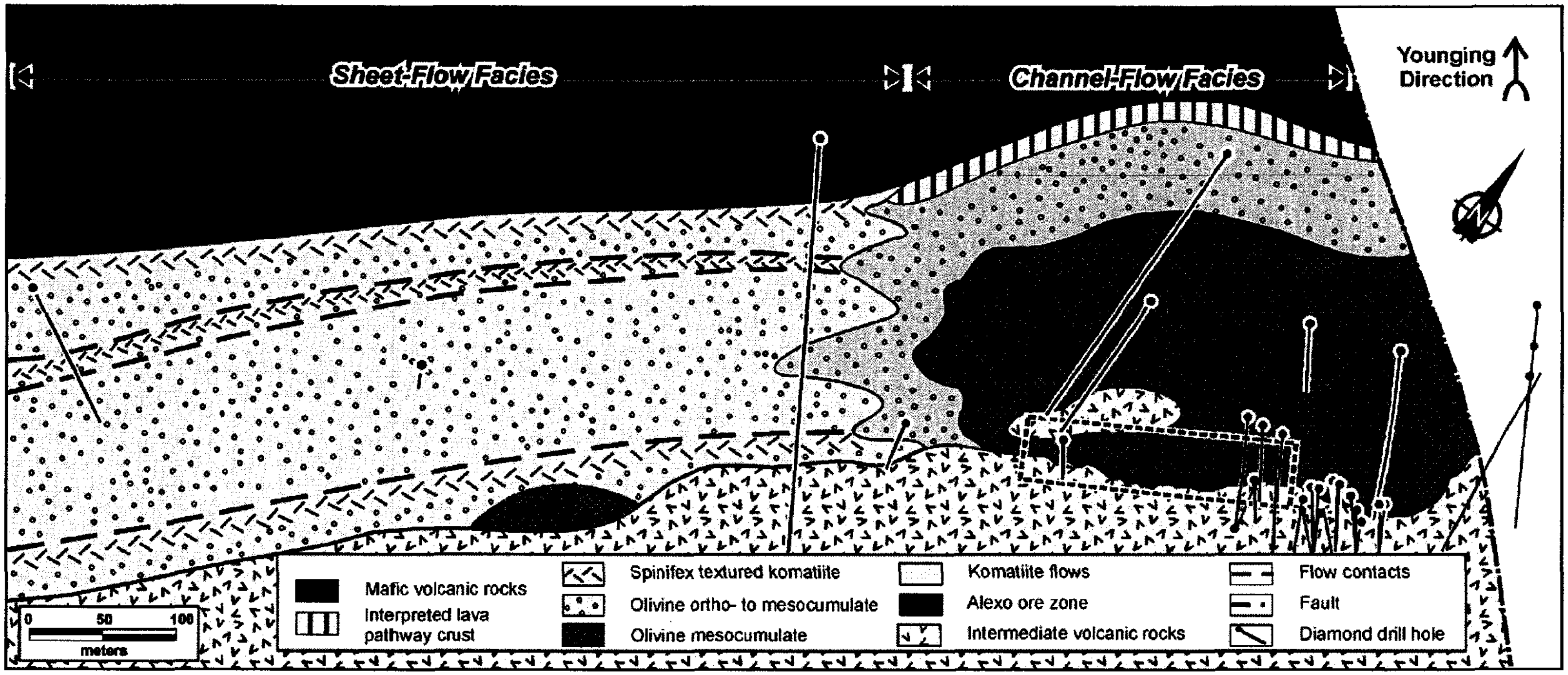

Figure 6.3 Interpreted surface plan of the volcanic facies at the Alexo mine (based on surface exposure and diamond core logs), illustrating the relatively massive central channel-flow facies, which exhibits a series of mineralized nested footwall embayments and the western sheet-flow facies, which is characterized by at least four different differentiated komatiitic units (spinifex/cumulate).

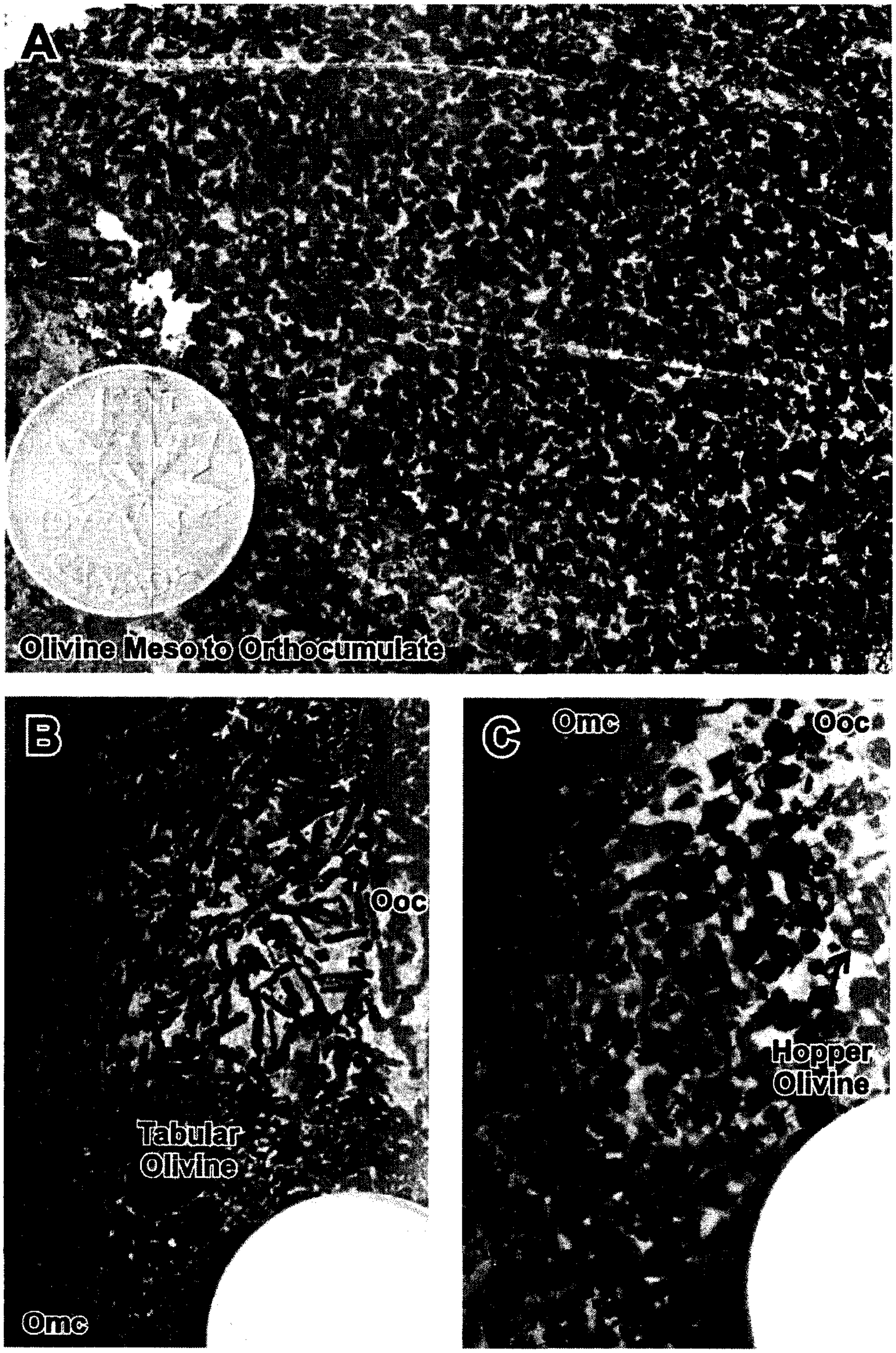

Figure 6.4 Representative olivine cumulate rocks at the Alexo mine (UTM 513862E, 5389472N, NAD 83, Zone 17). A) Olivine meso- (Omc) to orthocumulate komatiite (Ooc) from the stripped area. B) Olivine mesocumulate with patch of randomly-oriented tabular olivine orthocumulate. C) Olivine mesocumulate that contains areas of Ooc with hopper olivine crystals. Coin is ~20mm in diameter and used for scale in all photos.

6.4.3. Basal Contact Relationships

The basal contact was exposed over a strike length of ~200m east and west of the old Alexo mine shaft. The contact was obscured by slight shearing in a few places, probably reflecting flexural slip during regional folding, but many areas were perfectly preserved, especially along parts of the western area and eastern area (Fig. 6.5).

Detailed mapping of the basal contact reveals that 1) the contact between komatiite and andesite is very sharp but delicately scalloped, marked by a thin (<1 cm) selvedge of black devitrified glass, and clearly transgresses pillow structures and interpillow breccias in the andesite without any evidence of a regolith, shearing, or folding, producing multiple nested embayments on scales from 100s of meters to a few centimeteres; 2) the andesites have been contact metamorphosed and altered along the entire length of the outcrop and the degree of metamorphism/alteration is thicker and more intense around embayments; 3) xenoliths of andesite in komatiite are more common within embayments; and 4) komatiitic dikes penetrate downward into the host andesites, primarily along the lateral margins of embayment. These points are discussed in detail below.

6.4.3.1. Footwall Embayments

Virtually all of the ores in the Alexo mine zone are localized within a series of footwall embayments (Figs. 6.3 and 6.5A) that can be subdivided into several orders based on their depths and relationships to other embayments. The first-order embayment that localizes the entire Alexo mine host unit is asymmetric, concave, ~300m wide, and ~45m deep (Fig. 6.3). Although incomplete exposure of the footwall and hanging-wall stratigraphy does not permit us to completely preclude modification of the first-order embayment by folding, as discussed below, the highly irregular geometries of the smaller embayments are not consistent with folding or faulting. Second-order embayments are superimposed on and contained within the first-order embayment, and are 120-140m wide and 25-45m deep, but those at the ENE and WSW ends of the exposure are 10-15m wide and 5-6m deep. Third- and fourth-order embayments appear to be superimposed on second-order embayments and are 15-70m wide x 5-20m deep and 13-20m wide x 4-6m deep, respectively.

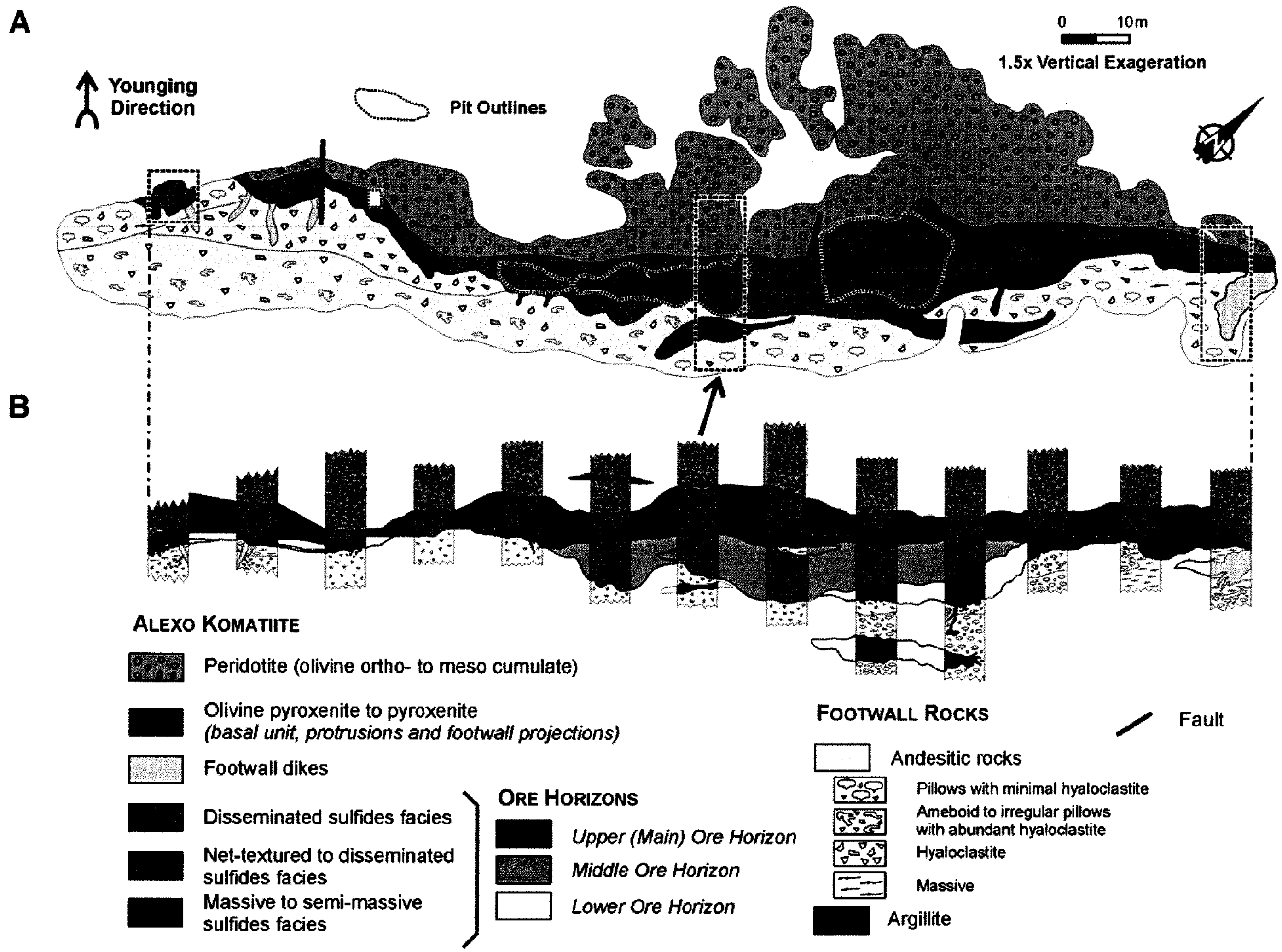

Figure 6.5 A) Simplified geological map of the Alexo stripped area (1.5x vertical exaggeration) in Dundonald Township, illustrating the localization of mineralization within a series of nested embayments along the basal contact (see also MAP B for details in back pocket). B) Composite section illustrating variations in the ore profile along the stripped area. Location of sections in A.

Larger embayments are generally concave in shape, whereas smaller embayments are concave to re-entrant in shape. Some embayments exhibit complex geometries (Fig. 6.6), but where the basal contact is covered by unmineralized komatiite, disseminated sulfides in komatiite, or net-textured ore, the embayments are normally concave, whereas where the basal contact is covered by massive sulfides, the embayments often re-entrant (Figs. 6.7 and 6.8). These geometries are similar to the least-deformed embayments at Kamblada, where massive sulfides in the re-entrant margins transgress massive, pillowed, or volcaniclastic basalt (Lesher, 1989).

At the westernmost part of the stripped area a concave to re-entrant embayment appears to have split into two subembayments separated by a pillar (Figs. 6.7 and 6.8). The western subchannel is characterized by significant undercutting of the both flanks by komatiite and massive sulfides, whereas the eastern subchannel is characterized by restricted undercutting by komatiite on the western flank and by no undercutting on the eastern flank. Smaller (m-scale to cm-scale) concave and re-entrant embayments and irregularities are superimposed on all of the embayments, resulting in a highly contorted footwall contact (Fig. 6.9). The contact the between the Alexo komatiite and its footwall rocks is very sharp but quite variable along strike. For example, the contact between komatiite and andesite and ranges from relatively planar and regular (Fig. 6.9a) and quite irregularly scalloped (Figs. 6.9b and 6.9c) to highly contorted (Figs. 6.9d and 6.9e).

There does not appear to be any consistent asymmetry and some embayments have more concave margins on one side and more re-entrant margins on the other (Figs. 6.6 and 6.7), similar to Raglan (Lesher, 2007) and Black Swan (Dowling et al., 2004), but quite different from the flat-floored embayments typical of least-deformed areas of Kambalda (Lesher, 1989; Evans et al., 1989).

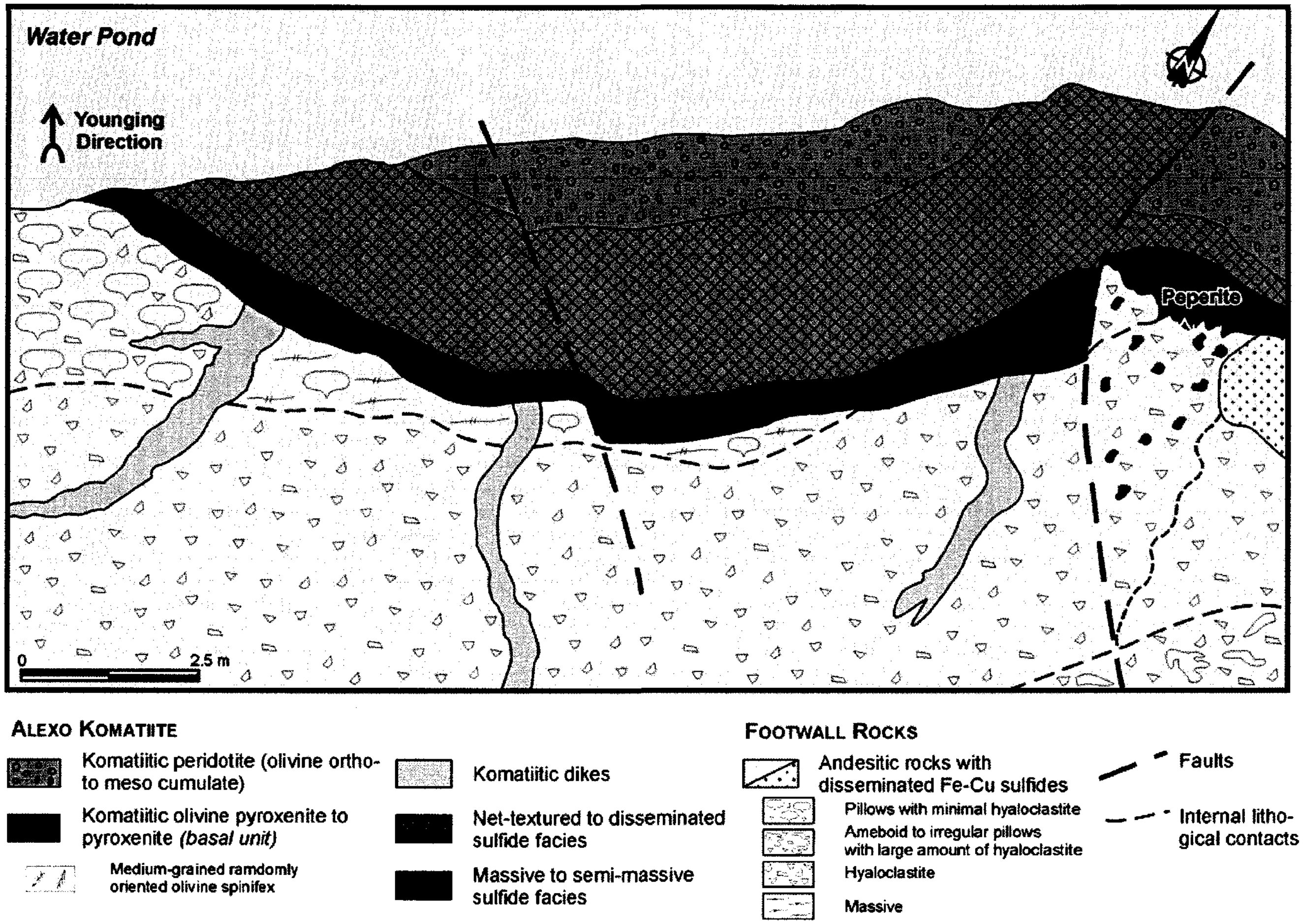

Figure 6.6 Concave third-order embayment along the stripped area at the Alexo mine (UTM 513780E, 5389422N, NAD 83, Zone 17). The embayment is asymmetric; the western side is characterized by a classic disseminated/an/net-textured /massive ore profile directly overlying andesite, whereas the eastern side is partly underlain by barren (to weakly mineralized) pyroxenite unit (basal unit). Spinifex-textured also occurs at the margins of the embayment.

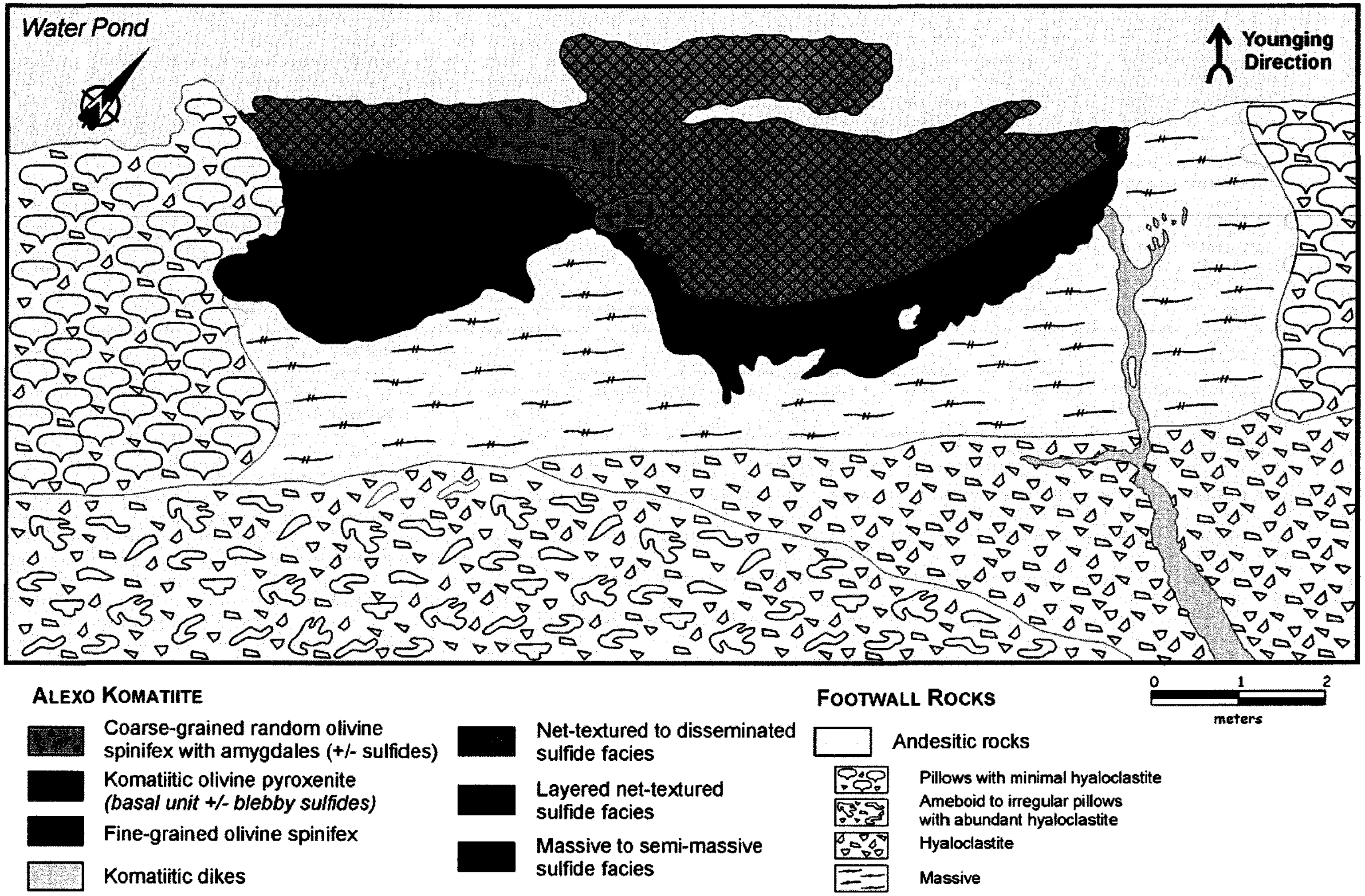

Figure 6.7 Concave to re-entrant second-order embayment in the westernmost part of the stripped area at the Alexo mine (UTM 513774E, 5389415N, NAD 83, Zone 17). The embayment has split into two third-order embayments and that undercut their flanks, leaving a central ridge. Both are broadly asymmetric, more undercut to the west, but the western embayment is undercut on both sides, whereas the eastern embayment is concave on the east side and re-entrant (undercut) along the west side.

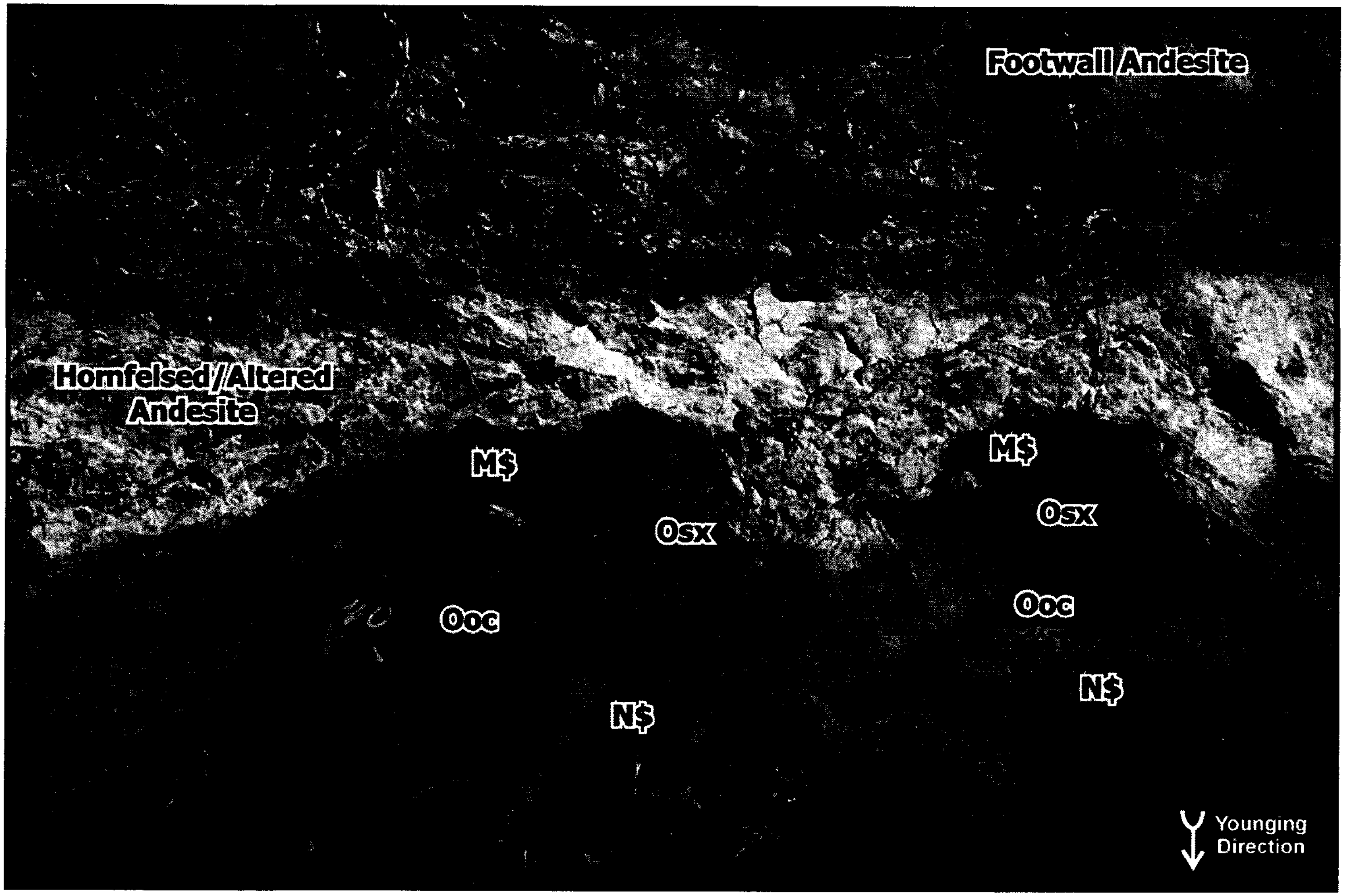

Figure 6.8 Photo of concave to re-entrant second-order embayment in the westernmost part of the stripped area (Fig. 6.7) at the Alexo mine (UTM 513774E, 5389415N, NAD 83, Zone 17). The second-order embayment is split in two third-order and that locally undercut their margins, leaving a central ridge. M$: massive sulfides, N$: net-textured sulfides, Ooc: olivine orthocumulate, Osx: olivine spinifex textures.

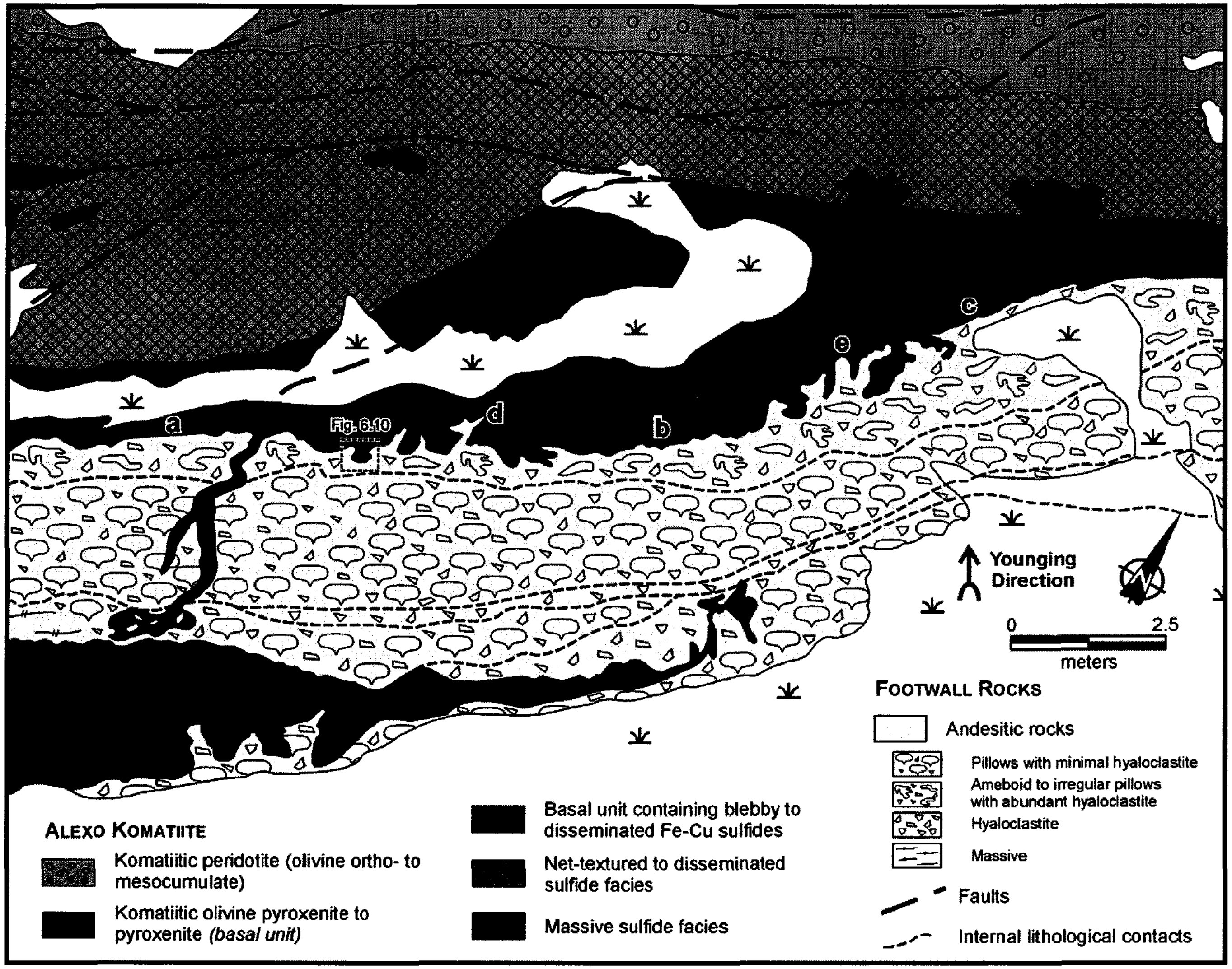

Figure 6.9 Irregular, scalloped, and highly-contorted basal contact between the Alexo komatiite (basal unit) and andesitic footwall rocks (UTM 513875E, 5389468N, NAD 83, Zone 17).

6.4.3.2. Basal Unit, Footwall Protrusions, Projections, and Dikes

The ore zone is commonly separated from the footwall rocks by a weakly mineralized to barren *basal unit* and the footwall rocks contain numerous *protrusions*, *projections*, and *dikes* of komatiite, most of which are also unmineralized.

The ***basal unit*** is preserved for ~20m along the western margin of the main embayment around the exploration shaft and for ~35m along the eastern margin of the main embayment east of the main Alexo shaft (Figs. 6.5, 6.6, 6.7, and 6.9). It is 0.5-4m thick, varies in composition from olivine pyroxenite to pyroxene peridotite, and locally feeds footwall projections (Fig. 6.9). The basal komatiitic unit that occurs between the Lower and the Middle ore horizons (see below) in the western part (Figs. 6.6 and 6.8) is most likely correlative with the basal komatiitic unit in the eastern part (Fig. 6.9) of the first-order Alexo embayment (Fig. 6.5).

Footwall protrusions are small (<0.5m) irregular embayments of unmineralized aphyric komatiite (Fig. 6.10A and 6.10B) or, less commonly, massive sulfide (Fig. 6.12A) that protrude into the andesite, sometimes extending laterally as thin (<1 cm) sills subparallel to the overlying contact (Figs. 6.10A and 6.10B). Komatiite protrusions are characterized by contamination and fracturing of the komatiite marked by a very thin (~2-5 mm) black chilled margin of komatiite with brownish aphyric komatiite core, and by silicification and brecciation of the adjacent andesites (Fig. 6.10).

Footwall projections are thin (0.2-3m), highly irregular intrusions of unmineralized aphyric komatiite that extend up to 6m from the host unit downward into underlying pillowed andesites (Fig. 6.9). They have wavy and irregular contacts where they invade massive andesites and peperitic contacts where they invade fragmental volcanic rocks. They appear to have exploited fractures generated by thermal cracking of the seawater-filled andesite and clearly cross-cut the selvages of andesite pillows. They normally terminate as bulbous pods that cross-cut the pillows.

Footwall dikes are narrow (0.2-3m), more regular intrusions of unmineralized pyroxene-phyric komatiites that extend up to 6m from the komatiite basal contact into the underlying pillowed andesites. They are clearly spatially associated with footwall embayments and are cross-cut by (rather than fed by) the overlying komatiites (Figs. 6.6 and 6.7). They are also locally cut by the ores (Figs. 6.6 and 6.7). Like footwall protrusions, they have wavy and irregular contacts where they invade massive andesites and peperitic contacts where they invade fragmental volcanic rocks. They commonly exhibit variolitic textures, which appear in thin section to represent alteration, rather than contamination (unmixed xenomelts - unlikely given that the protrusions do not contain any of this type of material), an immiscible liquid (unlikely for the same reason), or devitrification (unlikely, given that the rocks are not glassy) (see further discussion by Fowler et al., 2002).

6.4.3.3. Inclusions

The basal part of the Alexo komatiite and associated footwall protrusions, projections, and dikes contain some angular (mechanically-eroded) xenoliths, many subrounded (partially-melted) xenoliths, and many globular (completely-melted) xenomelts of andesitic volcanic rocks. They also occur in massive sulfides, but have not been observed in net-textured or disseminated sulfides. The inclusions vary widely in size, but are commonly less than 10 cm in diameter. The largest are slab-like blocks of andesite up to 10-15m long oriented subparallel to the basal contact (Baker, 1917).

6.4.3.4. Contact Metamorphism

The andesitic rocks beneath the Alexo komatiite have been contact metamorphosed along the entire length of the exposed outcrop, but the intensity and thickness is greater beneath second-order footwall embayments. The pillow structures in the andesitic rocks beneath the westernmost footwall embayment have been almost completely obliterated within 2m of the embayment (Fig. 6.7), leaving only a few incomplete pillow margins. The contact metamorphism is manifested as recrystallization and patchy silicification, which grades (with increasing distance from the contact) from bleached, silicified, and recrystallized (possibly melted) andesite through recrystallized andesite to weakly metamorphosed andesite over a distance of several meters (Figs. 6.11A and 6.11B). The basal contact ranges from relatively planar and regular (e.g., right side of Fig. 6.11A) and quite irregularly scalloped (e.g., left side of Figs. 6.11A and 6.11B) to highly contorted that is also reflected in the alteration patterns (Fig. 6.11A).

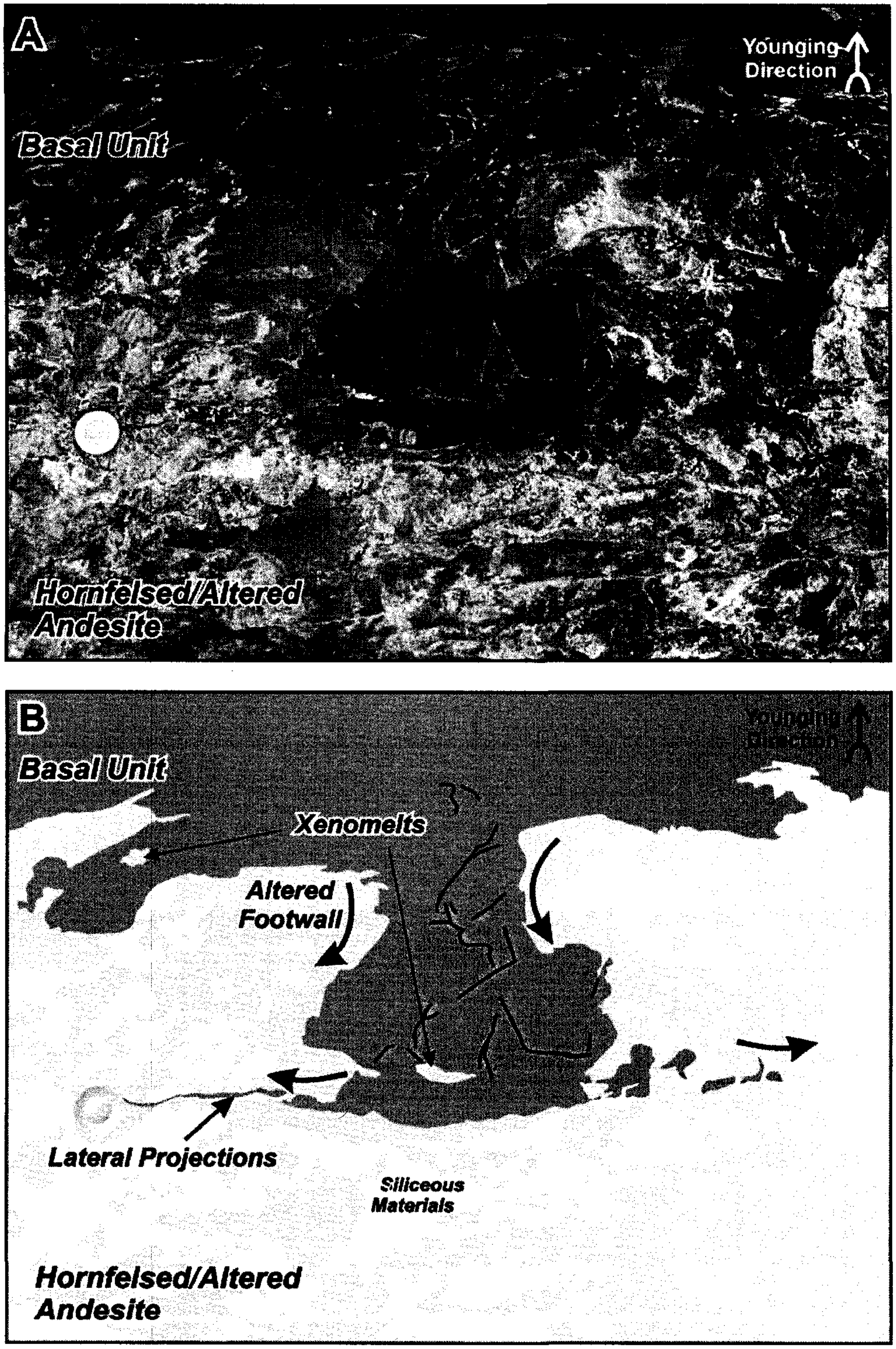

Figure 6.10 Komatiite protrusion along the basal contact at the Alexo mine (UTM 513875E, 5389468N, NAD 83, Zone 17). A) Photograph of the komatiite protrusion (dark grey) extending from basal unit (black) into andesite (light grey). B) Map of the same protrusion showing the komatiitic material extending downward and spreading out laterally as very thin komatiitic sills. Coin is ~24mm in diameter.

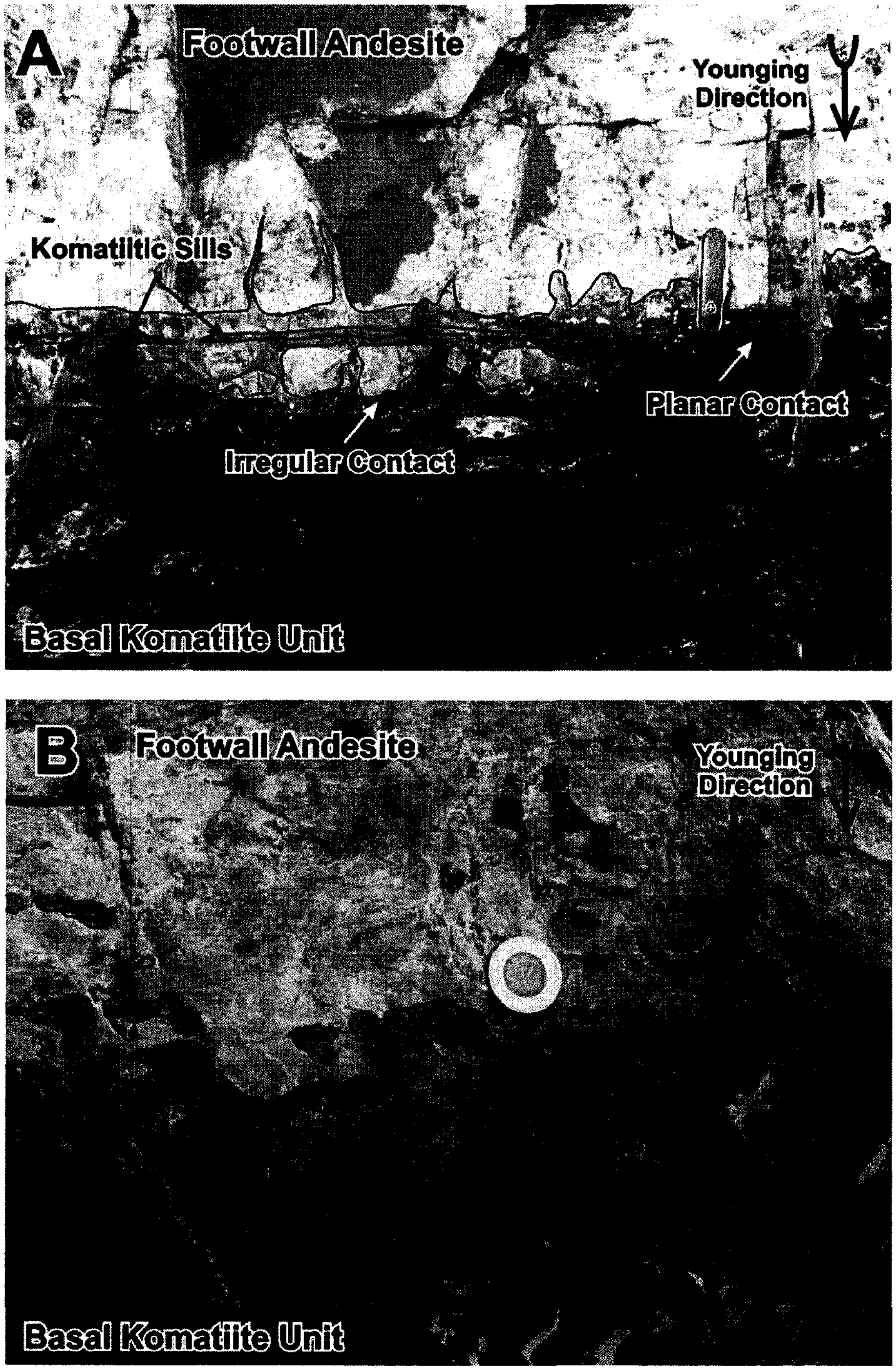

Figure 6.11 A) Basal contact relationship between the Alexo komatiite (basal unit) and andesitic footwall rocks (UTM 513879E, 5389475N, NAD 83, Zone 17). On the ride side, the contact is planar, whereas on the left side, the contact is quite irregular and scalloped, characterized by thin komatiitic injections downward and laterally. Knife is ~10cm long. B) Relatively planar but slightly undulatory contact between komatiite (black), contact metamorphosed andesite (brown), and altered andesite (light tan) (UTM 513877E, 5389473N, NAD 83, Zone 17). Coin is ~28 mm in diameter.

6.4.4. Ni-Cu-PGE Mineralization

The Ni-Cu-(PGE) mineralization at the Alexo mine is hosted by olivine ortho- to mesocumulate komatiites. The ores are localized within the larger first-order footwall embayment and further confined by smaller higher-order embayments in the underlying volcanic rocks. Locally, mineralization also extends into the footwall rocks as protrusions and small dikes, but as noted above, some of the ores are separated from the footwall rocks by a unit of weakly mineralized komatiite.

The mineralogy of the ores is typical of magmatic Ni-Cu-(PGE) deposits (Naldrett, 2004). The principal nickel-bearing sulfide minerals in the ores are pentlandite with subordinate heazlewoodite and violarite (Coad, 1979). Pyrrhotite, troilite, and pyrite are major components of the mineralization, whereas chalcopyrite is a ubiquitous accessory phase (Naldrett and Gasparrini, 1971). Minor amounts of magnetite occur in massive ores.

6.4.4.1. Sulfide Textural Facies

The Fe-Ni-Cu sulfides range in thickness from a few centimetres to greater than 8 metres, and are characterized by massive to semi-massive lenses overlain by net-textured and disseminated sulfides. The mineralization occurs as five main textural facies: 1) massive; 2) net-textured; 3) disseminated; 4) blebby; and 5) xenolithic sulfide facies.

The *massive sulfide facies* is composed of more than 85% Fe-Ni-Cu sulfides with fine inclusions of komatiite and footwall rocks (Fig. 6.12A). This facies occurs semi-continuously along the entire strike length of the stripped area and ranges in thickness from a few centimetres to up to 4 metres. Several enclaves of the footwall rocks and rare enclaves of disseminated to net-textured sulfides also occur within the massive sulfide facies. Apophyses of massive sulfide facies also occur locally at the base of the net-textured sulfide facies (Fig. 6.12B).

The *net-textured sulfide facies* at the Alexo mine is the type locality for net-textured sulfide facies (Naldrett, 1966, 1973) and comprises of a fine-grained olivine orthocumulate rock where the interstitial phase is composed a network of sulfides (Fig. 6.13A). This network is semi-continuous to continuous, depending on the abundance of sulfides (15 to 50%). This facies is the dominant mineralized facies at the Alexo mine and occurs continuously along the entire strike length of the stripped area and ranges in thickness from few centimetres to greater than 5 metres.

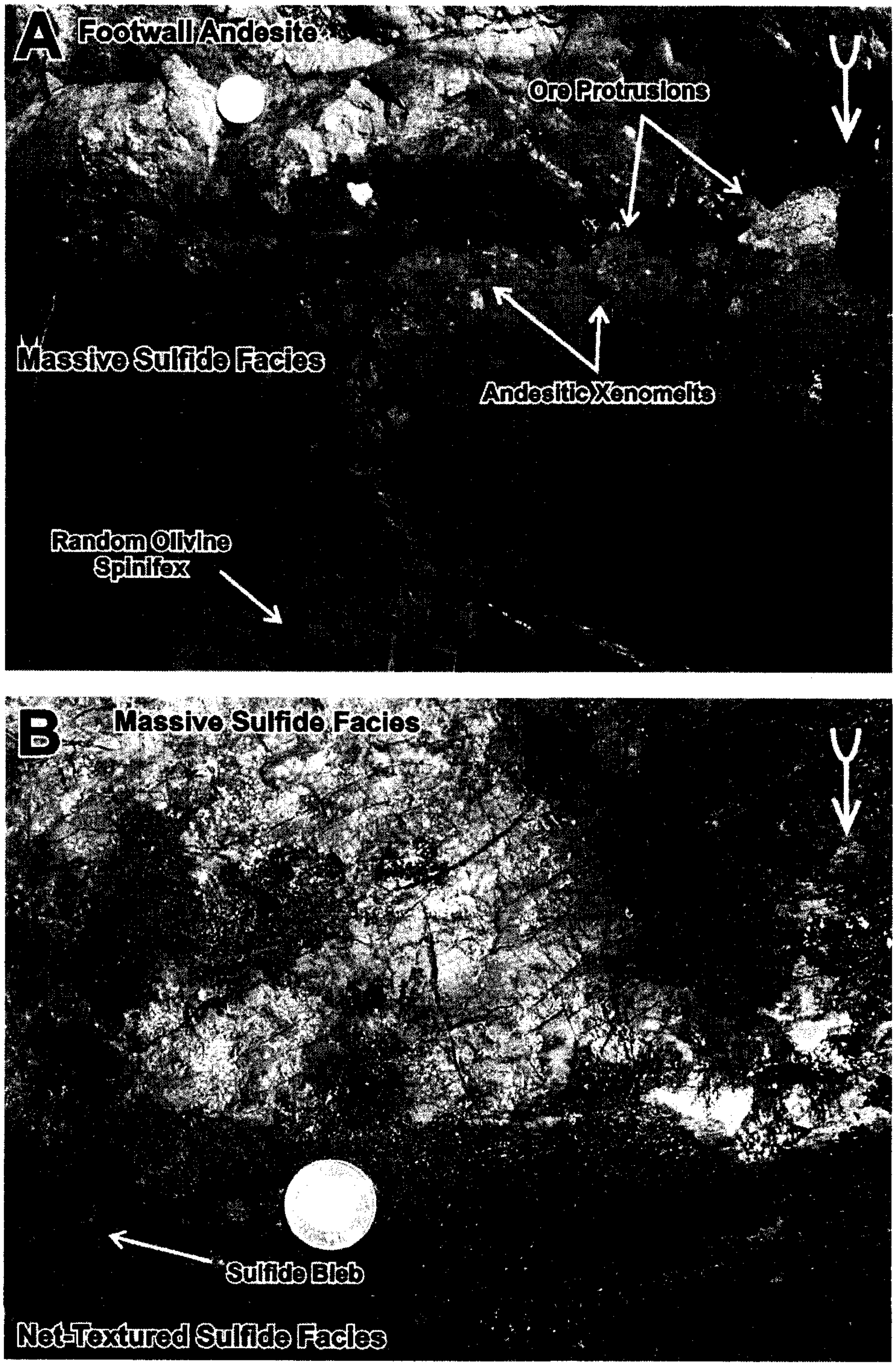

Figure 6.12 Massive sulfide facies at the Alexo Mine. A) Photograph of massive sulfide facies protrusion within the westernmost footwall embayment (UTM 513774E, 5389415N, NAD 83, Zone 17). Note andesitic pods (xenomelts) along the base of the massive sulfide facies. B) Massive and blebby sulfide facies within net-textured sulfide facies near the basal contact of the stripped area (UTM 513875E, 5389478N, NAD 83, Zone 17). Coin is 28 mm in diameter in both photos.

Centimeter-scale layering occurs locally at the base of the net-textured sulfide zone. A variant containing medium- to coarse-grained *blades* of olivine (Fig. 6.13B) occurs as patches in association with the massive sulfides facies. Net-textured ores commonly contain clasts of massive sulfide and barren olivine mesocumulate komatiite (Fig. 6.9).

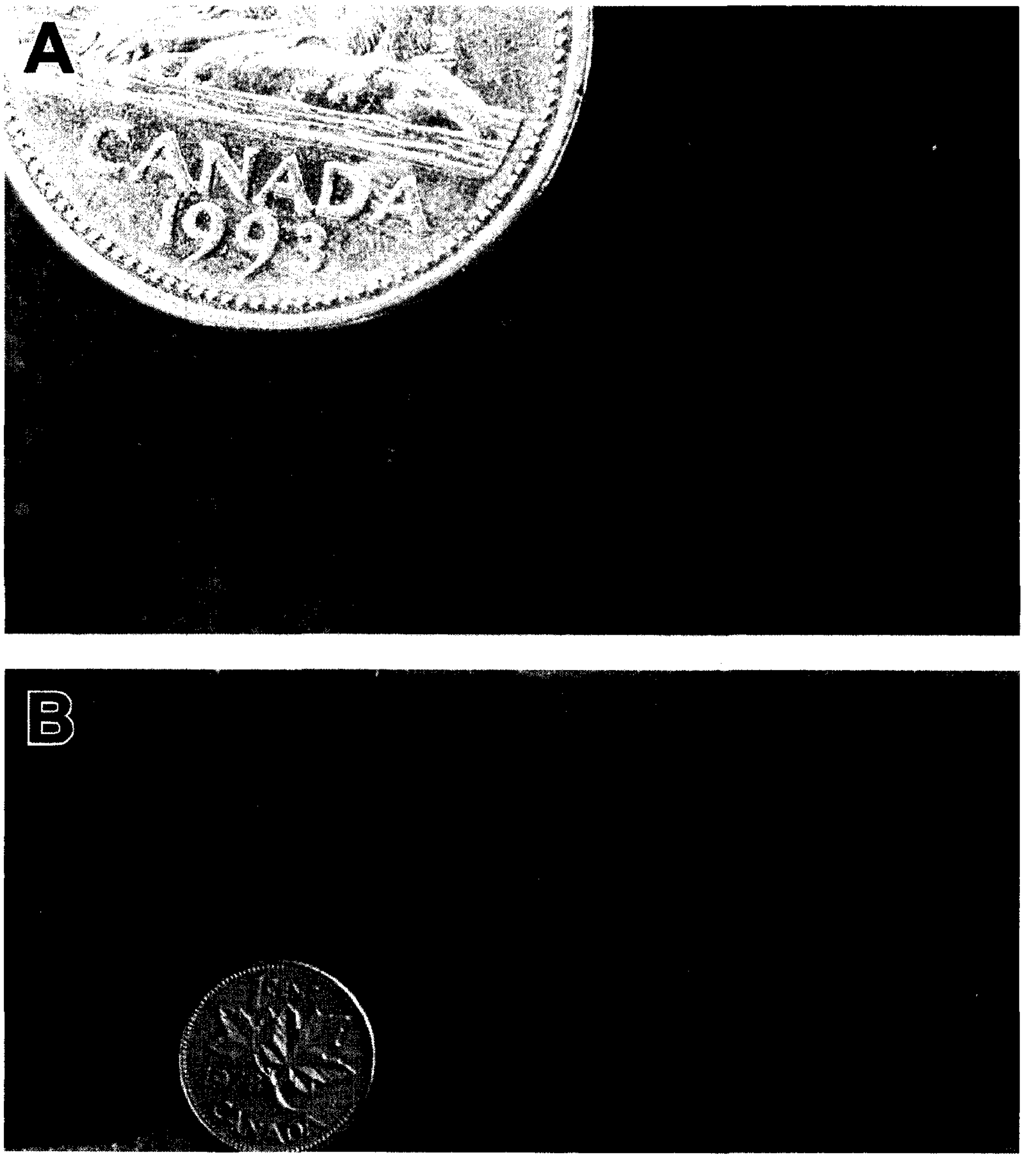

Figure 6.13 Net-textured sulfide facies at the Alexo Mine. A) Photograph of typical orthocumulate net-textured sulfide facies observed on the Alexo stripped area. Coin is 21 mm in diameter. B) Photograph of spinifex net-textured sulfide facies observed in drill core. Coin is 19 mm in diameter.

The *disseminated sulfide facies* occurs discontinuously above and locally within net-textured sulfide facies. It consists of up to 10% finely disseminated Fe-Ni-Cu sulfides within olivine mesocumulate komatiite.

The *blebby sulfide facies* occurs very discontinuously, normally as small (<20 cm) patches within net-textured sulfide facies. It consists of small (<1 cm) subspherical patches of Fe-Ni-Cu sulfides (up to 5-7%) within the host mesocumulate komatiite. The sizes and distributions of the blebs appear to be erratic.

The *inclusion-bearing sulfide facies* is rare, but it is generally closely associated with massive sulfide facies and only occurs at the bases of ore profiles. The inclusions include andesite xenoliths and komatiite autoliths (Fig. 6.11B). The xenoliths do not appear to have been rotated or experienced any displacement, and therefore represent footwall rocks that have been veined by sulfides rather than physically-incorporated fragments.

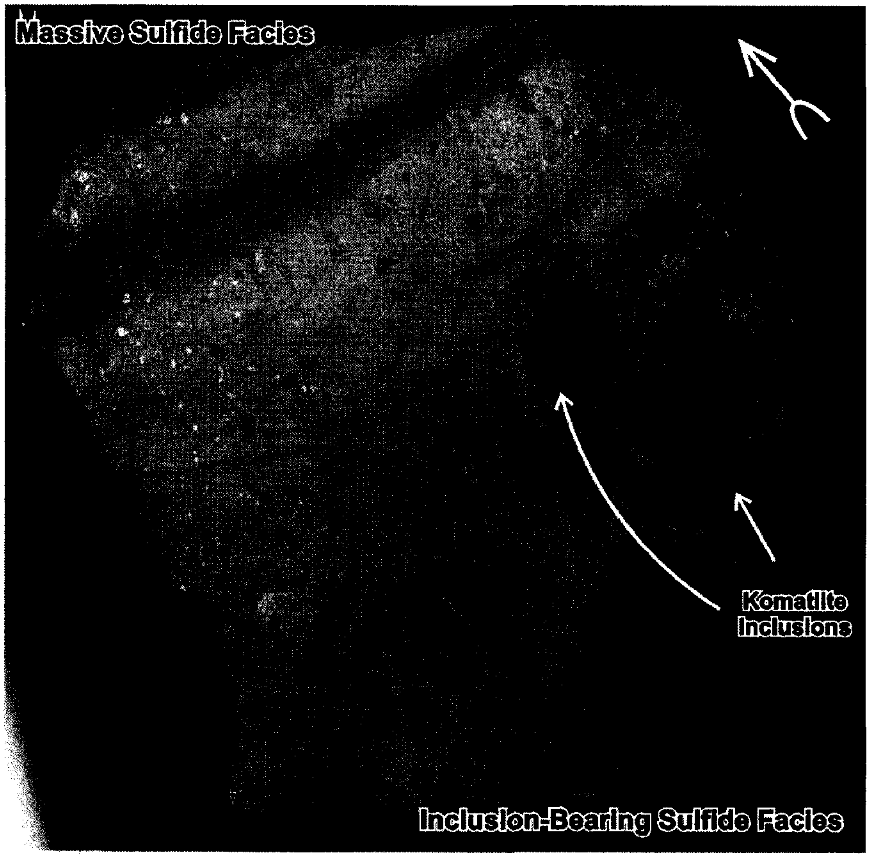

Figure 6.14 Photograph of typical *inclusion-bearing sulfide facies* located at the base of massive sulfide facies where inclusions are dominantly komatiitic in composition (photo courtesy of Brian Atkinson).

6.4.4.2. Ore Profile

Although some andesite \ massive sulfide, massive sulfide \ net-textured sulfide, and net-textured sulfide \ disseminated sulfide contacts at Alexo are sheared (modified magmatic) and a few are faulted (tectonic), most shearing has been accommodated by the more ductile massive sulfides (see discussion by Barrett et al., 1977), so most contacts remained unmodified. The most common ore profile at the Alexo mine (Fig. 6.15) is characterized by massive sulfide facies underlain by xenolitic sulfide facies and overlain by net-textured sulfide facies with local sulfide blebs. Most contacts are delicately scalloped and decorated with ferrochromites (Fig. 6.12A), indicating that they are primary magmatic contacts (Ewers et al., 1976; Marston et al., 1981; Lesher, 1989; Frost and Groves, 1989; Barnes et al., 2004).

The segregation of sulfides into a lower zone of massive sulfides overlain by net-textured sulfides and disseminated sulfides was first described at the Alexo mine (Naldrett, 1966) and has since been described at many other deposits of this type (Ewers and Hudson, 1972; see reviews by Lesher, 1989; Barnes, 2006; Lesher and Barnes, 2008). Alexo is the locality where Naldrett (1973) first applied his "billiard-ball" model to explain such profiles, the concept being that olivine (billiard balls) would settle through silicate magma containing fine disseminated sulfides (water) but float in sulfide melt (mercury), and that the thickness of the massive sulfide melt (mercury) would be determined by the thickness of the column of olivine (billiard ball) according to Archimedes' principle.

Although this ore profile occurs in the western and central parts of the stripped area at the Alexo mine, in many other parts the ore profile is more complex (Fig. 6.5A and 6.5B) where ~25% of the exposed contact is covered by massive sulfides, ~35% of the contact is covered by net-textured sulfides, and ~40% of the contact is covered by barren to weakly mineralized komatiite. Despite this complexity, three stratigraphically-distinct ore horizons may be defined based on the field relationships: an *Upper Ore Horizon* (UOH), a *Middle Ore Horizon* (MOH), and a *Lower Ore Horizon* (LOH) (Fig. 6.5B).

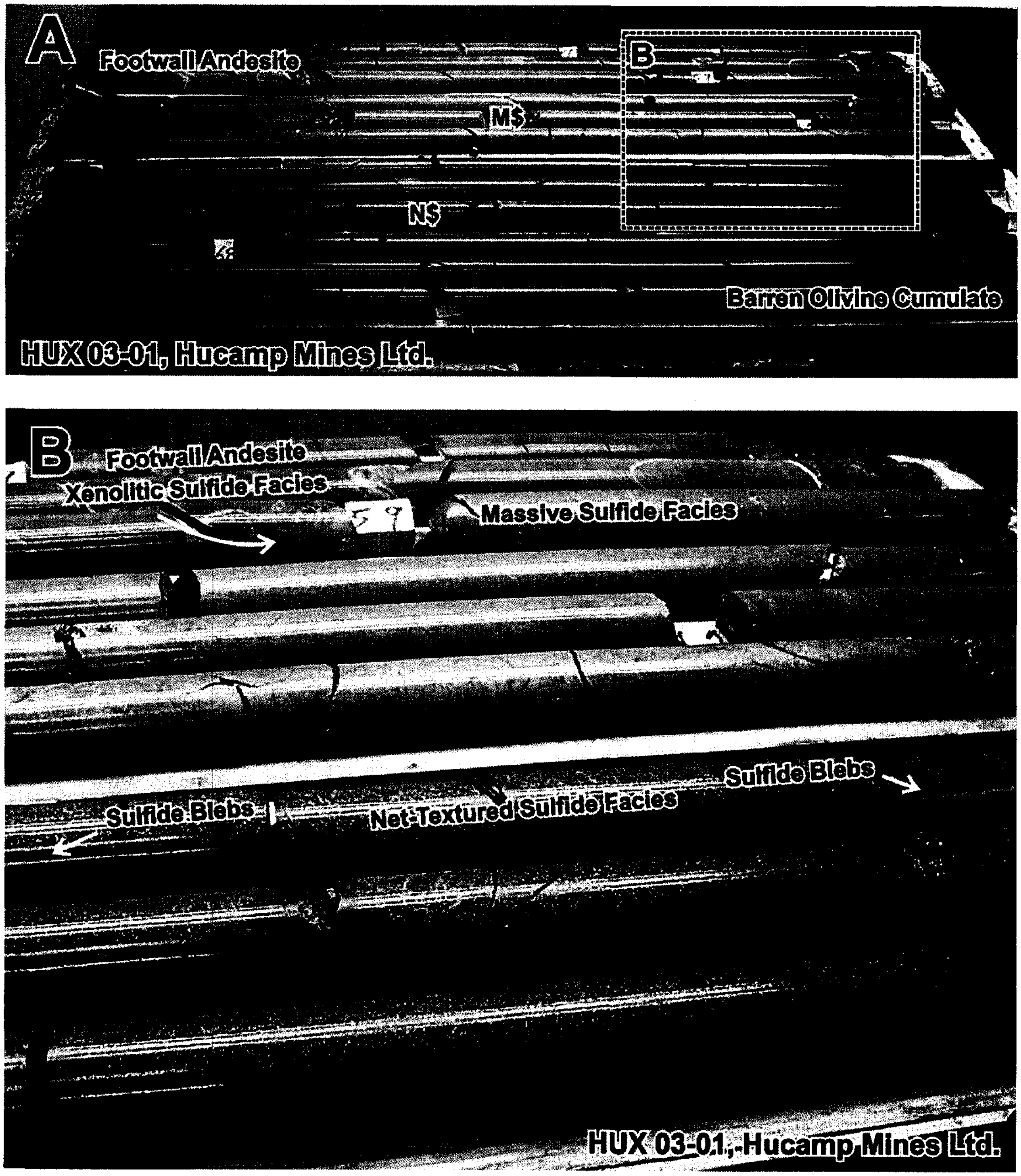

Figure 6.15 Common ore profile at the Alexo mine, HUX 03-01 (Hucamp Mines, Ltd.). A) Ore profile underlain by footwall andesite and overlain by barren olivine cumulate komatiite. The ore profile is characterized by (from base to top): inclusion-bearing sulfide facies, massive sulfide facies, and net-textured sulfide facies with local sulfide blebs. Vertical red lines mark major lithological contacts. Abbreviations: M$ = massive sulfide facies and N$ = net-textured sulfide facies. B) Close-up from 6.15A.

The *Upper Ore Horizon (UOH)* is the main ore horizon and is exposed over the entire strike length of the stripped area (Fig. 6.5). It normally comprises a 0.2-1.5m thick zone of massive sulfides, overlain by a 0.3-2.5m thick zone of net-textured sulfides, overlain by disseminated sulfides and/or barren cumulate komatiite. However, the net-textured sulfide facies is the only facies that is continuous over the entire exposure and, depending on location, directly overlies unmineralized komatiite, earlier net-textured sulfide facies, and footwall andesites. The massive sulfide facies locally contains large to small size enclaves of disseminated to net-textured sulfides, whereas the net-textured sulfide facies contains locally barren olivine cumulate enclaves.

The *Middle Ore Horizon (MOH)* is exposed over a strike length ~75m in the central part of the main Alexo embayment. It comprises a 0.3-4m-thick zone of net-textured sulfides with an internal zone of disseminated sulfides that directly overlies the andesitic footwall for ~45m in the west-central part of the first-order embayment and directly overlies the basal unit for ~30m in the east-central part of the first-order embayment (Fig. 6.5A). Massive sulfides do not occur as a coherent unit within the MOH, but occur as enclaves within the net-textured sulfide facies.

The *Lower Ore Horizon (LOH)* is only exposed over ~10m in the western part of the stripped area, within a subordinate embayment (Figs 6.5A, 6.6, and 6.7). It comprises a 0.2-0.9m thick zone of massive sulfide that contains locally xenoliths and xenomelts of the footwall rocks.

Although massive sulfides are normally overlain by net-textured sulfides, and net-textured sulfides are normally overlain by fine disseminated sulfides, the ore profiles at Alexo vary considerably along strike (Figs. 6.5A and 6.5B). Despite all of the variations, the profiles share many common features:

- Even where massive sulfides do not occur at the base of the profile or where the profile is complex; massive sulfides rarely occur more than halfway up an ore profile.
- As noted above, contacts between massive ores and footwall rocks are very sharp, but scalloped, and are normally marked by thin layers of ferrochromite. Where they occur along the basal contact, massive sulfides locally protrude into the footwall rocks, the margins of the protrusions are also marked by a layer of ferrochromites, and the protrusions are surrounded by a 1-3 cm thick zone of disseminated Fe-Ni-Cu sulfides in andesite (Fig. 6.12A).

- Massive and net-textured sulfides are commonly separated by a thin (10 to 15 cm) layer of weakly disseminated or blebby sulfides in orthocumulate komatiitic peridotite. The contact between this layer and the underlying massive ore horizon is very sharp and undulating, whereas the contact between this layer and the overlying net-textured ore horizon is gradational over a distance of ~5-10 cm. In some cases, the base of the net-textured ore horizon exhibits centimetre-scale layering. Locally, along the margins of embayments, the olivines in the intermediate zone are bladed, forming a spinifex-textured ore facies.
- Where an intermediate disseminated/blebby sulfide later is absent, the contact between massive sulfides and overlying net-textured sulfides is often sharp and planar, but massive sulfides sometimes protrude upwards into net-textured sulfides (Fig. 6.12B).
- Contacts between net-textured sulfides and overlying disseminated sulfides are normally gradational and undulating, but locally sharp and undulating.
- Contacts between net-textured sulfides and overlying massive sulfides are normally sharp and undulating.

6.5 Lithogeochemistry

The major and trace element geochemistry of the Alexo komatiite (see Appendix A) and associated protrusions, projections, and dikes will be presented elsewhere, but the results are briefly summarized here and in Figs. 6.16 and 6.17 to aid in establishing whether the ore-forming process involved assimilation of the footwall rocks and contamination of the komatiite magma.

Most barren to weakly mineralized cumulate peridotites that overlie the ores (some of which are mineralized) have major element compositions that are similar to other cumulate komatiites in the Alexo area, but *some* are slightly enriched in highly incompatible lithophile elements (HILE: U, Th, Nb, LREE) (Th/Yb_{MN} = *0.48 - 0.51;* La/Sm_{MN} = *0.52-0.87*) relative to moderately incompatible lithophile elements (MILE: Zr, MREE, Ti, Y, HREE) compared to the inferred parental liquid (Th/Yb_{MN} = *0.21;* La/Sm_{MN} = *0.47*: Lahaye and Arndt, 1996; Lahaye et al., 2001).

Some barren to weakly mineralized komatiites in the *basal unit* that underlies the ore along most parts of the embayment and occurs within the massive and net-textured sulfides in the western area have major element compositions similar to many cumulate komatiites in the Alexo area, but *many* are slightly to moderately enriched in HILE relative to MILE (*Th/Yb_{MN} = 0.34 – 0.48; La/Sm_{MN} = 0.60-0.80*) compared to the inferred parental liquid. The enrichments in HILE are sometimes, but not always accompanied by negative Nb and Ti anomalies.

Most footwall protrusions have major element compositions similar to non-cumulate komatiites in the Alexo area, but *some* are slightly enriched in HILE relative to MILE (*Th/Yb_{MN} = 0.34 – 0.46; La/Sm_{MN} = 0.56-0.74*) compared to the inferred parental liquid. The enrichments in HILE are commonly, but not always accompanied by negative Nb and Ti anomalies.

Most footwall projections have major element compositions similar to non-cumulate komatiites in the Alexo area, but *many* are slightly enriched in HILE relative to MILE (*Th/Yb_{MN} = 0.32 – 1.13; La/Sm_{MN} = 0.64-0.83*) compared to the inferred parental liquid. The enrichments in HILE are commonly, but not always accompanied by negative Nb and Ti anomalies.

Many footwall dikes have lower Mg contents, much higher Ti contents, and *all* are slightly enriched in HILE relative to MILE (*Th/Yb = 1.03 – 1.15; La/Sm_{MN} = 0.68-1.24*) compared to the inferred parental liquid. The enrichments in HILE are commonly, but not always accompanied by negative Nb and Ti anomalies.

Andesites have higher Si, Al, Ti, and lithophile element contents than komatiites, and *all* are slightly enriched in HILE relative to MILE (*Th/Yb = 0.49 – 0.65; La/Sm_{MN} = 0.69-0.96*) compared to komatiites. They do not exhibit negative Nb or Ti anomalies, more like tholeiites than arc andesites (Kerrich and Wyman, 1996).

Interflow graphitic sediments also have higher Si, Al, Ti, and lithophile element contents than komatiites, are enriched in HILE relative to MILE compared to komatiites (*La/Sm_{MN} = 3.6*), and exhibit pronounced negative Nb and Ti anomalies, typical of upper continental crustal rocks (Taylor and McLennan, 1985; McLennan, 2001).

The footwall protrusions, footwall projections, and dikes therefore have $[Nb/Th]_{MN}$ ratios that are slightly but significantly lower and La/Sm_{MN} ratios that are slightly but significantly higher than the inferred parental magma, with variable Nb and Ti anomalies suggesting variable degrees of crustal contamination by mixtures of andesite and interflow sediment.

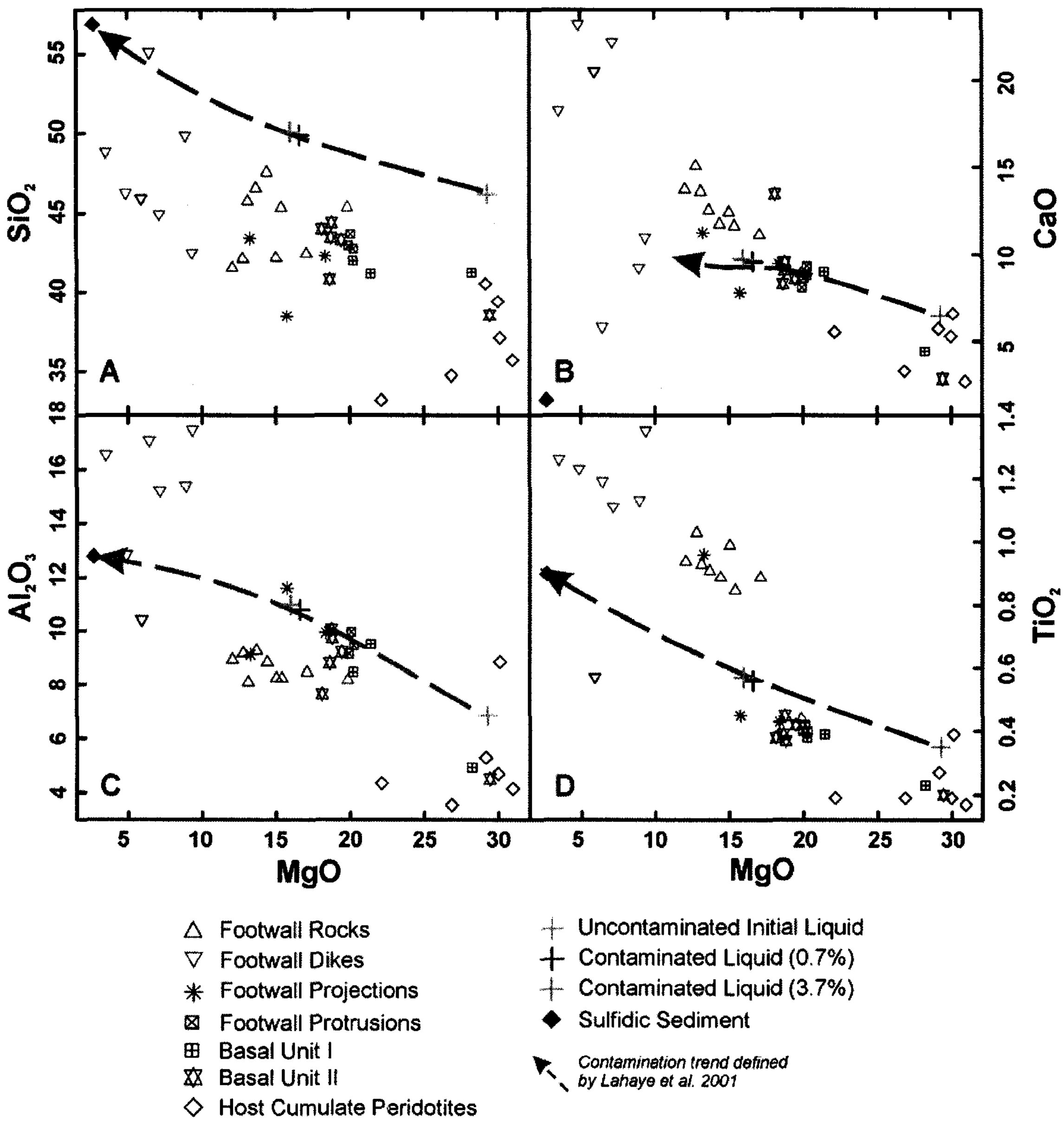

Figure 6.16 MgO variation diagrams showing compositional variations of main lithologies in the Alexo mine stripped area, including host cumulate peridotites, basal unit, footwall protrusions, footwall projections, footwall dikes, and footwall rocks. A) MgO-SiO_2, B) MgO-CaO, C) MgO-Al_2O_3, and D) MgO-TiO_2. Initial komatiitic liquid from Lahaye and Arndt (1996), 0.7% contaminated komatiitic liquid, 3.7% contaminated komatiitic liquid, and sulfidic, graphitic sediments from Lahaye et al. (2001).

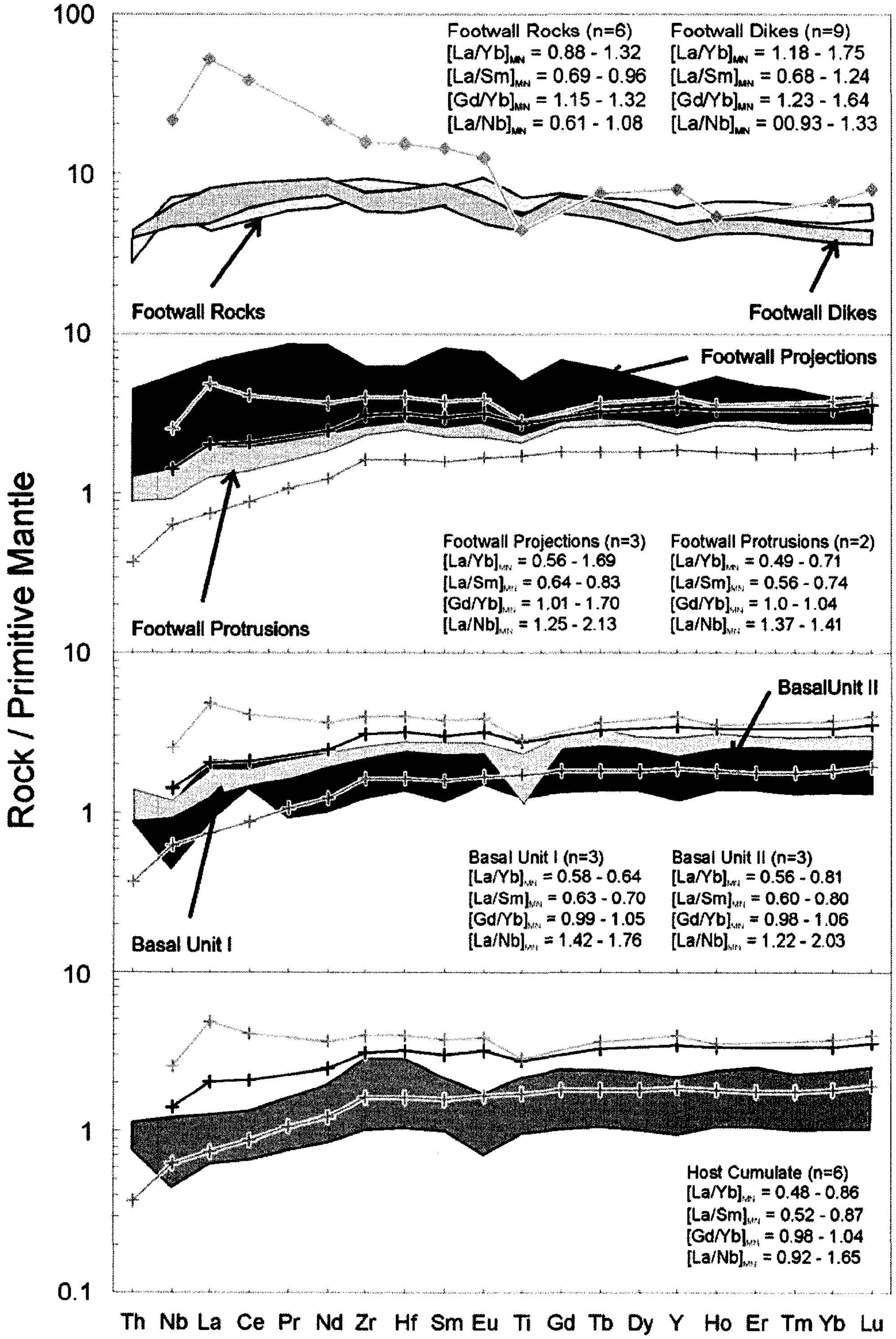

Figure 6.17 Primitive-mantle normalized variation diagrams of main lithologies from the stripped area, including A) host cumulate peridotites, B) basal unit, C) footwall protrusions and footwall projections, D) footwall dikes and and footwall rocks. Initial komatiitic liquid (orange) from Lahaye and Arndt (1996); 0.7% contaminated komatiitic liquid (dark blue); 3.7% contaminated komatiitic liquid (light blue); and sulfidic graphitic sediments (green) from Lahaye et al. (2001). Primitive mantle normalized values from McDonough and Sun (1995).

6.6 Discussion

6.6.1. Environment of Emplacement for the Alexo Komatiite

Contact relationships, especially upper contact relationships, are critical in establishing an extrusive or intrusive nature for a komatiitic unit (see discussion by Dann, 2000; Arndt et al., 2004; Houlé et al., 2008; see also Chapter 5). Unfortunately, the upper contact of the Alexo komatiite is not exposed, and the only drill core that pierced the contact was located ~300m west of the mine and no longer exists. Although that core intersected several thick weakly differentiated (spinifex-cumulate) units, the presence of spinifex texture is not unequivocal evidence for an extrusive origin (Arndt et al., 2004; Houlé et al., 2004) and there is no information about the nature of the contact with overlying rocks. Interflow sediments were not reported in this core, but interflow sediments and "flow-top breccias" were reported in cores further to the west. However, the cores were logged by different geologists, so we cannot assume that they were all logged in the same detail.

Nevertheless, there are several arguments for an extrusive origin FOR THE Alexo komatiite:

1) Some of the units 300-800m along strike from the mineralization have been reported to be differentiated spinifex-cumulate units with flow-top breccias (Muir, 1995). Unless the flow-top breccias were peperites, this suggests that at least the lateral parts of the Alexo komatiite were extrusive.
2) Barnes et al. (1983) and Arndt (1986) have established that the differentiated spinifex-cumulate units in the underlying Dundonald South member were extrusive based on the presence of unequivocal flow-top breccias along the upper contacts of some units.
3) Because peperites only form in unconsolidated, normally wet sediments (Skilling et al., 2002; White et al., 2000), the development of peperite along the margins of footwall projections and footwall dikes emanating from the Alexo komatiite indicates that it was emplaced immediately after the footwall andesites and associated interflow sediments. This does not require it to be extrusive, but it could not have been a markedly later intrusive.
4) The unit above the ore zone appears to be thicker, more magnesian, and less differentiated than the flanking units. Interflow sediments are present between the

thinner flanking units. This architecture is very similar to the much better constrained Silver Lake Member of the Kambalda Komatiite Sequence (Gresham and Loftus-Hills, 1981), which has been interpreted to represent a series of channelized sheet flows (Lesher et al., 1984; Cowden and Roberts, 1990; Beresford et al., 2002).

5) The Alexo mine sequence appears to represent a facies transition between komatiitic subvolcanic to volcanic components (see Chapter 5; Houlé et al., 2008): the Foundation member and Empire members are intrusive, the lower part of the Dundonald South member is intrusive, and the upper part of the Dondonald South member is extrusive.

Although we cannot completely exclude an intrusive origin for the Alexo komatiite, the best interpretation is that it is extrusive.

6.6.2. Nature of the Alexo Komatiite

The textural variations within the Alexo komatiite suggest that it is a compound unit, similar to the host units at Kambalda (Lesher, 1989; Beresford et al., 2002) and Raglan (Lesher, 2007). Some of the channel flow facies at Kambalda appear to correlate with multiple flanking sheet flows and exhibit internal textural and geochemical evidence of being composite units that represent beheading of underlying units and/or multiple pulses of lava emplacement (Cowden, 1988; Lesher, 1989; Beresford et al., 2002). Because no detailed stratigraphic geochemical data are available, we cannot establish whether the Alexo komatiite is a single cooling unit or whether it comprises multiple cooling units, but the variations in cumulus textures suggest that it was a dynamic unit in which lava flow and crystallization rates varied over time.

By analogy with similar stratigraphic relationships at Kambalda (Lesher, 1989; Roberts and Cowden, 1990), the relatively undifferentiated komatiites above the Alexo ore zone are interpreted to represent a thick *channel-flow facies*, whereas the more differentiated komatiites to the southwest that are locally separated by interflow sediments are interpreted to represent a *sheet flow-facies* (Fig. 6.3).

6.6.3. Nature of Embayments

Most komatiite-associated Ni-Cu-(PGE) deposits are localized within footwall embayments (Lesher, 1989; Barnes, 2006; Lesher and Barnes, 2008), but their origin has been controversial due to the often pervasive deformation and regional metamorphism that has affected Archean and Proterozoic greenstone belts. They have been interpreted to represent syn-*volcanic grabens* (e.g., Kambalda: Ross and Hopkins, 1975; Gresham and Loftus-Hills, 1981; Gresham, 1986; Brown et al., 1999; Beresford et al., 2000b), *volcanic topographic features* modified by thermomechanical erosion and/or deformation (e.g., Langmuir: Green and Naldrett, 1981; Kambalda: Lesher et al., 1984; Lesher, 1989), *thermomechanical erosional features* (e.g., Kambalda: Huppert et al., 1984; Huppert and Sparks, 1985; Evans et al., 1988; Perseverance: Barnes et al., 1988; Williams et al., 2002; Raglan: Chisholm et al., 1999; Lesher, 2007; Silver Swan: Dowling et al., 2004), or *post-volcanic structural features* (e.g., Kambalda: Cowden and Archibald, 1987; Cowden, 1988; Findlay, 1998; Stone and Archibald, 2004; Perseverance: Trofimovs et al., 2003). Although there finally appears to be a consensus that the embayments in the basalts at Kambalda represent volcanic topographic features *modified* by thermomechanical erosion and deformation (Lesher, 1989; Beresford and Stone, 2004; Stone et al., 2005; Barnes, 2006), the role of thermomechanical erosion has been debated (cf. Lesher, 1989; Williams et al., 1998, 2002; Cas and Beresford, 2001; Rice, 2001; Lesher and Keays, 2002; Barnes, 2006). Part of the problem is that komatiite-associated Ni-Cu-PGE deposits were deposited over wide variety of substrates, including pelitic sediments (e.g., Raglan, Damba-Silwane), felsic volcanic rocks (e.g., Perseverance, Silver Swan), andesites (e.g., Alexo, Langmuir), and basalts (e.g., Kambalda). Although one might argue that the evidence for only local thermomechanical erosion at Kambalda can be attributed to the low erodability of fine-grained basalt, the other substrates should have been more erodable (Williams et al., 1998) and the andesitic rocks at Alexo are a perfect place to test this hypothesis.

6.6.3.1. Deformation

The consistent younging directions within the komatiites and andesite, the absence of penetrative deformations, and the lack of any evidence of folding of other features at any scale (e.g., stratigraphic contacts between andesite units, stratigraphic contacts between ore facies, pillow margins, dikes) that match the irregularities along the lower contact indicate that they have not been formed by structural deformation. We cannot completely rule out the possibility that the first-order embayment has been slightly modified by deformation, as the entire volcanic sequence is folded on the megascopic scale, but the smaller embayments are localized within the first-order embayment, so they most likely formed by a similar, non-tectonic process.

6.6.3.2. Volcanic Topography

The floors of many least-deformed embayments at Kambalda are relatively flat and correlate with the contacts between footwall basalt flows defined by flow-top breccias and contacts between pillowed and massive flows (Lesher, 1989), suggesting that they represent topographic depressions between non-overlapping flows. However, the embayments at Alexo are much more irregular and appear to transgress multiple flow units (Fig. 6.3). So, although we cannot eliminate the possibility of some original topography on the andesite surface, the embayments at Alexo do not appear to have formed like those at Kambalda.

6.6.3.3. Thermomechanical Erosion

The markedly discordant footwall contact, the irregular geometries of the embayments, the presence of footwall protrusions and projections, the cross-cutting of pillow margins by komatiite, the presence of xenoliths and rare xenomelts, and the delicately scalloped contacts between komatiite and andesite provide unequivocal evidence for erosion of andesite by komatiite at Alexo. Although we cannot completely preclude the possibility of minor deformation or original topography (see above), the depth of first-order the embayment suggests removal of up to 25 meters, possibly up to 45 meters, of the footwall rocks. Preferential erosion beneath the mineralized part of the Alexo komatiite is supported by the greater depth and degree of contact metamorphism beneath ore-bearing embayments. Field evidence for thermomechanical erosion has been reported in many other komatiite localities, including Kambalda (Lesher et al., 1984; Groves et al., 1986; Evans, 1989; Frost and Groves, 1989; Lesher, 1989), Forrestania (Perring et al., 1995), Black Swan (Dowling et al., 2001; Dowling et al., 2004; Barnes et al., 2004), Langmuir (Greens and Naldrett, 1981), Sothman (Houlé et al., 2003), Mickel (Davis, 1999), Raglan (Lesher, 2007), and several localities in Zimbabwe (Prendergast, 2001), but the field evidence at Alexo appears to be the least equivocal.

Erosion by flowing lava flows or sills can occur via 1) *thermal erosion*, resulting from partial or wholesale melting of the substrate from heat of the flowing lava, 2) *mechanical erosion,* involving physical incorporation by plucking of lifting of the substrate, and 3) *thermomechanical erosion*, as a combination of both processes

(Williams et al., 2004). Thermomechanical erosion may involve melting of the material mechanically plucked by the flowing lava (Williams et al., 2004) or it may involve thermal weakening of the substrate followed by physical incorporation (e.g., Greeley et al., 1998). Both processes are sensitive to the degree of consolidation of the substrate (Williams et al., 1998; 2001). Both processes appear to have occurred at Alexo: the komatiite protrusions, ore protrusions, and scalloped contacts are consistent with mainly thermal erosion, whereas the projections, dikes, and sills are consistent with mainly mechanical erosion. However, in many cases they appear to have operated together via a thermomechanical process.

Mechanical erosion without assimilation will produce xenoliths, such as those described in many other magmatic Ni-Cu-PGE deposits (e.g., Duluth, Noril'sk, Sudbury, Voisey's Bay) and thermal erosion without assimilation will produce immiscible liquids, such as those rarely preserved at Kambalda (Frost et al., 1989). Only a few xenoliths and xenomelts have been observed at Alexo, suggesting that if the entire volume of the embayment was filled with now-eroded footwall rocks, the majority of the inclusions and/or xenomelts were assimilated or swept downstream. Komatiite magmas are much hotter and much less viscous than the basaltic magmas at Duluth, Noril'sk, and Voisey's Bay, which would have facilitated assimilation of andesite and argillite xenoliths into the magma.

Thermal erosion with assimilation will contaminate the magma, with the degree of contamination depending on the geochemical contrast between the magma and contaminant, and the amounts of the two components. The geochemical data suggest that the footwall protrusions, footwall projections, and komatiite dikes are contaminated, but the contaminant appears to have had significantly lower Nb/Th_{MN} and higher La/Sm_{MN} than the andesites. Lahaye et al. (2001) suggested that the contamination is best explained by assimilation of interflow argillites, which are strongly enriched in HILE relative to MILE and have pronounced negative Nb-Ta-(Ti) anomalies. The apparent absence of any contribution from the andesites, which are the predominant component that appears to have been eroded, can probably be explained by the much lower incompatible element contents of the andesites compared to the argillites and dilution in the lava channel (see discussion by Arndt and Lesher, 1995; Lesher et al., 2001). The geochemical aspects of the contamination of the Alexo komatiite are presently under investigation.

The type of erosion at Alexo appears to have varied locally with the nature of the substrate:

1) The small embayment at the western end of the exposed area (Fig. 6.8), which is underlain by pillowed andesites with little interpillow material, appears to have been generated by mainly thermal erosion. This embayment is reentrant and the lower contact is covered by massive sulfide, consistent with enhanced lateral erosion by very dense, very low viscosity, highly-conductive, and probably highly-corrosive sulfides (Groves et al., 1986; Lesher, 1989).

2) The step east of the exploration shaft (see Fig. 6.5A) that is underlain by peperite and andesitic hyaloclastite appears to have been generated by mainly mechanical erosion. This may be attributed to the greater amount of heat lost by vaporization of intersitital fluids by the development of peperitic texture.

3) The contact in the eastern part of the exposed area, which is underlain mainly by pillowed andesites with abundant interpillow hyaloclastite, appears to have formed by a combination of thermal and mechanical erosion. The footwall protrusions in this area (Figs. 6.9 and 6.10) are commonly flanked by thin sills, but are underlain by massive andesite, suggesting that the komatiite thermally eroded the andesite in the space previously occupied by the protrusion and then mechanically fractured the flanking rocks. What we see now is a snapshot of the intermediate stages of process, but one may easily imagine that the denser komatiite in the sills would then lift the less dense flanking andesite (Figs. 6.10 and 6.11A).

These variations, and the variations in the morphologies of embayments (Lesher, 1989; Lesher and Keays, 2002) and the abundances of xenoliths (Lesher et al., 2001) in other localities where erosion has been interpreted, suggest that substrate erosion should be considered as a complete spectrum from entirely mechanical to entirely thermal depending on magma composition (temperature and viscosity), substrate structure/texture/composition (unconsolidated vs. consolidated, glassy vs. phaneritic, felsic vs. mafic), flow regime (turbulent vs. laminar), and the degree of lava channelization.

The observations here very clearly indicate, contrary to the suggestions of Rice and Moore (2001), that channelized komatiites were quite capable of thermomechanical erosion, as interpreted for many terrestrial basalt lava tubes (e.g., Greeley, 1971; Greely and Hydes, 1972; Greeley et al.,1998; Swanson, 1973; Coombs et al., 1990; Peterson et al., 1994; Kauhikaua et al., 1998) and as predicted by many theoretical and analog models (e.g., Hulme, 1973; Huppert and Sparks, 1985; Jarvis, 1995; Williams et al., 1998, 2001). The process would have been even more efficient in komatiites because they were much hotter and much less viscous, which would have facilitated turbulent flow (Huppert and Sparks, 1985), but Fagents and Greely (2001) and Kerr (2001) have shown that even laminarly-flowing basalts are capable of thermomechanical erosion if they flow long enough.

The two third-order embayments located within the second-order embayment at the westernmost part of the stripped area (Figs. 6.8 and 6.9) exhibit different geometries, suggesting that they evolved separately. Huppert and Sparks (1985) produced a similar cross-sectional geometry by flowing hot water over wax; in some cases the stream split and rejoined, forming a midstream island. Huppert and Sparks (1985) and Jarvis (1995) attributed this to variable degrees of erosion caused by variations in flow thickness; more erosion beneath thicker parts of the flow and less erosion beneath thinner parts of the flow. Jarvis (1995) also proposed that embayment morphology may vary with the thickness of the flow within the embayment. If the flow fills the embayment, it will produce a concave morphology, whereas if the flow does not fill the embayment, it will most likely produce a re-entrant morphology. Re-entrant embayment morphologies at Alexo appear to be preferentially located (Fig. 6.7) at the westernmost part of the stripped area. This observation suggests that the edge of the Alexo embayment could have been isolated from the main embayment at some point in their history. The asymmetry of the embayments (concave to east, steep to undercut to west) suggest a northward plunge to the flow (see discussion by Lesher, 2007).

6.6.4. *Ore Genesis*

6.6.4.1. Ore Segregation Profile

The ore segregation profile at Alexo was interpreted by Naldrett (1973) to have formed in response to a static buoyancy contrast between dense sulfide liquid and a column of close-packed olivine crystals (the "billard ball" model). This model was criticized by Ussleman et al. (1979), who pointed out that molten sulfides would chill against the footwall rocks and that olivines might not pack in the way envisioned in the model. It is also possible that such a profile might result from flowage segregation (Hudson, 1972) or dynamic remelting (Lesher and Campbell, 1993). However, there are many features at Alexo that are inconsistent with these models, including the local presence of:

1) Repetitions in sulfide facies that depart from the "normal" massive\net-textured\disseminated ore profile,
2) Magmatic layering at the base of some net-textured facies,
3) Barren spinifex-bearing cumulates between massive and net-textured sulfides,
4) Sharp contacts between different facies in almost in all ore profiles,
5) Footwall clasts within massive sulfide facies,
6) Disseminated to net-textured sulfide clasts within massive sulfide facies,
7) Massive sulfide clasts and barren olivine ortho- to mesocumulate rocks within net-textured sulfide facies,
8) Subrounded to amoeboid massive sulfide clasts within the barren unit between the massive and net-textured sulfide facies,
9) Barren to weakly mineralized komatiite beneath the ores.

In common with the similarly complex ore profiles at Raglan (Chisholm, 1999; Lesher, 2007), the ore profiles at Alexo require a very dynamic environment involving multiple episodes of ore emplacement rather than a single stage implied by the other models.

The presence of subrounded to amoeboid massive sulfide clasts suggests that at least one of the pulses remelted underlying sulfides. If the magma was saturated in sulfide, which appears to have been the case here, it would not have dissolved much of the sulfide, but if it was undersaturated in sulfide, it could have dissolved some of the sulfide thereby increasing the tenor of the ores (Kerr and Leitch, 2005).

6.6.4.2. Sulfur Sources

Alexo is also the first place where an external source of S was proposed. Based on the similarity and non-mantle signatures of the S isotopes in the ores (+4.4 to +6.2 $\delta^{34}S$) and andesites (+3.6 to +5.1 $\delta^{34}S$), Naldrett (1966) suggested that the S in the ores was extracted from the andesites. Similar observations have been made at most magmatic sulfide deposits, where the ores and country rocks have similar non-mantle S isotopic compositions (Green and Naldrett, 1981; Lesher and Groves, 1986; Ripley, 1986; Ohmoto, 1986; Naldrett, 2004).

Actually, there are three possible S sources at Alexo. The andesitic footwall contains up to 2-3% disseminated pyrite and pyrrhotite, local pods of semi-massive exhalative sulfides in the andesite contain up to 40% pyrite and pyrrhotite, and interflow argillites contain up to 20% pyrite and pyrrhotite (Davis, 1999). As noted above, there is field evidence for incorporation of andesite (this study) and geochemical and isotopic evidence for incorporation of graphitic sulfidic argillite (this, study and Lahaye et al., 2001). More detailed S-Os-Pb isotopic and trace element geochemical work will be required to further constrain the relative abundances of the various S sources in the ores.

6.6.5. Evolution of Alexo Komatiite and Ore Zone

Although the subregional stratigraphic relationships are not very well defined (Fig. 6.3), the Alexo komatiite appears to be thicker, more olivine-enriched, and less differentiated near the Alexo Mine, and to comprise multiple thinner, less olivine-enriched, and more differentiated units separated by interflow sediments to the WSW and possibly to the ENE. As noted above, this suggests that it may represent a channelized sheet flow.

The emplacement and crystallization of channelized komatiite flows has recently been reviewed by Barnes and Lesher (2008). We do not have any of the detailed stratigraphic, geochemical, and isotopic data used by Barnes et al. (1988), Lesher and Arndt (1995), and Lesher (2007) to constrain the timing of emplacement of the channelized sheet flows at Kambalda, Perseverance, and Raglan, but by analogy, emplacement of the Alexo komatiite may be inferred to have involved emplacement of a thin sheet flow that inflated and became channelized during emplacement and crystallization. Barnes (1985; see also Hill, 2001) suggested that the spinifex A zones of inflated flows in the Dundonald South member of the Dundonald formation formed during inflation. However, based on arguments by Lesher (1989) and Barnes and Lesher (2008), the geochemical data presented in Arndt (1986) and Puchtel et al. (2004) indicate that only the upper chilled margins and perhaps the uppermost parts of the random spinifex-textured A1 zones could have formed during inflation.

We have more constraints on the timing of development of the lower part of the Alexo komatiite and ore zone in the Alexo Mine area where crosscutting relationships, inclusion populations (especially of massive sulfides within other rocks), and the principle of superposition indicates the following sequence of events:

1) Initial emplacement of komatiite, channelization in a paleotopographic low, and thermomechanical erosion of andesite to generate the main first-order embayment

and the small westernmost embayment. The initial komatiite is preserved as footwall dikes that are cross-cut by massive sulfides (Figs. 6.6 and 6.7) of the Lower Ore Horizon and weakly mineralized komatiite (Fig. 6.6). The absence of any sulfides in footwall protrusions, projections, and dikes indicates that thermomechanical erosion at the site of the present ore zone preceded emplacement of the ores.

2) Emplacement of the Lower Ore Horizon (massive sulfide in the westernmost embayment and along the step in the contact south of exploration shaft) and overlying weakly-mineralized komatiite. The contact between the two is very contorted (Fig. 6.7) and the weakly-mineralized komatiite contains inclusions of massive sulfide, suggesting partial remelting of the massive sulfides by this unit. It is possible that this unit did not form net-textured and/or heavy-disseminated sulfides, for example if the flow was thin enough at this stage, but it is also possible that overlying barren to weakly-mineralized komatiite eroded any net-textured or heavy disseminated sulfide facies that formed in the Lower Ore Horizon.

3) Emplacement of barren to weakly mineralized olivine pyroxenite (preserved south of the Exploration Shaft: Fig. 6.5 and in the eastern part of the outcrop: Figs. 6.5 and 6.9), footwall protrusions, and footwall projections. The olivine pyroxenite overlies the Lower Ore Horizon south of the Exploration Shaft, but overlies the footwall andesite in the eastern part of the outcrop, suggesting that the Lower Ore Horizon did not form or was completely eroded in the eastern part of the outcrop.

4) Emplacement of the Middle Ore Horizon (net-textured to disseminated sulfides), which contains inclusions of massive sulfide. The Middle Ore Horizon is characterized by the presence of net-textured sulfide overlain by disseminated sulfide and the absence of massive sulfides at the base of the ore profile. The numerous xenoliths of massive sulfides within the net-textured ores could have been derived from the base of the Middle Ore Horizon, now completely eroded, or from the Lower Ore Horizon.

5) Emplacement of the Upper (Main) Ore Horizon, which overlies (and has possibly beheaded parts of) the Middle Ore Horizon, and overlying cumulate komatiites. Massive sulfides of the Upper Ore Horizon appear to have been squeezed upward into the net-textured sulfides (Figs. 6.9 and 6.12B), possibly by compaction in response to the accumulation of olivine within the overlying channel-flow facies.

The Middle Ore Horizon also contains several xenoliths of disseminated to net-textured sulfide and barren olivine cumulate within the ore zones could have been derived from the Middle Ore Horizon, now completely partially eroded, or from the Lower Ore Horizon.

The normal abundances of PGEs in Alexo komatiites (Puchtel et al., 2004) and most other komatiites worldwide (Keays, 1982; Barnes et al. 1985; Naldrett and Barnes, 1986; Sproule et al., 2005) suggests that they were undersaturated in sulfide when they separated from their source and remained undersaturated during ascent, eruption, and emplacement (see discussion by Keays, 1982; Lesher and Groves, 1986). The absence of any mineralization during the first stages of emplacement and thermomechanical erosion of andesite at Alexo suggest that this contamination was not enough induce sulfide saturation. This may be because the parts of the andesite that were eroded (upstream) at this stage did not contain enough sulfide and/or that the flow rates were high enough to allow the sulfides to be assimilated without achieving sulfide saturation (see discussion by Lesher et al., 2001). The presence of mineralization during the later stages of emplacement suggests that the channel had eroded deeply enough to encounter more of the sulfide-rich material (sulfide pods and interflow sediments) in the andesites and/or that the flow rate had waned to a point where they were low enough to allow the magmas to exceed sulfide saturation.

During the initial stages of thermomechanical erosion, the rate of erosion likely exceeded the rate at which heat could be conducted into the footwall rocks (Huppert and Sparks, 1985), so there would have been only a very thin thermal aureole beneath the lava channel. However, as flow waned, the rate of thermomechanical erosion would have decreased, resulting in deeper conduction of heat into the footwall rocks. The footwall protrusions are interpreted to represent complete melting of the andesite within 10-30 cm of the contact, the quartz pods beneath the embayments are interpreted to represent partial melting of andesite within 0.1-1 m of the contact, and the destruction of pillow margins is interpreted to represent recrystallization in response to contact metamorphism extending up to 1-2m below the contact.

6.7 Conclusions

The principal conclusions of this study can be summarized as follows:

1) The Alexo Ni-Cu-(PGE) deposit is a small, high-grade body of massive/net-textured/disseminated sulfide localized within series of nested concave to

reentrant embayments at base of the olivine meso- to adcumulate komatiite channel-flow facies of a thick channelized sheet flow.

2) Cross-cutting relationships between komatiite and andesite, and the presence of xenoliths and xenomelts of andesite in komatiite, protrusions/projections/dikes of komatiite into andesite, and contaminated komatiitic rocks, all spectacularly preserved in glacially-polished outcrops, provide unequivocal evidence of thermomechanical erosion of andesite by komatiite. The embayments are bordered by a 20-30cm-thick zone of wholesale melting (footwall protrusions), partial melting (quartz pods), and strong recrystallization (obliteration of pillow margins) of andesite.

3) The ores were emplaced in at least 3 stages, forming a *Lower Ore Horizon* of massive sulfides, a *Middle Ore Horizon* of net-textured sulfides, and an *Upper (Main) Ore Horizon* of massive\net-textured\disseminated sulfides. The presence of xenoliths of massive sulfide in the Middle and Upper Horizons suggest that they eroded some of the earlier sulfides.

6.8 Acknowledgements

This paper is part of MGH's PhD dissertation at Laurentian University and the University of Ottawa. We very grateful to Hucamp Mines Ltd. (Kevin Montgomery), Larchex Inc. (Dave Larche), and Canadian Arrow Mines Ltd. (Dean MacEachern) for providing access to field exposures, drill cores, and geological data. Kevin Montgomery is thanked for thoughtful discussions on the geology of the area and for providing copies of his early geological mapping. This research has been supported by a collaborative agreement between the Ontario Geological Survey and the Mineral Exploration Research Centre (Laurentian University), a Natural Sciences and Engineering Research Council of Canada operating grant to CML, and a *Fonds de la nature et de la technologie* fellowship from the Province of Quebec, a *Hugh E. McKinstry Grant* from the Society of Economic Geologists, and a Graduate Scholarship from the University of Ottawa to MGH.

Appendix I: Analytical Methods

Major, minor, and selected trace elements (SiO_2, TiO_2, Al_2O_3, Fe_2O_{3t}, MnO, MgO, CaO, Na_2O, K_2O, P_2O_5, LOI, Ni, Cu, Co, Zn, Cr, and V) were determined by wavelength-dispersive X-ray spectrometry of fused glass disks and pressed powder pellets at the

University of Western Ontario (Dr. C. Wu, analyst). Rare-earth elements, Y, Zr, Hf, Nb, Ta, Th, U, Cs, Rb, Sr, and Ba were determined by inductively-coupled plasma mass spectrometry at the Ontario Geoscience Laboratories in Sudbury (Dr. O.M. Burnham, analyst) after a 10-day closed-beaker mixed-acid dissolution (Tomlinson et al., 1999). Details on sample preparation, analytical methods, accuracy, and precision are described in Sproule et al. (2002).

CHAPTER 7 - SUMMARY OF MAJOR CONCLUSIONS

The main objective of this thesis was to explore the physical volcanology of komatiites to better understand their modes of emplacement and implications for the genesis of komatiite-associated Ni-Cu-(PGE) deposits in the western part of the Abitibi greenstone belt. The major conclusions of this study are summarized below.

7.1 Thermomechanical Erosion by Komatiite Magmas

New field observations at the Alexo mine (Dundonald Township), the Sothman deposit (Sothman Township), and the C-Zone deposit and Thalweg occurrence (Bannockburn Township) provide unequivocal evidence to support the concept of thermomechanical erosion of footwall rocks by Archean komatiitic lava flows and sills in the western Abitibi greenstone belt.

Detailed mapping of the basal contact at the Alexo Mine (Houlé et al., 2002; submitted), indicates that the mineralized cumulate komatiite host unit thermomechanically eroded the andesitic substrate. The key evidence is 1) footwall embayments are nested (i.e., of multiple orders) on scales from 100s of meters to a few centimetres; 2) the morphologies of the embayments vary from concave to re-entrant; 3) the basal contact is very sharp but scalloped and clearly transgresses the footwall rocks without any evidence of a regolith, shearing, or folding; 4) there is evidence for contact metamorphism along the entire length of the contact, but it appears to be thicker and more intense around embayments; 5) xenoliths are more common within embayments; and 6) komatiitic dikes penetrate downward into the host andesites primarily along the lateral margins of embayments. When coupled with S-isotopic data suggesting a footwall source for the S in the ores (Naldrett, 1966), this provide a strong link between thermomechanical erosion and ore genesis.

Mapping at the Sothman deposit (Houlé et al., 2001; Houlé et al., 2003), reveals that the mineralized cumulate komatiite host unit occurs within a concave footwall embayment, also likely produced by thermomechanical erosion. This is supported by evidence of contact metamorphism along the basal contact, which is more pervasive beneath the embayment, and by felsic dikes, which cross-cut the komatiitic unit at high angles. These emanate from the basal contact, and appear to represent partial melts of andesite produced during thermal erosion of the andesitic volcanic rocks. The presence of barren cumulate komatiite within the main mineralized horizon and the subsequent disruption of mineralized zones by olivine pyroxenites suggests that the ore-forming process was more dynamic than many deposits of this type. These observations suggest that the Sothman deposit represents a mineralized channelized sill (or flow) characterized by successive replenishment of magma and sulfides into the channel (Houlé et al., 2003).

Reconnaissance mapping at the C and Thalweg zones in Bannockburn Township (Houlé et al., 2005) also revealed evidence of the interaction between the komatiitic units and their footwall rocks. This interaction is manifested at the C-Zone by the presence of a metamorphic zone (and possibly a contamination zone) along the basal contact, expressed as a sharp to gradational change from black aphyric komatiite through browner (contaminated?) aphyric komatiite, hornfelsed plagioclase-phyric to plagioclase-phyric intermediate footwall volcanic rocks. The presence in the eastern part of the komatiitic unit of poorly-sorted (1 to 60 cm) autoclastic komatiite breccia containing subangular to rounded fragments of olivine phyric komatiite, aphyric komatiite, and spinifex-textured komatiite within a spinifex-textured komatiitic matrix suggests a different volcanic environment than most deposits of this type. Contact metamorphism along the basal contact and fragments of the footwall rocks in the komatiite were observed at Thalweg.

These new observations made at several different Fe-Ni-Cu sulfide deposits associated with komatiites in the WAGB provide unequivocal evidence that komatiites were capable of both mechanical and thermal erosion. It also demonstrates that thermomechanical erosion was a critical factor in the genesis of Fe-Ni-Cu sulfide mineralization in the WAGB.

7.2 Komatiitic Flows and Intrusions

This study has shown that komatiitic rocks in the Abitibi greenstone belt occur not only as lava flows, but also as high-level intrusions. The re-interpretation of *some* of these units as intrusions rather lava flows applies to several locations in the Abitibi belt, including Boston Creek (Round Lake Dome area), Dundonald Beach (Dundonald Township), Pyke Hill (Munro Township), and Serpentine Mountain (McArthur Township).

The Boston Creek ferropicrite extends over ~36 km along the eastern margin of the Round Lake Dome. It was interpreted by Stone et al (1987; 1995a,b) as a thick differentiated lava flow, but has been re-interpreted by Houlé et al., (2004) as a thick semi-conformable differentiated sill. This interpretation is supported by detailed mapping of the upper contact of the Boston Creek unit at four locations, where its intrusive nature is supported by the presence of: 1) xenoliths of the overlying volcaniclastic rocks in the upper part of the unit; 2) apophyses of the upper border zone projecting into the overlying intermediate volcanic rocks; 3) transgression of the overlying hanging wall rocks; and 4) localized peperite development.

Dundonald Beach is a mechanically- and hydraulically stripped outcrop on the south limb of the Dundonald anticline in the southwestern part of the Dundonald Township. Komatiitic basalts and komatiites in this area were interpreted by Muir and Comba (1979) as lava flows, but several of these units have been re-interpreted as high-level intrusions by Arndt et al. (2004) and Houlé et al. (accepted). This re-interpretation is supported by trangressive upper contacts and multiple generations of peperites along the upper contacts of many komatiitic basalt and komatiite units.

Thin spinifex-bearing komatiite units that occur within komatiite flows at Pyke Hill and Serpentine Mountain were recognized by Pyke et al. (1973) and Arndt et al. (1977) and interpreted as late stages internal segregation veins. New observations by Houlé et al. (accepted) have demonstrated evidence of interaction between those sills and their wall rocks providing a basis for a re-interpretation of the spinifex-textured sills as having been new pulses of magma into cooler, semi-consolidated but locally permeable cumulate materials during inflation of lava conduits (i.e., lava tubes or lava channels). This interpretation is supported by coarsening of olivine crystals along both margins of the sills, and concentric overgrowth shells, or dendritic olivine overgrowths that extend from the cumulate-sill contact toward the sill interior. The dendrites grew on pre-existing olivine cumulate at the contact in response to a sharp temperature gradient imposed by the intrusion of hot material, whereas the concentric overgrowths formed as new melt percolated into the unconsolidated groundmass of the host-flow cumulate material. Furthermore, within thicker sills, a more complex organization of the spinifex-textured zone occurs in comparison of what is observed generally in lava flows. This complexity is characterized by striking coarse dendritic spinifex zones composed of very large olivine crystals, up to several centimetres long and up to 1 cm thick, in addition to zones of medium-grained random olivine spinifex and coarse platy spinifex crystals similar to that found in komatiite lava flows. These intrusions suggest that these systems represent preferred lava pathways or tubes that focused lava flow. Thus far, thin spinifex-textured sills have been observed within almost all komatiitic sequences in the Abitibi greenstone belt but appear to more common within certain localities (e.g., Bartlett Dome, Shaw Dome).

These observations are critical for better understanding the physical volcanology of komatiite in the Abitibi greenstone belt and elsewhere. The observations at Boston Creek and Dundonald Beach corroborate the interpretations of Donaldson (1974; 1976), Arndt et al. (2004), Houlé et al. (2004), and Faure et al. (2006) that spinifex textures simply reflect rapid crystallization and must not be used as the primary evidence for an extrusive or intrusive origin. The observations at Dundonald Beach indicate that the komatiite stratigraphy may be complicated by the presence of multiple trangressive relationships between different cooling units. The re-interpretation of some of the komatiite units to be high-level intrusions rather than lava flows indicate that komatiitic intrusions may also host "Kambalda-style" komatiite-associated Ni-Cu-(PGE) mineralization.

7.3 Komatiitic Volcanic Architecture

The recognition that intrusive komatiitic rocks may represent a significant portion of komatiitic sequences and the linkage between intrusive and extrusive komatiites in Dundonald Township also provides critical insights on the architecture of komatiite volcanic sequences (Houlé et al., 2008b).

The subvolcanic-volcanic architecture of komatiites reflects, in part, the different geodynamic environments into which komatiitic magmas have been emplaced. These environments range from old continental crust overlain by thick sequences of basaltic strata (e.g., Kambalda), through continental margins containing a combination of basaltic and sedimentary strata (e.g., Bulawayan belt: Zimbabwe, Cape Smith Belt: Canada), to island arcs/back arcs containing a combination of felsic and mafic volcanic, volcaniclastic, and sedimentary strata (e.g., Abitibi Belt: Canada). These associations suggest that ambient stress field, the relative densities of the magma and lithosphere, and other physical properties of komatiitic magmas determine the level to which they will rise (Lesher and Keays, 2002), but that near-surface parameters govern the mode of emplacement. Once in the near-surface environment, the density and rheology of the near-surface rocks (dense lava flows vs. intermediate density sedimentary rocks vs. low-density unconsolidated sediments or volcaniclastic deposits) govern whether they are emplaced as lava flows, invasive flows, or sills. Where near-surface strata are dense and competent (i.e., flow-dominated or consolidated sedimentary/volcaniclastic successions), komatiitic magma erupts as flows and forms extensive lava shields (e.g., Kambalda). However, where near-surface strata are not competent (i.e., unconsolidated volcaniclastic/sediment-dominated successions), komatiitic magmas typically are emplaced as high-level sills that increase the bulk density of the volcano-sedimentary pile and eventually allow the eruption of lava, and the construction of complex subvolcanic-volcanic lava shields (e.g., Dundonald, Shaw Dome, Raglan, Thompson).

7.4 Regional Perspectives on Komatiite Volcanology

Komatiitic rocks are known to represent only a small proportion of the Abitibi greenstone belt (Figures 7.1 to 7.3) and other Archean and Proterozoic greenstone belts around the world (Arndt et al., 2008). Regional compilations by the Ontario Geological Survey (Ayer et al., 1998; 1999; 2000; 2002; 2005) permit semi-quantitative estimates of the proportions of komatiites within the western Abitibi greenstone belt and each host assemblage.

Komatiitic rocks represent only minor component of each of the four komatiite-bearing assemblages in the western Abitibi greenstone belt (Figure 7.4). The distribution of komatiites is variable within assemblages and is often relatively discontinuous. In some areas (e.g., Shaw Dome, Dundonald: Figure 7.1), komatiites represent a common rock type whereas they are rare in other areas (e.g., west of Kidd Creek: Figure 7.1). The *Pacaud assemblage (2750-35 Ma)* represents less than one percent of the assemblages of the western AGB and contains ~4% komatiitic rocks. Low-Mg komatiites and komatiitic basalts are the dominant komatiitic rock types within this assemblage (Sproule et al., 2003). The *Stoughton-Roquemaure assemblage (*2723-20 Ma*)* represents approximately 14% of the assemblages of the western AGB and contains ~3% komatiitic rocks. Low-Mg komatiites / komatiitic basalts and high-Mg komatiites / cumulate komatiites occur roughly in the same proportion of komatiitic rock types within this assemblage (Sproule et al., 2003). The *Kidd-Munro assemblage (*2719-11 Ma*)* represents only 11% the assemblages of the western AGB, but contains 11% komatiitic rocks. High-Mg komatiites / cumulate komatiites are the most common komatiitic rock types within this assemblage (Sproule et al., 2003). The *Tisdale assemblage (*2710-04 Ma*)* represents 28% of the assemblages of the western AGB and contains ~7% of komatiitic rocks. High-Mg komatiites / cumulate komatiites are the most common komatiitic rock types within this assemblage (Sproule et al., 2003).

This regional investigation of komatiite physical volcanology has also revealed some fundamental differences between each of the komatiite-bearing assemblages (Chapter 2; Figure 7.4, Tables 7.1 and 7.2). The *Pacaud assemblage* contains undifferentiated non-cumulate pillowed komatiitic basalts and lesser differentiated non-cumulate komatiitic basalts. Cumulate lava channels or channelized sheet flows have not been identified in this assemblage. The *Stoughton-Roquemaure assemblage* contains undifferentiated non-cumulate pillowed komatiites and komatiitic basalts and lesser differentiated non-cumulate komatiites and komatiitic basalts. Cumulate lava channels or channelized sheet flows have not been identified in this assemblage. The *Kidd-Munro assemblage* contains differentiated non-cumulate komatiite and komatiitic basalt lobes, undifferentiated non-cumulate lava lobes and sheet flows, differentiated cumulate komatiites and komatiitic basalt lava channels and channelized sheet flows, rare undifferentiated non-cumulate pillowed komatiites and komatiitic basalts, and very rare volcaniclastic komatiitic basalts. The *Tisdale assemblage* also contains differentiated non-cumulate komatiite and komatiitic basalt lobes, undifferentiated non-cumulate lava lobes and sheet flows, differentiated cumulate komatiite and komatiitic basalt lava channels and channelized sheet flows, rare undifferentiated non-cumulate pillowed komatiites and komatiitic basalts, and very rare volcaniclastic komatiitic basalts.

Importantly, the younger assemblages (Kidd-Munro and Tisdale) contain larger volumes of komatiitic rocks, in particular larger volumes of thick, highly magnesian cumulate lava channels and channelized sheet flows than the older assemblages (Pacaud and Stoughton-Roquemaure). This suggests that the magma discharge rates were higher and/or that they formed more proximal to the eruptive site (Lesher et al., 1984; Lesher, 1989; Hill et al., 1995; Lesher and Keays, 2002) or that thick cumulate komatiites have been selectively preserved within the younger assemblages suggested by their preferential location at the margin of major felsic complex (e.g., Pacaud).

7.5 Implications for the localization of Komatiite-Associated Ni-Cu-(PGE) Mineralization

Several factors have been proposed as being critical to the genesis of economically significant magmatic sulfide deposits associated with komatiites (e.g., Lesher, 1989; Lesher and Keays, 2002; Barnes, 2006; Lesher and Barnes, 2008), including: 1) the magma must be initially undersaturated in sulfide so that it contains sufficient concentrations of Ni, Cu, and PGE; 2) the magma must have access to an external sulfur source to achieve early sulfide saturation (prior to significant fractionation) and to segregate a significant abundance of immiscible sulfides at a high crustal levels; 3) the sulfides must be concentrated in a physical trap (embayment, inflection); and 4) the ores must form in a dynamic system where the magmas can interact with country rocks (to extract S) and where the sulfides can equilibrate with a sufficient amount of magma to generate high chalcophile element contents (i.e., high R factor).

These factors highlight the importance of the physical volcanology in the understanding of the genesis of those types of deposits. The present study and a complementary study (Sproule et al., 2005) have corroborated the interpretations of Lesher et al. (1984), Lesher (1989), Hill et al. (1990; 1995), Barnes et al. (1999), Barnes (2006), and Lesher and Barnes (2008) that the single most important parameter in assessing the mineral potential of komatiites is the physical volcanology. This study also provides new insights on the implications for Fe-Ni-Cu sulfide deposits in the western part of the Abitibi greenstone belt.

First, all known komatiite-associated Ni-Cu-(PGE) deposits/prospects/showings in the AGB occur in the 2719-2710 Ma Kidd-Munro assemblage (e.g., Alexo, Dundonald South, Dumont, Marbridge) and the 2710-2703 Ma Tisdale assemblage (e.g., Langmuir, McWatters, Redstone, Texmont, Sothman, Bannockburn). Thus far, no deposits have been discovered in the 2750-2735 Ma Pacaud and 2723-2720 Ma Stoughton-Roquemaure assemblages. The fact that younger komatiite-bearing assemblages are mineralized and older komatiite-bearing assemblages are barren is interpreted to reflect differences in the physical volcanology of those assemblages, as the Kidd-Munro and the Tisdale assemblages (younger assemblages) contain larger volumes of komatiitic rocks, in particular larger volumes of thick, highly magnesian cumulate lava channels and channelized sheet flows than the Pacaud and Stoughton-Roquemaure assemblages (older assemblages).

Second, almost all komatiite-associated Ni-Cu-(PGE) deposits in the Abitibi greenstone belt (e.g., Dundeal, Dundonald South/Beach, Hart, Langmuir #1 and #2, Redstone, Galata, and Mickel) and all of those include in this study (Alexo, Sothman, and C-Zone) are localized within transgressive footwall embayments produced or enhanced via thermomechanical erosion. They exhibit evidence of magma-wallrock interaction (e.g., xenoliths, geochemical contamination) consistent with formation within dynamic systems. Lava pathway/magma conduits represent only a small portion of the lava flow field/lava-sill complex and not all pathways are mineralized depending on the flow rate and access to sulfur (Lesher, 1989; Barnes, 2006; Lesher and Barnes, 2008). In addition to the thick cumulate host units and transgressive embayments reported within other komatiite-associated Ni-Cu-(PGE) deposits worldwide, the contact metamorphism, footwall projections, and footwall dikes identified in this study may also be used as exploration tools to aid in the identification and delineation of lava channelways that could potentially host Ni-Cu-PGE mineralization within subvolcanic-volcanic komatiite lava flow fields. Thin spinifex-textured sills, described only within unmineralized komatiite flows, may also be used as exploration tool for these types of deposits. Those sills are interpreted to have been developed within thin komatiitic flows during inflation of proximal, larger lava pathways that could potentially host Ni-Cu-(PGE) mineralization within komatiite lava flow fields.

Third, the linkages between intrusive and extrusive komatiitic rocks established within this study provide important constraints on the architecture of the komatiite volcanic-subvolcanic sequences in the Abitibi greenstone belt. If the density and rheology of the near-surface rocks governs whether they will be emplaced as lava flows, invasive flows, or sills, these factors must also influence the localization of Ni-Cu-(PGE) sulfide deposits. The initial eruptions in lava-dominated environment are typically most voluminous (Lesher, 1989; Lesher and Keays, 2002; Lesher, 2007) and, if erupted at sufficient flow rates, form channelized flows conducive to thermomechanical erosion of S-bearing footwall rocks. In subvolcanic-volcanic environments, however, channelized units may occur within the subvolcanic plumbing system and/or within overlying lavas. Where only the sills are channelized (e.g., Thompson belt), mineralization will occur only within the subvolcanic environment, where only the flows are channelized (e.g., Damba-Silwane), mineralization will occur only within the volcanic environment, but where both sills and lava flows are channelized (e.g., Dundonald, Shaw Dome, possibly Raglan), the distribution of the mineralization is more diverse and may occur within both environments as sub-seafloor and seafloor Ni-Cu-(PGE) sulfide deposits.

7.6 Areas for further Research

Since the recognition of komatiite as ultramafic volcanic rocks in the late 1960s, a tremendous amount of work has been conducted to improve our knowledge of these fascinating rocks and their spectacular textures and structures. However, there are still numerous points of uncertainty that are hotly debated in the scientific community. The following sections discuss some potential guides for future studies.

7.6.1. Physical volcanology

Although, a significant amount of volcanological work has been carried out on komatiites, our understanding of their physical volcanology is still very limited and inspired largely by mafic analogues that might not be necessarily appropriate for komatiites (Barnes and Lesher, 2008).

The physical volcanology of komatiite is one of the most important factors for the genesis of komatiite-associated Ni-Cu-(PGE) deposits and better knowledge and understanding of their volcanology may help to better understand the localization of Ni-Cu-(PGE) deposits. Numerous challenges remain, at all scales (regional- to local-scale), in developing a practical volcanological model for komatiites in the Abitibi greenstone belt. Because, the AGB is one of the best preserved Archean greenstone belts it might permit the resolution of the following problems:

Outcrop-Scale (m-scale) / Property-Scale (km-scale)

1) Identify and characterize textural and morphological facies variations laterally and up section within single flow units and volcanic sequences to define the main parameters that control the mode of emplacement and solidification of komatiite flows, and why similar komatiite flows may exhibit significantly different textural facies (e.g., thin spinifex-bearing and spinifex-free sheet flows).

2) Describe komatiite/footwall interaction in many other locations to further constrain the timing relationships between thermomechanical erosion and segregation of Fe-Ni-Cu sulfide mineralization.

Camp/District-Scale (10km-scale)

3) Describe and document contact relationships regionally to better understand the linkages between intrusive and extrusive komatiites that occur in some parts of the AGB, which are critical to understanding the architecture of komatiite magmatism.

4) Document geological settings and relationships between the various deposits at the camp scale to better constrain the main controls on the localization and segregation of Ni-Cu-(PGE) ores.

5) Identify and characterize komatiite volcanic facies and their lateral and up-section variation from proximal to distal settings from a volcanic centre, to define volcanic facies variations within a komatiite volcano and why some volcanic facies are so rare (e.g., vent facies).

Belt-Scale (100km-scale)

6) Determine and characterize the volcanic facies at the scale of the greenstone belt to constrain the overall volcanic architecture and to establish if the komatiitic volcanism erupted from one or several volcanic centres.

7) Characterize the spatial and temporal distribution of komatiite within the entire Abitibi greenstone belt to understand why komatiites are a major component of some areas and absent in others, and if they were generated from one or several plume events or from subduction-like process.

Characterization of komatiite flow fields at all scales from outcrop to belt using facies analysis will significantly advance our ability to constrain volcanic facies variations, aid in the interpretation of the volcanic architecture of komatiite flow fields, and provide vectors toward the most prospective environments for the genesis of Ni-Cu-(PGE) deposits.

7.6.2. Experimental work

Although a significant amount of experimental work has been carried out on komatiites, little experimental work has been done on komatiite flow morphology. Almost all experimental work has been confined to the cooling history of komatiite lava flows and spinifex growth. An avenue that could be fruitful for future experimental work would be to study komatiite lava flow morphology via analog modelling of the type initially done by Huppert and Sparks (1985). Such research could potentially lead to the recognition of how parameters such as extrusion rate, flow interior, underlying topography, etc. influence the architecture of komatiite volcanoes. Studying the dynamics of lava flows through laboratory modelling could bring new insights regarding komatiites that that are impossible to deduce by comparison with more mafic modern analogues that are characterized by different physical and chemical properties.

References

Allègre, C.J., 1982, Genesis of Archaean komatiites in a wet ultramafic subducted plate: in Komatiites, Arndt, N.T. and Nisbet, E.G. (Editors), Unwin and Allen, London, p. 495-500.

Anderson, S.W., Stofan, E.R., Smrekar, S.E ., Guest, J.E., and Wood, B.J., 2000, Reply to Self et al discussion of "Pulsed inflation of pahoehoe lava flows; implications for flood basalt emplacement": Earth and Planetary Science Letters, v. 179, p. 425-428.

Arndt, N.T., 1977, Ultrabasic magmas and high-degree melting of the mantle: Contributions to Mineralogy and Petrology, v. 64, p. 205-221.

Arndt, N.T. 1986, Spinifex and swirling olivines in komatiite lava lake, Munro Township, Canada: Precambrian Research, v. 34, p. 139-155.

Arndt, N.T., 1986, Differentiation of komatiite flows: Journal of Petrology, v. 27, p. 279-301.

Arndt, N.T., 1994, Archean komatiites: in Condie K.C. (Editor), Archean crustal evolution: Elsevier, Amsterdam Lausanne New York Oxford Shannon Tokyo, p. 11-44.

Arndt, N.T. and Nisbet, E.G. (Editors), 1982, Komatiites: Allen and Unwin, London, 526p.

Arndt, N.T. and Fowler, A.D, 2004, Textures in komatiites and variolitic basalts. In: The PreCambrian Earth: Tempos and Events. Pat Eriksson, Wlady Altermann, David Nelson, Wulf Muller, and Octavian Catuneanu (Editors), Developments in Precambrian Geology 12, p. 298-311.

Arndt, N.T., Lesher, C.M. and Barnes S.J., 2008, Komatiite: Cambridge University Press, New York, NY, United States, 456p.

Arndt, N.T., Francis, D., and Hynes, A.J. 1979, The field characteristics and petrology of Archean and Proterozoic komatiites: Canadian Mineralogist, v. 17, p. 147-163.

Arndt, N.T., Naldrett, A.J., and Pyke, D.R., 1977, Komatiitic and Fe-rich tholeiitic lavas of Munro Township, northeastern Ontario: Journal of Petrology, v. 18, p.319-369.

Arndt, N.T., Lesher, C.M., Houlé, M.G., Lewin, E., and Lacaze, Y., 2004, Intrusion and crystallization of a spinifex-textured komatiite sill in Dundonald Township, Ontario: Journal of Petrology, v. 45, p. 2555-2571.

Atkinson, B.T., 1999, Geology and mineral potential of the Serpentine Mountain area, Timmins: in Summary of Field Work and Other Activities 1999, Ontario Geological Survey, Open File Report 6000, p. 13-1 to 13-8.

Ayer, J.A. and Trowell, N.F., 2000, Geological compilation of the Kirkland Lake area, Abitibi greenstone belt: Ontario Geological Survey, Preliminary Map P.3425, scale 1:100 000.

Ayer, J.A., Trowell, N.F., Madon, Z., and Corfu, F., 1997, Geological compilation of the Abitibi greenstone belt in Ontario: the correlation of metallogenic potential with stratigraphy: in Summary of Field Work and Other Activities 1997, Ontario Geological Survey, Miscellaneous Paper 168, p. 3-9.

Ayer, J.A., Trowell, N.F., Amelin, Y., and Corfu, F., 1999a, Geological compilation of the Abitibi greenstone belt in Ontario: toward a revised stratigraphy based on compilation and new geochronology results: in Summary of Field Work and Other Activities 1998, Ontario Geological Survey, Miscellaneous Paper 169, p. 14-24.

Ayer, J.A., Trowell, N.F., Amelin, Y., and Corfu, F., 1999b, Compilation of the Abitibi greenstone belt in the Timmins–Kirkland Lake area: revisions to stratigraphy and new geochronology results: in Summary of Field Work and Other Activities 1999, Ontario Geological Survey, Open File Report 6000, p. 4-1 to 4-14.

Ayer, J.A., Amelin, Y., Corfu, F., Kamo, S., Ketchum, J., Kwok, K., and Trowell, N., 2002, Evolution of the southern Abitibi greenstone belt based on U-Pb geochronology; autochthonous volcanic construction followed by plutonism, regional deformation and sedimentation: Precambrian Research, v. 115, p. 63-95.

Ayer, J.A., Thurston, P.C., Bateman, R., Dubé, B., Gibson, H.L., Hamilton, M.A., Hathaway, B., Hocker, S., Houlé, M.G., Hudak, G., Lafrance, B., Lesher, C.M., Ispolatov, V., MacDonald, P.J., Péloquin, A.S., Piercey, S.J., Reed, L.E., and Thompson, P.H., 2005, Overview of Results from the Greenstone Architecture Project: Discover Abitibi Initiative; Ontario Geological Survey, Open File Report 6154, 146p.

Baird, A.M., 1999, Geochemistry and petrogenesis of chromite in intrusive and extrusive komatiites in the Shaw Dome area, Abitibi greenstone belt, Ontario: Unpublished M.Sc. thesis, University of Alabama, Tuscaloosa, Alabama, 189p.

Baker, H.B., 1917. Alexo nickel mine; Timiskaming District:Ontario Bureau of Mines Report no. 26, p. 258-272.

Baragar, W.R.A., 1983, The Circum-Ungava belt of eastern Hudson Bay: geology of the Cape Smith region: in Current Research, Part A, Geological Survey of Canada, Paper 83-1A, p. 325-328.

Barnes, S.-J., 1983, The origin of the fractionation of platinum group elements in Abitibi komatiites: Unpublished Ph.D. thesis, University of Toronto, Toronto, 231p.

Barnes, S.-J., 1985, The petrology and geochemistry of komatiite flows from the Abitibi greenstone belt, Canada, and a model for their formation, Lithos, v. 18, p. 241-270.

Barnes, S.-J., and Naldrett, A.J., 1986, Variations in platinum group element concentrations in the Alexo mine komatiite, Abitibi greenstone belt, northern Ontario, Geological Magazine, v. 123, p. 515-524.

Barnes, S.-J., and Naldrett, A.J., 1987, Fractionation of platinum group elements and gold in some komatiites of the Abitibi Greenstone Belt, northern Ontario, Economic Geology, v. 82, p. 165-183.

Barnes, S.-J., Gorton, M.P., and Naldrett, A.J., 1983, A comparative study of olivine and clinopyroxene spinifex flows from Alexo, Abitibi Greenstone Belt, Ontario, Canada: Contributions to Mineralogy and Petrology, v. 83, p. 293-308.

Barnes, S.-J., Naldrett, A.J., and Gorton, M.P., 1985, The origin of the fractionation of platinum-group elements in terrestrial magmas: Chemical Geology, v. 53, p. 303-323.

Barnes, S.J., 2004, Introduction to nickel sulfide orebodies and komatiite of the Black Swan area, Yilgarn Craton, Western Australia: Mineralium Deposita, v. 39, p.679-683.

Barnes, S.J., 2006, Komatiite-hosted nickel sulfide deposits: geology, geochemistry, and genesis, Chapter 3, in Barnes, S.J. (Editor), Nickel Deposits of the Yilgarn Craton: Geology, Geochemistry, and Geophysics Applied to Exploration: Special Publication 13, Economic Geology, p. 51-97.

Barnes, S.J., and Perring, C.S., 2006, Appendix: Summary of geological features of nickel sulfide deposits of the Yilgarn Craton: in Barnes, S.J. (Editor), Nickel Deposits:of the Yilgarn Craton: Geology, Geochemistry, and Geophysics Applied to Exploration: Special Publication 13, Economic Geology, p. 99-118.

Barnes, S.J., and Lesher, C.M., 2008, Physical Volcanology, Chapter 9: in N.T. Arndt, Lesher, C.M., and Barnes, S.J. (Editors), Komatiites, Cambridge University Press, New York, NY, United States, p. 243-294.

Barnes, S.J., Hill, R.E.T., and Gole, M.J., 1988, The perseverance ultramafic complex, Western Australia: The product of a komatiite lava river: Journal of Petrology, v. 29, p. 305-331.

Barnes, S.J., Hill1, R.E.T., and Evans, N.J., 2004, Komatiites and nickel sulfide ores of the Black Swan area, Yilgarn Craton, Western Australia. 3: Komatiite geochemistry, and implications for ore forming processes: Mineralium Deposita, v. 39, p. 729-751.

Barrett, F.M., Binns, R.A., Groves, D.I., Marston, R.J., and McQueen, K.G., 1977, Structural history and metamorphic modification of Archean volcanic-type nickel deposits, Yilgarn block, Western Australia: Economic Geology, v. 72, p. 1195-1223.

Barrie, C.T., Corfu, F., Davis, P.C., Coutts, A.C., and MacEachern, D., 1999, Geochemistry of the Dundonald komatiite-basalt suite and genesis of Dundeal Ni deposit, Abitibi Subprovince, Canada: Economic Geology, v. 94, p. 845-866.

Benson, D., 2005, Report on the 2004 summer mapping and sampling program on the Powell Property, Powell and Bannockburn townships, Ontario for Mustang Minerals Corp.: Kirkland Lake Resident Geologist office, assessment file # KL-5415.

Beresford, S.W., and Cas, R.A.F., 2001, Komatiitic invasive lava flows, Kambalda, Western Australia: The Canadian Mineralogist, v. 39, p. 525-535.

Beresford, S.W., and Stone, W.E., 2004, Komatiite-hosted Ni–Cu–PGE deposits of the Kambalda nickel camp - an overview: in: Neumayr, P., Harris, M., and Beresford, S. W. (Editors), Gold and nickel deposits in the Norseman–Wiluna greenstone belt, Yilgarn Craton, Western Australia — a field guide: Western Australia Geological Survey, Record 2004/16, p. 5-8.

Beresford, S.W., Cas, R.A.F., Lambert, D.D., and Stone, W.E., 2000a, Vesicles in thick komatiite lava flows, Kambalda, Western Australia: Journal of the Geological Society of London, v.. 157, p. 11-14.

Beresford, S.W., Cas, R.A.F., Lahaye, Y., Lambert, D.D., Jane, M., and Stone, W.E., 2000b, New insights into komatiite-hosted NiS ore genesis, Workshop on Volcanic Environments and Massive Sulfides, Abstract Volume, University of Tasmania, p. 9-10.

Beresford, S.; Cas, R.; Lahaye, Y.; Jane, M., 2002, Facies architecture of an Archean komatiite-hosted Ni-sulphide ore deposit, Victor, Kambalda, Western Australia; implications for komatiite lava emplacement: Journal of Volcanology and Geothermal Research, v. 118, p. 57-75.

Bereton, W.E., 2003, Report on the Bannockburn Nickel Property, Bannockburn, Matachewan area, Ontario for Mustang Minerals Corp.: NI43-101 compliant, Unpublished report, MPH Consulting Limited, 59p.

Berger, B.R., and Leblanc, G., 2002, Geology of Cairo Township, District of Timiskaming; in Summary of Field Work and Other Activities 2002: Ontario Geological Survey, Open File Report 6100, p. 8-1 to 8-7.

Berger, B.R., and Préfontaine, S., 2005, General Geology of Powell Township, District of Timiskaming: in Summary of Field Work and Other Activities 2002: Ontario Geological Survey, Open File Report 6172, p. 5-1 to 5-10.

Bowen, N.L., 1927, The origin of ultrabasic and related rocks: American Journal of Sciences, v. 14, p. 89.

Brown, M.A.N., Jolly, R.J.H., Stone, W.E. and Coward, M., 1999, Nickel ore troughs in Archaean volcanic rocks, Kambalda, Western Australia: indicators of early extension: Geological Society Special Publication 155, p. 197-211.

Burnham, O.M., Halden, N., Layton-Matthews, D., Lesher, C.M., Liwanag, J., Heaman, L., Hulbert , L., Machado, N., Michalak, D., Pacey, M., Peck, D.C., Potrel, A., Theyer, P., Toope, K., and Zwanzig, H., 2003, Geology, Stratigraphy, Petrogenesis, and Metallogenesis of the Thompson Nickel Belt, Manitoba: Final Report for CAMIRO Project 97E-02, 410 p., (11 Appendices).

Busby-Spera, C.J., White, J.D.L., 1987, Variation in peperite textures associated with differing host-sediment properties: Bulletin of Volcanology, v. 93, p. 765-775.

Campbell, I.H., and Naldrett, A.J., 1979, The influence of silicate:sulphide ratios on the geochemistry of magmatic sulphides: Economic Geology, v. 74, p. 1503-1505

Cas, R.A.F., Self, S., and Beresford, S.W. 1999, The behaviour of the fronts of komatiite lavas in medial to distal settings: Earth and Planetary Science Letters, v. 172, p. 127-139.

Cas, R.A.F., and Beresford, S.W., 2001, Field characteristics and erosional processes associated with komatiitic lavas: implications for flow behavior: The Canadian Mineralogist, v. 39, p. 505-524.

Champagne, C., 2004, Volcanologie physique et geochimie des komatiites de Spinifex Ridge, Formation de La Motte-Vassan, Abitibi: Unpublished M.Sc. thesis, Université du Québec à Chicoutimi, Chicoutimi, 155p.

Chisholm, K.M., 2002, Nature and origin of ore-localizing embayments at the Katinniq Ni-Cu-(PGE) sulphide deposit, Cape Smith Belt, northern Quebec: Unpublished M.Sc. thesis, Laurentian University, Sudbury, Canada, 166p.

Chitwood, L.A., 1994, Inflated basaltic lava—examples of processes and landforms from central and southeast Oregon: Oregon: Geology, v. 56, p. 11–21.

Chown, E.H., Daigneault, R., Mueller, W., and Mortensen, K., 1992, Tectonic evolution of the Northern Volcanic Zone, Abitibi Belt, Québec: Canadian Journal of Earth Sciences, v. 29, p. 2211-2225.

Coad, P.R., 1979, Nickel sulphide deposits associated with ultramafic rocks of the Abitibi belt and economic potential of mafic-ultramafic intrusions: Ontario Geological Survey, Study 20, 84p.

Coombs, C.R., Hawke, B.R., Wilson, L., 1990, Terrestrial analogs to lunar sinuous rilles: Kauhako crater and channel, Kalaupapa, Molokai, and other Hawaiian lava conduit systems: in Proceedings of the 20th Lunar Planetary Science Conference, Lunar Planetary Institute, Houston, Texas, p 195–206.

Cowden, A., 1988, Emplacement of komatiite lava flows and associated nickel sulfides at Kambalda, Western Australia: Economic Geology, v. 83, p. 436-442.

Cowden, A., and Archibald, N.T., 1987, Massive-sulfide fabrics at Kambalda and their relevance to the inferred stability of monosulfide solid-solution: The Canadian Mineralogist, v. 25, p. 37-50.

Cowden, A., and Roberts, D.E., 1990, Komatiite hosted nickel sulphide deposits, Kambalda: in Hughes, F.E. (Editor), Geology of the Mineral Deposits of Australia and Papua New Guinea, Australasian Institute of Mining and Metallurgy: Monograph 14, p. 567-581.

Dann, J.C., 2000, The 3.5 Ga Komati Formation, Barberton Greenstone Belt, South Africa, Part I: New maps and magmatic architecture: South African Journal of Geology, v. 103, number 1, p.47-68.

Dann, J.C., 2001, Vesicular komatiites, 3.5-Ga Komati Formation, Barberton Greenstone Belt, South Africa: inflation of submarine lavas and origin of spinifex zones: Bulletin of Volcanology, v. 63, p. 462-481.

Davis, P.C., 1996, Thalweg Nickel Showing, Bannockburn Property: Unpublished report, Outokumpu Mines Ltd., 13p., including 5 appendices.

Davis, P.C., 1997, Volcanic stratigraphy of the late Archean Kidd-Munro assemblage in Dundonald and Munro Townships and genesis of associated nickel and copper-zinc volcanogenic massive sulfide deposits, Abitibi greenstone belt, Ontario, Canada: Unpublished M.Sc. thesis, University of Alabama, Tuscaloosa, 201p.

Davis, P.C., 1999, Physical volcanology of komatiites flows at Dundonald Beach and Alexo Mine, Dundonald and Clergue Townships, Kidd-Munro Assemblage, Ontario portion and the Abitibi Greenstone Belt. Day 2: Guidebook Series, v. 1, Mineral Exploration Research Centre, Laurentian University, p. 27-44.

Davis, P.C. and Shore, M., 1999, Physical volcanology of komatiite flows at Pyke Hill and Dee's Flow, Munro Township, Kidd–Munro Assemblage, Ontario portion and the Abitibi Greenstone Belt. Day 1: in Classic komatiite localities and magmatic Fe-Ni-Cu-(PGE) sulphide deposits of the Abitibi Greenstone Belt, Ontario–Québec; Laurentian University, Sudbury, Ontario, Mineral Exploration Research Centre, Guidebook Series, v. 1, p. 11-26.

Dawson, J.B., Pinkerton, H., Norton, G.E., Pyle, D.M., 1990, Physicochemical properties of alkali carbonatite lavas: data from the 1988 eruption of Oldoinyo Lengai, Tanzania: Geology, v. 18, p. 260–263.

Dimroth, E., Cousineau, P., Leduc, M., and Sanschagrin, Y., 1978, Structure and organization of Archean subaqueous basalt flows, Rouyn-Noranda area, Quebec, Canada: Canadian Journal of Earth Sciences, v. 15, p. 902-918.

Dimroth, E., Imreh, L., Rocheleau, M., and Goulet, M., 1982, Evolution of the south-central segment of the Archean Abitibi belt, Québec. Part I: Stratigraphic and paleogeographic model: Canadian Journal of Earth Sciences, v. 19, p. 1729-1758.

Donaldson, C.H., 1974, Olivine crystal types in harrisitic rocks of the Rhum pluton and Archean spinifex rocks: Geological Society of America Bulletin, v. 85, p. 1721-1726.

Donaldson, C.H., 1976, An experimental investigation of olivine morphology: Contributions to Mineralogy and Petrology, v. 57, p. 187–213.

Donaldson, C.H., 1982, Spinifex-textured komatiites: a review of textures, mineral compositions and layering: in Komatiites, Arndt, N.T. and Nisbet, E.G. (Editors), George Allen and Unwin, London, p. 213-242.

Donaldson, M.J., Lesher, C.M., Groves, D.I., and Gresham, J.J, 1986, Comparison of Archaean dunites and komatiites associated with nickel mineralization in Western Australia: Implications for dunite genesis, Mineralium Deposita, v. 21, p. 296-305.

Dowling, S.E., Hill, R.E.T., and Barnes, S.J., 2001, Plumose inclusions and primary contacts, Silver Swan Nickel Deposit: in Cassidy, K.F. et al. (Editors), 4th International Archaean Symposium 2001 Extended Abstracts, AGSO-Geoscience Australia, Record 2001/37, p. 146-148.

Dowling, S. E., Barnes, S.J., Hill1, R.E.T., and Hicks, J.D., 2004, Komatiites and nickel sulfide ores of the Black Swan area, Yilgarn Craton, Western Australia. 2: Geology and genesis of the orebodies: Mineralium Deposita, v. 39, p. 707-728.

Duke, J.M., 1986, Petrology and economic geology of the Dumont Sill; an Archean intrusion of komatiitic affinity in northwestern Quebec: Economic Geology Report, Geological Survey of Canada, v. 35, 56p.

Evans, D.M., Cowden, A., and Barratt, R.M., 1989, Deformation and thermal erosion at the Foster nickel deposit, Kambalda-St. Ives, Western Australia: in Prendergast, M.D., and Jones, M.J. (Editors), Magmatic Sulphides – The Zimbabwe Volume, London, Institution of Mining and Metallurgy, p. 215-220.

Ewers, W.E., and Hudson, D.R., 1972, An interpretive study of a nickel-iron sulfide ore intersection, Lunnon shoot, Kambalda, Western Australia: Economic Geology, v. 67, p. 1075-1092.

Fagents, S.A., and Greeley, R., 2001, Factors influencing lava-substrate heat transfer and implications for thermomechanical erosion: Bulletin of Volcanology, v. 62, p. 519-532.

Faure, F., Arndt, N., and Libourel, G., 2006, Formation of spinifex texture in komatiites: an experimental study: Journal of Petrology, v. 47, p. 1591-1610.

Findlay, D., 1998, Boudinage on radial fractures: an alternative to magmatic models for the emplacement of nickel ores, Lunnon Shoot, Kambalda, Western Australia: Australian Journal of Earth Sciences, v. 45, p. 943-954.

Fowler, A.D., Berger, B., Shore, M., Jones, M.I., and Ropchan, J., 2002, Supercooled rocks: development and significance of varioles, spherulites, dendrites and spinifex in Archaean volcanic rocks, Abitibi Greenstone belt, Canada: Precambrian Research, v. 115, p. 311-328.

Frost, K.M., and Groves, D.I., 1989a, Magmatic contacts between immiscible sulfide and komatiite melts: Implications for genesis of Kambalda sulfide ores, Economic Geology, v. 84, p. 1697-1704.

Frost, K.M., and Groves, D.I., 1989b, Ocellar units in the Kambalda-Widgiemooltha komatiite sequence: evidence for sediment assimilation by komatiite lavas, in Prendergast, M.D., and Jones, M.J. (Editors), Magmatic Sulphides - The Zimbabwe Volume, London, Institution of Mining and Metallurgy, p. 207-214.

Fyfe, W.S., 1978, The evolution of the Earth's crust; modern plate tectonics to ancient hot spot tectonics?: Chemical Geology, v. 23, p. 89-114.

Gamble, A.P.D., 2000, Geology of the Potter Cu-Zn-Co-Ag VMS mineralization and exploration progress report to March 31, 2000 at Millstream Mines Ltd. Potter Mine Exploration project: Dave Gamble Geoservices Inc., Unpublished company report.

Gamble, A.P.D., and Gibson, H.L., 2000, The geologic setting of Cu-Zn-Co-Ag VMS mineralization at the Potter Mine, Munro Township, Ontario: abstract in Northeastern Ontario Mineral Symposium 2000, Sudbury Prospectors and Developers Association.

Gibson, H.L., Morton, R.L., and Hudak, G., 1999, Submarine volcanic processes, deposits, and environments favorable for the location of volcanic-associated massive sulfide deposits. in Barrie, C. T. and. Hannington, M.D, eds., Volcanic-Associated Massive Sulfide Deposits: processes and examples in modern and ancient settings: Reviews in Economic Geology, v. 8, p. 13-51.

Gibson, H.L., Ames, D., Bailes, B., Tardit, N., Devine, C., and MacLachlan, K., 2003, Invasive flows, peperite and Paleoproterozoic massive sulphide, Flin Flon, Manitoba and Saskatchewan: Programme with Abstract, GAC-MAC Annual Meeting, Vancouver, British Columbia.

Gillies, S.L., 1993, Physical volcanology and genesis of the Katinniq peridotite complex and associated Fe-Ni-Cu sulfide mineralization, Cape Smith Belt, New Québec: Unpublished M.Sc. thesis, University of Alabama, Tuscaloosa, Alabama, 146p.

Greeley, R., 1971, Observations of actively forming lava tubes and associated structures: Hawaii: Modern Geology, v. 2, p. 207-223.

Greeley, R., and Hyde, J.H., 1972, Lava tubes of the Cave Basalt, Mount St. Helens, Washington: Geological Society of American Bulletin, v. 83, p. 2397-2418.

Greeley, R., Fagents, S.A., Harris, R.S., Kadel, S.D., Williams, D.A., and Guest, J.E., 1998, Erosion by flowing lava: field evidence: Journal of Geophysical Research, v. 103, p. 27325-27346.

Green, A.H., and Naldrett, A.J., 1981, Langmuir volcanic peridotite-associated nickel deposits: Canadian equivalents of the Western Australian occurrences: Economic Geology, v. 76, p. 1503-1523.

Gresham, J.J., 1986, Depositional environments of volcanic peridotite-associated nickel sulphide deposits with special reference to the Kambalda dome: in Friedrich, G.H., Genkin, A., Naldrett, A.J., Ridge, J.D., Sillitoe, R.H., and Vokes, F.M. (Editors), Geology and Metallogeny of Copper Deposits, Proceedings of the Twenty-Seventh International Geological Congress, Moscow, Springer-Verlag, Berlin, p. 63-90.

Gresham, J.J., and Loftus-Hills, G.D., 1981, The geology of the Kambalda nickel field, Western Australia: Economic Geology, v. 76, p. 1373-1416.

Grove, T.L., and Parman, S.W, 2006, The development of spinifex textures I komatiites: Programme with Abstracts, GAC-MAC Annual Meeting, Montréal, Québec, v. 31, p. 61.

Grove, T. L., Gaetani, G. A., and deWit, M. J., 1994, Spinifex textures in 3.49 Ga Barberton Mountain Belt komatiites: evidence for crystallization of water-bearing, cool magmas in the Archean: EOS Transactions, American Geophysical Union 75, 354.

Grove, T. L., Gaetani, G. A., Parman, S., Dann, J., and deWit, M. J., 1996, Origin of spinifex textures in 3.46 Ga komatiite magmas from the Barberton Mountainland, South Africa: EOS Transactions, American Geophysical Union 77, p. 281.

Grove, T.L., de Wit, M., S.W., and Dann J.C., 1997, Komatiites from the Komati type section, Barberton South Africa, in de Wit, M.J., Ashwal, L.D. (Editors), Tectonic Evolution of Greenstones Belts, Oxford University Press, p. 438-453.

Grove, T.L., Parman, S.W., Nuka, P., de Wit, M., and Dann, J., 2002, Influence of H2O on the development of spinifex textures in komatiites: Geochimica Cosmochimica Acta, v. 66, p. A294.

Groves, D.I., Korkiakoski, E.A., McNaughton, N.J., Lesher, C.M., and Cowden, A., 1986, Thermal erosion by komatiites at Kambalda and genesis of nickel ores: Nature, v. 319, p. 136-139.

Harron, G.A., 2005, Technical report on Bannockburn Nickel Property, Bannockburn, Doon, Montrose, Hincks and Zavitz townships, Ontario for Mustang Minerals Corp.: NI43-101 compliant, MPH Consulting Limited, 50p.

Heather, K.B. 1998, New insights on the stratigraphy and structural geology of the South Western Abitibi Greenstone belt: Implications for the tectonic evolution and setting of mineral deposits in the Superior Province: in Technical Papers, Annual Meeting, Prospectors and Developers Association of Canada, p. 63-101.

Herzberg, C., Ratteron, P., and Zhang, J., 2000, New experimental observations on the anhydrous solidus for peridotite KLB-1: Geochemistry, Geophysics, Geosystems (G^3) 1, Paper number 2000GC000089.

Hill, R.E.T., 2001, Komatiite volcanology, volcanological setting and primary geochemical properties of komatiite-associated nickel deposits: Geochemistry - Exploration, Environment, Analysis, v. 1, p. 365-381.

Hill, R.E.T., and Perring, C.S., 1996, The evolution of Archaean komatiite flow fields—are they inflationary sheet flows?: in Whitehead, P.W., eds., Long lava flows: Chapman Conference on Long Lava Flows, Townsville, Australia, 1996, Abstracts, p. 18–21.

Hill, R.E.T., Gole, M.J., and Barnes, S.J., 1990, Physical volcanology of komatiites: A field guide to the komatiites between Kalgoorlie and Wiluna, Eastern Goldfields Province, Yilgarn Block, Western Australia: Excursion Guide Book No.1, Geological Society of Australia, Western Australian Division, Perth, 100p.

Hill, R.E.T., Barnes, S.J., Gole, M.J., and Dowling, S.E., 1995, The volcanology of komatiites as deduced from field relationships in the Norseman–Wiluna greenstone belt, Western Australia: Lithos, v. 34, p. 159-188.

Hoaston, D.M., Jaireth, S., and A.L. Jaques, 2006, Nickel sulfide deposits in Australia: Characteristics, resources, and potential: Ore Geology Reviews, v. 29, p. 177–241

Hon, K., Kauahikaua, J., Denlinger, R. and Mackay, K. 1994, Emplacement and inflation of pahoehoe sheet flows: Observations and measurements of active lava flows on Kilauea Volcano, Hawaii: Geological Society of America Bulletin, v. 106, p. 351–370.

Houlé, M.G., 2006, Geological and mineral potential of McArthur Township in the Bartlett Dome, Abitibi greenstone belt: Open File Report 6192, p6.1 to 6.14.

Houlé, M.G. and Solgadi, F., 2007, Geological and mineral potential of Bartlett and Geikie townships in the Bartlett dome, Abitibi greenstone belt: in Summary of Field Work and Other Activities 2007, Ontario Geological Survey, Open File Report 6213, p.7-1 to 7-15.

Houlé, M.G., and Montgomery, K., in preparation, Alexo Stripped Area, Dundonald Township: Ontario Geological Survey, Preliminary Map, various scales.

Houlé, M., Lesher, C.M., Gibson, H.L., Fowler, A.D., and Sproule, R.A., 2001, Physical Volcanology of Komatiites in the Abitibi Greenstone Belt: in Summary of Field Work and Other Activities 2001, Ontario Geological Survey, Open File Report 6070, p.13-1 to 13-16.

Houlé, M.G., Davis, P.C., Lesher, C.M., Arndt, N.T., 2002a, Extrusive and intrusive komatiites, komatiitic basalt and peperite and ore genesis at the Dundonald Ni-Cu-(PGE) Deposit, Abitibi Greenstone Belt, Canada: 9th International Platinum Symposium Abstract Volume, Billings, Montana, p. 181-184.

Houlé, M.G., Gibson, H.L., Lesher, C.M., Davis, P.C., Arndt, N.T., 2002b, The role of subvolcanic sills and peperites in facilating the eruption of Archean komatiitic flows at the Dundonald Beach Ni-Cu-(PGE) Deposit, northern Ontario: GSA Annual Meeting, Denver, U.S.A., Arizona, p. 513.

Houlé, M.G., Lesher, C.M., Gibson, H.L., and Sproule, R.A., 2002c, Recent Advanced in Komatiite Volcanology in the Abitibi Greenstone Belt, Ontario: in Summary of Field Work and Other Activities 2002, Ontario Geological Survey, Open File Report 6100, p. 7.1 to 7-19.

Houlé, M.G., Lesher, C.M., and Davis, P.C., 2003, Alexo and Sothman Ni-Cu-(PGE) deposits in the Abitibi greenstone belt, Canada: Thermomechanical erosion and multiple mineralization events: CIM Annual Meeting, Mining Industry Conference and Exhibition, Montreal, Québec, p. 188-189.

Houlé, M.G., Lesher, C.M., and Gibson, H.L., 2004, The Significance of Spinifex Textures in Constraining the Volcanic Settings of Precambrian Komatiitic and Ferropicritic Rocks: The Boston Creek Sill, Programme with Abstracts, GAC-MAC Annual Meeting, St-Catharines, Ontario, p.417.

Houlé, M.G., Préfontaine, S. and Berger, B.R., 2005., Physical Volcanology and Economic Potential of Komatiite-Associated Ni-Cu-(PGE) Deposits, Bannockburn Township Area : in Summary of Field Work and Other Activities 2005, Ontario Geological Survey, Open File Report 6172, p. 7-1 to 7-18.

Houlé, M.G., Lesher, C.M., Sproule, R.A., and Gamble, A.D.P., 2006a, Physical Volcanology of Komatiitic lava Flows at Pyke hill and "Lava Lake", Potter Mine, Munro Township, Ontario: Program with Abstract, GAC-MAC Annual Meeting, Montréal, Québec, p. 69.

Houlé, M.G., Hall, L.A.F., and Gibson, H.L., 2006b, The Anatomy of an Archean Komatiitic Sequence in the Shaw Dome area, Western Abitibi greenstone belt, Ontario, Canada: Program with Abstract, GAC-MAC Annual Meeting, Montréal, Québec, p. 69.

Houlé M.G., Gibson H.L., Lesher C.M., Davis P.C., Cas R.A.F., Beresford S.W., and Arndt N.T., 2008, Komatiitic basalt sills and multi-generational peperite at Dundonald Beach, Abitibi Greenstone Belt, Ontario: Implications for the Stratigraphic Architecture of Komatiite Volcanoes and Distribution of Subseafloor and Seafloor Komatiite-Associated Ni-Cu-(PGE) Deposits: Economic Geology, v.103, no.6.

Hudson, D.R., 1972, Evaluation of genetic models for Australian sulphide nickel deposits: Australasian Institute of Mining and Metallurgy Conference, Newcastle, p. 59-68.

Hulme, G., 1973, Turbulent lava flow and the formation of lunar sinuous rilles: Modern Geology, v. 4, p. 107-117.

Huppert, H.E. and Sparks, R.S.J., 1985, Komatiites I: eruption and flow: Journal of Petrology, v. 26, p. 694-725.

Huppert, H.E., Sparks, R.S.J., Turner, J.S., and Arndt, N.T., 1984, Emplacement and cooling of komatiite lavas: Nature, v. 309, p. 19-22.

Imreh, L., 1980, Variations morphologiques des coulées méta-ultramafiques komatiitiques du sillon Archéen de La Motte-Vassan, Abitibi-Est, Québec : Precambrian Research, v. 12, p.3-30.

Jackson, S.L., 1994, The Precambrian geology of Pacaud and Catharine townships and portions of adjacent townships, District of Timiskaming, Ontario: Ontario Geological Survey, Open File Report 5884, 86p.

Jackson, S.L., and Fyon, A.J., 1991, The western Abitibi subprovince in Ontario; in Geology of Ontario: Ontario Geological Survey, Special Volume 4, Part 1, p. 405-482.

Jackson, S.L., Fyon, A.J., and Corfu, F., 1994, Review of Archean supracrustal assemblages of the southern Abitibi Greenstone Belt, in Ontario, Canada: products of microplate interaction within large-scale plate-tectonic setting: Precambrian Research, v. 65, p. 183-205.

Jarvis, R.A., 1995, On the cross-sectional geometry of thermal erosion channels formed by turbulent lava flows: Journal of Geophysical Research, v. 100, p. 10,127-10,140.

Jensen, L.S. 1976. A new cation plot for classifying sub-alcalic volcanic rocks: Ontario Division of Mines, Miscellaneous Paper 66, 22p.

Jensen, L.S., 1985, Stratigraphy and petrogenesis of Archean metavolcanic sequences, southwestern Abitibi Subprovince, Ontario: Geological Association of Canada, Special Paper 28, p. 65-87.

Jolly, W.T., 1982, Progressive metamorphism of komatiites and related Archean lavas of the Abitibi area, Canada: in Komatiites, Arndt, N.T., and Nisbet, E.G. (Editors), George Allen and Unwin, London, p. 246-266.

Kauahikaua, J., Cashman, K.V., Mattox, T.N., Heiliker, C.C., Hon, K.A., Manhan, M.T., and Thornbur, C.R., 1998, Observations on basaltic lava streams in tubes from Kilauea volcano, Hawaii: Journal of Geophysical Research, v. 103, p. 27303-27324.

Kauahikaua, J., Sherrod, D.R., Cashman, K.V., Heliker, C., Hon, K., Mattox, T.R., and Johnson, J.A., 2003, Hawaiian Lava-Flow Dynamics During the Pu'u 'Ö'ö-Küpaianaha Eruption: A Tale of Two Decades: U.S. Geological Survey Professional Paper 1676, p. 63-87.

Keays, R.R., 1982, Palladium and iridium in komatiites and associated rocks: Application to petrogenetic problems, in N.T. Arndt and E.G. Nisbet (Editors), Komatiites, George Allen and Unwin, London, p. 435-457.

Kerr, A., and Leitch, A.M., Self-destructive sulfide segregation systems and the formation of high-grade magmatic ore deposits: Economic Geology, v. 100, p. 311-332.

Kerr, A.C. and Arndt, N.T., 2001, A note on the IUGS reclassification of the high-Mg and picritic volcanic rocks: Journal of Petrology, v. 42, p. 2169-2171.

Kerr, R.C., 2001, Thermal erosion by laminar lava flows: Journal of Geophysical Research, v. 106, p. 26,453- 26,465.

Kerrich, R., and Wyman, D.A., 1996, The trace element systematics of igneous rocks in mineral exploration: an overview: in Wyman D. (Editor), Igneous Trace Element Geochemistry: Applications for Massive Sulphide Exploration, Geological Association of Canada, Short Course Notes, v. 12, p. 1-50.

Lahaye, Y., and Arndt, N.T., 1996, Alteration of a komatiite flow from Alexo, Ontario, Canada: Journal of Petrology, v. 37, p. 1261-1284.

Lahaye, Y., Barnes, S.-J., Frick, L.R., and Lambert, D., 2001, Re-Os isotopic study of komatiitic volcanism and magmatic sulphide formation in the southern Abitibi Greenstone Belt, Canada: Canadian Mineralogist, v. 39, p. 473-490.

Larson, M.S., 1996, Physical volcanology and petrogenesis of intrusive and extrusive komatiites in the Shaw Dome area, Abitibi greenstone belt, Ontario, Canada; Unpublished M.Sc. thesis, University of Alabama, Tuscaloosa, Alabama, 259p.

Le Bas, M.J., 2000, IUGS reclassification of the high-Mg and picritic volcanic rocks: Journal of Petrology, v. 41, p.1467-1470.

Le Bas, M.J., 2001, Reply to comment by Kerr and Arndt: Journal of Petrology, v. 42, p.2173-2174.

Leblanc, G., and Berger, B.R., 2003, Precambrian geology, Cairo Township: Ontario Geological Survey, Preliminary Map P.3522, scale 1:20 000.

Lesher, C.M., 1989, Komatiite-associated nickel sulfide deposits: in Ore Deposits Associated with Magmas, Whitney J.A. and Naldrett A.J. (Editors), Reviews in Economic Geology, 4, Society of Economic Geologists, p. 44-101.

Lesher, C.M., 2007, Ni-Cu-(PGE) Deposits in the Raglan area, Cape Smith Belt, New Quebec, in Goodfellow, W.D., ed., Mineral Deposits of Canada: A synthesis of Mineral Deposit-Types, District Metallogeny, the Evolution of Geological Provinces, and Exploration Methods: Special Publication 5, Mineral Deposits Division, Geological Association of Canada, p. 351-386.

Lesher C.M., and Groves, D.I., 1984, Geochemical and mineralogical criteria for the identification of mineralized komatiites in Archaean greenstone belts of Australia, in Petrology: Igneous and Metamorphic Rocks, Proceedings of the 27th International Geological Congress, v. 9. VNU Science Press, Utrecht, p. 283-302.

Lesher, C.M., and Groves, D.I., 1986, Controls on the formation of komatiite-associated nickel-copper sulfide deposits, in Friedrich, G.H., Genkin, A., Naldrett, A.J., Ridge, J.D., Sillitoe, R.H., and Vokes, F.M. (Editors), Geology and Metallogeny of Copper Deposits, Proceedings of the Twenty-Seventh International Geological Congress, Moscow, Springer-Verlag, Berlin, p. 43-62.

Lesher, C.M., and Campbell, I.H., 1993, Geochemical and fluid dynamic modelling of compositional variations in Archean komatiite-hosted nickel sulfide ores in Western Australia: Economic Geology, v. 88, p. 804-816.

Lesher, C.M., and Arndt, N.T., 1995, REE and Nd isotope geochemistry, petrogenesis and volcanic evolution of contaminated komatiites at Kambalda, Western Australia: Lithos, v. 34, p. 127-157.

Lesher, C.M., and Keays, R.R., 2002, Komatiite-Associated Ni-Cu-(PGE) Deposits: Mineralogy, Geochemistry, and Genesis, in Cabri, L.J. (Editor), The Geology, Geochemistry, Mineralogy, and Mineral Beneficiation of the Platinum-Group Elements, Canadian Institute of Mining, Metallurgy and Petroleum, Special Volume 54, p. 579-617.

Lesher, C.M., and, Barnes, S.J., 2008, Komatiite-Associated Ni-Cu-PGE Deposits, Chapter 10: in N.T. Arndt, Lesher, C.M., and Barnes, S.J. (Editors), Komatiites, Cambridge University Press, New York, NY, United States, p. 295-327.

Lesher, C.M., Arndt, N.T. and Groves D.I., 1984, Genesis of komatiite-associated nickel sulphide deposits at Kambalda, Western Australia: A distal volcanic model, in Buchanan D.L. and Jones M.J., (Editors), Sulphide Deposits in Mafic and Ultramafic Rocks: , Institution of Mining and Metallurgy, London, p. 70-80.

Lesher, C.M., Burnham, O.M., Keays, R.R., Barnes, S.J., and Hulbert, L., 2001, Geochemical discrimination of barren and mineralized komatiites associated with magmatic Ni-Cu-(PGE) sulphide deposits: Canadian Mineralogist, v. 39, p. 673-696.

Lévesque, M., Lesher, C.M., and Charland, A., 2003, Volcanic or subvolcanic emplacement of the Raglan Formation in the Zone 3, Zone 2, and the Katinniq Ni-Cu-(PGE) deposits, Cape Smith Belt, Nouveau-Québec: CIM Annual Meeting, Mining Industry Conference and Exhibition, Montreal, Québec, p. 145-146.

Ludden, J., Hubert, C., and Gariépy, C., 1986, The tectonic evolution of the Abitibi greenstone belt of Canada: Mineralogical Magazine, v. 123, p. 53-166.

MacEachern, D., 2006. Canadian Arrow Mines Limited: lecture, Annual General Meeting, Toronto, June 30.

Marston, R.J., Groves, D.I., Hudson, D.R., and Ross, J.R., 1981, Nickel sulfide deposits in Western Australia: A review, Economic Geology, v. 76, p. 1330-1363.

Mattox, T.N., Heliker, C.C., Kauahikaua, J.P., and Hon, K.A., 1993, Development of the 1990 Kalapana flow field, Kilauea Volcano, Hawaii: Bulletin of Volcanology, v. 55, p. 407–413.

McLennan, S. M., 2001, relationship between the Trace Element composition of sedimentary rocks and Upper Continental Crust.: G-cubed, v. 2000GC, p. 000109.

Melezhik, A., Hudson-Edwards, K.A., Green, A.H. and Grinenko, L.N., 1994, The Pechenga area, Russia. 2. Nickel-copper deposits and related rocks: Transactions, Institution of Mining and Metallurgy, B 103, p. 46-161.

Montgomery, J.K., 2004, Report on the 2004-2005 diamond drilling program and surface exploration work on the Dundonald Property, Northeastern Ontario, July 2004-December 2005: Unpublished First Nickel Inc. report, 50p.

Mueller, W.U., Champagne, C., Barnes, S.-J., and Pilote, P., 1999, Physical volcanology of komatiites flows at Spinifex Ridge, La Motte Vassan Formation, Malartic Block, Québec portion, Abitibi Greenstone Belt. Day 3: in Classic komatiite localities and magmatic Fe-Ni-Cu-(PGE) sulphide deposits of the Abitibi Greenstone Belt, Ontario–Québec; Laurentian University, Sudbury, Ontario, Mineral Exploration Research Centre, Guidebook Series, v. 1, p. 5-53.

Muir, J. E., and Comba, C. D. A., 1979, The Dundonald deposit; an example of volcanic-type nickel-sulfide mineralization: The Canadian Mineralogist, v. 17, p. 51-359.

Muir, T.L., 1979, Discrimination between extrusive and intrusive Archean ultramafic rocks in the Shaw Dome area using selected major and trace elements: Canadian Journal of Earth Sciences, v. 16, p. 80-90.

Muir, T.L., 1995, Geology of Dundonald Township: Ontario Geological Survey, Preliminary Map, Map P.45, scale 1: 20 000.

Mullen, D.V., 1983, Report on the geology of the Sothman greenstone belt, districts of Sudbury and Temiskaming, Ontario: Unpublished internal report, Falconbridge Ltd., 53p.

Naldrett, A.J., 1966, Ultrabasic rocks of the Porcupine and related deposits: Unpublished Ph.D. thesis, Queen's University, Kingston, 264p.

Naldrett, A.J., 1966, The role of sulphurization in the genesis of iron-nickel sulphide deposits of the Porcupine District, Ontario, Canadian Institute of Mining and Metallurgy, Transactions, v. 69, p. 147-155.

Naldrett, A.J., 1973, Nickel sulphide deposits - their classification and genesis with special emphasis on deposits of volcanic association: Canadian Institute of Mining and Metallurgy, Bulletin, v. 66, p. 45-63.

Naldrett, A.J., 2004, Magmatic Sulfide Deposits: Geology, Geochemistry and Exploration: Springer-Verglag, Berlin, 727p.

Naldrett, A.J. and Mason, G.D., 1968, Contrasting Archean ultramafic igneous bodies in Dundonald and Clergue Townships, Ontario: Canadian Journal of Earth Sciences, v. 5, p. 111-143.

Naldrett, A.J., and Gasparini, E.L., 1971, Archaean nickel sulphide deposits in Canada, Their classification, geological setting and genesis with some suggestions as to exploration, in Glover, J.E. (Editor), The Archaean Rocks, Proceedings of the First Symposium on Archaean Rocks: Special Publication 3, Geological Society of Australia, Adelaide, p. 201-225.

Naldrett, A.J. and Turner A.R., 1977, The geology and petrogenesis of a greenstone belt and related nickel sulfide mineralization at Yakabindie, Western Australia: Precambrian Research, v. 5, p. 43-103.

Nesbitt, R.W., 1971, Skeletal crystal forms in the ultramafic rocks of the Yilgarn Block, Western Australia; evidence for an Archaean ultramafic liquid: Special Publication - Geological Society of Australia, v. 3, p. 331-346.

Nesbitt, R. W., Sun, S. S., 1976, Geochemistry of Archean spinifex-textured peridotites and magnesian and low-magnesian tholeiites: Earth and Planetary Science Letters, v. 31, p. 433-453.

Nisbet, E.G., 1982, Tectonic setting and petrogenesis of komatiite: in Komatiites, Allen and Unwin, London, p. 501-518.

Nisbet, E.G., Bickle, M.J., Martin, A., 1977, The mafic and ultramafic lavas of the Belingwe Greenstone Belt, Rhodesia: Journal of Petrology, v. 18, p. 521-566.

Olivier J.L., Rebagliati C.M., and Haslinger R.J., 1999, Summary exploration report – Potter mine property, Munro Township, Ontario for the HDG Potter Exploration Limited Partnership of Hunter Dickinson Group Inc. and Millstream Mines Limited: Internal Company Report Hunter Dickinson Group Inc., p 1.1 to 11.3.

Ontario Geological Survey, 1999, Single master gravity and aeromagnetic data for Ontario: Ontario Geological Survey, ERLIS Data Set 1036.

Ontario Geological Survey, 2005, Mineral Deposit Inventory Version 2 (MDI2): Ontario Geological Survey.

Parman, S.W., Grove, T.L., Dann, J.C., and de Wit, M.J., 2004, subduction origin for komatiites and cratonic lithospheric mantle: South African Journal of Geology, v. 107, p. 107-118.

Perring, C.S., Barnes, S.J., and Hill, R.E.T., 1995, The physical volcanology of Archaean komatiite sequences from Forrestania, Southern Cross Province, Western Australia: Lithos, v. 34, p.1 89-207.

Peterson D.W., Holcomb, R.T., Tilling, R.I., Christiansen, R.L., 1994, Development of lava tubes in the light of observations at Mauna Ulu, Kilauea Volcano, Hawaii: Bulletin of Volcanology, v. 56, p. 343–360.

Préfontaine, S., 2003, Origin of spinifex texture in ultramafic sills at Serpentine Mountain and Pyke Hill, Abitibi Ontario: Unpublished B.Sc., University of Ottawa, Ottawa, 30p.

Préfontaine, S., and Berger, B.R., 2005, Geology of Bannockburn and Montrose Townships, District of Timiskaming: in Summary of Field Work and Other Activities 2002: Ontario Geological Survey, Open File Report 6172, p. 6-1 to 6-7.

Prendergast, M.D., 2001, Komatiite-hosted Hunters Road nickel deposit, central Zimbabwe: physical volcanology and sulfide genesis, Australian Journal of Earth Sciences, v. 48, p. 681-694.

Puchtel, I.S., Humayun, M., Campbell, A., Sproule, R.A., and Lesher, C.M., 2004, Platinum group element geochemistry of komatiites from the Alexo and Pyke Hill areas, Ontario, Canada: Geochimica et Cosmochimica Acta, v. 68, p. 1361-1383.

Pyke, D.R., 1978, Geology of the Peterlong Lake area, districts of Timiskaming and Sudbury: Ontario Geological Survey, Report 171, 53p.

Pyke, D.R., 1982, Geology of Timmins area, District of Cochrane: Ontario Geological Survey, Report 219, 141p.

Pyke, D.R., Naldrett, A.J., and Eckstrand, A.P., 1973, Archean ultramafic flows in Munro Township, Ontario: Geological Society of America Bulletin, v. 84, p. 955-978.

Rice, A., and Moore, J., 2001, Physical modeling of the formation of komatiite-hosted nickel deposits and a review of the thermal erosion paradigm, Canadian Mineralogist, v. 39, p. 491-503.

Rosengren, N.M., Beresford, S.W., Grguric, B.A., and Cas, R.A.F., 2005, An intrusive origin for the komatiitic dunite-hosted Mount Keith disseminated nickel sulfide deposit, Western Australia: Economic Geology, v.100, p.149-156.

Ross, J.R., and Hopkins, G. M. F., 1975, Kambalda nickel sulfide deposits; in Knight, C. L., Ed., Economic Geology of Australia and Papua-New Guinea, I. Metals, Monograph 5: Australasian Institute of Mining and Metallurgy, Parkville, p. 100-121.

Schofield, R.E., 1982, Petrology of the Dundonald komatiites, Dundonald, Ontario: Unpublished Ph.D. thesis, Rutgers University, New Brunswick, New Jersey, 285p.

Scott, C.R., Mueller, W.U., and Pilote P., 2002, Physical volcanology, stratigraphy, and lithogeochemistry of an Archean volcanic arc: evolution from plume-related volcanism to arc rifting of SE Abitibi Greenstone Belt, Val d'Or, Canada: Precambrian Research, v. 115, p. 223-260.

Self, S., Thordarson, T., Keszthelyi, L., Walker, G. P. L., Hon, K., Murphy, M. T., Long, P., and Finnemore, S. 1996, A new model for the emplacement of Columbia River Basalts as large, inflated pahoehoe lava flow fields: Geophysical Research Letters, v. 23, p. 2689–2692.

Self, S., Thordarson, T., and Keszthelyi, L. 1997, Emplacement of continental flood basalt lava flows, in Large Igneous Provinces: in: Mahoney, J. J. and Coffin, M. (eds) Geophysical Monograph Series, 100. AGU, Washington DC, p. 381–410.

Self, S., Keszthelyi, L.P., and Thordarson, T., 1998, The importance of pähoehoe: Annual Review of Earth and Planetary Sciences, v. 26, p. 81–110.

Shore, M., 1996, Cooling and crystallization of komatiite flows: Unpublished PhD thesis, University of Ottawa, Ottawa, Ontario, 211p.

Shore, M., and Fowler, A.D., 1999, The origin of spinifex texture in komatiites: Nature, v.397, p.691-693.

Skilling, I., White, J.D.L., and McPhie, J., 2002, Peperite: review of magma-sediment mingling: Journal of Volcanology and Geothermal Research, v. 114, p. 1-17.

Sproule, R.A., Lesher, C.M., Ayer, J.A., and Thurston, P.C., 2002, Spatial and temporal variations in the geochemistry of komatiitic rocks in the Abitibi greenstone belt and implications for their tectonic setting: Precambrian Research, v. 115, p. 153-186.

Sproule, R.A., Lesher, C.M., Ayer, J.A., and Thurston, P.C., 2003, Geochemistry and petrogenesis of komatiitic rocks in the Abitibi greenstone belt, Ontario, Canada: Ontario Geological Survey, Open File Report, 119p.

Sproule, R.A., Lesher, C.M., Houlé, M.G., Keays, R.R., Ayer, J.A., and Thurston, P.C., 2005, Chalcophile element geochemistry and metallogenesis of komatiitic rocks in the Abitibi greenstone belt, Canada: Economic Geology, v. 100, p. 1169-1190.

Squire, R.J., and McPhie, J., 2002, Characteristics and origin of peperite involving coarse-grained host sediment: Journal of Volcanology and Geothermal Research, v. 114, p. 45-61.

Stone, M.S., and Stone, W.E., 2000, A crustally contaminated komatiitic dyke-sill-lava complex, Abitibi greenstone belt, Ontario: Precambrian Research, v. 102, p. 21-46.

Stone, W.E., and Archibald, N.J., 2002, Structural controls on Kambalda NiS ore shoots; the trough controversy revisited: Bulletin, Australian Institute of Geoscientists, v. 36, p. 205-208.

Stone, W.E., and Archibald, N.J., 2004, Structural controls on nickel sulphide ore shoots in Archaean komatiite, Kambalda, WA; the volcanic trough controversy revisited: Journal of Structural Geology, v. 26, p. 1173-1194.

Stone, W.E., Jensen, L.S., and Church, W.R., 1987, Petrography and geochemistry of an unsual Fe-rich basaltic komatiite from Boston Township, northeastern Ontario: Canadian Journal of Earth Sciences, v. 24, p. 2537-2550.

Stone, W.E., Crocket, J.H., Dickin, A.P., and Fleet, M.E., 1995a, Origin of Archean ferropicrites: geochemical constraints from the Boston Creek Flow, Abitibi greenstone belt, Ontario, Canada: Chemical Geology, v.121, p. 57-71.

Stone, W.E., Crocket, J.H., Fleet, M.E., 1995b, Differentiation processes in an unusual iron-rich alumina-poor Archean ultramafic/mafic igneous body, Ontario: Contributions to Mineralogy and Petrology, v. 119, p. 287-300.

Stone, W.E., Crocket, J.H., Fleet, M.E., and Larson, M.S., 1996, PGE mineralization in Archean volcanic systems: geochemical evidence from thick, differentiated mafic-ultramafic flows, Abitibi greenstone belt, Ontario, and implications for exploration: Journal of Geochemical Exploration, v. 56, p. 237-263.

Stone, W.E., Beresford, S.W., and Archibald, N.J., 2005, Structural setting and shape analysis of nickel sulfide shoots at the Kambalda dome, Western Australia: Implications for deformation and remobilization: Economic Geology, v. 100, p. 1441–1455.

Swanson, D.A., 1973, Pahoehoe flows from the 1969–1971 Mauna Ulu eruption, Kilauea Volcano, Hawaii: Geological Society of America Bulletin, v. 84, p. 615–626

Taylor, S. R., and McLennan, S. M., 1985, The continental crust: its composition and evolution: Oxford, Blackwell Scientific, 312p.

Taranovic, V., Lesher, C.M., Houlé, M.G., and Bédard, J.H., 2008. Physical Volcanology and Metallogenesis of Komatiite-Associated Ni-Cu-(PGE) Mineralization in the C-Zone, Bannockburn Township, Ontario: Program with Abstract, GAC-MAC Annual Meeting, Québec, Québec.

Thompson, P.H., 2005, A New Metamorphic Framework for Gold Exploration in the Timmins–Kirkland Lake Area, Western Abitibi Greenstone Belt: Discover Abitibi Initiative: Ontario Geological Survey, Open File Report 6162, 104p.

Thomson, B., 1989, Petrology and stratigraphy of some texturally well preserved thin komatiites from Kambalda, Western Australia: Geological Magazine, v. 126, p. 249-261.

Thurston, P.C., Ayer, J.A., Goutier, J., and Hamilton, M.A., 2008, Depositional gaps in Abitibi greenstone belt stratigraphy: a key to exploration for syngenetic mineralization: Economic Geology, v.103, no.6.

Trofimovs, J., Tait, M., Cas, R.A.F., Macarthur, A., and Beresford, S. 2003, Can the role of thermal erosion in strongly deformed komatiite-Ni-Cu-(PGE) deposits be determined? Perseverance, Agnew-Wiluna Belt, Western Australia: Australian Journal of Earth Sciences, v. 50, p.199-214.

Trofimovs, J., Cas, R., and Davis, B.K., 2004, Contemporaneous ultramafic and felsic intrusive and extrusive magmatism in the Archaean Boorara Domain, Eastern Goldfields Superterrane, Western Australia, and its implications: Precambrian Research, v. 131, p.283-304.

Ussleman, T.M., Hodge, D.S., Naldrett, A.J., and Campbell, I.H., 1979, Physical constraints on the characteristics of nickel-sulfide ore in ultramafic lavas, Canadian Mineralogist, v. 17, p. 361-372.

Vicker, P.A., 1991, Petrographic and Geochemical Examination of the Empire Komatiite Flow, Dundonald Township, Northern Ontario: Unpublished B.Sc. thesis, University of Western Ontario, London, 79p.

Viljoen, M.J., and Viljoen, R.P., 1969, Evidence for the existence of a mobile extrusive peridotitic magma from the Komati Formation of the Onverwacht group: in Upper Mantle Project, Geological Society of South Africa, Special Publication, v. 2, , p. 87-112.

Walker, G.P.L., 1972, Compound and simple lava flows and flood basalts: Bulletin of Volcanology, v. 35, p. 579-590.

Walker, G.P.L., 1991, Structure, and orgin by injection of lava under surface crust, of tumuli, "lava rises", "lava-rise pits", and "lava-inflation clefts" in Hawaii: Bulletin of Volcanology, v. 53, no. 7, p. 546–558.

Watkins, J.J., 1972, The Sothman sill nickel deposit: Unpublished B.Sc. thesis, Queen's University, Kingston, Ontario, 32p.

White, J.D.L., McPhie, J., and Skilling, I., 2000, Peperite: a useful genetic term: Bulletin of Volcanology, v. 62, p. 65-66.

Williams, D.A.C., 1979, The association of some nickel sulfide deposits with komatiitic volcanism in Rhodesia: Canadian Mineralogist, v. 17, p. 337-349.

Williams, D.A., Kadel, S.D., Greeley, R., Lesher, C.M., and Clynne, M.A., 2004, Erosion by flowing lava: Geochemical evidence in the Cave Basalt, Mount St. Helens, Washington, Bulletin of Volcanology, v. 66, p. 168-181.

Williams, D.A., Kerr, R.C., and Lesher, C.M. 1998, Emplacement and erosion by Archean komatiite lava flows at Kambalda: revisited: Journal of Geophysical Research, v. 103, p. 27 533-27 549.

Williams, D.A., Kerr, R.C., and Lesher, C.M., 1999, Thermal and fluid dynamics of komatiitic lavas associated with magmatic Ni-Cu-(PGE) sulphide deposits, in Keays, R.R., Lesher, C.M., Lightfoot, P.C., and Farrow, C.E.G. (Editors), Dynamic

Processes in Magmatic Ore Deposits and their Application to Mineral Exploration, Geological Association of Canada Short Course, v. 13, p. 367-412.

Williams, D.A., Kerr, R.C., Lesher, C.M., and Barnes, S.J., 2001, Analytical/Numerical Modeling of Komatiite Lava Emplacement and Thermal Erosion at Perseverance, Western Australia, Journal of Volcanology and Geothermal Research, v. 110, p. 27-55.

Woodall, R., and Travis, G.A., 1969, The Kambalda nickel deposits, Western Australia: Ninth Commonwealth Mining and Metallurgy Congress, Publication 2, p. 517-533.

Wyman, D.A., Bleeker, W., Kerrich, R., 1999, A 2.7 Ga komatiite, low Ti tholeiite, arc tholeiite transition, and inferred proto-arc geodynamic setting of the Kidd Creek deposit: evidence from precise trace element data: Economic Geology, Monograph 10, p. 511-528.

Appendix A – Whole Rock Major and Trace Element Geochemistry

Table A1. Abbreviations

n.a.: Not analyzed
n.d.: Not detected

Rock Types

And: Andesite (intermediate volcanic rocks)
Kb: Komatiitic basalt
Kk: Komatiite
Kpd: Komatiitic peridotite
Kpx: Komatiitic pyroxenite
Osx: olivine spinifex-textured rock

Unit Types

FW: Footwall rock
FWD: Footwall dike
FWP: Footwall projection
PR: Protrusion
BU: Basal unit
HU: Host unit
HUD: Host unit dike

Table A1. Major and trace elements analyses from the Alexo Stripped Area.

Sample	01-MGH-004	02-MGH-049	02-MGH-052A1AD	02-MGH-128	02-MGH-132
Rock Type	And	And	And	And	And
Unit Type	FW	FW	FW	FW	FW
Major Elements in wt% (XRF)					
SiO_2	48.81	55.08	42.50	45.92	44.92
TiO_2	1.26	1.19	1.35	0.57	1.11
Al_2O_3	16.54	17.06	17.45	10.40	15.19
Fe_2O_{3t}	6.46	5.42	11.70	13.45	4.90
MnO	0.08	0.07	0.13	0.24	0.13
MgO	3.50	6.43	9.35	5.91	7.12
CaO	18.27	5.78	10.98	20.50	22.19
Na_2O	0.00	0.61	0.09	0.00	0.00
K_2O	0.00	4.89	1.39	0.00	0.00
P_2O_5	0.14	0.10	0.10	0.06	0.18
LOI	5.18	2.59	3.81	2.25	3.16
Total	100.24	99.22	98.85	99.30	98.90
Trace Elements in ppm (XRF)					
Cr	274	298	317	812	626
Ni	165	211	1005	8202	1058
Co	59	59	59	330	53
Zn	21	68	115	45	27
V	243	236	304	131	190
Mn	700	628	1144	2091	1180
Trace Elements in ppm (ICP-MS)					
La	2.82	n.a.	3.83	2.06	5.01
Ce	8.4	n.a.	11.01	5.84	14.19
Pr	1.5	n.a.	1.7	0.944	2.179
Nd	7.62	n.a.	8.67	4.74	10.98
Sm	2.56	n.a.	2.79	1.44	3.27
Eu	1.26	n.a.	1.486	0.524	1.3
Gd	3.55	n.a.	3.54	1.811	4.03
Tb	0.63	n.a.	0.612	0.302	0.69
Dy	3.77	n.a.	3.991	1.956	4.35
Ho	0.87	n.a.	0.848	0.417	0.911
Er	2.4	n.a.	2.514	1.198	2.696
Tm	0.37	n.a.	0.372	0.175	0.4
Yb	2.17	n.a.	2.48	1.12	2.58
Lu	0.362	n.a.	0.38	0.166	0.391
Rb	n.d.	n.a.	2.6	0.18	0.24
Sr	11.01	n.a.	106.5	6.9	14.5
Nb	4.63	n.a.	4.4	1.9	4.7
Cs	0.01	n.a.	1.629	0.133	0.054
Hf	2.15	n.a.	2.4	1	2.5
Ta	n.d.	n.a.	0.3	n.d.	0.31
Th	0.26	n.a.	0.27	0.11	0.3
U	0.1	n.a.	0.278	0.055	0.152
Y	23.15	n.a.	22.82	10.71	24.31
Zr	84.02	n.a.	90.7	37.4	96.9

Table A1. *(Continued)*

Sample	02-MGH-138	02-MGH-150	01-MGH-009	02-MGH-054	02-MGH-055
Rock Type	And	And	Kb	Kb	Kpx
Unit Type	FW	FW	FWD	FWD	FWD
Major Elements in wt% (XRF)					
SiO_2	46.26	49.84	45.80	47.59	45.40
TiO_2	1.23	1.13	0.93	0.89	0.44
Al_2O_3	12.82	15.37	8.10	8.85	8.18
Fe_2O_{3t}	8.74	7.75	14.13	11.85	10.75
MnO	0.11	0.08	0.21	0.13	0.12
MgO	4.86	8.89	13.11	14.39	19.84
CaO	23.23	9.22	13.67	11.80	8.93
Na_2O	0.00	0.42	0.04	0.25	0.15
K_2O	0.00	3.65	0.61	1.17	0.00
P_2O_5	0.13	0.11	0.06	0.07	0.04
LOI	2.02	2.43	3.21	1.79	4.37
Total	99.40	98.89	99.87	98.78	98.22
Trace Elements in ppm (XRF)					
Cr	327	370	1407	1316	1772
Ni	174	221	509	537	1354
Co	31	41	91	69	87
Zn	96	46	73	53	80
V	265	266	218	226	168
Mn	951	675	1640	1086	1093
Trace Elements in ppm (ICP-MS)					
La	3.65	3.92	4.52	3.77	2.48
Ce	9.46	10.765	12.2	11.03	5.64
Pr	1.571	1.682	1.95	1.745	0.794
Nd	8.51	8.41	9.38	8.92	3.94
Sm	2.94	2.55	2.69	2.58	1.25
Eu	0.945	0.973	1.09	0.941	0.487
Gd	3.996	3.301	3.39	3.236	1.656
Tb	0.694	0.565	0.58	0.532	0.295
Dy	4.56	3.763	3.34	3.235	1.881
Ho	0.985	0.793	0.72	0.651	0.398
Er	2.905	2.358	1.92	1.866	1.173
Tm	0.432	0.343	0.28	0.266	0.169
Yb	2.82	2.28	1.68	1.7	1.09
Lu	0.43	0.352	0.274	0.254	0.166
Rb	0.2	5.01	0.56	0.7	0.95
Sr	12.9	168.8	18.59	33.9	9.7
Nb	4.2	3.7	3.5	3.2	1.2
Cs	0.014	0.104	0.29	0.098	0.272
Hf	2.2	2	1.85	1.7	0.8
Ta	0.29	0.2	n.d.	0.28	n.d.
Th	0.25	0.22	0.35	0.33	1.06
U	0.055	0.034	0.12	0.06	3.38
Y	26.25	20.44	18.36	16.86	10.36
Zr	83.5	73.9	65.59	63	28.9

Table A1. *(Continued)*

Sample	02-MGH-056	02-MGH-053	02-MGH-125	02-MGH-126	02-MGH-127
Rock Type	Kb	Kb	Kb	Kb	Kb
Unit Type	FWD	FWD	FWD	FWD	FWD
Major Elements in wt% (XRF)					
SiO_2	45.39	46.61	42.18	42.24	42.51
TiO_2	0.85	0.91	1.03	0.99	0.89
Al_2O_3	8.25	9.28	9.18	8.26	8.48
Fe_2O_{3t}	13.25	11.92	14.80	15.89	14.77
MnO	0.17	0.15	0.23	0.22	0.24
MgO	15.38	13.66	12.77	15.01	17.08
CaO	11.68	12.58	15.10	12.47	11.18
Na_2O	0.12	0.05	0.02	0.01	0.04
K_2O	0.24	0.00	0.00	0.00	0.00
P_2O_5	0.07	0.07	0.09	0.08	0.07
LOI	2.68	2.63	2.87	3.41	3.60
Total	98.08	97.86	98.27	98.58	98.86
Trace Elements in ppm (XRF)					
Cr	1386	1428	1491	1425	1291
Ni	514	495	481	491	458
Co	69	70	82	83	95
Zn	77	73	211	79	60
V	230	231	235	214	221
Mn	1481	1328	1997	1905	2100
Trace Elements in ppm (ICP-MS)					
La	3.76	3.14	5.11	5.19	3.77
Ce	11.18	10.1	13.97	14.54	10.755
Pr	1.809	1.782	2.237	2.302	1.752
Nd	9.22	9.48	11.35	11.51	9
Sm	2.71	2.88	3.33	3.46	2.76
Eu	0.92	0.946	1.098	1.025	0.739
Gd	3.251	3.426	3.98	3.986	3.344
Tb	0.539	0.568	0.65	0.644	0.539
Dy	3.236	3.489	3.904	4.021	3.429
Ho	0.658	0.711	0.79	0.807	0.691
Er	1.906	2.054	2.249	2.277	1.939
Tm	0.27	0.282	0.319	0.324	0.266
Yb	1.72	1.81	1.99	2.05	1.73
Lu	0.256	0.271	0.298	0.294	0.253
Rb	0.75	0.67	0.7	0.47	0.49
Sr	13.9	33	19.6	13.6	11.8
Nb	3.1	3.4	3.9	4.1	3.3
Cs	0.413	0.319	0.499	0.53	0.514
Hf	1.7	1.8	2.2	2.2	1.9
Ta	0.24	0.25	0.28	0.3	0.2
Th	0.32	0.34	0.4	0.42	0.33
U	0.083	0.08	0.126	0.124	0.113
Y	17.38	18.15	20.32	20.69	17.24
Zr	62.6	66.6	77.2	80.8	67

Table A1. *(Continued)*

Sample	02-MGH-124	01-MGH-003	02-MGH-044	02-MGH-045A2	02-MGH-129
Rock Type	Kb	Kb	Kpx	Kb	Kpx
Unit Type	FWD	FWP	FWP	FWP	PR
Major Elements in wt% (XRF)					
SiO_2	41.61	43.43	42.31	38.50	42.78
TiO_2	0.94	0.96	0.43	0.45	0.40
Al_2O_3	8.94	9.11	9.93	11.61	9.45
Fe_2O_{3t}	17.29	16.25	12.85	18.28	11.41
MnO	0.17	0.20	0.19	0.20	0.16
MgO	12.04	13.26	18.35	15.73	20.25
CaO	13.79	11.27	9.49	7.80	9.34
Na_2O	0.03	0.06	0.09	0.06	0.06
K_2O	0.00	0.94	0.03	0.00	0.04
P_2O_5	0.07	0.07	0.03	0.03	0.03
LOI	3.29	3.98	4.92	5.42	4.69
Total	98.17	99.53	98.62	98.08	98.61
Trace Elements in ppm (XRF)					
Cr	1477	1512	2531	2932	2576
Ni	462	565	693	726	727
Co	100	81	89	119	84
Zn	292	63	84	106	54
V	230	220	173	219	179
Mn	1441	1573	1663	1717	1360
Trace Elements in ppm (ICP-MS)					
La	3.9	4.38	1	1.47	0.81
Ce	11.485	12.82	2.75	4.83	2.275
Pr	1.877	2.2	0.468	0.813	0.397
Nd	9.61	10.86	2.57	4.12	2.3
Sm	2.97	3.31	0.98	1.31	0.9
Eu	1.016	1.18	0.427	0.713	0.341
Gd	3.591	3.69	1.526	1.821	1.396
Tb	0.585	0.61	0.282	0.324	0.262
Dy	3.651	3.63	1.894	2.138	1.824
Ho	0.721	0.78	0.413	0.474	0.396
Er	2.023	2.05	1.27	1.431	1.18
Tm	0.281	0.3	0.186	0.211	0.171
Yb	1.8	1.76	1.22	1.36	1.13
Lu	0.266	0.276	0.186	0.207	0.173
Rb	0.64	1.65	1.78	2.13	0.92
Sr	24.7	41.04	20.4	12.8	7.3
Nb	3.4	3.57	0.7	0.7	0.6
Cs	0.275	0.56	0.474	1.354	0.724
Hf	2	1.81	0.8	0.8	0.7
Ta	0.2	n.d.	n.d.	n.d.	n.d.
Th	0.35	0.36	0.07	0.08	0.07
U	0.108	0.08	0.025	0.026	0.027
Y	18.1	19.83	11.12	12.59	10.32
Zr	69.3	66.27	25.7	27	23.8

Table A1. (*Continued*)

Sample	02-MGH-130	02-MGH-131	01-MGH-008A	02-MGH-042	02-MGH-043
Rock Type	Kpx	Kpx	Kpd	Kpx	Kpx
Unit Type	PR	PR	BU	BU	BU
Major Elements in wt% (XRF)					
SiO_2	43.71	42.97	38.55	43.35	43.50
TiO_2	0.42	0.40	0.20	0.42	0.45
Al_2O_3	9.95	9.14	4.50	9.21	10.06
Fe_2O_{3t}	11.19	12.81	10.96	12.00	12.16
MnO	0.18	0.20	0.15	0.15	0.15
MgO	20.07	19.92	29.41	19.43	18.74
CaO	8.65	8.09	2.84	8.59	9.11
Na_2O	0.14	0.12	0.01	0.16	0.16
K_2O	0.49	0.39	0.00	0.67	0.51
P_2O_5	0.03	0.03	0.01	0.03	0.03
LOI	4.31	4.60	12.49	3.95	3.99
Total	99.14	98.67	99.12	97.96	98.86
Trace Elements in ppm (XRF)					
Cr	2390	2381	2879	2518	2484
Ni	700	690	1636	690	1489
Co	76	71	125	80	98
Zn	53	41	56	112	66
V	181	194	90	182	180
Mn	1550	1744	1235	1151	1179
Trace Elements in ppm (ICP-MS)					
La	1.25	0.91	1.2	1.04	0.98
Ce	3.26	2.555	3.14	2.785	2.65
Pr	0.542	0.425	0.54	0.47	0.445
Nd	2.87	2.3	2.83	2.57	2.58
Sm	1.06	0.93	1.08	0.96	0.97
Eu	0.416	0.308	0.42	0.384	0.372
Gd	1.544	1.387	1.62	1.471	1.412
Tb	0.286	0.256	0.32	0.269	0.271
Dy	1.892	1.796	1.99	1.818	1.796
Ho	0.418	0.388	0.46	0.393	0.395
Er	1.247	1.142	1.29	1.182	1.176
Tm	0.185	0.168	0.2	0.173	0.175
Yb	1.2	1.11	1.28	1.13	1.15
Lu	0.186	0.172	0.201	0.171	0.176
Rb	0.62	0.86	1.53	0.68	0.83
Sr	8.9	9	8.12	12.1	9.5
Nb	0.9	0.6	0.77	0.6	0.7
Cs	0.536	0.936	0.9	0.368	0.405
Hf	0.8	0.7	0.78	0.7	0.7
Ta	n.d.	n.d.	n.d.	n.d.	n.d.
Th	0.1	0.07	0.11	0.08	0.08
U	0.033	0.022	0.03	0.032	0.023
Y	10.89	9.83	12.52	9.91	10.51
Zr	27.2	23.3	26.81	24.4	24.9

Table A1. (*Continued*)

Sample	02-MGH-057	02-MGH-058	02-MGH-151	01-MGH-010	02-MGH-050
Rock Type	Kpx	Kpx	Kpx	Kpd	Kpx
Unit Type	BU	BU	BU	BU	BU
Major Elements in wt% (XRF)					
SiO_2	44.43	44.02	40.83	41.27	42.02
TiO_2	0.37	0.38	0.39	0.23	0.38
Al_2O_3	9.74	7.65	8.80	4.93	8.46
Fe_2O_{3t}	11.61	10.83	16.25	10.15	13.58
MnO	0.12	0.15	0.18	0.14	0.16
MgO	18.78	18.11	18.62	28.20	20.21
CaO	9.58	13.49	8.32	4.43	8.81
Na_2O	0.15	0.02	0.08	0.03	0.02
K_2O	0.58	0.00	0.00	0.38	0.00
P_2O_5	0.03	0.01	0.03	0.02	0.03
LOI	3.53	3.98	5.10	9.50	4.94
Total	98.92	98.64	98.60	99.28	98.61
Trace Elements in ppm (XRF)					
Cr	2481	2292	2417	1776	2570
Ni	800	2380	13452	2029	1467
Co	80	129	184	106	98
Zn	47	76	97	45	72
V	185	149	180	101	155
Mn	1063	1340	1634	1101	1296
Trace Elements in ppm (ICP-MS)					
La	1.22	0.67	0.83	0.6	0.84
Ce	3.18	2.18	2.41	2.455	2.33
Pr	0.499	0.432	0.409	0.239	0.407
Nd	2.59	2.6	2.32	1.31	2.23
Sm	0.93	0.97	0.91	0.49	0.87
Eu	0.449	0.323	0.383	0.234	0.355
Gd	1.372	1.458	1.324	0.741	1.306
Tb	0.255	0.273	0.25	0.14	0.244
Dy	1.716	1.795	1.669	0.967	1.627
Ho	0.364	0.389	0.366	0.21	0.359
Er	1.146	1.182	1.107	0.628	1.077
Tm	0.165	0.172	0.164	0.09	0.158
Yb	1.11	1.09	1.06	0.61	1.02
Lu	0.163	0.166	0.163	0.091	0.158
Rb	0.78	0.38	2.33	1.3	1.4
Sr	11.5	7.5	8.6	3.6	7
Nb	0.6	0.4	0.7	0.3	0.7
Cs	0.339	0.224	1.265	0.407	0.565
Hf	0.7	0.7	0.7	0.4	0.7
Ta	n.d.	n.d.	n.d.	n.d.	n.d.
Th	0.08	0.07	0.07	n.d.	n.d.
U	0.026	0.01	0.012	0.016	0.024
Y	9.62	10.17	9.76	5.3	9.56
Zr	22.4	22.9	22.8	13.2	23.1

Table A1. (*Continued*)

Sample	02-MGH-051A3	01-MGH-011	01-MGH-012	02-MGH-048A2	02-MGH-188
Rock Type	Kk (Osx)	Kpd	Kpd	Kk (Osx)	Kpd
Unit Type	BU	HU	HU	HU	HUD
Major Elements in wt% (XRF)					
SiO_2	41.22	34.76	40.55	39.42	37.14
TiO_2	0.39	0.19	0.27	0.19	0.39
Al_2O_3	9.50	3.54	5.29	4.69	8.84
Fe_2O_{3t}	11.33	19.04	8.26	10.42	6.39
MnO	0.17	0.12	0.15	0.17	0.19
MgO	21.40	26.84	29.13	29.96	30.10
CaO	9.01	3.26	5.71	5.28	6.57
Na_2O	0.03	0.02	0.01	0.02	0.00
K_2O	0.00	0.00	0.26	0.00	0.00
P_2O_5	0.03	0.01	0.02	0.01	0.07
LOI	5.43	11.19	10.16	8.97	10.00
Total	98.51	98.97	99.81	99.13	99.69
Trace Elements in ppm (XRF)					
Cr	2852	1880	1926	3730	2490
Ni	1324	3627	1730	1864	862
Co	71	263	97	85	45
Zn	111	46	36	54	39
V	171	101	97	98	179
Mn	1461	946	1156	1397	1542
Trace Elements in ppm (ICP-MS)					
La	1.35	0.47	0.82	0.42	0.73
Ce	3.56	1.175	1.995	1.17	2.26
Pr	0.566	0.198	0.333	0.202	0.414
Nd	2.87	1.07	1.76	1.15	2.45
Sm	1.06	0.39	0.59	0.43	0.88
Eu	0.371	0.155	0.24	0.114	0.262
Gd	1.478	0.561	0.834	0.652	1.298
Tb	0.272	0.107	0.151	0.118	0.239
Dy	1.805	0.723	1.017	0.795	1.591
Ho	0.394	0.158	0.219	0.177	0.361
Er	1.168	0.467	0.652	0.532	1.084
Tm	0.175	0.069	0.095	0.082	0.157
Yb	1.13	0.45	0.65	0.53	1.03
Lu	0.169	0.07	0.097	0.083	0.168
Rb	1.28	1.33	0.77	0.7	0.19
Sr	8.4	3.5	3.9	1.9	4.3
Nb	0.7	0.4	0.5	0.3	0.8
Cs	0.332	0.288	0.239	0.157	0.051
Hf	0.7	0.3	0.5	0.3	0.8
Ta	n.d.	n.d.	n.d.	n.d.	n.d.
Th	0.07	n.d.	0.06	n.d.	0.09
U	0.024	0.018	0.027	0.01	0.02
Y	10.44	4	5.71	4.77	9.32
Zr	24.1	10.8	16.7	11.1	29.9

APPENDIX B - SCIENTIFIC CONTRIBUTIONS

Refereed Publications

1. **Houlé, M.G.**, Lesher, C.M., and Davis, P.C., ***To be Submitted***. Komatiite-Hosted Alexo Nickel Deposit, Abitibi Greenstone Belt: Thermomechanical Erosion and Sulfide Genesis: Economic Geology or Mineralium Deposita.

2. **Houlé, M.G.**, Préfontaine, S., Fowler, A.D., and Gibson, H.L., ***In press***. Endogenous Growth in Komatiite Lava Flows: Evidence from Spinifex-Textured Sills at Pyke Hill and Serpentine Mountain, Western Abitibi Greenstone Belt, Northeastern Ontario, Canada: Bulletin of Volcanology.

3. **Houlé, M.G.**, Gibson, H.L., Lesher, C.M., Davis, P.C., Cas, R.A.F., Beresford, S.W., and Arndt, N.T., ***2008***. Komatiitic Basalt Sills and Multi-Generational Peperite at Dundonald Beach, Abitibi Greenstone Belt, Ontario: Implications for Komatiite Volcanic-Subvolcanic Architecture and Seafloor-Subseafloor Nickel Sulfide Distribution: Economic Geology, vol. 103, no. 6.

4. Sproule, R.A., Lesher, C.M., **Houlé, M.G.**, Keays, R.R., Ayer, J.A., and Thurston, P.C., **2005**. Chalcophile Element Geochemistry and Metallogenesis of Komatiitic Rocks in the Abitibi Greenstone Belt, Canada: Economic Geology, vol. 100, p. 1169-1190.

5. Arndt, N.T., Lesher, C.M., **Houlé, M.G.**, Lewin, E., and Lacaze, Y., **2004**. Intrusion and Crystallization of a Spinifex-Textured Komatiite Sill in Dundonald Township, Ontario: Journal of Petrology, vol. 45, p. 2555-2571.

Government Publications

6. **Houlé, M.G.**, Préfontaine, S. and Berger, B.R., **2005**. Physical Volcanology and Economic Potential of Komatiite-Associated Ni-Cu-(PGE) Deposits, Bannockburn Township Area : in Summary of Field Work and Other Activities 2005, Ontario Geological Survey, Open File Report 6172, p. 7-1 to 7-18.

7. Péloquin, S.A., **Houlé, M.G.**, and Gibson, H.L., **2005**. Geology of the Kidd-Munro assemblage in Munro Township, and the Tisdale and Lower Blake River assemblages in Currie Township: Discover Abitibi Initiative; Ontario Geological Survey, Open File Report 6157, 94p.

8. Ayer, J.A., Thurston, P.C., Bateman, R., Dubé, B., Gibson, H.L., Hamilton, M.A., Hathaway, B., Hocker, S., **Houlé, M.G.**, Hudak, G., Lafrance, B., Lesher, C.M., Ispolatov, V., MacDonald, P.J., Péloquin, A.S., Piercey, S.J., Reed, L.E., and Thompson, P.H., **2005**. Overview of Results from the Greenstone Architecture Project: Discover Abitibi Initiative; Ontario Geological Survey, Open File Report 6154, 146p.

9. **Houlé, M.G.**, Lesher, C.M., and Hall, L.A.F., **2003**. Komatiitic Rocks in the Shaw Dome Area : Volcanology and Their Economic Potential : in Summary of Field Work and Other Activities 2002, Ontario Geological Survey, Open File Report 6120, p. 38.1 to 38-4.

10. **Houlé, M.G.**, Lesher, C.M., Gibson, H.L., and Sproule, R.A., **2002**. Recent Advanced in Komatiite Volcanology in the Abitibi Greenstone Belt, Ontario: in Summary of Field Work and Other Activities 2002, Ontario Geological Survey, Open File Report 6100, p. 7.1 to 7-19.

11. **Houlé, M.**, Lesher, C.M., Gibson, H.L., Fowler, A.D., and Sproule, R.A., **2001**. Physical Volcanology of Komatiites in the Abitibi Greenstone Belt: in Summary of Field Work and Other Activities 2001, Ontario Geological Survey, Open File Report 6070, p.13-1 to 13-16.

12. **Houlé, M.**, Lesher, C.M., Fowler, A.D., Sproule, R.A., Ayer, J.A., Gibson, H.L., and Thurston, P.C., **2000**. Physical volcanology and metallogenesis of komatiites in the Abitibi Greenstone Belt, Superior Province, Canada: in Summary of Field Work and Other Activities 2000, Ontario Geological Survey, Open File Report 6032, p.11-1 to 11-8.

Abstracts

13. Gibson, H.L., Thurston, P.C., and **Houlé, M.G.**, **2007**. Archean base metal metallogeny in light of new tectonic models: Old rocks, new tricks: PDAC Convention 2007, Prospectors and Developers Association of Canada Annual Meeting, Toronto, Ontario.

14. **Houlé, M.G.**, Pilote, P., and Lesher, C.M., **2006**. Potential and Distribution of komatiite-Associated Ni-Cu-(PGE) Deposits in the Abitibi Greenstone Belt, Superior Province: Ontario Exploration and Geoscience Symposium 2006, Ontario Prospectors Association Annual Meeting, Sudbury, Ontario.

15. **Houlé, M.G.**, Pilote, P., Lesher, C.M., **2006**. Potentiel et distribution des gîtes de Ni-Cu-(ÉGP) associés aux komatiites dans la ceinture de roches vertes de l'Abitibi, Province du Supérieur: Québec Exploration 2006, Congrès Annuelle de l'AEMQ-MRNFQ, Québec, Québec.

16. Beresford, S.W., Cas, R.A.F., Lesher, C.M., and **Houlé, M.G., 2006**. Devolatisation of sulphidic sediments during shallow komatiitic sill emplacement, Dundonald Beach Ni-Cu-PGE deposit, Abitibi, Canada: Australian Earth Sciences Convention 2006, Melbourne, Australia.

17. Sproule, R.A., Lesher, C.M., **Houlé, M.G.,** Keays, R.R., Ayer, J.A., and Thurston, P.C., **2006**. Metallogenesis of komatiitic rocks in the Abitibi Greenstone Belt, Canada: Australian Earth Sciences Convention 2006, Melbourne, Australia.

18. **Houlé, M.G.**, Gibson, H.L., Lesher, C.M., Davis, P.C., Beresford, S.W., Arndt, N.T., and Cas, R.A.F., **2006.** Komatiitic Sills and Multi-Generational Peperite at Dundonald Beach, Abitibi Belt: Implications for the Architecture of Komatiite Volcanoes and Distribution of Subseafloor and Seafloor Komatiite-Associated

Deposits: Program with Abstract, GAC-MAC Annual Meeting, Montréal, Québec, p. 68-69.

19. **Houlé, M.G.**, Hall, L.A.F., and Gibson, H.L., **2006.** The Anatomy of an Archean Komatiitic Sequence in the Shaw Dome area, Western Abitibi greenstone belt, Ontario, Canada: Program with Abstract, GAC-MAC Annual Meeting, Montréal, Québec, p. 69.

20. **Houlé, M.G.**, Lesher, C.M., Sproule, R.A., and Gamble, A.D.P., **2006**. Physical Volcanology of Komatiitic lava Flows at Pyke hill and "Lava Lake", Potter Mine, Munro Township, Ontario: Program with Abstract, GAC-MAC Annual Meeting, Montréal, Québec, p. 69.

21. **Houlé, M.G.**, Fowler, A.D., Préfontaine, S., and Gibson, H.L., **2006**. Endogenous Growth in Komatiite Lava Flows: Evidence from Spinifex-Textured Sills at Pyke Hill and Serpentine Mountain, western Abitibi Greenstone Belt, Ontario: Program with Abstract, GAC-MAC Annual Meeting, Montréal, Québec, p. 68.

22. **Houlé, M.G.,** and Gibson, H.L., **2005**. Potential for komatiitic Ni-Cu-(PGE) sulphide mineralization in the Abitibi greenstone belt: Ontario Exploration and Geoscience Symposium 2005, Ontario Prospectors Association Annual Meeting, Toronto, Ontario, p. 18-20.

23. **Houlé, M.G.**, Lesher, C.M., and Gibson, H.L., **2004**. The significance of spinifex textures in constraining the mode of emplacement of Precambrian komatiitic and ferropicritic rocks: Program with Abstract, GAC-MAC Annual Meeting, St-Catharines, Ontario, p. 417.

24. **Houlé, M.G.**, Lesher, C.M., and Sproule, R.A., **2004**. Potential for komatiitic-associated Ni-Cu-(PGE) deposits in the Western Abitibi greenstone belt: Northeastern Ontario Minerals Symposium, Ontario Prospectors Association Annual Meeting, Sudbury, Ontario, p. 11.

25. Cas, R.A.F., Beresford, S., **Houlé, M.**, Lesher, M., Fowler, A., Trofimovs, J., Rosengren, N., Thurston, P., and Arndt, N., **2003**. Are spinifex-cumulate textured komatiitic rock units necessarily lavas? Archean example from Dundonald Beach, Abitibi greenstone belt, Canada : 17th Australian Geological Convention, Hobart, Australia, p. 60.

26. Cas, R.A.F., **Houlé, M.**, Beresford, S., Lesher, M., Fowler, A., Trofimovs, J., Rosengren, N., Thurston, P., and Arndt, N., **2003**. Are spinifex-cumulate textured komatiitic rock units necessarily lavas? Archean example from Dundonald Beach, Abitibi greenstone belt, Canada : 23rd IUGG General Assembly, Sapporo, Japan, p. A.500.

27. Sproule, R.A., **Houlé, M.G.**, Lesher, C.M., Keays, R.R., Ayer, J.A. and Thurston, P.C., **2003**. Chalcophile element geochemistry of komatiitic rocks in the Abitibi Greenstone Belt, Canada: Implications for their source region and metallogenesis: Program with Abstract, GAC-MAC Annual Meeting, Vancouver, British Columbia, Canada.

28. **Houlé, M.G.**, Lesher, C.M., and Davis, P.C., **2003**. Alexo and Sothman Ni-Cu-(PGE) deposits in the Abitibi greenstone belt, Canada: Thermomechanical erosion and multiple mineralization events: CIM Annual Meeting, Mining Industry Conference and Exhibition, Montreal, Québec, p. 188-189.

29. Sproule, R.A., Lesher, C.M., **Houlé, M.**, Keays, R., Thurston, P., Ayer, J., **2003**. Chalcophile element geochemistry of komatiites in the Abitibi greenstone belt and implications for their source region and metallogenesis: CIM Annual Meeting, Mining Industry Conference and Exhibition, Montreal, Québec, p. 187-188.

30. **Houlé, M.G.**, Lesher, C.M, Davis P.C., Sproule, R.A, and Montgomery, J.K., **2002**. Thermomechanical Erosion of Footwall Andesites by Komatiites at the Alexo Ni-Cu-(PGE) Deposit, Abitibi Greenstone belt, Canada: 9th International Platinum Symposium Abstract Volume, Billings, Montana, p. 189-192.

31. **Houlé, M.G.**, Davis, P.C., Lesher, C.M., Arndt, N.T., **2002**. Extrusive and intrusive komatiites, komatiitic basalt and peperite and ore genesis at the Dundonald Ni-Cu-(PGE) Deposit, Abitibi Greenstone Belt, Canada: 9th International Platinum Symposium Abstract Volume, Billings, Montana, p. 181-184.

32. **Houlé, M.G.**, Gibson, H.L., Lesher, C.M., Davis, P.C., Arndt, N.T., **2002**. The role of subvolcanic sills and peperites in facilating the eruption of Archean komatiitic flows at the Dundonald Beach Ni-Cu-(PGE) Deposit, northern Ontario: GSA Annual Meeting, Denver, U.S.A., Arizona, p. 513.

33. Lesher, C.M., **Houlé, M.G.**, Lévesque, M., Gibson, H.L., Williams, D.A., and Kerr, R.C., **2002**. Geochemical, mineralogical, textural, and fluid dynamic constrains on endogenous growth in differentiated cumulate komatiite flows: Goldschimdt 2002, 12th Annual VM Goldschimdt Conference, Davos, Switzerland, p. A449.

34. Sproule, R.A., Lesher, C.M., **Houlé, M.G.**, Keays, R.R., Ayer, J.A., and Thurston, P.C., **2002**. Geochemistry, Petrogenesis and Metallogenesis of Komatiites in the Abitibi Greenstone Belt: 9th International Platinum Symposium Abstract Volume, Billings, Montana, p. 439-442.

35. **Houlé, M.**, Lesher, C.M., Gibson, H.L., and Fowler, A.D., **2001**. Komatiite Lava Flow Classification: Extended Abstracts, 4th International Archaean Symposium 2001, Perth, AGSO-Geoscience Australia, Record 2001/37, 161-163.

36. **Houlé, M.**, Lesher, C.M., Gibson, H.L., Fowler, A.D, and Sproule, R.A., **2001**. Komatiite Lava Flow Classification: Morphologic, Lithologic, and Volcanic Facies: Program with Abstract, GAC-MAC Annual Meeting, St-John's, Newfoundland, p. 66.

37. Sproule, R.A., **Houlé, M.**, Lesher, C.M., Ayer, J.A., and Thurston, P.C., **2001**. Ni-Cu-(PGE) Potential of Komatiites in the Archean Abitibi Greenstone Belt, Canada: Northeastern Ontario Minerals Symposium, Annual Meeting, Sudbury, Ontario, p. 21.

38. **Houlé, M.**, Lesher, C.M., Sproule, R.A., Ayer, J.A., **2000**. Physical Volcanology and Metallogeny of Komatiitic Rocks in the Abitibi Greenstone Belt, Ontario-

Québec / Volcanologie Physique et Métallogénie des Roches Komatiitiques de la ceinture de roches vertes de l'Abitibi, Ontario-Québec : Explore in Québec: rediscover Abitibi, Geological Research Information Seminar/Explorer au Québec: redécouvrir l'Abitibi, Séminaire d'Information sur la Recherche Géologique, Ministère des Ressources naturelles du Québec. Program with Abstracts/Programme et résumés. DV 2000-04 / DV 2000-03, p. 44.

Field Trip Guidebooks

39. **Houlé, M.G.**, Péloquin, S.A, and Gibson, H.L., **2006.** Day 3: Physical Volcanology of Komatiite-Basalt association in Munro Township, Kidd-Munro Assemblage, Ontario Portion, Abitibi Greenstone Belt, *in* Mueller, W.U, Daigneault, R., Pearson, V., **Houlé, M.**, Dostal, J., and Pilote, P. (eds), The Komatiite-Komatiitic Basalt- Basalt Association in Oceanic Plateaus and Calderas: Physical Volcanology and Textures of Subaqueous Archean Flow Fields in the Abitibi Greenstone Belt: Field Trip A3 Guidebook, GAC-MAC Annual Meeting, Montréal, Québec, p. 45-61.

40. Atkinson, B., **Houlé, M.**, and Seim, G., **2005**. Nickel Field Trip, South of Timmins, Abitibi Greenstone Belt, Northeastern Ontario: Field Trip Guide, October 13th 2005, Ontario Geological Survey, 15p.

APPENDIX C – GEOLOGICAL MAPS AND OTHER MATERIALS

Map A

Detailed geological map of the eastern section of the Western Part of the Dundonald Stripped Area in Dundonald Township (scale 1:100).

Map B

Detailed geological map of the Alexo Stripped Area in Dundonald Township (scale 1:100).

Poster A

Distribution of Komatiites and Fe-Ni-Cu Sulfide Mineralizations within the Western Abitibi Greenstone Belt, Ontario. This includes Figures 7.1 to 7.4 and Tables 7.1 and 7.2.